TRANSCRIPTIONAL CONTROL OF HYPOTHALAMIC TANYCYTE DEVELOPMENT

By

Ana Lucia Miranda-Angulo

A dissertation submitted to the Johns Hopkins University in conformity with the requirements for the degree of Doctor of Philosophy

Baltimore, Maryland

March 2013

Abstract

The wall of the ventral third ventricle is composed of two distinct cell populations; tanycytes and ependymal cells. Tanycytes support several hypothalamic functions but little is known about the transcriptional network which regulates their development. We explored the developmental expression of multiple transcription factors by *in situ* hybridization and found that the retina and anterior neural fold homeobox transcription factor (Rax) was expressed in both ventricular progenitors of the hypothalamic primordium and differentiating tanycytes. Rax is known to participate in retina and hypothalamus development but nothing is known about its function in tanycytes. To explore the role of Rax in hypothalamic tanycyte development we generated Rax haploinsufficient mice. These mice appeared grossly normal, but careful examination revealed a thinning of the third ventricular wall and reduction of tanycyte and ependymal markers. These experiments show that Rax is required for tanycyte and ependymal cell progenitor proliferation and/or survival. Rax haploinsufficiency also resulted in ectopic presence of ependymal cells in the α2 tanycytic zone were few ependymal cells are normally found. Thus, the presence of ependymal cell in this zone suggests that Rax was required for α2 tanycyte differentiation. These changes in the ventricular wall were associated with reduced diffusion of Evans Blue tracer from the ventricle to the hypothalamic parenchyma. Furthermore, we have provided *in vivo* and *in vitro* evidence suggesting that RAX protein is secreted by tanycytes, and subsequently internalized by adjacent and distal cells. Finally, we generated an inducible Rax:CreER^{T2} mouse line which we have found to be selectively active in hypothalamic tanycytes, and will be a useful tool for manipulating gene function in these cells. In conclusion, we

have provided evidence that during development Rax is necessary to control tanycyte and ependymal cell progenitor proliferation and for α2 tanycyte differentiation. We also show that RAX protein is secreted from tanycytes and internalized by proximal and distal cells. Finally, the inducible Rax:CreER$^{T2/+}$ mouse line generated in this study will provide an invaluable tool for future studies of tanycyte development and function.

Thesis advisor: Seth Blackshaw, Ph.D.

Reader: Adam Kaplin M.D, Ph.D.

Acknowledgements

I would like to thank my advisor Seth Blackshaw for his guidance, understanding and support over the past seven years. Seth´s passion for science has always been an inspiration. His enthusiasm for discovering new things and for accomplishing complex projects always challenged me beyond what I thought I could do both personally and scientifically. He gave me enough freedom to think for myself, solve problems and generate new ideas while at the same time being supportive and providing needed guidance. I thank him for believing that I could always accomplish more.

I also want to thank all the current and previous members of Seth´s lab who I had the opportunity to interact with. They made my days much better and the challenges easier. I especially want to thank Mardi Byerly, a previous postdoc in Seth´s lab, who helped me during some of the hardest times. She not only encouraged me but also spent many hours helping me with critical experiments even when she was exhausted. I want to thank Jimmy de Melo for his discussions about science and life, and for letting me use his critical eye and experience. He was encouraging and supportive at difficult times and did not hesitate to listen and help. I would like to thank Hong Wang for her dedication, efficiency, and patience when performing all my genotyping and lab ordering. Her assistance made many of my experiments possible. I would like to thank Thomas Pak for his dedication and efforts to make the functional characterization of our knock-in mice possible. I also would like to thank Lizhi, our previous technician and a good friend. She was always willing to make probes or anything else I needed. Her smile and willingness to work were inspiring. I thank Janny, a rotating undergrad, who was a great companion during the last months of my graduate training and who helped me with image analysis. I

thank Thuzar and Liz for their gracious ways and ability to create a friendly lab environment. I also would like to thank them for giving me a very nice photo album that will never let me forget the people I met during this period of my life. Thanks to Juan for letting me speak Spanish to him in the lab to feel a little closer to my home country, and Kai for sharing his enthusiasm and curiosity for science which reminded me how much fun science can be. I want to thank Dan, who joined Seth's lab at the same time than I did. Together we accepted the challenge of studying tanycytes for the first time in this lab, his findings and technical expertise were very helpful for the development of my experiments. Thanks to Erin, Eric, and E.J. for their positiveness and friendship at all times. I would also like to thank Nicole and Aki, the first two members of Seth's lab, who welcomed me and guided me during my first years of training. I want to thank Vani, a former undergrad in the lab. She helped start our great adventure studying tanycytes in Seth's lab.

I want to thank all the people from other labs in the neuroscience department at Johns Hopkins who helped me with advice and/or reagents, especially Caitlin Engelhard, a previous member of David Ginty's lab. Caitlin kindly and patiently walked me through the generation of the knock-in constructs. I would also like to thank Shin Kang, a previous member of Dwight Bergles lab. He gave me helpful advice and contributed reagents for the generation of the knock-in constructs. Many thanks to Michelle Pucak for her guidance with experiments and valuable help with the Imaris software and to Claudia Ruiz, a neuroscience graduate student who rotated in our lab and made possible to obtain data necessary to start the knock-in mouse project.

People from Hopkins facilities were indispensable to me during my graduate studies. I want to give a special thanks to Barbara, Mike, Loza, Scot and Ester from the Microscope Core Facility for their hospitality, friendliness, and willingness to assist me in every step of imaging and analysis. I also thank Chip and Holly from the Johns Hopkins transgenic core. They made possible the generation of the knock-in mice. Also, thanks to the people in the mouse facility who took great care of my mice.

I want to specially thank the members of my thesis committee: David Ginty, Nicholas Gaiano, Hongjun Song, and Adam Kaplin; for their guidance not only in the academic area, but also during personal difficulties. They were all very helpful in pushing me to accomplish my goals.

I want to thank Beth and Rita, as well as other administrative members who helped make possible the existence of this wonderful graduate program, and for making me feel as an important member of the neuroscience department family.

I thank my previous advisors during my postdoctoral fellowship at NIMH. Dr. Cynthia Weickert and Daniel Weinberger were both great mentors and gave me a great deal of support and allowed me to be able to move toward my graduate training at Hopkins.

I want to thank the PAHO and NIH for giving me the opportunity to obtain my postdoctoral training at NIMH and for their financial support. Also, I thank the Universidad de Antioquia in Colombia for its financial support during all my training in the United States. I especially thank Dr. Carlos Palacio, the vice dean of the Universidad de Antioquia, who helped me solve all kind administrative difficulties necessary for me to finish my graduate training.

I thank all our collaborators who donated mice or helped with experiments: Tomomi Shimogori, Jin Woo Kim, Peter Mathers, Gordon Fishell, Xinzhong Dong, and Jeremy Nathans.

I want to thank my friends Lindsay, Lauren, Prya, Rob, Heather and Mala who made my time at Hopkins and in Baltimore a happy one.

Thanks to all who kindly helped editing this thesis Mardi, Jimmy, Lindsay, Juan, and Wendy.

I want to thank my family. My mother, who traveled back and forward from my home county, every year for eight years, to help me taking care of my children which was essential to me during my graduate studies. Without her help I would not have had peace of mind during my long lab hours. I thank my cousin Melisa who entertained my energetic younger son allowing me to write my thesis. I especially want to thank my husband Luis. He was my rock during all the challenging circumstances that arose. He supported and encouraged me and would always be there to remind me that I could achieve my goals and that he would do everything he could to help me make it possible. His positivity and love were essential for me during the most difficult times. I also thank him for being the great father that he is and for making sure the kids had all they needed when I could not be there during my long days in the lab. I thank my son Tomas who most of the time was able to patiently wait for me to be able to spend time with him. Although I stretched his patience to the limit he always gave me a smile and a hug and reminded me that he was there for me and loved me very much. I thank my little Mateo who is a wonderful gift from God and who makes me laugh and find joy every day.

Finally, and most importanty, I want to thank God who provided and keeps providing all I need, every day. I thank him for awakening in me a desire to explore and understand one of his most wondrous creations, the human brain. He keeps demonstrating to me that through Him everything is possible.

Table of Contents

List of Figures

List of Tables

Chapter 1

Chapter 2

List of abreviations

AAV1	Adeno-associated virus
AgRP	Agouti related peptide
ArcN	Arcuate nucleus
ATP	Adenosine-5'-triphosphate
BAC	Bacterial artificial chromosome
BBB	Blood brain barrier
BDNF	Brain-derived neurotrophic factor
bFGF	Basic fibroblast growth factor
BrdU	Bromodeoxyuridine
CA	Catecolaminergic
Ca^{2+}	Calcium
Cai^{2+}	Intracellular calcium
CART	Amphetamine-regulated transcript peptide
cGMP	Cyclic guanosine monophosphate
CNTF	Ciliary neurotrophic factor
COX	Cyclooxygenase
CPHNA	N-1-carboxy-2-phenylethyl (Nim-benzyl)-histidyl-βNA
CPPs	Cell penetrating peptides
Cre	Cre recombinase
CreER	Cre recombinase estrogen receptor
CSF	Cerebrospinal fluid
CVOs	Circunventricular organs

Cy	Cyanine
DAPI	4',6-diamidino-2-phenylindole
DIO2	Iodothyronine deiodinase 2
DMH	Dorsomedial nucleus
DP	Deflection point
Dta	Diphtheria toxin A-fragment
E2	17β-estradiol
EB	Evans blue
EDTA	Ethylenediaminetetraacetic acid
EGFP	Enhanced green fluorescent protein
eIF4E	Eukaryotic translation initiation factor 4E
EL	Ependymal layer
EM	Electron microscopy
En1/2	Engrailed 1 and engrailed 2
Ep	Ependymal cell
ErbB1	Epidermal growth factor receptor1
ErbB2	Epidermal growth factor receptor2
ERs	Estrogen receptors
ES	Embryonic stem cells
EtOH	Ethanol
fISH	Fluorescent *in situ* hybridization
FITC	Fluorescein
FL	Fiber layer

Foxj1	Forkhead box protein J1
FSH	Follicle-stimulating hormone
G-TUB	Detyrosinated alpha tubulin
GCL	Ganglion cell layer
GFAP	Glial fibrillary acidic protein
GFP	Green fluorescent protein
GK	Glucokinase
GLAST	Glial high-affinity glutamate transporter
GLUT-1	Glucose-transporter 1
GLUT-2	Glucose-transporter 2
GnRH	Gonadotropin releasing hormone
GPR50	G protein-coupled receptor 50 protein
Gpr50	G protein-coupled receptor 50 gene
H_2O_2	Hydrogen peroxide
Hes1	Hairy and enhancer of split
Hes 5	Hairy and enhancer of split
HPG axis	Hypothalamus-pituitary-gonad axis
HPT axis	Hypothalamus-pituitary-thyroid gland axis
HPZ	Hypothalamic proliferative zone
HRP	Horseradish peroxidase
i.c.v	Intracerebroventricular
i.p	Intraperitoneal
IGF-1	Insulin growth factor 1

IGFR-1	Insulin growth factor 1 receptor
IGFRBP-2	IGF-1 receptor binding protein-2
IHC	Immunohistochemistry
INL	Inner nuclear layer
IR	Infundibular recess
JAMs	Junction adhesion molecules
K^+	Potassium
KO	Knockout
LA	Long arm
LEIR	Lateral evaginations of the infundibular recess
LH	Lateral hypothalamus
LH	Luteinizing hormone
LHA	Lateral hypothalamic area
Lhx	LIM homeobox
LiCl	Lithium chloride
MAGUK	Membrane associated guanylate kinase homologues
MCT8	Monocarboxylate transporter 8
mDA	Mesecephalic dopaminergic
MDCK	Madin-Darby Canine Kidney Epithelial Cells
ME	Median eminence
MG	Müller glia
mG	Membrane targeted EGFP
MPTP	1-methyl-4-phenyl-1,2,3,6-tetrahydropyridine

mRNA	Ribonucleic acid messenger
MSG	Monosodium glutamate
MTC1/4	Monocarboxylate transporter 1 and 4
Ndufs	NADH dehydrogenase [ubiquinone] iron-sulfur protein 3
neo	Neomycin
NES	Nuclear export sequence
Nfia	Nuclear factor I/A-type
NLS	Nuclear localization sequence
NO	Nitric oxide
NPY	Neuropeptide Y
O/N	Overnight
OATP1C1	Organic anion transporter polypeptide 4C1
OCT	Optimum cutting temperature Tissue-Tek®
ONL	Outer nuclear layer
OT	Oxytocinergic
PB	Phosphate buffer
PBS	Sodium phosphate buffer
PD	Parkinson's disease
Pdx	Pancreatic and duodenal homeobox 1
PFA	Paraformaldehyde
PGE2	Prostaglandin E2
PGFα	Prostaglandin F alpha
pGK-	Phosphoglycerate kinase promoter

PHA	Posterior hypothalamic area
PIGFM	Prospective inducible genetic fate mapping
PL	Palisade layer
PMH	Posteriormedial hypothalamus
POD	Peroxidase (Horseradish roots) enzyme
POMC	Pro-opiomelanocortin
PPII ,	EC 3.4.19.6 pyroglutamyl peptidase II
PT	Pars tuberalis
PVN	Paraventricular nucleus
RT-PCR	Real-time reverse-transcription PCR
R26	Rosa26
Rarres2	Retinoic acid receptor responder 2
Rax	Retina and anterior neural fold homeobos gene
RAX	Retina and anterior neural fold homeobox protein
RaxKI	Rax knock-in mouse
RL	Reticular layer
ROI	Region of interest
RPCs	Retinal progenitor cells
RT	Room temperature
SA	Short arm
SCN	Suprachiasmatic nucleus
SE	Serotoninergic
SE	Subependymal

Shh	Sonic hedgehog
Six	Sine-oculis realted homeobox
SRY	Sex determining region Y-box 2
SUMO	Small Ubiquitin-like Modifier
SVZ	Subventricular germinal zone
T3	Triiodothyronine
T4	Thyroxine
Tan	Tanycyte
TetOp-Cre	Tetracycline operator-Cre recombinase
Tfs	Transcrition factors
TGFα	Transforming growth factor alpha
TGFβ	Transforming growth factor beta
TL	Tanycyte layer
TRH	Thyrotropin releasing hormone
TSA	Tyramide amplification reaction
TSH	Thyroid-stimulating hormone
TSHβR	TSH Thyroid-stimulating hormone receptor β subunit
Vim	Vimentin
VMH	Ventromedial nucleus
VP	Vasopressinergic
WGA	Wheat germ agglutinin
Xhmgb3	Xenopus high mobility group 3
Xrx1	Xenopus retina and anterior homeobox 1

YFP	Yellow fluorescent protein
Z/EG	LacZ/EGFP
ZO	Zona occludens protein
3V	Third ventricle
4-OHT	4-Hydroxytamoxifen

Chapter 1

Introduction

All organisms are exposed to environmental challenges, and the corresponding appropriate responses to those challenges allow them to reach the internal equilibrium necessary for adaptation and survival. This equilibrium, often called homeostasis or allostasis, is regulated in vertebrates by the hypothalamus, which is located in the medial basal part of the brain adjacent to the third ventricle (Garcia-Segura, 2009). Fundamental homeostatic functions such as feeding, reproduction, sleep, circadian rhythm, stress response, blood pressure and temperature, among many other functions, are all orchestrated by around twenty well-defined nuclei classically distributed in three rostro-caudal regions (anterior, tuberal or medial and mammillary or posterior), and three ventricle-adjacent areas (periventricular, medial and lateral) (Paxinos, 1994; Swaab, 1999). These nuclei receive input from multiple origins including retina, olfactory system, adrenal glands and autonomic system which are processed by these hypothalamic nuclei to generate two basic outputs; i) neuronal projections to other brain regions, brain stem and spinal cord and ii) hormonal release into the blood stream of the portal circulation or directly into the posterior pituitary (Paxinos, 1994). The complex multi-organ response orchestrated by the hypothalamus allows the organisms to reach equilibrium and survive in a challenging and variable environment (Garcia-Segura, 2009).

In addition to the function performed by the different neurons present in the hypothalamic nuclei, hypothalamic functions are constantly influenced by the cells lining

the walls of the third ventricle, in particular by the tanycytes. Tanycytes are considered specialized ependyma or radial glia-like cells which are located in circunventricular organs (CVOs) (Didier et al., 1986; Mullier, Bouret, Prevot, & Dehouck, 2010; Siso, Jeffrey, & Gonzalez, 2010), in the subventricular germinal zone (SVZ) of the lateral ventricles (Doetsch, Garcia-Verdugo, & Alvarez-Buylla, 1997) and the central canal of the spinal cord of the adult murine brain (Bruni, 1998). Also, they are particularly abundant in the third ventricular wall of the adult murine medial basal hypothalamus (Rodriguez et al., 2005). Their enrichment and strategic location in the hypothalamus caught the attention of many researchers between the 1960s and 1980s, resulting in a great advance in their anatomical characterization. However, due to the lack of appropriate tools, little progress was made in understanding of their functions during this period (Rodriguez et al., 2005). More recently, interest in exploration of tanycyte functions is starting to resume using better strategies, even though the optimal tools are still lacking. For this reason, I investigated the development of tanycytes in the adult mouse brain in order to better understand their function and to also develop tools which will contribute towards revealing their fascinating complexity.

1.1. Localization, Morphology, connectivity and immunohistochemistry of hypothalamic tanycytes

Tanycytes were named based on their morphology from the Greek word *tanus* which means “elongated”. They are characterized by a cell body localized in the ventricular layer whose more apical surface is in direct contact with the cerebrospinal fluid (CSF). Emerging from their cells bodies is a single long basal process that projects toward the median eminence (ME) or the hypothalamic parenchyma, which is in contact

with endothelial cells and probably glia and neurons (Millhouse, 1971; Rodriguez, Gonzalez, & Delannoy, 1979; Bleier, 1971). There are four types of hypothalamic tanycytes; alpha one (α1), alpha two (α2), beta one (β1) and beta two (β2) (Figure 1.1). Each of them has different locations along the third ventricle; as well as different morphology, connectivity and functions which are summarized below.

1.1.1. Distribution of tanycytes in the third ventricular wall of the medio-basal hypothalamus

The ventricular layer of the third ventricle is composed mainly of two cell populations, ependymal cells and tanycytes. These cells have a distinct distribution along the ventricular wall of the third ventricle of the medial hypothalamus (Mathew, 2008). Tanycytes are the only cell population in the most ventral part of the third ventricular wall, and their density progressively decreases dorsally until ependymal cells become the only cell population in the roof of the third ventricle. Based on the abundance of each of these cell types, the ventricular wall of the third ventricle in the tuberal hypothalamus can be divided in three ventro-dorsal zones: The **tanycytic zone,** which is composed almost exclusively by tanycytes; the **transition zone,** which contains tanycytes and ependymal cells; and the **ependymal zone,** which is composed only by ependymal cells. The tanycytic zone includes β1 and β2 tanycyte cell bodies whose processes project to the median eminence (ME), as well as ventral α2 tanycytes that project to the arcuate nucleus (ArcN) and the ventromedial hypothalamus (VMH). The transition zone is composed of α1 tanycytes cell bodies whose processes project to the dorsal portion of the VMH and to the dorsomedial hypothalamus (DMH). This zone also contains ependymal cells in close association with tanycytes. Finally, the ependymal zone is composed exclusively of

ependymal cells, which lack a process, and are located in the ventricular wall adjacent to the most dorsal portion of the DMH (Mathew, 2008) (Figure 1.2).

1.1.2. α tanycytes

α tanycytes have cylindrical cell bodies which are joined together by zonula adherence while the terminal portion of their processes is joined by thigh junctions (Krisch & Leonhardt, 1978). Their perikarya contain all the endocytic machinery and their apical surface have abundant microvilli and/or a single cilium which is in direct contact with the CSF. The apical surface and proximal portion of both α tanycyte processes contain abundant polyribosomes, but only α2 tanycytes have the characteristic subventricular neck enriched with spines that contain tightly packed polyribosomes. α1 and α2 tanycytes have similar morphology and differ mainly in their location. α1 tanycytes are more dorsal, with cells bodies located in the transition zone and processes that follow a dorsolateral trajectory projecting to the VMH or the DMH (Rodriguez et al., 2005). α2 tanycyte cell bodies are located in the lateral walls of the infundibular recess (IR) ventral to the α1 tanycytes cell bodies. Their processes follow a dorsoventral trajectory within the ArcN and some of them terminate in the lateral regions of the pars tuberalis (PT). Both types of α tanycytes have been observed in contact with blood vessels and are likely to be in contact neurons and glia (Bleier, 1971; Millhouse, 1971; Rodriguez et al., 1979).

1.1.3. β tanycytes:

β1 tanycyte have cylindrical cell bodies with elongated nuclei and are located in the ventricular wall of the lateral evaginations of the infundibular recess (LEIR). Their apical surface contains abundant microvilli, small spherical protrusions containing

endosomes, and large protrusions enriched with polyribosomes projecting to the ventricle. An interesting β1 tanycyte characteristic is the presence of numerous lipid inclusions in the perikaryon, which is associated with a highly developed smooth endoplasmic reticulum. Rodríguez *et al.* 2005 have suggested that this finding indicates that β1 tanycytes are involved in steroid or lipid synthesis or in lipid metabolism. This idea is also supported by the presence of enzymes involved in lipid metabolism, as detected by immunohistochemistry (Rodriguez et al., 1979). β1 tanycyte processes project to the lateral region of the ME where they form multiple branches in close association with blood vessels of the pars tuberalis (PT). β1 tanycyte processes also form abundant synaptoid contacts with the axonal terminals of neurosecreory neurons that release the gonadotropin releasing hormone (GnRH) to the portal circulation (Rodriguez et al., 1979).

β2 tanycyte cell bodies are cylindrical and are located in the floor of the IR in the ependymal layer of the ME. Some cell bodies have been found in the subventricular zone of the ME or even deeper (Rodriguez et al., 1979). Their processes follow a more or less straight trajectory toward portal capillaries of the ME where they terminate, forming multiple branches that surround blood vessels of the portal circulation. Interestingly, the processes of β2 tanycytes receive multiple synaptoid contacts from oxitocinergic and vasopressinergic axons as well as from other neuronal hypothalamic axons traveling across the ME. A number of molecular markers can be used to identify different tanycyte subtypes. These immunocytochemical markers are summarized in Table 1.1.

1.2. Functions attributed to tanycytes

Despite the broad anatomical characterization of tanycytes, their role in hypothalamic function is not completely understood, and most tanycyte functions remain speculative (Table 1.2).

1.2.1. Transport and barrier

It has being proposed that tanycytes may establish communications between the CSF and blood vessels, neurons in hypothalamic nuclei (α tanycytes), and, in the case of β tanycytes, with the portal circulation. This is supported by the connectivity of tanycytes, and their ability to endocytose and transcytose tracers compounds (Rodriguez et al., 2005). Interestingly, in β1 tanycytes, the presence of several components of the endocytic pathway in their cell bodies and their process terminals suggest that they can absorb molecules not only from the CSF but also from the portal circulation. In fact, both horseradish peroxidase (HRP) injected into the blood stream, and circulating apolipoprotein A-IV accumulate in tanycytes (Rodriguez et al., 2005). This suggests a possible bi-directional transport from CSF to blood and vice versa, where tanycytes serve as a bridge.

However, the physiological implications of tanycyte-mediated endocytosis and transport have being poorly investigated. One of the very few studies that addresses this aspect of tanycyte function shows that, although these cells do not express Insulin growth factor 1 (IGF-1) mRNA, they can accumulate IGF-1 protein in their cell bodies and processes via endocytosis (Duenas et al., 1994). Interestingly, this accumulation can be blocked with IGFR-1 receptor antagonists (Fernandez-Galaz et al., 1997). Thus, it has being suggested that tanycytes may absorb IGF-1 from the CSF (Fernandez-Galaz,

Torres-Aleman, & Garcia-Segura, 1996). Interestingly, IGF-1 levels in tanycytes fluctuate with the estrous cycle and are known to be regulated by estrogen and progesterone (Duenas et al., 1994). In order to better understand the regulation of the cyclic fluctuation of IGF-1, Cardona-Gomez *et al.* explored the changes in IGF-1 receptor (IGF1R) and IGF-1 receptor binding protein-2 (IGFRBP-2) in the apical surface of the tanycytes, after injection of estrogen and progesterone in ovarectomized rats. They found that progesterone decreased IGF1R and IGFRBP-2 immunoreactivity, whereas estrogen increased IGFRBP-2 immunoreactivity in tanycyte microvilli. The authors concluded that estrogen and progesterone may show opposing effects on the cyclic accumulation of IGF-1 in tanycytes during the estrous cycle, where progesterone could block the absorption of IGF1 whereas estradiol seems to promote it (Cardona-Gomez, Chowen, & Garcia-Segura, 2000) . The fact that estrogen did not stimulate IGF-R expression in the apical surface of tanycytes but can increase IGF-1 absorption suggests that the upregulation of IGF-1R stimulated by estrogen might be taking place in tanycyte terminals. This is supported by studies that have shown that tanycytes can take up IGF-1 from peripheral blood (Duenas et al., 1994).

The fate of the molecules absorbed by tanycytes is now becoming clear. Studies done with wheat germ agglutinin (*WGA*) have shown that the molecules that enter tanycytes by endocytosis follow three pathways (Rodriguez et al., 2005); degradation, transcytosis and some molecules are stored in their terminals, apparently waiting for stimulus to induce their secretion. This last option seems to be the fate of IGF-1 taken up by tanycytes. Since IGF-1 accumulation in tanycytes has been associated with ovulation and the beginning of puberty (Duenas et al., 1994; Hiney, Srivastava, Nyberg, Ojeda, &

Dees, 1996), and since tanycytes are known to regulate GnRH release during those events, it is likely that the absorbed IGF-1 is secreted by tanycyte terminals in response to estrogen to induce tanycyte-mediated GnRH release in these two hormone mediated events (Garcia-Segura, Lorenz, & DonCarlos, 2008). The neurons and astrocytes of the ArcN represent another potential target for IGF-1. Since they both express IGF-1R and they are in close contact with tanycyte terminals it is likely that IGF-1R mediates the response of ArcN neurons and astrocytes to estrogen during the estrous cycle (Garcia-Segura, Rodriguez, & Torres-Aleman, 1997; Fernandez-Galaz et al., 1997).

In summary, IGF-1 represents an elegant example of the dual sources from where tanycytes can incorporate molecules (CFS and blood), and their distribution to a wide variety of targets such as neuropeptide containing axon terminals, neurons and astrocytes. However, more direct evidence is necessary to understand the mechanism of estrogen-induced endocytosis for IGF-1 by tanycyte and to reveal other absorbed molecules.

While tanycytes serve as a bi-directional bridge between the CSF and the hypothalamus, they also have the ability to form barriers. β2 tanycyte cell bodies form tight junctions which create a barrier between the CSF and axons crossing the ME, isolating them from direct contact with the CSF, where there are abundant signaling molecules. Also, the processes of β1 tanycytes are joined by *zonula occludens* (ZO) to form bundles that separate the ME, where there is no blood brain barrier (BBB), from the ArcN. This conclusion is based on experiments with monosodium glutamate (MSG) injected in peripheral blood. It has been previously shown that MSG damages ArcN neurons if it is injected during the first postnatal week, when tanycytes are still immature (Olney, 1971). In contrast, when MSG is injected in the fourth postnatal week, when

tanycytes are fully mature, there is no damage to ArcN neurons (Olney, 1971). This suggests that β1 tanycyte process bundles are necessary to protect ArcN neurons from blood borne molecules. Furthermore, these barriers have been studied using tracers and may be important in protecting the hypothalamus from CSF and peripheral blood molecules (Rodriguez, Blazquez, & Guerra, 2010). However, the effect of disrupting these barriers in the mature hypothalamus has not yet been studied.

1.2.2. Glucosensing

Tanycytes express the glucose-sensing molecules glucokinase (GK), Glucose-transporter 1 (GLUT-1), Glucose-transporter 2 (GLUT-2) and ATP-sensitive K^+ channels (Millan et al., 2010; Garcia et al., 2003; Thomzig et al., 2001; Harik et al., 1993). Intracerebroventricular (i.c.v) injection of alloxan, a GK inhibitor, in the third ventricle leads to destruction of tanycytes and alters glucose levels and feeding behavior in rats. Interestingly, these defects in feeding behavior are reversed over the course of time, and are associated with recovery of the tanycytes (Sanders, Dunn-Meynell, & Levin, 2004). Furthermore, it is known that the VMH and the ArcN contain neurons that respond to changes in glucose concentrations, eliciting a systemic regulatory response consisting of changes in food intake and insulin secretion (Fehm, Kern, & Peters, 2006).

The expression of the glucose-sensing molecules, the phenotype observed with Alloxan, and the strategic location of tanycytes with direct contact to the CSF and neurons of the VMH and the ArcN, all led to speculation that tanycytes might be involved in the detection of glucose levels in the CSF and in the neuronal response to glucose changes (Rodriguez et al., 2005). However, the mechanism by which tanycytes detect gluocose, their response to changes in glucose levels and the resulting effect on the

function of adjacent neurons is only starting to be studied. Recently, it was shown that tanycytes can take up glucose through GLUT-2 receptors and connexin-43 *in vitro,* and that glucose uptake leads to an ATP-mediated increase in free intracellular calcium (Ca_i^{2+}) (Orellana et al., 2012). However, how the Ca_i^{2+} increase in tanycytes is translated to specific changes in neuronal activity is still unknown.

Another study has shown that lactate is involved in the translation of glucose changes, detected by tanycytes, to ArcN and VMH neurons. It is known that neurons in the VMH and ArcN depolarize in response to lactate by increased ATP production that results in the closing of K_{ATP} channels (Song & Routh, 2005). Interestingly, it has being shown *in vitro* that tanycytes can produce lactate through the glycolytic pathway in response to glucose, and release it through the lactate transporters Monocarboxylate Transporter 1 and 4 (MTC1/MTC4) to adjacent neurons which express MCT2 (Cortes-Campos et al., 2011; Cortes-Campos et al., 2013). Thus, lactate produced by tanycytes apparently can activate glucose-excited neurons from the ArcN and the VMH.

Taken together, these findings suggest that tanycytes sense glucose and initiate a lactate/ATP and/or Ca^{2+}-mediated communication with adjacent neurons in the VMH and ArcN, which might contribute to the regulation of feeding behaviors. However, additional *in vivo* studies are necessary to demonstrate the participation of tanycytes in the glucosensing network and in the neuronal response of the VMH and ArcN to changes in glucose levels.

1.2.3. Regulation of the neuroendocrine system

Tanycytes participate in the regulation of the neuroendocrine system through several mechanisms: i) Dynamic control of gonadotropin-releasing hormone (GnRH) release into

the portal circulation, ii) thyroid hormone synthesis, iii) extracellular degradation of thyrotropin releasing hormone (TRH) in the ME.

1.2.3.1. Dynamic control of GnRH release

In female vertebrates, reproduction depends on cyclic changes of reproductive hormones. These cyclic changes are tightly regulated and are known as the hypothalamus-pituitary-gonadal axis (HPG axis) (Charlton, 2008). Hypothalamic neurons of the preoptic area secrete GnRH into the portal circulation of the median eminence. GnRH travels through the portal circulation to the anterior pituitary to stimulate the production and release into the blood stream of gonadotropins, luteinizing hormone (LH) and follicle-stimulating hormone (FSH). In this way gonadotropins reach the ovaries and induce morphological changes that result in the production and secretion of estrogen and progesterone, which leads to the induction of ovulation and preparation of the uterus for possible fertilization.

Estrogen and progesterone have opposite but complementary effects on the regulation of the HPG axis to maintain homeostasis. Estrogen induces a positive feedback loop, stimulating synthesis of more GnRH by the hypothalamic neurons in preparation for a possible fertilized egg. On the other hand, progesterone induces a negative feedback mechanism that inhibits GnRH synthesis. If the egg is not fertilized, a prostaglandin produced by the uterus, PGFα, blocks progesterone production and consequently ends the negative feedback of GnRH, leading to the beginning of another cycle (Larsen, Kronenberg, Melmed, & Polonsky, 2002). Classically, estrogen-mediated regulation of the HPG axis occurs in the hypothalamic neurons through the regulation of GnRH expression (Gharib, Wierman, Shupnik, & Chin, 1990). However, several investigations have shown that another level of regulation is happening in the ME,

particularly at the neurohemal junction of the ME where abundant tanycytic processes are found in close association with GnRH fibers (Prevot et al., 1999; Yamamura, Hirunagi, Ebihara, & Yoshimura, 2004; Kozlowski & Coates, 1985; King & Rubin, 1994).

It has been shown that during the diestrus and early proestrus phase, β1 tanycytes envelop neurosecretory axonal terminals containing gonadotropin releasing hormone (GnRH) and interpose between these neurosecretory terminals and the portal capillaries. In contrast, during the oestroge surge, tanycyte processes retract, allowing neuropeptide axons to access the vasculature to release GnRH into the portal circulation (Prevot et al., 1999). This phenomenon is the result of a synchronized tanycyte-neuron-endthelial structural plasticity of which estradiol (E2) is apparently the master regulator. When E2 binds to estrogen receptors (ERs) in tanycytes, there is an induction of synthesis and secretion of prostaglandin E2 (PGE2), which stimulates tanycyte processes retraction. Meanwhile, E2 binding to endothelial cells of the portal circulation induces nitric oxide (NO) synthesis and release; the NO freely diffuses and penetrates tanycytes to regulate their structural plasticity. In tanycytes, NO binds to NO-sensitive guanylyl cyclase and activates cyclooxygenase 1 (COX1) and cyclooxygenase 2 (COX2), and as a result there is an increase in cyclic guanosine monophosphate (cGMP) and PGE2 production, which induces retraction of tanycyte processes. This allows a direct apposition of GnRH axonal terminals with the portal circulation and consequent GnRH release (de Seranno et al., 2010; de Seranno et al., 2004). In addition to E2 and NO, there are growth factors that are known to stimulate GnRH release in the portal circulation, but the signaling pathways involved are not well understood. It is well accepted that TGFα, TGFβ and neuregulins participate in GnRH release; however there are no ErbB receptors in the GnRH axonal

terminals (Ma, Berg-von der Emde, Moholt-Siebert, Hill, & Ojeda, 1994; Voigt et al., 1996). Interestingly, epidermal growth factor receptor (ErbB1) and epidermal growth factor receptor (ErbB2) receptors have being found in astroglia of the ME (Ma et al., 1994), suggesting that TGFs do not affect GnRH release directly but do so by regulating the activity of glia surrounding GnRH terminals. Indeed, TGFα has been shown to interact with tanycyte ErbB receptors, thereby affecting tanycyte plasticity (Prevot, Cornea, Mungenast, Smiley, & Ojeda, 2003). *In vitro* binding of TGFα to tanycyte ErbB1 and ErbB2 receptors induces a biphasic response. Initially, TGFα induces tanycytes process extension, however after sustained TGFα signaling there is an increased synthesis of PGE2 which induces TGFβ production and leads to tanycyte process retraction.

In conclusion, these findings establish estrogen-NO-mediated tanycyte plasticity as an important phenomenon in the regulation of the HPG axis by determining the access of the GnRH fibers to portal circulation. It remains an open question as to whether TGF initiates an estrogen-independent mechanism of plasticity in tanycytes, or if estrogen-induced production of PGE2 can potentiate the TFG-mediated plasticity.

1.2.3.2. Thyroid hormone synthesis

Thyroid hormones are essential for the regulation of cell proliferation, differentiation and metabolic balance (Mohacsik, Zeold, Bianco, & Gereben, 2011). As a consequence, their dysregulation during development leads to a severe neurodevelopmental defect known as congenital hypothyroidism. In the adult brain, altered thyroid hormone levels lead to mood disorders as well as memory, cognitive and motor deficits (Mohacsik et al., 2011). The hormones triiodothyronine (T3) and

thyroxine (T4) are tyrosine-based hormones produced in the thyroid. T4 is released into the blood stream from the thyroid gland to reach their target tissues, including the brain. However, T4 is a pro-hormone that does not bind any receptor, and needs to be converted to active T3 by iodothyronine deiodinase 2 (D2) (Croteau, Davey, Galton, & St Germain, 1996). In the brain, more than 75% of T3 is derived D2-mediated local conversion of T4. This enzyme is present in astrocytes of different brain regions, but by far the highest levels of D2 are found in tanycytes of the mediobasal hypothalamus (Guadano-Ferraz, Obregon, St Germain, & Bernal, 1997; Tu et al., 1997).

There is a traditional feedback mechanism to regulate the hypothalamus-pituitary-thyroid (HPT) axis in order to maintain appropriate energy levels. In this feedback mechanism, systemic reduction of T3 leads to increased TRH synthesis in the parvocellular neurons of the paraventricular nucleus (PVN), which is transported to the ME to be released into the portal circulation. TRH then travels to the pituitary, which responds by releasing thyroid-stimulating hormone (TSH) to the blood stream. Finally, TSH reaches the thyroid gland and increases the production of T4, which is then transported to target tissues to be converted to T3. In this way, T3 levels are restored to maintain an energy balance. In this feedback mechanism there is an inverse relationship between the thyroid hormone levels and TRH synthesis (Segerson et al., 1987).

Interestingly, in response to fasting and infection there is a reduction of T4 and T3 along with a paradoxical HPT axis response consisting of low to normal TSH and low TRH levels, in contrast to the expected increase in these two hormones necessary for the restoration of T3 levels. This altered HPT axis response is known as “nonthyroidal illness syndrome” or “euthytoid sick syndrome” in humans (De Groot, 1999). It is still

under debate whether this abnormal HPT axis response is a normal physiological response to limit energy expenditure and protein catabolism under food deprivation and illness, or if it might be a pathological condition by itself (De Groot, 1999). Moreover, the origins of the abnormal HPT axis response remain enigmatic. Changes in gene expression in murine tanycytes in response to lipopolysaccharides (LPS) and fasting shed some light on the origin of the euthytoid sick syndrome (De Groot, 1999). In response to infection (LPS injection) and fasting, there was a fast increase of D2 mRNA in tanycytes and, as a consequence, more hypothalamic T3 production accompanied by reduction of TRH mRNA in PVN neurons (Diano, Naftolin, Goglia, & Horvath, 1998; Fekete et al., 2004). Interestingly, i.c.v infusion of iopanoic acid, a D2 inhibitor, in the third ventricle of rats prevented the decrease of TRH under fasting conditions (Coppola, Meli, & Diano, 2005).

Taken together, these observations suggest that during infection and fasting, hypothalamic tanycyte D2 activity differs from peripheral D2 activity, and the paradoxical decrease of TRH mRNA synthesis seems to be determined by tanycytic D2 activity. Therefore, the paradoxical TRH feedback during illness and infection has revealed an independent local feedback mechanism in which tanycytes are a key component (Lechan & Fekete, 2004). Some studies have suggested that in this local feedback mechanism, tanycytes uptake T4 from the CSF or blood vessels of the ME through thyroid transporters Monocarboxylate transporter 8 (MCT8) and Organic anion transporter polypeptide 4C1 (OATP1C1), convert it to T3 and transport back to the blood stream, to the ME, the CSF and to ArcN neurons. Locally produced T3 affects excitability of Pro-opiomelanocortin (POMC) and Neuropeptide Y (NPY) neurons in the

ArcN, which then reach PVN neurons through the monosynaptic connection between ArcN and PVN or through retrograde transport (Fliers, Unmehopa, & Alkemade, 2006; Herwig, Ross, Nilaweera, Morgan, & Barrett, 2008).

In addition to fasting and infection, another stimulus that is able to affect D2 expression in tanycytes is the length of daylight exposure (Mohacsik et al., 2011). It has been demonstrated that D2 mRNA expression, and as a consequence T3 production by hypothalamic tanycytes, is influenced by light, with consequences in the reproductive behavior of birds (e.g. Japanese quail). Nakao et al. have shown that Japanese quail show circannual changes in TSH synthesis in the PT as a result of changes in T3 synthesis in β2 tanycytes induced by seasonal day length variation. The first wave of gene expression changes in response to long-day conditions consisted of an increase in the TSH receptor β subunit (TSHβR) mRNA in the PT, followed by an increase in tanycytic D2 mRNA expression. These expression changes correlated with a peak in LH leading to gonadal growth. These suggested that TSH was triggering photoinduced gene expression changes in both tanycytes and PT cells which initiated reproductive behaviors. Indeed, i.c.v injection of TSH in short-day conditions induced increase of TSHβR in PT and D2 mRNA in tanycytes as well as gonadal growth that was indistinguishable from those in long-day conditions. These findings suggested a connection between photoperiodic changes in TSH and GnRH release into to portal circulation, which seems to be mediated by tanycytes (Nakao et al., 2008).

In summary, fasting and LPS injection in mice have revealed a local thyroid hormone feedback mediated by tanycytes, which although both interesting and highly probable, is currently still speculative. Experiments that include specific elimination of

tanycytes coupled to fasting or infection, followed by measurement of changes in ArcN and PVN neuronal excitability and TRH mRNA production, are necessary to confirm these assumptions. Furthermore, tanycytes seem to be the cellular mediator of the interaction between the HPT and the HPG axis during changes in daylight length. Specific elimination of tanycytes would help to confirm and further understand this interaction.

1.2.3.3. Extracellular degradation of TRH

Another level of regulation of the HPT axis mediated by tanycytes takes place in the β tanycytes process located in the external layer of the ME. β tanycytes express pyroglutamyl peptidase II (PPII, EC 3.4.19.6) mRNA, which encodes a highly specific membrane-bound metallopeptidase that inactivates TRH in the extracellular space (Charli et al., 1998). Sanchez et al. have shown that PPII protein is abundant in the terminals of β tanycytes of the rat ME, and that it co-localizes with the tanycyte marker vimentin which is expressed in tanycyte processes. They also found that PPII mRNA levels increased in response to T4 injection and that T4 induced an 80% increase of PPII enzymatic activity in β tanycytes. Moreover, the increase in PPII mRNA and in PPII enzymatic activity induced by T4 was associated with lower levels of circulating TSH, indicating that there was a reduction in the availability of TRH protein. These findings suggest that tanycytes participate in the classical feedback regulation of TSH secretion by the anterior pituitary through a PPII-mediated degradation of TRH in the ME. This was supported by their *in vivo* and *in vitro* PPII inhibition experiments. In those experiments the authors showed that i.p, injection of a specific PPII inhibitor into rats that had high TRH levels due to i.p. TRH injection or cold-stress led to high TSH levels in plasma.

Furthermore, *in vitro* application of another PPII inhibitor N-1-carboxy-2-phenylethyl (Nim-benzyl)-histidyl-βNA (CPHNA) increased TRH recovery from ME cultures compared to vehicle treated cultures (Sanchez et al., 2009).

Taking in account that, first, TSH secretion from pituitary depends on TRH secretion at the ME, and second, that TRH availability in the ME depends on TRH synthesis in the PVN and on PPII degradation by β tanycytes, Marsili et al. compared PPII mRNA levels in tanycytes with TRH mRNA levels in the PVN to determine the chronology of these two events necessary for the regulation of TSH secretion. The authors found an increase in PPII mRNA in β tanycytes 5h after injection of T3 in D2 knock-out (KO) hypothyroid mice, and no change in TRH mRNA in the PVN. These suggested that PPII mediated degradation of TRH occurs more rapidly than the reduction of TRH synthesis by the PVN neurons (Marsili et al., 2011). However, as these experiments were conducted in D2 KO mice, in which T3 is not produced from T4 in any cells including tanycytes, it remains unclear if the level of T3 locally produced by tanycytes is sufficient to regulate PPII activity.

This finding, along with the thyroid hormone synthesis findings described in the previous section, suggest that tanycytes might regulate the HPT axis at two levels. Firstly, tanycytes may regulate TRH mRNA synthesis in the PVN neurons and secondly, by degrading TRH protein in the ME. Between them, the PPII-mediated degradation of TRH seems to be a faster response. However, experiments addressing the specific role of tanycytes in the regulation of the TRH axis, such as mouse models in which tanycytes are selectively eliminated, are necessary to confirm the assumptions described above.

1.2.4. Neurogenesis

Another possible tanycyte function is that of neurogenesis. Low to moderate levels of hypothalamic neurogenesis have been reported in response to growth factors including BDNF (Pencea, Bingaman, Wiegand, & Luskin, 2001; Mohacsik et al., 2011), CNTF (Kokoeva, M. V (Kokoeva, Yin, & Flier, 2005), bFGF (Xu et al., 2005), and IGF-1 (Perez-Martin et al., 2010). The cellular source of hypothalamic neurogenesis is unknown, but some evidence suggests that tanycytes might be involved. Tanycytes share morphological, spatial and molecular characteristics with neural progenitors (Rodriguez et al., 2005). These characteristic include i) radial glia-like morphology, ii) location in the epithelia of a cerebral ventricle, iii) expression of radial glia and astrocytic markers (GFAP, GLAST, Nestin), and iv) expression of progenitor related genes such as Rax, Notch1 and its canonical targets Hes1 and Hes5 (Lee et al., 2012). In fact, we have recently shown that β2 tanycytes proliferate in postnatal and in adult mice forming the hypothalamic proliferative zone (HPZ) and that these tanycytes can differentiate into neurons. Furthermore, the ability of tanycytes to give rise to neurons is increased by a high fat diet. Interestingly, elimination of tanycyte proliferation by focal irradiation abolished the body weight changes induced by a high fat diet and increased oxygen consumption, energy expenditure and total activity, suggesting an increased metabolic rate (Lee et al., 2012).

One way to interpret the metabolic changes observed after irradiation is that the newly form neurons are inducing reduction of metabolic rate in order to increase energy storage (Lee et al., 2012). As an alternative, the metabolic changes might have originated from changes in ArcN and/or α2 tanycyte proliferation. This is supported by the finding

that α2 tanycytes can proliferate in response to IGF-1 (Perez-Martin et al., 2010) and that neurogenesis and proliferation in the ArcN have been reported (Kokoeva et al., 2005). Interestingly, proliferation in the hypothalamus is better appreciated when BrdU is injected i.c.v instead of i.p due to increased accessibility to the brain (Cifuentes et al., 2011). We observed an almost complete absence of ArcN or α2 tanycyte proliferation in our study (Lee et al., 2012), perhaps due to the use of i.p BrdU delivery. If it is assumed that only β2 tanycytes proliferate, focal irradiation would have affected only that cell population; however, since there are proliferating cells in the ArcN and the entire ArcN received irradiation, it is possible that the metabolic changes are in part mediated by damage induced to α2 tanycytes and/or to the adjacent ArcN; a well established hypothalamic nucleus required for the maintenance of the energy balance to which neurogenesis has being linked (Kokoeva et al., 2005).

Furthermore, taking in account that tanycytes are the major source of T3 in the brain, and that β2 tanycytes express high levels of D2 (Guadano-Ferraz et al., 1997; Tu et al., 1997) it is likely that when β2 tanycytes were irradiated T3 production was disrupted and as a consequence, the metabolic changes resulting from irradiation can not only be attributed to blocking ME neurogenesis but also to a dysregulation of the HPT axis.

In summary, compelling information implicates tanycytes as a source of hypothalamic neurogenesis with important implications in the regulation of energy balance. However, it is necessary to develop more specific methods of tanycyte elimination in order to reveal the role of tanycyte-mediated neurogenesis in controlling energy balance and other hypothalamic functions.

1.2.5. Axonal regeneration

The robust regenerative capacity of the neurohypophysial system in adult mammals has been known for decades (Dellmann, Lue, & Bellin, 1987). It is believed that the ability of this region to regenerate is mainly due to the presence of tanycytes. *In vivo* and *in vitro* studies have explored the ability of tanycytes to promote axonal regeneration. *In vivo* studies have shown that when the ME is surgically lesioned and magnocellular axons are transected, vasopressinergic (VP) and especially oxytocinergic (OT) axons regenerate toward the external layer of the ME that projects toward the perivascular region in close association with tanycytic processes (Chauvet, Parmentier, & Alonso, 1995). Furthermore, tanycytes promote regeneration of different types of axons such as catecolaminergic (CA) and serotoninergic (SE). This regeneration is only observed in catecolaminergic and serotoninergic axons located in the VMH where tanycytes are present (Chauvet, Prieto, & Alonso, 1998). Also, cultures grafted in spinal cords support regeneration of descending afferent axons (Prieto, Chauvet, & Alonso, 2000). Moreover, it has been shown that *in vitro* survival and neurite outgrowth of several types of neurons improves significantly when neurons are co-cultured with ME tanycytes (Chauvet, Privat, & Alonso, 1996).

Despite all this compelling information, the mechanism by which tanycytes promote axonal regeneration remains a topic of controversy. It is widely accepted that the failure of the CNS to regenerate is mainly because the intrinsic ability of the axon to regenerate is inhibited by the microenviroment surrounding the injured axons. This environment consist of reactive astrocytes and their secreted proteoglycans (glial scar), as well as oligodendrocytes and degenerating myelin (myelin inhibitors) (Selzer, 2003).

Chauvet et al. have suggested that tanycytes provide a permissive environment for axonal regeneration by modifying properties of reactive astrocytes, and as a consequence disrupts the formation of glial scar (Chauvet et al., 1995; Prieto et al., 2000). Other investigators have explored the possibility that tanycytes secrete growth factors (Givalois, Arancibia, Alonso, & Tapia-Arancibia, 2004). In contrast, Villar M. J. et al. have hypothesized that the selective survival and regeneration of OT axons depends on injury-induced gene expression changes in these axons instead of it being a tanycyte-mediated process (Villar et al., 1994). Collectively, these data suggest that tanycytes may promote not only regeneration of axons *in vivo* and *in vitro* but also support neuronal survival. However, more experiments are necessary to reveal the tanycyte mediated mechanism involved in these processes.

In conclusion, tanycytes represent an intriguing hypothalamic cell population that can be considered an essential integrator of stimuli in the hypothalamus. Tanycytes can detect changes in glucose, light, lipids, growth factors and hormones, and respond by proliferating and differentiating into neurons, by absorbing, synthesizing and secreting a variety of molecules, as well as by undergoing plastic morphological changes and supporting regeneration. As a result tanycytes are able to regulate the activity of adjacent and distal hypothalamic neurons, leading to changes in hypothalamic functions such as reproduction and energy balance. Despite advances in the understanding of tanycyte function in the hypothalamus, precise experimental models that allow direct observation of tanycyte function *in vivo* are still necessary to confirm their role in hypothalamic function, and to reveal as yet unknown tanycyte-mediated functions.

1.3. Hypothalamic tanycyte development

The hypothalamus develops from the ventral diencephalon under the direction of morphogens such as sonic hedgehog (Shh) and Wnt which are required to determine the ventrodorsal and rostrocaudal patterning of the neuroepithelium, and to direct diencephalic progenitors to their hypothalamic fate (Kapsimali, Caneparo, Houart, & Wilson, 2004; Ohyama, Das, & Placzek, 2008). In addition, several dynamically expressed transcription factors, acting both independently or by interacting with each other, regulate the development of the different hypothalamic nuclei in a way that is still unclear. (Shimogori et al., 2010; Blackshaw et al., 2010).

In the mouse hypothalamus, neurogenesis occurs between E10 to E16 in an inside-out sequence, such that the most lateral nuclei are generated first while the more medial nuclei are generated last. As a result, for example, the neurons of the lateral hypothalamus (LH) are generated earlier than the neurons of the ArcN (Markakis, 2002). By E15, hypothalamic nuclei can be distinguished and gliogenesis only starts after neurogenesis is completed (Byerly & Blackshaw, 2009). In contrast, there is virtually no information about cytogenesis of the hypothalamic ventricular glia , ependymal cells and tanycytes, in the mouse. An early study reported that tanycytes can be found first in the mouse embryo at E17 (de, Picart, Jacque, & Tixier-Vidal, 1981). Most studies of tanycyte and ependymal birthdating have being performed in the rat using ^{3}H-thymidine. These studies have reported that ependymogenesis occurs between E14 and E19 from a caudal to rostral direction along the neural tube, with the pick of ependymal cell generation in the hypothalamic third ventricle occurring at E17 and E18 (Altman & Bayer, 1978; Rutzel & Schiebler, 1980; Hajos & Basco, 1984). On the other hand,

tanycytes start forming at the very end of embryonic development (E19) apparently from local radial glia (Rutzel & Schiebler, 1980; Hajos & Basco, 1984) and continue to be generated during the first and second postnatal week (Altman & Bayer, 1978). Based on cytological, histochemical and ultrastructural criteria, tanycytes reach their complete morphological and functional maturity during the first month of life (Monroe & Paull, 1974; Altman & Bayer, 1978; Walsh, Brawer, & Lin, 1978; Rutzel & Schiebler, 1980; Seress, 1980). However, the terminal differentiation of tanycytes seems to vary among different subtypes. It has being shown that ventral tanycytes (α2 tanycytes) acquire adult morphology as early as the first postnatal week, and the most dorsal tanycytes (α1 tanycytes) need longer to mature (Walsh et al., 1978). Interestingly, a more recent study, that incidentally refers to tanycyte generation in the mouse hypothalamus, reported that some tanycytes of the median eminence might be originated as early as E8.5 from midline Shh^{+} progenitors which were labeled using a genetic inducible fate mapping strategy (Alvarez-Bolado, Paul, & Blaess, 2012).

In addition to this incidental finding, virtually nothing is known about cell autonomous and non-cell autonomous factors involved in tanycyte development. Understanding the transcriptional control of tanycyte development will shed light not only on the role of tanycytes in the development of the hypothalamus, but will also contribute to the generation of tools that allow the full characterization of tanycyte functions beyond descriptive observations.

Figure 1.1.

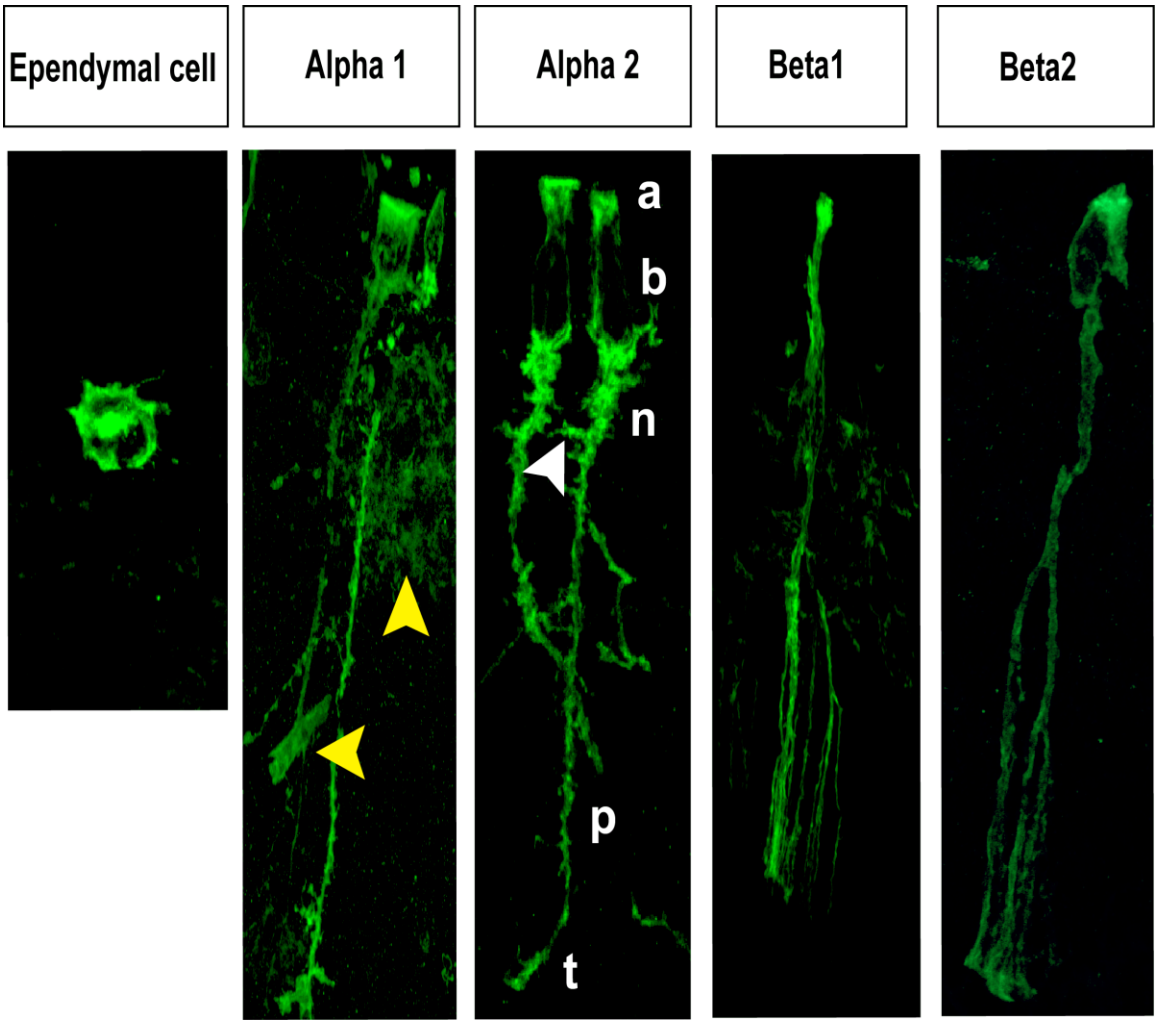

Figure 1.1. Tanycytes and ependymal cells morphology
Nestin:CreERT2$^{/+}$, TdTomEGFP$^{/+}$ adult mice (P45) stained for GFP. Ependymal cells do not have a process. Tanycytes have a long cell process sometimes associated with blood vessels and astrocytes (yellow arrow heads). Characteristic α2 tanycyte morphology: (a) apical surface facing the third ventricle, (b) elongated cell body, (n) neck with abundant spines (white arrow head), (p) process, (t) terminal, β tanycytes have ramified terminals.

Figure 1.2.

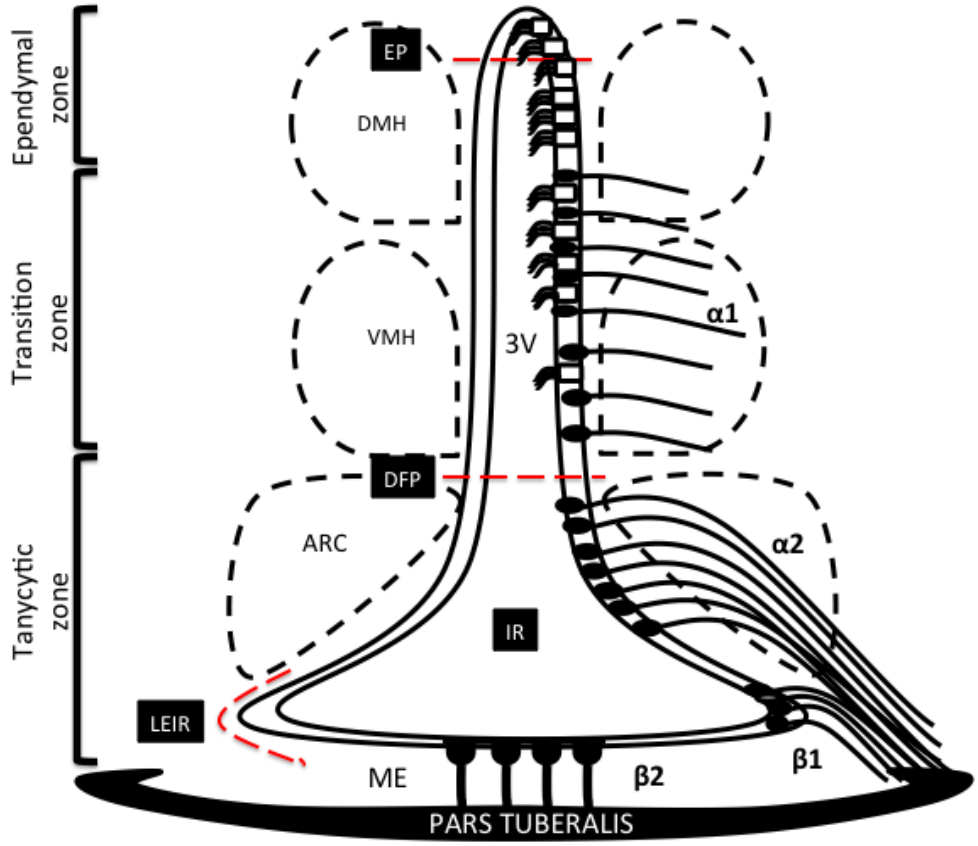

Figure 1.2. Schematic representation of the distribution of tanycytes and ependymal cells in the hypothalamic third ventricular wall
The third ventricular wall of the medial hypothalamus is composed of two types of cells, ependymal cells and tanycytes. Tanycytes are more abundant ventrally and have a cell body facing the ventricle and a process projecting to the adjacent hypothalamic nuclei. Ependymal cells do not have a process and are more abundant dorsally. There are three zones along the wall: i) the **tanycytic zone**, which is composed almost exclusively by tanycytes, the ii) **transition zone**, which contains tanycytes and ependymal cells and the iii) **ependymal zone**, which is composed only by ependymal cells (EP). There are four kind of tanycytes; beta 2 (β2) tanycytes located at the floor of the infundibular recess (IR) and whose processes project to the medial portion of the median eminence (ME). Beta 1 tanycytes (β1) are located in the lateral evaginations of the infundibular recess (LEIR) and whose processes project to the lateral portion of the ME. The alpha 2 tanycytes (α2) are located ventral to the point where the third ventricle starts opening to form the IR, we named this reference point the deflection point (DFP). Finally, the alpha 1 (α1) tancyytes which are located in the transition zone dorsal to the DFP and ventral to the EP.

Table 1.1. Best characterized markers of hypothalamic tanycytes and ependymal cells

Protein name	Symbol	Cell
Glial high affinity glutamate transporter	GLT-1	α1 and α2 tanycytes
Glutamate/aspartate transporter	GLAST	β1 and β2 tanycytes
Glucose transporter type 1	GLUT-1	α1, α2 and β1 tanycytes
Glucose transporter type 2	GLUT-2	α1, α2 and β1 tanycytes
Vimentin	Vim	Tanycytes and ependyma
Alpha-detyrosinated tubulin	Glu-tub	Ependymal cells [*1]
Nestin	Nes	Tanycytes and ependyma
Glial fibrillary acidic protein	GFAP	Tanycytes
G protein-coupled receptor 50	GPR50	Tanycytes[*2]
Forkhead box J1	Foxj1	Ependyma

*1 Also labels tanycytes single cilia

*2 Also present in a population of DMH neurons

Table 1.2. Functions attributed to tanycytes

Functions	Tanycytes	References
Endocitosis		Rodríguez *et al.* 2005 (review)
Transcytosis of IGF-1	α and β	Dueñas *et al.* 1994, Fernandez-Galaz *et al.* 1997, Cardona-Gómez *et al.* 2000
Barrier	β1 and β2	Rodríguez *et al.* 2010 (review)
Neurogenesis	β2, α?	Xu, Y. *et al.* 2005, Pérez-Martín M. *et al.* 2010, Lee D. *et al.* 2010,
Promote axonal regeneration	β2	Chauvet N. *et al.* 1995, 1996,1998, Prieto M. *et al.* 2000
Glucosensing	α and β	Sanders NM. *et al.* 2004, Orellana JA. *et al.* 2011, Frayling *et al.* 2011
Regulation of HPT axis	α2 and β	Lechan RM. and Fekete C. 2004, Sanchez E. *et al.* 2009,Marsili A. *et al.* 2011
Regulation of HPG axis	β	Prevot V. *et al.* 1999, Yamamura T. *et al.* 2004, Kozlowski GP. *et al.* 1986

HPT: hypothalamus–pituitary–thyroid axis

HPG: hypothalamius-pituitary-gonad axis

1.4. Main objectives of this thesis

In this thesis we studied the role of the retina and anterior neural fold homeobox transcription factor (Rax) in tanycyte development. First, we characterized Rax expression in the hypothalamus and we found that Rax was expressed in developing and terminally differentiated tanycytes and in cells of unknown identity within the median eminence **(Chapter 2)**. Then, we analyzed the cellular phenotype of the Rax haploinsuficient which revealed that these mice had a thinner ventricular wall suggesting that Rax was required for tanycyte and ependymal cell progenitor proliferation. We also found that there was an ectopic presence of ependymal cells in the α2 tanycytic zone indicating that Rax was required for α2 tanycyte cell fate specification **(Chapter 3)**. To determine if changes in the composition of the ventricular wall of Rax haploinsuficient mice could disrupt the proper function of the CSF-brain barrier, we injected the Evans Blue tracer in their ventricles and found that there was a reduced diffusion from the ventricle to the distal hypothalamic parenchyma **(Chapter 4)**. To begin deciphering the function of Rax in terminally differentiated tanycytes, we characterized Rax protein (RAX) distribution in the hypothalamus and we found that RAX protein was present not only in α and β tanycytes but also in hypothalamic cells which do not have the Rax transcript including; ependymal cells, adjacent parenchymal cells and neurons in the lateral hypothalamic area (LHA) suggesting that Rax was secreted and internalized by cells adjacent and distal to α tanycytes. Also we found that in the median eminence, RAX protein was synthesized in β tanycyte cell bodies and processes and that it was secreted in the most external layer of the median eminence from where it might diffuse to more internal layers. RAX protein secretion was further supported by the presence of a

conserved secretion and internalization sequence within the RAX homeodomain region and by the demonstration of RAX protein secretion *in vitro* **(Chapter 5)**. In Chapter 5 we also described our attempt to eliminate Rax in terminally differentiated tanycytes. Finally, since Rax heterozygouos mice had a normal phenotype and Rax mRNA was expressed in developing and terminally differentiated hypothalamic tanycytes, we generated the inducible Rax:CreER^{T2} mouse line to study hypothalamic tanycyte development and function **(Chapter 6)**.

1.5. Disclosures

All experiments were designed and conducted under the supervision of my thesis advisor Dr. Seth Blackshaw. The transcription factor expression data in developing and mature tanycytes was extracted from the published genomic atlas of mouse hypothalamic development in whose generation I participated together with other members of the Blackshaw laboratory in collaboration with Dr. Tomomi Shimogori of the RINKEN-BSI in Japan (**Chapter 1**, Figure 2.1 A,B, Table 2.1).

Recombineering experiments for the generation of Rax:CreER$^{T2/+}$ and Rax:lox-EGFP-stop-lox-DTa constructs were performed with assistance from Caitlin Engelhard in David Ginty´s laboratory at the Johns Hopkins School of Medicine.

Dr. Mardi Byerly from Dr. William Wong's laboratory at the Johns Hopkins School of Medicine performed the intracerebroventricular (i.c.v) injections of Evans Blue for the evaluation of the CSF-brain barrier integrity (**Chapter 4**, Figure 4.1) and the AVV1 i.c.v injections in mice used in **Chapter 5**.

Dr. Jin Woo Kim from KAIST, in Korea, performed the Rax *in vitro* secretion experiments and analysis (**Chapter 5**, Figure 5.13).

The Johns Hopkins Transgenic core facility performed the ES cell electroporations, ES pronuclear injections, karyotyping and generation of Rax:CreER^{T2} mouse chimeras. Also, they performed all ES cell electroporations of Rax:lox-EGFP-stop-lox-DTa.

Seth Blackshaw´s Laboratory technician, Hong Wang, performed all the mouse genotyping, ES cell genotyping and Southern blots. Laboratory technician Thomas Pak, carried out the mouse breeding to generate Rax:CreER$^{T2/+}$; Ai9tdTomato$^{/+}$ mice. He also performed all the tissue preparation, immunohistochemical staining and imaging of these mice for the spatiotemporal characterization of Rax:CreER^{T2} activity in the brain (**Chapter 6**, Figures 6.2,6.3,6.4).

Dr. Jimmy de Melo in Dr. Seth Blackshaw´s laboratory, performed tissue preparation, immunhistochemical staning and imagining of retinas from Rax:CreER^{T2}, Ai9tdTomato$^{/+}$ mice (**Chapter 6**, Figure 6.5).

Chapter 2

Characterization of Rax gene expression in embryonic and adult murine hypothalamus

2.1. Introduction

The retinal and anterior fold homeobox gene (Rax) encodes a homeobox TF which is expressed in both the hypothalamus and the retina. Rax expression is required for the formation of the eye field and ventral forebrain (Mathers, Grinberg, Mahon, & Jamrich, 1997). Rax expression can be weakly detected as early as E7.5 in the anterior neural plate of the developing mouse brain, with strong expression by E8.5. By E10.5 Rax expression becomes restricted to the optic vesicle and ventral forebrain with further expression identifiable in the posterior pituitary by E12.5. Ultimately, retinal Rax expression becomes restricted to photoreceptors and Müller glia by postnatal day (P)6.5. Rax expression declines with time in the retina, with Rax expression levels becoming undetectable by P13.5 (Furukawa, Kozak, & Cepko, 1997; Mathers et al., 1997).. In contrast, strong Rax expression persists in the hypothalamus and in the posterior pituitary throughout adulthood (Asbreuk, van Schaick, Cox, Smidt, & Burbach, 2002; Medina-Martinez et al., 2009). In 2008, Osakada et al. inserted GFP into the Rax locus generating the RaxKI mouse line (Osakada et al., 2008). *In vitro* studies of these mice have shown that Rax^+ GFP^+ ES cells from pituitary can form a functional gland (Suga et al., 2011), retinal Rax^+ GFP^+ ES cells can form a complete retina (Eiraku et al., 2011), and Rax^+ GFP^+ ES cell-derived neuroectodermal cells can give rise to VMH and ArcN neurons (Wataya et al., 2008). These studies highlight the essential role of Rax in

neurogenesis and gliogenesis of components of the neuroendocrine system and confirm its known fundamental role in retina development.

The retina and hypothalamus are derived from adjacent regions in the developing ventral diencephalon, and then diverge in cell type and organization (Byerly & Blackshaw, 2009). However, the retina and hypothalamus feature two cell types that share common characteristics; Müller glia and tanycytes. Müller glia (MG) are the specialized glia cells in the mouse retina, whereas tanycytes are the specialized glia cells in the hypothalamus. Tanycytes and MG are morphologically similar and are required for the proper function of the hypothalamus and retina, respectively (Liu & Rao, 2004; Bringmann & Wiedemann, 2012; Rodriguez et al., 2005). MG extends their processes throughout the entire thickness of the retina, excluding the photoreceptor outer segments. Their cell bodies are located in the retinal inner nuclear layer (INL) and project processes to the basal and apical neuroretina forming endfeet. These endfeet form the inner and outer limiting membranes which compartmentalize the neuroretina (Reichenbach et al., 1993). MG are necessary for the columnar organization of the retina; each MG envelops adjacent neuronal cells, dendrites, and axons resulting in a functional unit spanning the retina in an apical-basal column (Reichenbach et al., 1993). Also, MG interact with blood vessels as an intermediary for the metabolic exchange between blood and neurons (Reichenbach et al., 1993). Similarly, tanycytes consist of a cell body facing the third ventricle and a long single process extending toward the hypothalamic parenchyma terminating in an end foot which contacts astrocytes, blood vessels and neurons (Rodriguez et al., 2005). It is hypothesized that tanycytes contact these cell types to regulate their function, however very little data exists (see **Chapter 1**). The fundamental

role of MG and tanycytes in the proper function of the retina and hypothalamus respectively, is made evident under circumstances when these tissues are disrupted. Lesions of the retina induce reactive gliosis of MG which may act to protect the retina from further damage. Conversely, MG reactive gliosis may result in neurotoxicity in retinal neurons exacerbating damage (Bringmann et al., 2009). Interestingly, in some species MG can also respond to injury by de-differentiating and generating new neurons (Garcia & Vecino, 2003). Although a lot is known about MG response to retinal injury, little is known about how tanycytes respond to hypothalamic injury. Intracerebroventricular administration of alloxan, a GK inhibitor, induces destruction of tanycytes in the third ventricle leading to a significant reduction of food intake and altered response to glucose challenge. Interestingly, this resulting phenotype is reversed within two weeks and it was associated with the regeneration of tanycytes (Sanders et al., 2004). Also, it has being shown that tanycytes participate in axonal regeneration of vassopressinergic and oxytocinergic axons after they have being surgically transected (Chauvet et al., 1995), (see **Chapter 1**).

In addition to similarities in morphology and function; tanycytes and MG share developmental origins. They both originate from the same neuroepithelia that gives rise to the retina and hypothalamus and both are the last cell type generated during the development of these structures (Young, 1985; Byerly & Blackshaw, 2009). Although much is known about the regulation of MG development, little is known about tanycyte development.

Tanycytes start forming at the very end of embryonic development (E19) and continue their differentiation during the first postnatal week with most tancytes reaching

their complete maturity (morphological and functional) during the first month of life (Bruni, 1998; Gould, Howard, & Papadaki, 1990). Virtually nothing is known about how tanycyte cell fate specification during development is regulated. In contrast, several transcription factors (TFs) and cell surface receptors have being shown to be involved in MG development including Notch1, Hes1 and Rax (Furukawa, Mukherjee, Bao, Morrow, & Cepko, 2000). In the retina, Rax is necessary for progenitor cell proliferation, cell fate specification of embryonic photoreceptors and the differentiation of MG (Muranishi et al., 2011; Furukawa et al., 2000). Since Rax is necessary for differentiation of MG and since there are many similarities between MG and tanycytes as well as between retinal and hypothalamic development, it is possible that Rax also participates in tanycyte cell fate specification and differentiation. This is further substantiated by the fact that Rax gene expression is found in the ventral portion of the wall of the third ventricle in the developing and mature hypothalamus (Asbreuk et al., 2002; Medina-Martinez et al., 2009; Shimogori et al., 2010).

In order to better understand the role of Rax in developing and mature hypothalamic tancytes, we characterized Rax expression in the murine hypothalamus. Using *in situ* hybridization, we have found that Rax is expressed in progenitors located along the ventricular wall of the third ventricle, as well as in some neuronal progenitor cells of the ventral hypothalamus. We also showed that Rax gene expression is present from early developmental stages and persists through adulthood when its expression becomes restricted to hypothalamic tanycytes and the median eminence.

2.2. Results

2.2.1. Rax mRNA is expressed in progenitor cells of the developing hypothalamus

Through microarray analysis and high throughput *in situ* hybridization, we characterized the expression profile of genes during development of the murine hypothalamus, generating a genomic atlas for mouse hypothalamic development (Shimogori et al., 2010). As a result, we detected genes temporally regulated in different hypothalamic nuclei and specific cell subtypes including tanycytes. We were particularly interested in transcription factors expressed in the developing hypothalamus which continued to be expressed into adulthood and whose expression patterns became restricted to the wall of the ventral portion of the third ventricle, a region which corresponds to the location of terminally differentiated tanycytes. Based on these criteria, we identified nine candidate genes of interest and focused our efforts on studying Rax because of its strong and specific expression in the ventral portion of the third ventricle (Table 2.1). We then used *in situ* hybridization to characterize Rax expression in the developing and mature hypothalamus.

Rax gene expression was observed in the hypothalamic primordium at E11.5. Rax was present along the ventral lateral walls of the hypothalamic primordium and was co-expressed with Shh in a localized ventral region of the midline (Figure 2.1A). From E12.5 to E16.5 Rax, in addition to being expressed along the ventricular wall, was expressed in ventral progenitors (Figure 2.1 B). By E16.5, Rax gene expression in the hypothalamus was present along the entire wall of the third ventricle and absent from all other hypothalamic regions. From P0 through adulthood, Rax became restricted to the ventral portion of the third ventricular wall and was excluded from the dorsal portion of

the third ventricle (Figure 2.1A)

2.2.2. Rax mRNA is expressed in terminally differentiated tanycytes and is absent from mature ependymal cells

In the hypothalamus of adult mice, P30 and older, Rax gene expression was restricted to the third ventricle of the anterior, tuberal and posterior hypothalamus, along the ventral floor where the tanycytes are located (Figure 2.3). In the anterior hypothalamus, Rax was expressed as a continuous ventricular band at the floor and lateral walls of the infundibular recess (IR) (Figure 2.2A,A'). In the tuberal hypothalamus, Rax expression expanded more dorsally reaching the walls of the third ventricle adjacent to the VMH and DMH. At level of the VMH and DMH, Rax expression is discontinuous, thereby reflecting the presence of ependymal cells which do not express Rax (Figure 2.2 B, B'). Finally, in the posterior hypothalamus, Rax was strongly expressed in the ventral and lateral walls of the third ventricle but it was completely absent from the roof of the third ventricle, which is composed of ependymal cells (Figure 2.2 C, C'). Rax gene expression in the ventricular wall suggested that it was present in tanycytes. To confirm this, we performed double-label fluorescence *in situ* hybridization (double fISH) for Rax and G protein-coupled receptor 50 (Gpr50), a known tanycyte marker (Batailler *et al.* 2012), followed by immunohistrochemistry (IHC) for the neurofilament protein Vimentin (Vim). We used Vim because it is known to be expressed in the cell bodies and processes of tanycytes, as well as in the cell bodies of ependymal cells (Rodriguez et al., 2005). The double fISH demonstrated that Gpr50 expression matched the expression pattern of Rax along the ventricular wall (Figure 2.4). We also observed Gpr50 expression in the DMH as it has being previously reported (Batailler et al., 2012) but Rax

was not present in this hypothalamic nucleus. Furthermore, we found that Rax was expressed in tanycytes identified by a Vim^+ cell body extending a vimentin-positive process to the hypothalamic parenchyma. In contrast, Rax was completely absent from the ependymal cells characterized by a Vim^+ cell body lacking a process.

In the tanycytic and transition zone of the third ventricle, tanycytes and ependymal cells are closely associated and tightly packed together, which makes differentiating Rax gene expression between tanycytes and ependymal cells difficult when using only Vim staining. One way to unambiguously see the differences in Rax expression between both tanycyte and ependymal cells, would be to use a strategy that allows a mosaic expression of a reporter line in which only few tanycytes and ependymal cells are labeled. Therefore, we investigated Rax gene expression in individual cells utilizing $Rax^{+/+}$;Nestin:$CreER^{T2/+}$; tdTomatoEGFP$^{/+}$ mice. The tdTomatoEGFP reporter has loxP sites flanking a membrane-targeted td-Tomato cassette and expresses strong red fluorescence in all tissues and cell types. Cre mediated recombination allows the expression of a membrane targeted EGFP (mG) cassette, ideal for morphology visualization (Muzumdar, Tasic, Miyamichi, Li, & Luo, 2007). As a consequence, tamoxifen induction of these mice should lead to GFP expression in Nestin-positive cells. In the hypothalamus, the neurofilament protein Nestin, is selectively expressed in tanycytes (Wei et al., 2002; Lee et al., 2012) but has also being reported in ependymal cells of the third ventricle (Rodriguez et al., 2005). Furthermore, it has being reported that the Nestin:$CreER^{T2}$ line that we chose for our experiments has a mosaic expression (Balordi & Fishell, 2007).

As a consequence $Rax^{+/+}$; Nestin:$CreER^{T2/+}$; tdTomatoEGFP$^{/+}$ mice should

display mosaic expression of GFP due to the properties of the Nestin:CreER^{T2} line. Indeed, we found that 4-hydroxytamoxifen (4-OHT) induction of Rax$^{+/+}$; Nestin:CreER$^{T2/+}$; tdTomatoEGFP$^{/+}$ mice at P45, was mosaic and allowed us to clearly visualize individual GFP^{+} tanycytes and ependymal cells. Therefore, we performed Rax fISH and GFP IHC staining in these mice and demonstrated that Rax gene expression was specific to tanycyte cell bodies located in the third ventricle and it was absent from ependymal cells (Figure 2.5).

2.2.3. Rax mRNA is expressed in the floor of the third ventricle as well as in deeper median eminence layers

Using confocal imaging we observed that Rax mRNA was not only localized in cell nuclei of β tanycyes in the ependymal layer of the median eminence, but was also expressed in some cell nuclei localized in deeper layers of the ME. In addition, some Rax mRNA was not associated with any nuclei, but was associated with tanycyte processes. Interestingly, Gpr50, a tanycyte marker, showed similar expression in the ME, suggesting that some Rax^{+} nuclei in the ME parenchyma might correspond to tanycytes (Figure 2.6).

2.3. Discussion

Our data shows that Rax is expressed in progenitors located along the ventricular wall of the third ventricle, as well as some neuronal progenitors in the ventral hypothalamus. Also, we have demonstrated that Rax gene expression persisted through adulthood when its expression became restricted to hypothalamic tanycytes and to the median eminence. Rax expression in mature tanycytes was confirmed by co-localization with Vim and the tanycyte marker Gpr50 as well as by the its expression in GFP^{+}

tanycytes from tamoxifen-injected $Rax^{+/+}$; Nestin:$CreER^{T2/+}$; tdTomatoEGFP $mice^{/+}$.

Rax mRNA is expressed in progenitor cells of the developing hypothalamus

We found that Rax is expressed in the ventricular wall of the hypothalamic primordium as well as in ventral progenitors away from the ventricular wall. Since radial glia give rise to tanycytes and ependymal cells located in the ventricular zone of the developing hypothalamus (Bruni, Del Bigio, & Clattenburg, 1985; Del Bigio, 1995) and since Rax is expressed in the same region as radial glia cells during the timeframe when tanycytes and ependymal cells are being generated (E16 to E19), we propose that Rax may be participating in hypothalamic radial glia cell proliferation and in tanycyte differentiation. Also, based on the embryonic stage and location of ventral progenitors expressing Rax, it is likely that they might give rise to neurons of the retrochiasmatic nucleus, the suprachiasmatic nucleus (SCN), the VMH, the ArcN and the posteriormedial hypothalamus (PMH). Indeed, recently publihsed data suggest that Rax is required for the specification of VMH and ArcN neurons (Lu et al., 2013). However, the limitations of the cre line used in that study makes necessary to generate a more specific inducible Rax:Cre mouse line to perform prospective fate mapping of Rax progenitors to delineate the contribution of Rax to hypothalamic neuronal differentiation (see **Chapter 6**).

It has being shown that Rax null mice have lethal abnormalities of the anterior neural tube, including complete absence of hypothalamus, craniofacial defects and anophthalmia (Voronina, Kozlov, Mathers, & Lewandoski, 2005). In addition, reduction of Rax has being associated with hypothalamic abnormalities in the SCN of the eyeless inbred mouse strain ZRDCT (Tucker et al., 2001). In these mice there is a reduction in the Rax protein due to a mutation in an alternative translation initiation site (the second

ATG) of the Rax gene originating a M10L amino acid substitution, ey-1 mutation, which affects protein translation. This mutation is necessary, but not sufficient, to produce anophthlamia in the ZRDCT strain, which is in agreement with the polygenic nature of anophthalmic phenotypes (Tucker et al., 2001; Verma & Fitzpatrick, 2007). Interestingly, the ZRDCT strain has abnormalities in the SCN and circadian rhythm disturbances (Laemle & Rusa, 1992; Silver, 1977). Although the SCN abnormality in these mice may be associated with a reduction in Rax protein, it may be difficult to make a definite conclusion pertaining to Rax because it is only transiently expressed in the SCN (VanDunk (VanDunk, Hunter, & Gray, 2011). Furthermore, the ZRDCT strain might carry mutations in other genes required for retina and hypothalamus development (Tucker et al., 2001). *et al.* 2001). Unfortunately, information about additional abnormalities that involve other hypothalamic nuclei present in the ZRDCT mice is missing. The hypothalamic phenotype of Rax null and ZRDCT mice suggest that this gene is necessary for the proliferation of some neuronal hypothalamic progenitors.

In contrast to the evidence of Rax participation in the development of hypohtlamic nuclei, the role of Rax in radial glia that give rise to tanycytes and ependymal cells has not yet been explored. We will investigate this by characterizing the phenotype of Rax heterozygous mice (see **Chapter 3).**

Rax mRNA is specifically expressed in terminally differentiated tanycytes and is not expressed in mature ependymal cells.

We found that Rax is expressed in maturing and terminally differentiated tanycytes but not in mature ependymal cells, suggesting that Rax is necessary for tanycyte maturation and maintenance, but not for the same final stages of ependymal cell

development. The persistence of Rax, a TF required for retinal progenitor (RPCs) proliferation and the expression of several progenitor-specific genes, such as Lhx2, Sox9, Nestin and the members of the Notch pathway, Hes1 and Hes5 in terminally differentiated tanycytes (Shimogori et al., 2010; Lee et al., 2012), may indicate that mature tanycytes can proliferate and behave as hypothalamic neural progenitors. In fact, we have shown that mature tanycytes proliferate within a hypothalamic proliferative zone (HPZ) and that this proliferation is potentiated by a high fat diet (Lee et al., 2012). Also, we have demonstrated that postnatal β2 tanycytes not only proliferate but also give rise to neurons in the ME (Lee et al., 2012).

Although there is some literature on non-cell autonomous signals regulating tanycyte proliferation and differentiation (Xu et al., 2005; Perez-Martin et al., 2010; Lee et al., 2012) nothing is known about which cell autonomous factors regulate the progenitor potential of terminally differentiated tanycytes. To address this, we will characterize the phenotype resulting from conditional knockout of Rax in mature tanycytes, (see **Chapter 5).**

Rax is expressed within the Median Eminence.

The median eminence is a CVO which implies that there is no blood brain barrier (BBB). This allows an open communication between axons and cells located in the ME and peripheral blood. At the same time, the absence of the BBB allows for the release of hormones from the hypothalamic neurosecretory axons into the portal circulation (Rodriguez et al., 2005). The ME is composed of five layers organized from the floor of the third ventricle to the portal vessels (Ojeda, Lomniczi, & Sandau, 2008). We found that in addition to the expression of Gpr50 and Rax mRNA in β tanycytes, there was also

expression of these genes in deeper layers of the ME. Rax and Gpr50 gene expression outside the ependymal layer of the ME might correspond to displaced β tanycyte nuclei (Rodriguez et al., 1979), astrocytes, or microglia (Ojeda et al., 2008). An electron microscopy (EM) analysis of the ME reported the presence of displaced β2 tanycyte nuclei in the subependymal layer of the ME (Rodriguez et al., 1979), which is further supported by our finding that Rax^+, $Gpr50^+$ nuclei are associated with Vim in this region. However, the ME is populated by astrocytes and microglia, which also express Vim. Consequently, Vim staining alone can not differentiate between Rax and Gpr50 expression in tanycytes from gene expression in other glia cells of the ME. Therefore, only co-staining with other glia specific markers that are not expressed in tanycytes coupled to morphological characteristics for each cell type will help to solve these questions.

Finally, Rax and Gpr50 mRNA were also found in association with tanycyte processes, signifying that they might be transported and translated along their processes and in their distal segment. This is possible since tanycytes have polyribosomes located at different cell body locations, such as the cytoplasmic area projecting to the ventricle (α and β tanycytes), the spine-like protrusions present in their neck (α tanycytes) and in the distal segment of the basal process (β tanycytes) (Rodriguez et al., 2005). Transport of Rax and Gpr50 mRNA along the tanycytic process might indicate a requirement for having these proteins available in the distal segment to be secreted to the extracellular space. Interestingly, GPR50 protein is found in tanycytic cell bodies as well as in their processes and terminals (Batailler et al., 2012). Since Gpr50 mRNA and GPR50 protein are both found in the tanycyte processes this strongly suggests that this protein is

translated along the tanycyte processes. A similar situation might be happening with Rax since its mRNA is found associated with tanycyte processes. In fact, we have found that RAX protein is present in tanycyte processes of β tanycytes (See **Chapter 5).**

Taken together, the expression pattern of Rax during development suggests that Rax participates in radial glia proliferation as well as in tanycyte specification and differentiation. Also, Rax might be essential for proliferation of progenitors which give rise to several ventral hypothalamic nuclei. On the other hand, the specific expression of Rax in mature tanycytes and its TF profile enriched in progenitor-specific genes, suggests that Rax might participate in tanycyte maintenance as progenitors. However, elimination of Rax during development and in adult mice will be required to confirm these assumptions.

Finally, Rax expression in adult mice is present not only in tanycytes but also within the ME. This expression might correspond to displaced tanycytes, neurons, astrocytes or microglia which can not be discriminated with the staining used in our experiments. Future research is necessary to identify the origin of Rax gene expression in the ME as well as its functional implications.

Figure 2.1.

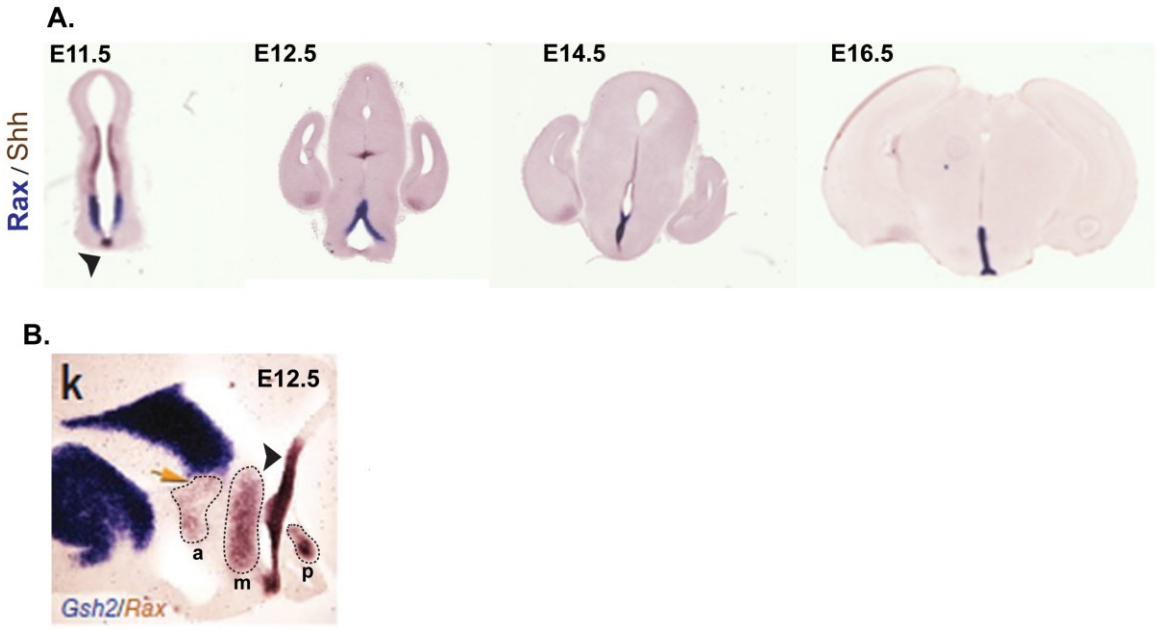

Figure 2.1. Rax mRNA expression in developing hypothalamus
A. Double chromogenic *in situ* hybridization of Rax and Shh mRNA in developing hypothalamus. Coronal sections from E11.5 to E16.5 show Rax expression restricted to the ventricular region of the hypothalamic primordium (blue). At E11.5 Shh and Rax are co-expressed in progenitors localized in the ventral midline (black arrow head).**B.** Sagital section of E12.5 developing hypothalamus double labeled for Gsh2 and Rax mRNA using chromogenic *in situ* hybridization. Gsh2 labels prethalamic progenitors whereas Rax labels hypothalamic progenitors. Both are expressed at the border of prethalamus and hypothalamus (orange arrow). Rax is not only expressed in the ventricular wall (black arrow head), but also in progenitors of the anterior (a), medial (m) and mammillary hypothalamus (p) (dotted areas). Adapted from Shimagori *et al.* 2010.

Table 2.1. Transcription factors expressed in developing as well as in terminally differentiated tanycytes

Gen name	Symbol
Hairy and enhancer of split 1	Hes1
Hairy and enhancer of split 5	Hes5
Sine oculis-related homeobox 3 homolog	Six3
Sine oculis-related homeobox 6 homolog	Six6
SRY-box containing gene 2	Sox2
SRY-box containing gene 9	Sox9
Nuclear factor I/A	Nfia
LIM homeobox protein 2	Lhx2
Retina and anterior neural fold homeobox	**Rax***

* Expressed exclusively in tanycytes

Figure 2.2.

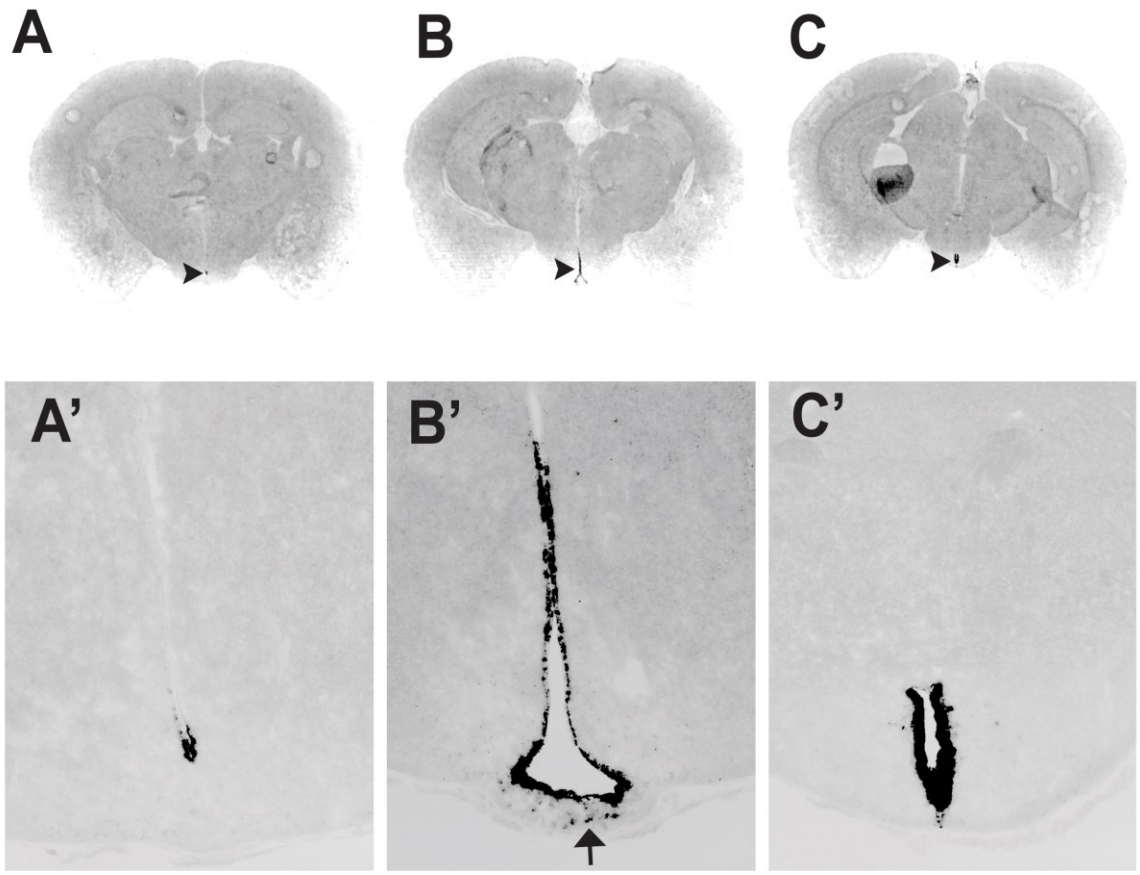

Figure 2.2. Rax mRNA expression in adult hypothalamus is restricted to the third ventricular wall.
Chromogenic *in situ* hybridization for Rax in brain sections from adult C57BL/6 wild type mice (P40). -Rax is only expressed in the third ventricle (black arrow head) of the anterior (**A, A'),** medial (**B**, **B')** and posterior **(C, C')** hypothalamus. Some expression is present in the median eminence of the medial hypothalamus (black arrow in **B'**).

Figure 2.3.

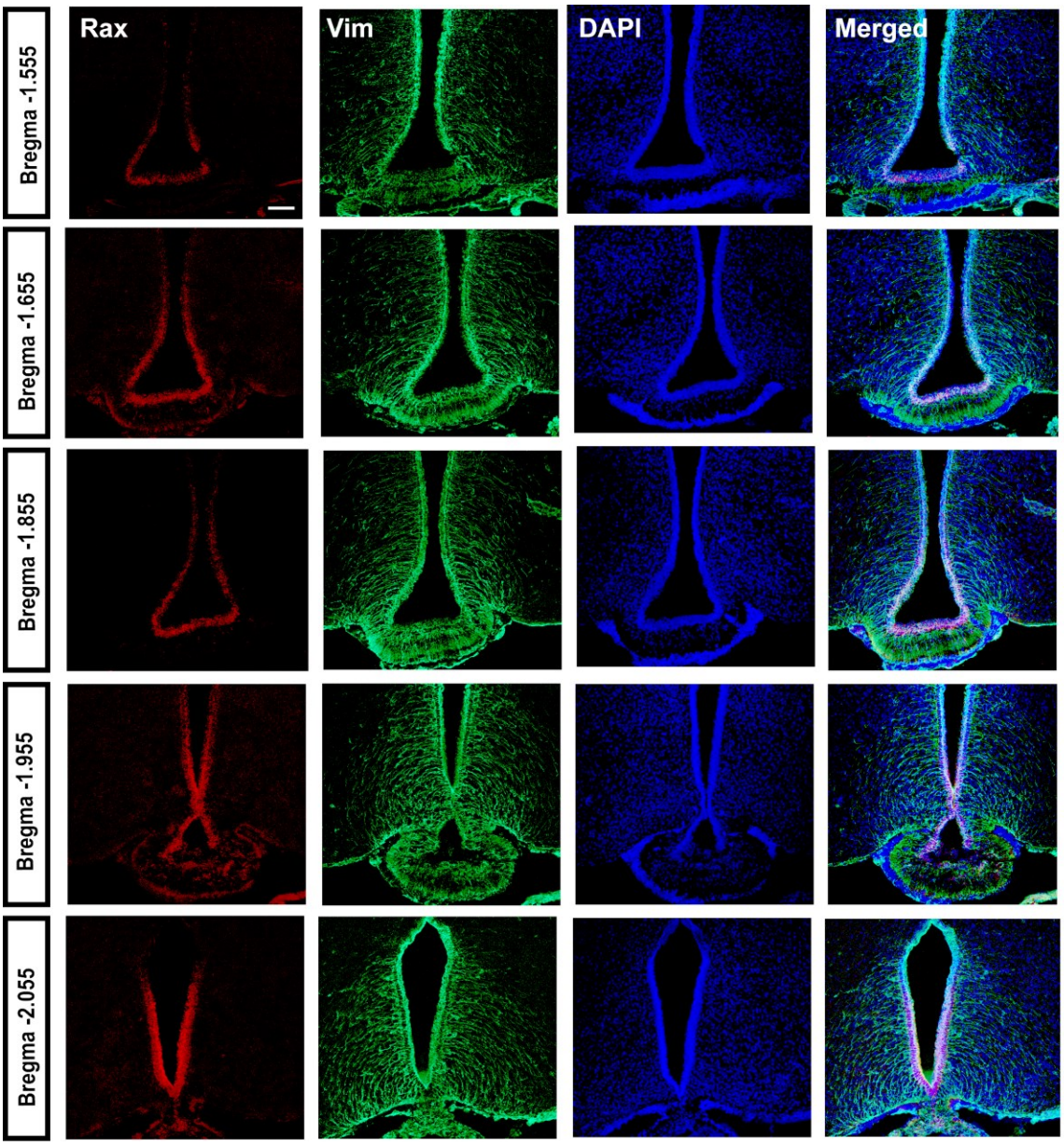

Figure 2.3. Rax mRNA and Vimentin protein expression in adult hypothalamus
Confocal *z*-stack reconstruction of Rax fluorescent *in situ* hybridization (fISH) (red) and Vimentin immunohistochemistry (IHC) (Vim) (green) of adult C57BL/6 wild type mice (P40). Rax is expressed along the anterior-posterior axis of the ventral hypothalamus and colocalizes with vimentin in the wall of the third ventricle. Scale bar: 100µm

Figure 2.4.

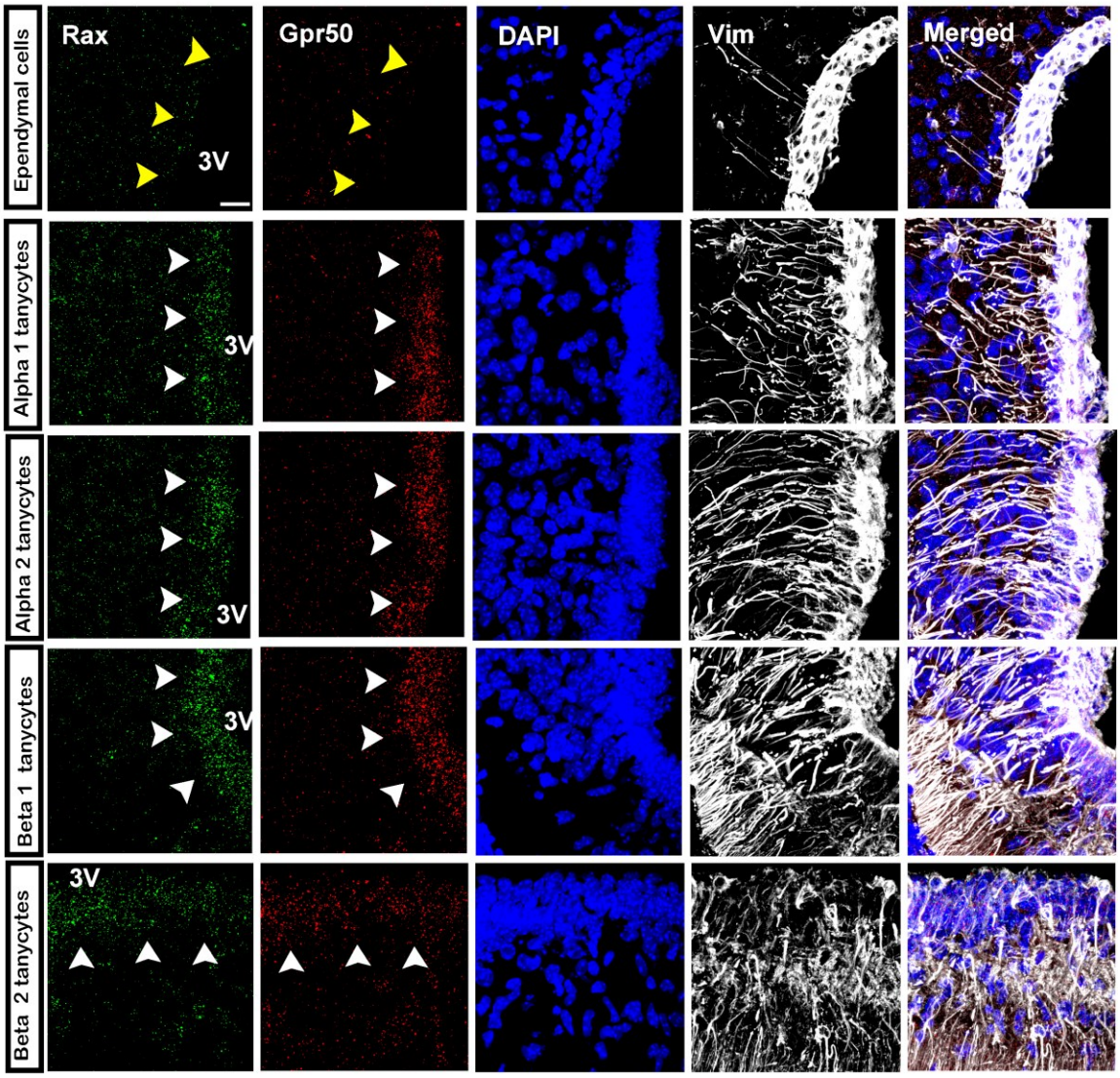

Figure 2.4. Rax is co-expressed with other tanycyte markers
Confocal *z*-stack reconstruction of double fISH for Rax (green), Gpr50 (red) mRNA and IHC for Vimentin (Vim) (white) in adult C57BL/6 wild type mice (P45). Rax and Gpr50 are expressed by tanycytes (Vim^+ cells with process, white arrow heads) and they are absent from ependymal cells (Vim^+ cells without process, yellow arrow heads). 3V: third ventricle. Scale bar: 20µm

Figure 2.5.

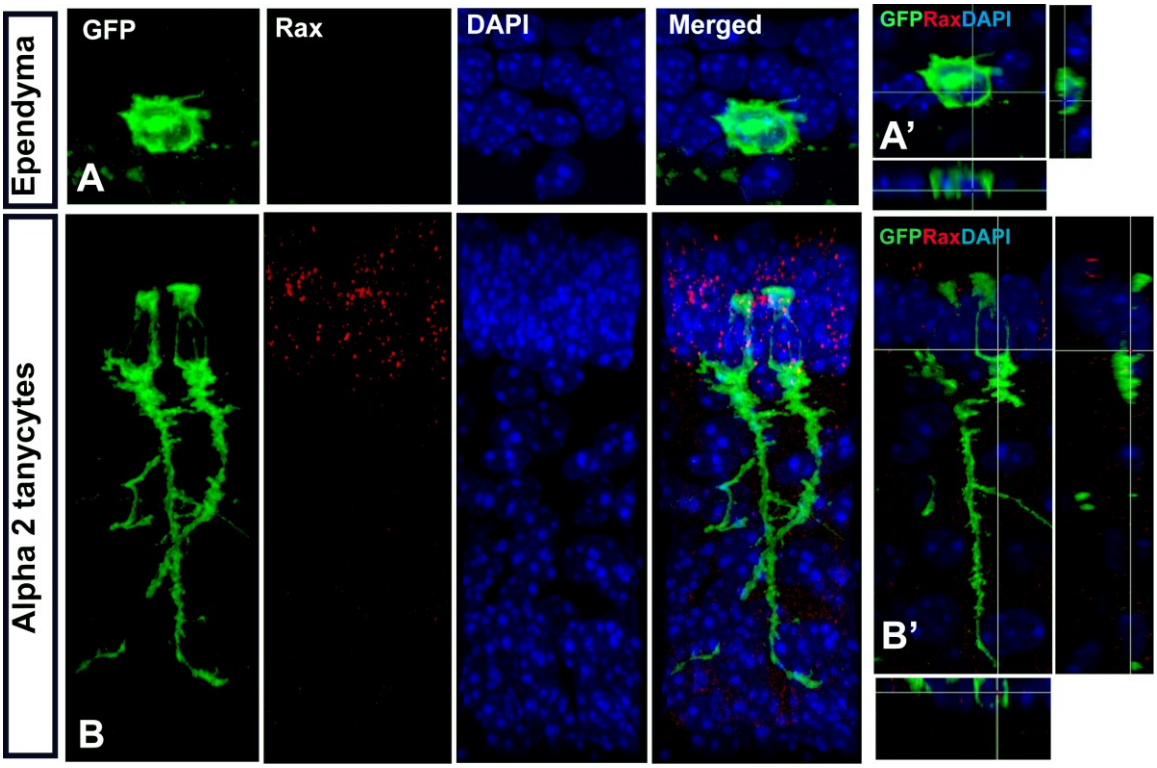

Figure 2.5. Rax is specifically expressed in tanycytes.
A,B. Rax fISH (red), GFP IHC (green) in adult $Rax^{wt/wt}$, $NestinCreERT2^{/+}$, TdTomEGFP mouse (P48). Rax is expressed in α2 tanycytes **(B)** but not in ependymal cells **(A).** **A'** and **B'** orthogonal view of merged channels in ependymal cells and α2 tanycytes (**A',B')**. Scale bar: 20μm.

Figure 2.6.

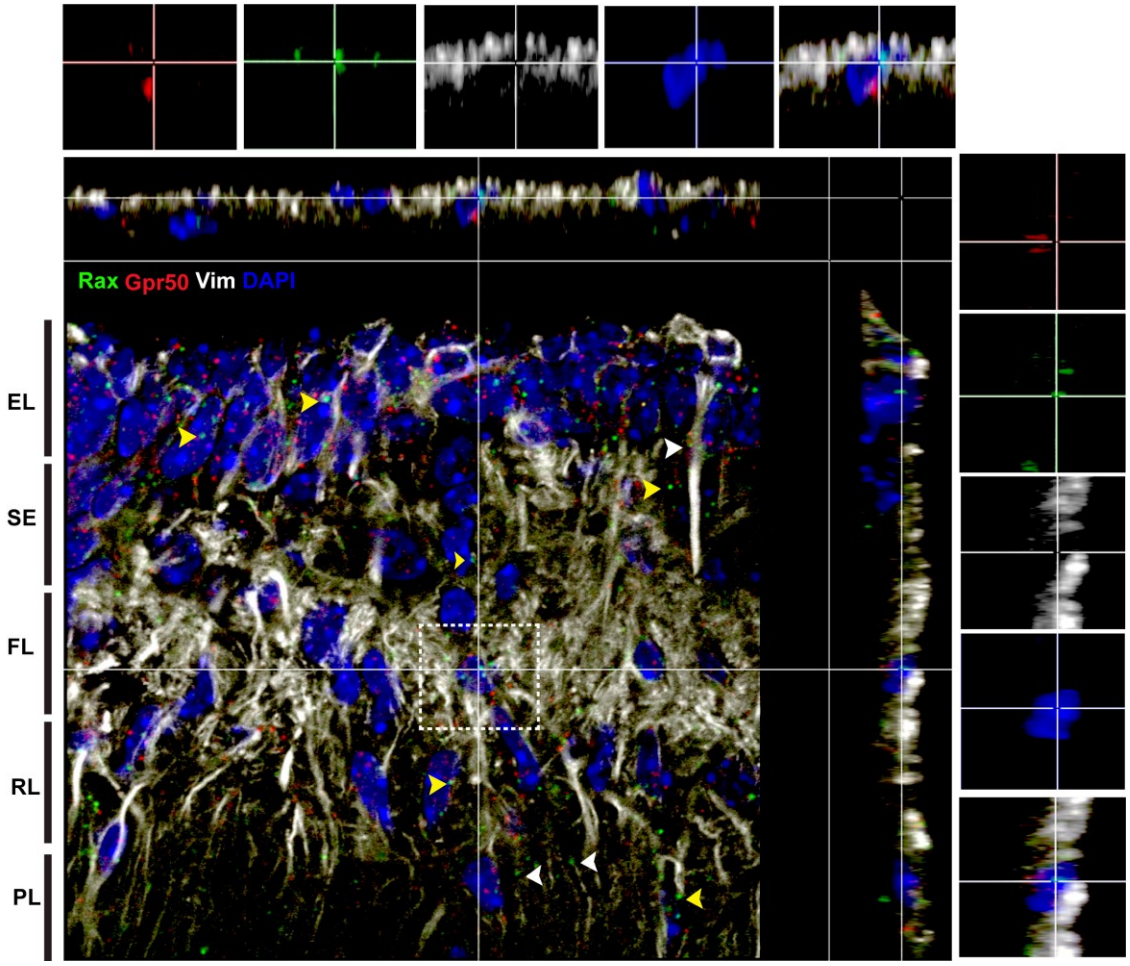

Figure 2.6. Rax is expressed within the median eminence
Orthogonal view of Rax and Gpr50 double fISH combined with Vim IHC in the median eminence (ME) of adult mouse hypothalamus. Rax is not only expressed in β tanycytes located in the ependymal layer (EL) of the ME but also in all the other layers of the ME (yellow arrows). Some Rax mRNA seems to be within tanycyte processes (white arrows). Rax^{+}, $Gpr50^{+}$ nuclei can be found in the fiber layer in close association with Vim (dashed square area). EL, Ependymal layer, SE, subependymal layer, FL, fiber layer, RL, reticular layer, PL, palisate layer.

2.4. Materials and Methods

Mice, Microarray analysis, high throughput *in situ* hybridization, high quality *in situ* hybridization and image analysis

The materials and methods used for the developmental characterization of Rax were performed as part of the previously published genomic atlas of mouse hypothalamic development (Shimogori et al., 2010).

Mice

All mice used in these studies were maintained and euthanized according to protocols approved by the Institutional Animal Care and Use Committee at the Johns Hopkins School of Medicine.

tdTomatoEGFP were obtained from Jackson lab (stock 007576). This reporter has loxP sites flanking a membrane-targeted td-Tomato cassette and expresses strong red fluorescence in all tissues and cell types. Cre mediated recombination allows the expression of membrane targeted EGFP (mG) cassette located downstream the tdTomato cassette. These mice were bred to Nestin:CreER$^{T2/+}$ to generate Rax$^{+/+}$;Nestin:CreER^{T2} ;tdTomatoEGFP mice$^{/+}$.

Six to seven week old wild type C56BL/6 and CD1 were purchased from Charles Rivers and sacrificed next day after arrival.

Tamoxifen preparation and administration

4-hydroxytamoxifen powder (4-OHT) (Sigma) was dissolved in 100% ethanol (EtOH) to a concentration of 0.1mg/ml. 4-OHT dissolved in EtOH was mixed with corn oil (sigma) in a ratio of 1:5 (4-OHT:oil). EtOH was evaporated from the mixture and 4-OHT precipitated in the oil by vacuum centrifugation and heat for 5 minutes. The oil

containing the 4-OHT was vortexed again and placed in a water sonicator for 15 minutes. Then, P45 $Rax^{+/+}$, Nestin:$CreERT2^{/+}$, tdTomato$EGFP^{/+}$ received an intraperitoneal injection (i.p) of 4-OHT daily for two consecutive days at a dose of 0.15mg/gr. Mice were sacrificed one day after the last dose (P48).

Brain tissue collection

Mice were anesthetized with 100ul of Nembutal and subjected to cardiac perfusion with 4% paraformaldehyde (4% PFA) in 1X sodium phosphate buffer (PBS 1X). Brains were extracted from the skull and immediately post-fixed in 4% PFA with rotation for 18-20 h at 4°C. Then, brains were washed in phosphate buffer 1X (PB 1X), cryoprotected in 30% sucrose for 48h, embedded in optimum cutting temperature Tissue-Tek® O.C.T. Compound, (Sakura® Finetek) and stored at -80 °C. Coronal hypothalamic free floating sections were collected by sectioning in a cryostat at 40 μm starting from the middle of the anterior hypothalamus to the end of the posterior hypothalamus. Sections were floated in RNase free PB 0.5X serially distributed in individual wells of an RNAse free 48 well plate (Falcon). Right after cutting, sections where examined under the light microscope to choose sections containing only the tuberal hypothalamus and the anterior region of the posterior hypothalamus for a total of ten to twelve sections per brain. Sections where mounted in four Superfrost Plus slides (Fisher) per brain organized as follow; alternate sections were mounted in the first group of two slides and the remaining alternate sections were mounted in the second group of two slides. Each group of two slides was used for a different *in situ* hybridization/IHC staining. Mounted sections were dried overnight at room temperature and stored at -80°C until they were used for the experiments.

Genotyping

DNA for mice genotyping was obtained from tail tips collected carefully with razor blades to avoid cross contamination. Tails were incubated at 55°C overnight in lysis solution containing proteinase K (0.1µg/ul). Rax flox and null allele were genotyped using the previously described set of primers (Voronine *et al.* 2005). Cre recombinase was genotyped using the sense primer 5'-TTCCCGCAGAACCTGAAGAT-3' and the antisense primer 5'-CCCCAGAAATGCCAGATTAC-3', GFP was genotyped using the sense primer 5'-ATGTGATCGCGCTTCTCGTTG-3' and the antisense primer 5' TGCAGTGCTTCAGCCGCTACC-3'. Cre, GFP and Rax PCR genotyping protocol was: 94°C for 5 min, 94°C for 30 sec, 55°C for 30 sec, 72°C for 1.3 min, steps 2 to 4 were repeated 30 times, 72°C for 5 min, 4°C hold.

Digoxigenin (DIG) and fluorescein probe labeling for *in situ* hybridization

Clones carrying cDNA for Rax BE951347 and Gpr50 BI28943 were amplified with T3/T7 primers using a Ready to use Taq PCR mix (Sigma). The amplified PCR product was checked for size and quality using agarose electrophoresis. Good quality PCR products were then used for generating a labeled RNA probe. Probe labeling with DIG or Fluorescein was conducted under RNAse-free conditions and using an RNA DIG labeling kit (Roche) as recommended by the manufacturer. After RNA amplification the labeling reaction was precipitated by overnight incubation with 4M lithium chloride (LiCl) and 100% EtOH. Pellets were washed with EtOH 70% and resuspended in 100 ul of 10mM EDTA, pH 8.0. Band size was checked again using agarose electrophoresis. Labeled probes were store at -80°C.

Chromogenic *in situ* hybridization

Chromogenic *in situ* hybridizations were performed following Tabin's online protocol (http://genepath.med.harvard.edu/~cepko/protocol/insituprotocol.pdf). Except that proteinase K treatment and the RNase treatment were done for 25 minutes. Also, instead of using MABT for washing before and after antibody incubation we used B1T (2M Tris pH7.5, 3M NaCl and 0.1% Tween-20).

Fluorescent *in situ* hybridization (fISH) and immunohistochemistry (IMH)

We combined our modified Tabin's protocol with the Tyramide amplification reaction (TSA) (Perkin Elmer) generating a fluorescent *in situ* hybridization (fISH) protocol as follows. Prehybridization and stringency washes were done as in Tabin's modified protocol (see previous section). Washes were followed by quenching in 3% hydrogen peroxide (H_2O_2) in PBS 1X for 30 min at RT and blocking in TNB (0.1 M Tris HCl pH7.5, 0.15 M NaCl and 0.5% w/v Blocking buffer from Perkin Elmer) 1h at RT. Anti DIG-POD was diluted in TNB 1:10000 whereas anti-Fluoresceine-POD was diluted 1:5000 and incubated overnight at 4°C in a humidified chamber. Cy3, Cy5 and Fluoresceine were prepared in a 1:50 dilution in amplification buffer provided in the kit (Perkin Elmer) and the optimal time for reaction for each probe was determine experimentally: Rax-Cy3 16-18h, Rax- fluorescein 6h, Gpr50-Cy3 and Gpr50-Cy5 1h. When a two color fISH was performed, the TSA reaction was stopped using B1T and it was followed by quenching in 1% H_2O_2 for 15 min. When single fISH was performed, the B1T washes were followed by IMH as follows: Permeabilization/blocking was performed using PBS plus solution (0.3% Triton 100X and 5% normal horse serum in 0.1M PBS 1X) for 15 minutes and followed by blocking in Superblock (ScyTek) for 5 minutes. Slides were incubated O/N at 4°C with primary antibodies prepared in

permeabilizing/blocking solution. Next day, slides were incubated with Alexa secondary antibodies in PBS plus for 2 hrs at RT at 1:500 dilution. Primary antibodies used were; chicken anti-vimentin (1:1500) from Millipore and chicken anti-GFP (1:1000) from Aves Lab. DAPI staining was performed by submerging the slides in a DAPI solution 1:5000 in PBS1X. When the staining was finished, 100ul of Vectashield hard-set Mounting Medium with DAPI (Vector laboratories) was applied to the slides and covered with a cover slip. Vectashield was allowed to dry in the dark for 1 hour and stored at 4°C until the image acquisition.

Image acquisition

Low resolution images of chromogenic *in situ* hybridization and DAPI were obtained in an axioskop 2 mot plus from Carl Zeiss equipped with an Axiovision software and using a 10X objective. *z* stack images were taken in a Zeiss LSM510 Meta confocal microscope using a 63X or 100X objective and digital zoom 0.7 or 1 and equipped with a Zen 2009 software. The landmarks used for the identification of the different tanycytes along the ventro-dorsal axis of the medial hypothalamus were the following (see Figure 1.1): Medial zone of the ME (β2 tanycytes), lateral evagination of the infundibular recess (LEIR) (β1 tanycytes), immediately ventral the deflection point (DFP) (α2 tanycytes), immediately dorsal to the DFP (α1 tanycytes), roof of the third ventricle (ependymal cells). Identification of bregma points along the anterior-posterior axis was done comparing our images with the Allen Mouse Brain Atlas (Sunkin et al., 2013) and using the shape of the ME, the lateral region of *par tuberalis* and the shape of the different hypothalamic nuclei stained with DAPI as landmarks.

Chapter 3

Rax is required for the proliferation of hypothalamic tanycytes and ependymal cell progenitors during development

3.1. Introduction

Tancytes and ependymal cells develop from radial glia (Rutzel & Schiebler, 1980; Bruni et al., 1985). Most data supports that ependymogenesis in the third ventricle of the rat occurs between E17 and E18 along a caudal to rostral trajectory in the developing brain; however maturation of ependymal cells extends until the first postnatal week (Bruni et al., 1985; Del Bigio, 1995). Tanycytes start forming after ependymal cells, at the very end of embryonic development (E19) and many are generated in the first and second postnatal week (Altman & Bayer, 1978). The majority of tanycytes do not reach complete maturity (morphological and functional) until the first month of life (Monroe & Paull, 1974; Altman & Bayer, 1978; Walsh et al., 1978; Rutzel & Schiebler, 1980; Seress, 1980). In contrast, in the mouse Shh-expressing progenitors appear in the most ventral midline of the hypothalamic primordium as early as E8.5 (Alvarez-Bolado et al., 2012). We found that Rax is expressed in the midline of the developing hypothalamus also at E8.5 and that it is co-expressed with Shh in the ventral midline of the third ventricle at E11.5 (Shimogori et al., 2010), (see **Chapter 2**). Taken together this data, suggests that Rax might interact with Shh in the proliferation of progenitors that give rise to tanycytes. Based on the expression profile of Rax during development and that the

retina and hypothalamus are derived from adjacent Rax expressing regions of the ventral diencephalon, we hypothesize that Rax will play an essential role in the developing hypothalamus. Indeed, previous studies have associated Rax deficiency with severe hypothalamic abnormalities but there is no evidence of Rax participation specifically in hypothalamic tanycyte development (Agnati, Zoli, Stromberg, & Fuxe, 1995; Voronina et al., 2005; Lu et al., 2013).

Based on the expression of Rax in the developing hypothalamus and knowing the role of Rax in the proliferation of RPCs we wanted to determine if Rax was required for the proliferation of tanycyte progenitors. Using a Rax haploinsuficient mouse, we identified a reduction of tanycytic and ependymal cell specific genes reflecting a reduction in the number of tanycytes and ependymal cells in the ventricular wall. Interestingly, in addition to the overall reduction of ependymal cells, some are ectopically located in the ventral portion of the wall of the third ventricle (α2 tanycytic zone) where ependymal cells are rarely found.

3.2. Results

3.2.1. Reduced expression of tanycytic and ependymal markers in Rax haploinsuficient mice

After the generation of Rax heterozygous ($Rax^{f/-}$) mice we confirmed the reduction of hypothalamic Rax mRNA in adult mice using image quantification and RT-PCR. Image quantification of Rax fISH signal in the α2 tancytes showed a significant reduction in Rax mRNA when compared with Rax homozygous ($Rax^{f/f}$) whose phenotype is identical to Rax wild type mice (Voronina et al., 2005) (Figure 3.1). This finding was confirmed by a two-fold reduction in Rax mRNA measured by RT-PCR

performed on hypothalamic tissue dissected from adult $Rax^{f/-}$ mice (Figure 3.2). In addition, the mRNA of other genes that are known to be expressed in developing and terminally differentiated tanycytes was significantly reduced in the $Rax^{f/-}$ as determined by RT-PCR. These genes included the Hes1, Hes5, and Gpr50 (Figure 3.2). Finally, mRNA levels of the ependymal marker forkhead box protein J1 (Foxj1) (Yu, Ng, Habacher, & Roy, 2008) were also significantly reduced in the hypothalamus of $Rax^{f/-}$ mice. In contrast, vimentin and GFAP did not show any significant difference in expression in the compared groups. Taken together, our observations showed that there is a reduction in expression of both tanycyte and ependymal markers in Rax heterozygous mice.

3.2.2. Rax haploinsuficient mice show a reduced volume of the third ventricular wall

The reduction in all tanycyte and ependymal markers of the $Rax^{f/-}$ mice suggested that Rax heterozygous mice might have fewer cells in the ventricular wall of the third ventricle. Quantification of total cell number in the walls of the third ventricle using confocal images was not possible due to the tight packing of tanycytes and ependymal cells. However, the nuclei in the ventricular layer, which correspond exclusively to tanycytes and/or ependymal cells, can be easily separated from the subventricular zone and hypothalamic parenchyma and its volume can be measured using digital analysis. We measured the volume of the wall of the third ventricle using digital quantification of confocal *z*-stack reconstruction images of DAPI staining in the ventricular layer. Using this approach we measured the volume of the cell nuclei present in the ventricular wall of the tuberal hypothalamus located at the lateral evaginantions of the infundibular recess

(LEIR) containing β1 tanycytes, the region ventral to the deflection point (DP) containing α2 tanycytes, and the ependymal zone. We found that the Rax heterozygous mice showed a significant reduction in volume. Interestingly, the region dorsal to the DP (α1 tanycytes) did not show any significant difference in volume (Figure 3.3). β2 tanycytes were not examined because most sections lose the ME during sectioning or staining. In summary, this data shows that that there is a reduction in the number of ependymal cells and α2 and β1 tanycytes in the third ventricle of Rax haploinsuficient mice.

3.2.3. Rarres2 is specifically expressed in ependymal cells

To visualize and quantify the reduction of ependymal cells with image analysis we attempted to perform IHC for Foxj1 without any success. As a consequence we used the Allen brain atlas to find other genes that were expressed exclusively in ependymal cells. This was particularly difficult because tanycytes express many genes that are commonly used to identify ependymal cells (Rodriguez et al., 2005). As a result of this search we found Rarres2 (retinoic acid receptor responder 2) which codes for chemerin, a secreted protein which functions as an adipokine, which is involved in immune response and inflammation (Ernst & Sinal, 2010). Although Rarres2 is expressed in ependymal cell of the lateral and third ventricle, nothing is known about its function on these cells. Using *in situ* hybridization we found that Rarres2 expression in the hypothalamus was restricted to the dorsal ventricular wall of the anterior, tuberal and posterior hypothalamus (Figure 3.4). Also, Rarres2 expression was absent from the ventral portion of the ventricular wall were tanycytes are located. This expression pattern matches the distribution of the ependymal cells in the third ventricle and was opposite to Rax expression which is more abundant ventrally (Figure 3.5). To confirm that Rarres2 was

expressed in ependymal cells we used the detyrosinated alpha tubulin (G-TUB) as a marker of cilia and examined the presence of Rarres2 in ciliated cells. We found that Rarres2 expression matches G-TUB expression in the anterior, medial and posterior hypothalamus (Figure 3.6A). Moreover, Rarres2 mRNA was located in the cell nuclei right beneath the multiple cilia of ependymal cells of the dorsal third ventricle (Figure 3.6B). Visualization of individual ependymal cells from $Rax^{+/+}$,$Nestin:CreER^{T2/+}$, $tdTomatoEGFP^{/+}$ demonstrated the presence of Rarres2 in ependymal cells and its absence from tanycytes (Figure 3.7). Taken together, these data suggested that we could use Rarres2 as a marker of ependymal cells to determine if there is a reduction in ependymal cells in Rax haploinsuficient mice.

3.2.4. Rax haploinsuficient mice feature a ventralization of Rarres2 expression

We quantified Rarres2 in fISH confocal images taken at the level of the α2 tanycytic zone of the tuberal hypothalamus (Bregma -1.655). Interestingly, we found that Rax haploinsuficient mice showed significatively higher levels of Rarres2 mRNA in the ventricular wall of the α2 tanycytic zone (Figure 3.8 A and B). We wanted to know if this difference persisted along the anterio-posterior axis. To do that, we measured Rarres2 expression at two other Bregma points inside the tuberal hypothalamus (Bregma -1.755 and -1.855). There was no significant difference in Rarres2 expression between the $Rax^{f/f}$ and the $Rax^{f/-}$ in the two latter Bregma points (Figure 3.8C). However, we noticed that, while not statistically significant, the Rarres2 signal at the latter two Bregma points was persistently higher in the Rax haploinsuficient mice than in the controls. We calculated the overall signal and we found that the cumulative signal including the first Bregma point was statistically increased in the $Rax^{f/-}$ mice (Figure 3.8 C). This data

shows that there is a ventralization of Rarres2 expression in Rax haploinsuficient mice, suggesting an ectopic presence of ependymal cells in the tanycytic zone.

3.2.5. Ependymal cells are found in the tanycytic zone of Rax haploinsuficient mice

To confirm the presence of ependymal cells in the tanycytic zone suggested by Rarres2 ventralization we use G-TUB which has being shown to be expressed in the cilia of ependymal cells (Mullier et al., 2010). Confocal *z*-stack visualization of G-TUB in the α2 tanycytic zone showed an increased in cilia projecting to the ventricular lumen (Figure 3.9). However, we noticed that G-TUB was present not only in the motile cilia (multiple cilia) of the ependymal cells but also in non-motile cilia (primary cilia) which can be found in some α2 tanycytes but it is more abundant in β1 and β2 tanycytes (data not shown). Primary cilia in tanycytes and motile cilia of the ependymal cells can be differentiated by their length and arrangement. Primary cilia are shorter than motile cilia, <1 μm for primary cilia and >2-8 μm for motile cilia (O'Callaghan, Sikand, & Rutman, 1999) and, more importantly for discrimination between the two, motile cilia are found in clusters whereas primary cilia are found as solitary cilia arising from the cell body (Satir & Christensen, 2007). Taking these differences in account, we quantified the clusters of cilia longer than 2 μm in the tanycytic zone of three Bregma points in each slide of our confocal *z*-stacks. We found that there was a significant increase in the number of cilia clusters in the tanycytic zone of the Rax haploinsufficient mice at each Bregma location examined (Figure 3.9). The increase of cilia clusters in the tanycytic zone confirms the ectopic presenc of ependymal cells in the α2 tantycytic zone of Rax haploinsuficient mice was previously suggested by the increase of ventral Rarres2 signal.

3.3. Discussion

In the current study we found that haploinsufficiency of Rax during development leads to a reduction of tanycytes and ependymal cells as demonstrated by the reduction of tanycyte and ependymal markers and the reduced volume of the ventricular wall. In addition, we found that Rax haploinsufficient mice have ectopic presence of ependymal cells in the α2 tanycytic zone.

Rax regulates the proliferation of tanycytes and ependymal cell progenitors

It is known that hypothalamic tanycytes and ependymal cells originate from radial glia progenitors located in the wall of the third ventricle (Rutzel & Schiebler, 1980; Bruni et al., 1985). However, the molecular factors involved in progenitor proliferation and the differentiation of progenitors giving rise to tanycytes and ependymal cells are poorly characterized. We reported that Rax haploinsufficient mice show a reduced volume of the ventricular wall. This could be due to the dose reduction of Rax during development reducing proliferation of radial progenitors similar to what is observed in RPC proliferation in Rax knockout mice (Mathers et al., 1997). Rax is very well conserved across species including human, mouse, chicken, fish and Xenopus. Inhibition of Xrx1, the *Xenopus* ortholog of Rax, results in reduced eye and brain size due to reduced proliferation (Andreazzoli et al., 2003; Casarosa et al., 2003). Terada and Furukawa have shown that Xrx1 binds to the chromatin modulator Xhmgb3 (Xenopus high mobility group 3) and to the Six family transcription factor XOptx2 (Six6) synergistically regulating cell proliferation in the eye and brain. They have also shown that Xhmgb3, binds to the SUMO E2 ligase UBC9 and inactivates transcription of the kinase inhibitor p27Xic1 promoting proliferation of retinal progenitor cells (Terada & Furukawa, 2010).

Six6 and high mobility box 2 (hmgb2), another high mobility box protein from same family of hmgb3 with a chromatin remodeling function, are expressed in the ventricular wall of the hypothalamic primordium (Shimogori et al., 2010) suggesting that Rax might be regulating the proliferation of hypothalamic ventricular radial glia through a similar mechanism. As a consequence, reduction of Rax would lead to an increase in p27 which could result in reduced proliferation. Another explanation for the reduced number of tanycytes and ependymal cells is that reduction of Rax might induce apoptosis during development and/or in terminally differentiated ependymal cells and tanycytes. One of the targets of p27 is cyclin D1 (Geng et al., 2001), cyclin D1 knockouts show a dramatic reduction in all retinal layers due to a reduction of proliferation, and display apoptosis in photoreceptors (Ma, Papermaster, & Cepko, 1998). Cyclin D1 is expressed in the developing retina and hypothalamus (Sicinski et al., 1995). Based on these data we might predict that reduction of Rax during the development of tanycytes and ependymal cells could result in the reduction of cyclinD1 due to the increase in p27, leading to apoptosis. Since we did not perform any staining in the Rax haploinsuficient mice to detect apoptosis we can not rule out this possibility.

Rax haplonsufficiency is associated with increase multiple cilia in the tanycytic zone

Under normal conditions, there are few ependymal cells in the walls of the ventral third ventricle where α2 tanycytes are located. However, we found that in Rax haploinsuficient mice there was an increase in the number of cells with motile cilia, characteristic of ependymal cells, in this region. We think there are three possible mechanisms that can explain this finding. First, the reduction in Rax expression levels during the development of the heterozygous mice could lead to reduced proliferation of

radial progenitors with premature exit from the cell cycle resulting in the formation of ectopic ependymal cells, the first cell type generated during the development of the ventricular wall. This would be in agreement with what is known about the cell fate specification of several cell types in the brain (Edlund & Jessell, 1999). However, if this were the case we would expect to observe an increase in ependymal cells throughout the hypothalamic ependymal region. It seems that this happened specifically to ventral radial glia progenitors located in the α2 tanycytic zone. It is possible that in addition to reduction in Rax dosage other cell-autonomous or cell non-autonomous signals present in the ventral developing wall could influence premature cell cycle exit promoting the generation of more ependymal cells in the ventral tanycitic zones. In this way, Rax would be necessary for tanycyte cell fate specification.

Alternatively, some ventral tanycytes with reduced Rax levels might be able to dedifferentiate and give rise to ependymal cells. For years, the possibility of tanycytes themselves behaving as neural progenitors was suggested but not demonstrated *in vivo* until we showed that postnatal β2 tanycytes give rise to neurons under basal conditions and that this is potentiated by a high fat diet (Lee et al., 2012). This highlights the ability of tanycytes to behave as progenitors under certain conditions and at specific developmental stages leaving open the possibility that they may generate other cell types including ependymal cells. The potential of tanycytes to give rise to ependymal cells has not being demonstrated, but some studies have produced some descriptive evidence of this potential. In 1990 Gould et al. using histology and electron microscopy in the developing human fetal brain found that some tanycytes of the lateral ventricles were a transitional cell type that could give rise to ependymal cells (Gould et al., 1990). The

authors proposed that this transition consists of the acquisition of multiple cilia and the degeneration of their basal process. However, the definitive developmental relationship between these two cell types requires a prospective genetic labeling analysis.

Interestingly, it has been recently shown that motile cilia can develop from single ciliated cells during the development of the airway (Jain et al., 2010). Ciliogenesis is very similar across several tissues as is demonstrated by the broad spectrum of systemic alteration found in inherited ciliopathies which, not surprisingly, includes the presence of hydrocephaly (Fliegauf, Benzing, & Omran, 2007). This opens the possibility that single ciliated cells in the brain, such as tanycytes, could develop motile cilia in response to cell-autonomous and non-cell autonomous cues similar to what happens in the airway. Two key cell-autonomous regulators of muticiliogenesis, multicilin and micro RNA 449, promote cilia formation in skin, kidney and airway act by blocking Notch signaling (Stubbs, Vladar, Axelrod, & Kintner, 2012; Marcet et al., 2011). Interestingly, components of Notch signaling are expressed the developing and mature tanycytes but not in ependymal cells (Shimogori et al., 2010).

From these studies we hypothesize that Notch signaling might be necessary for the inhibition of cilia formation in tanycytes. In the retina, Rax and Notch form a transcriptional network in which Rax is upstream Notch in the regulation of Müller glia differentiation (Furukawa et al., 2000). However, such an interaction has not being demonstrated in tanycytes. We have found some evidence suggesting that Rax is acting upstream of Notch1 in terminally differentiated tanycytes as is suggested by the reduction of Hes1 and Notch1 mRNA in Rax $^{f/-}$ mice (data not shown). Assuming that this interaction is also present during tanycyte differentiation, we propose that Rax dose

reduction might result in a reduction of Notch signaling promoting the formation of multiple cilia.

Finally, the multiple cilia observed in the tanycytic zone might correspond to a population of hybrid tanycytes with both ependymal cell and tanycyte characteristics. Hybrid tanycyte-ependyma cells were recently described in a study where the authors investigated the role of the Six3 transcription factor in the maturation of ependymal cells (Lavado & Oliver, 2011). The authors demonstrated that the conditional loss of function of Six3 during the maturation of ependymal cells gave rise to formation of cells with mixed ependymal and radial glia characteristics. Based on the location, morphology and immunoreactivity described by the authors of this paper, the postnatal radial glia likely correspond to tanycytes. The authors also concluded that in the lateral ventricles Six3 is required for the maturation of ependymal cells, when Six3 is not present, the transition from "radial glia" to ependyma was defective. Using vimentin staining, we are unable to discriminate between a tanycyte with multiple cilia or an ependymal cell located directly on top of the tanycyte cell body giving the appearance of a ciliated tanycyte. Analysis of the morphology of individual tanycytes using mice such as the Nestin:CreER$^{T2/+}$;tdTomatoEGFP$^{/+}$ and co-labeling with a cilia marker such as G-TUB would allow us to determine the existence of this hybrid tanycyte-ependymal cell in Rax haploinsuficient mice.

Ventralization of Rarres2 does not affect ArcN function

The ventralization of ependymal cells was accompanied by ventralization of Rarres2 expression in the lateral walls of the infundibular recess adjacent to the the ArcN of the Rax haploinsuficient mice. As we mentioned before, Rarres2 codes for chemerin which is

involved in inflammation and metabolism (Ernst MC (Ernst & Sinal, 2010). Since α2 tanycytes are in direct contact with ArcN neurons, it could be expeculated that an increase in chemerin in the ventricular wall of the ArcN might affect the function of this nucleus. The ArcN plays a key role in energy homeostasis through the function of two main populations of neurons: the neuropeptide Y (NPY) and Agouti related peptide (AgRP) co-expressing neurons which stimulate food intake, and the cocaine and amphetamine-regulated transcript peptide (CART) and pro-piomelanocortin (POMC) expressing neurons which inhibit food intake (Sainsbury & Zhang, 2010). There is only one study in which chemerin has been studied in the context of ArcN function (Brunetti et al., 2011). In that study chemerin and other adipokines were injected in the ArcN and the subsequent changes in the expression of feeding-related genes was evaluated as were the resulting changes in food intake. Interestingly, chemerin stimulated both orexogenic AgRP and anorexogenic POMC gene expression resulting in a null effect in food intake. Although more studies are required to support this finding, especially a characterization of chemerin receptors in the ArcN, it is in agreement with our observation of normal feeding behavior of our Rax haploinsuficient mice despite the potential increase in chemerin signaling in the ArcN.

In conclusion, we have shown that Rax reduction during development results in a decrease number of tanycytes and ependymal cells in the hypothalamic third ventricular wall probably due to a reduced radial progenitor proliferation. Also, we found that Rax haploinsuficiency induces the presence of ectopic ependymal cells in the α2 tanycytic zone which might be originated from a premature exit of tanycyte progenitors from the cell cycle and acquisition of an ependymal cell fate or it might correspond to the

induction of α2 tanycytes transdifferentiation toward an ependymal phenotype. In either case our data suggest that Rax is necessary for tanycyte cell fate specification and maintenance (Figure 3.10).

Figure 3.1.

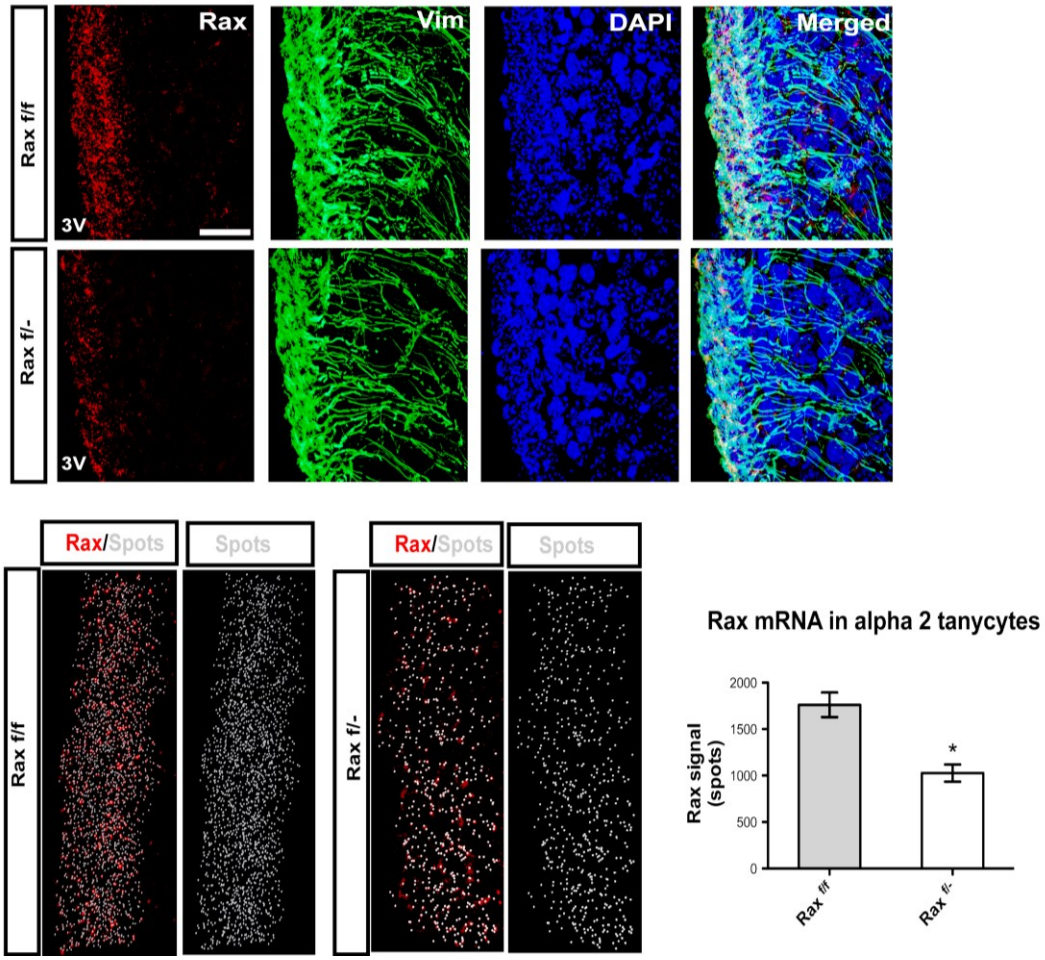

Figure 3.1. Rax mRNA is reduced in Rax heterozygous mice
A. Confocal *z*-stack reconstruction of Rax fISH (red) and Vim IHC (green) in α2 tanycytes. Rax mRNA signal is reduced in Rax heterozygous mice ($Rax^{f/-}$) compared to Rax homozygous mice ($Rax^{f/f}$). **B.** Three dimensional reconstruction and **C.** quantification of Rax mRNA signal using the spot tool of the Imaris software. Unpaired t-test (n=3), p=0.01. 3V: third ventricle. Scale bar 20μm.

Figure 3.2.

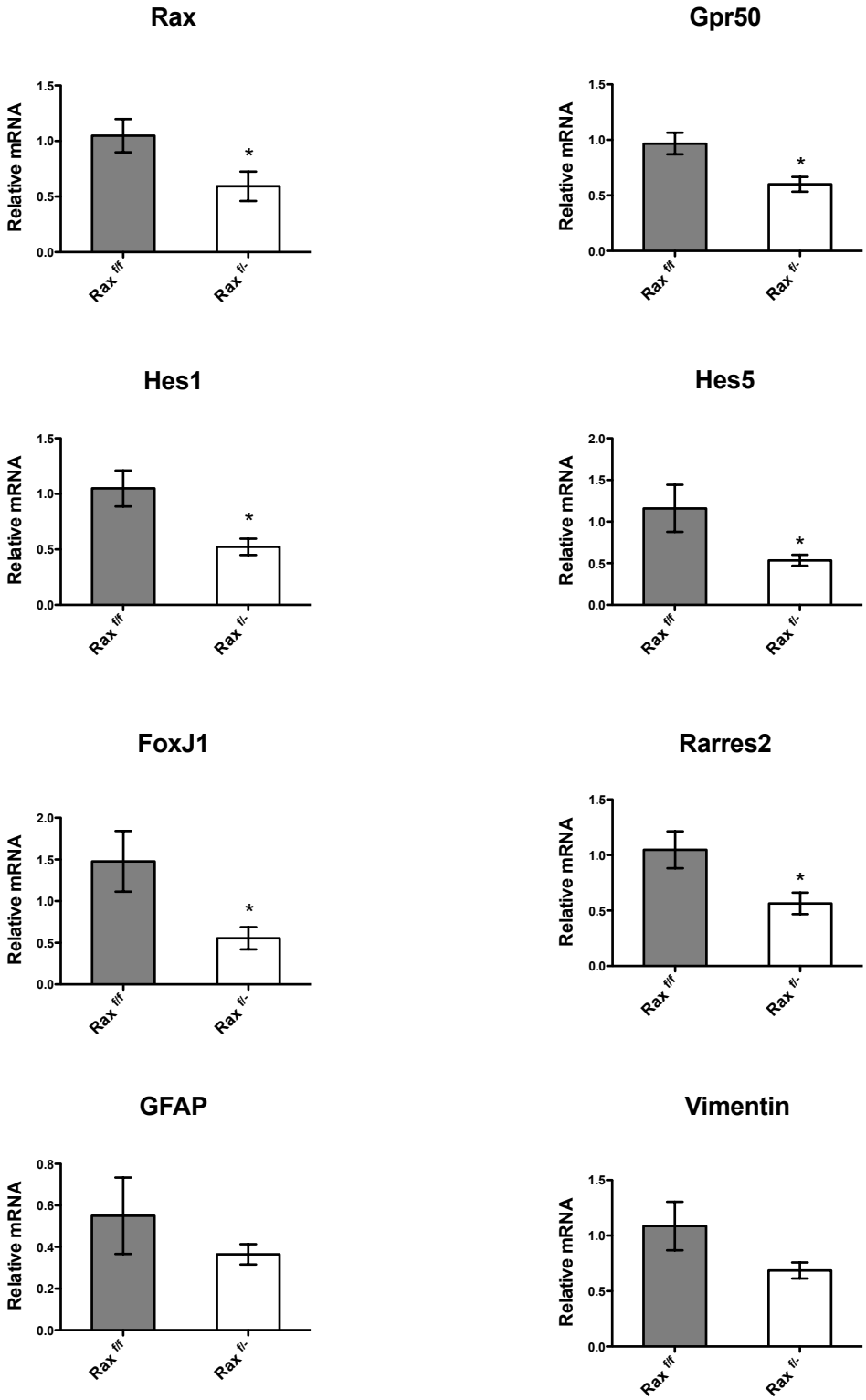
Rax
Relative mRNA
1.5
1.0
0.5
0.0
*
Rax fl/f
Rax fl/-
Gpr50
Relative mRNA
1.5
1.0
0.5
0.0
*
Rax fl/f
Rax fl/-
Hes1
Relative mRNA
1.5
1.0
0.5
0.0
*
Rax fl/f
Rax fl/-
Hes5
Relative mRNA
2.0
1.5
1.0
0.5
0.0
*
Rax fl/f
Rax fl/-
FoxJ1
Relative mRNA
2.0
1.5
1.0
0.5
0.0
*
Rax fl/f
Rax fl/-
Rarres2
Relative mRNA
1.5
1.0
0.5
0.0
*
Rax fl/f
Rax fl/-
GFAP
Relative mRNA
0.8
0.6
0.4
0.2
0.0
Rax fl/f
Rax fl/-
Vimentin
Relative mRNA
1.5
1.0
0.5
0.0
Rax fl/f
Rax fl/-

Figure 3.2. Relative mRNA of ependymal and tanycyte genes is reduced in the hypothalamus of Rax haploinsuficient mice

mRNA from adult mouse hypothalamus quantified by RT-PCR. Two fold reduction of Rax heterozygous mice ($Rax^{f/-}$) p=0.05. Other genes expressed by mature tanycytes (Gpr50 p= 0.01, Hes1 p=0.01, Hes5 p=0.04.) also have a significant reduction of relative mRNA. Ependymal genes Foxj1 (p=0.03) and Rarres2 (p=0.03) are significantly reduced in $Rax^{f/-}$ .There is no change in GFAP and Vimentin relative mRNA. Unpaired t-test $Rax^{f/f}$ (n=5), $Rax^{f/-}$ (n=6).

Figure 3.3.

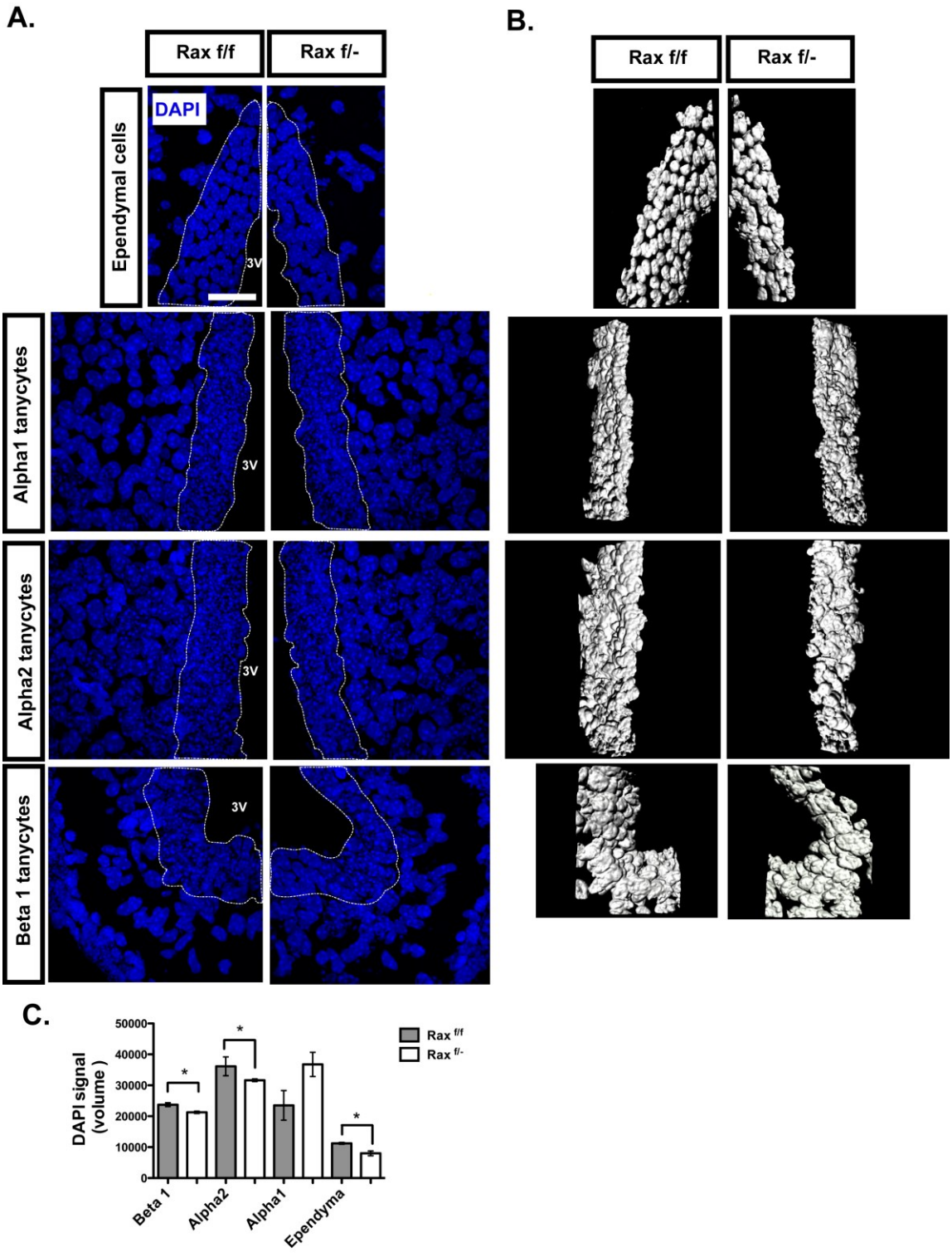
A.
Rax f/f
Rax f/-
DAPI
Ependymal cells
3V
Alpha1 tanycytes
Alpha2 tanycytes
Beta 1 tanycytes
B.
Rax f/f
Rax f/-
C.
DAPI signal (volume)
50000
40000
30000
20000
10000
0
Rax f/f
Rax f/-
*
Beta 1
Alpha2
Alpha1
Ependyma

Figure 3.3. Reduction of volume in third ventricular wall of the medial hypothalamus in Rax heterozygous mice

A. Confocal *z*-stack reconstruction of DAPI staining along the third ventricular wall of the medial hypothalamus (dotted area). **B.** Three-dimensional reconstruction of the wall of the third ventricle in the doted areas of **A**. **C.** Quantification of volume in the third ventricular wall using the cell tool of the Imaris software. Unpaired t-test (n=3), β1 tanycytes p=0.01, α2 tanycytes p=0.03, α1 tanycytes p=0.08, ependymal cells p=0.02. 3V: third ventricle. Scale bar: 50μm.

Figure 3.4

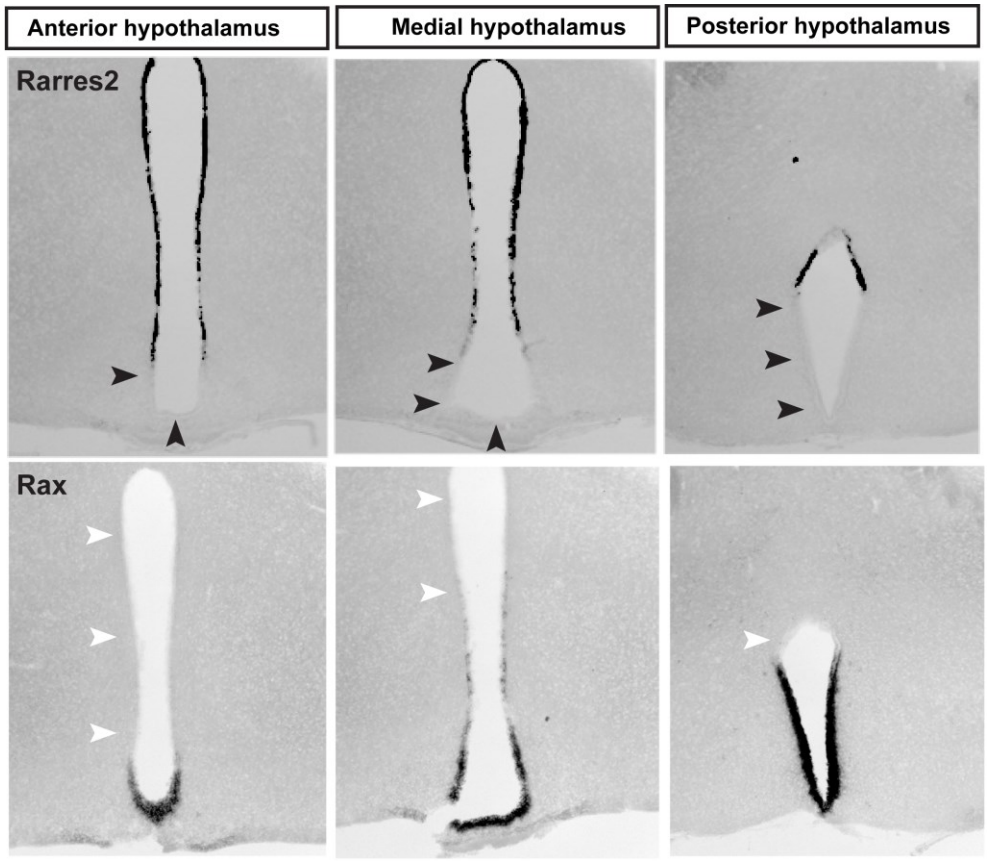

Figure 3.4. Rax and Rarres2 mRNA expression along the anterior-posterior axis of the hypothalamus

Rax and Rarres2 chromogenic *in situ* hybridization in adult C57BL/6 wild type mice (P45). Rarres2 mRNA is absent from the ventral portion of the third ventricular wall where tanycytes are located (black arrow heads). Rax mRNA expression is absent from the dorsal portion of the third ventricular wall were ependymal cells are located (white arrow heads). Rarres2 and Rax mRNAs are not expressed in the same zones along the anterior to posterior axis of the hypothalamic third ventricular wall.

Figure 3.5.

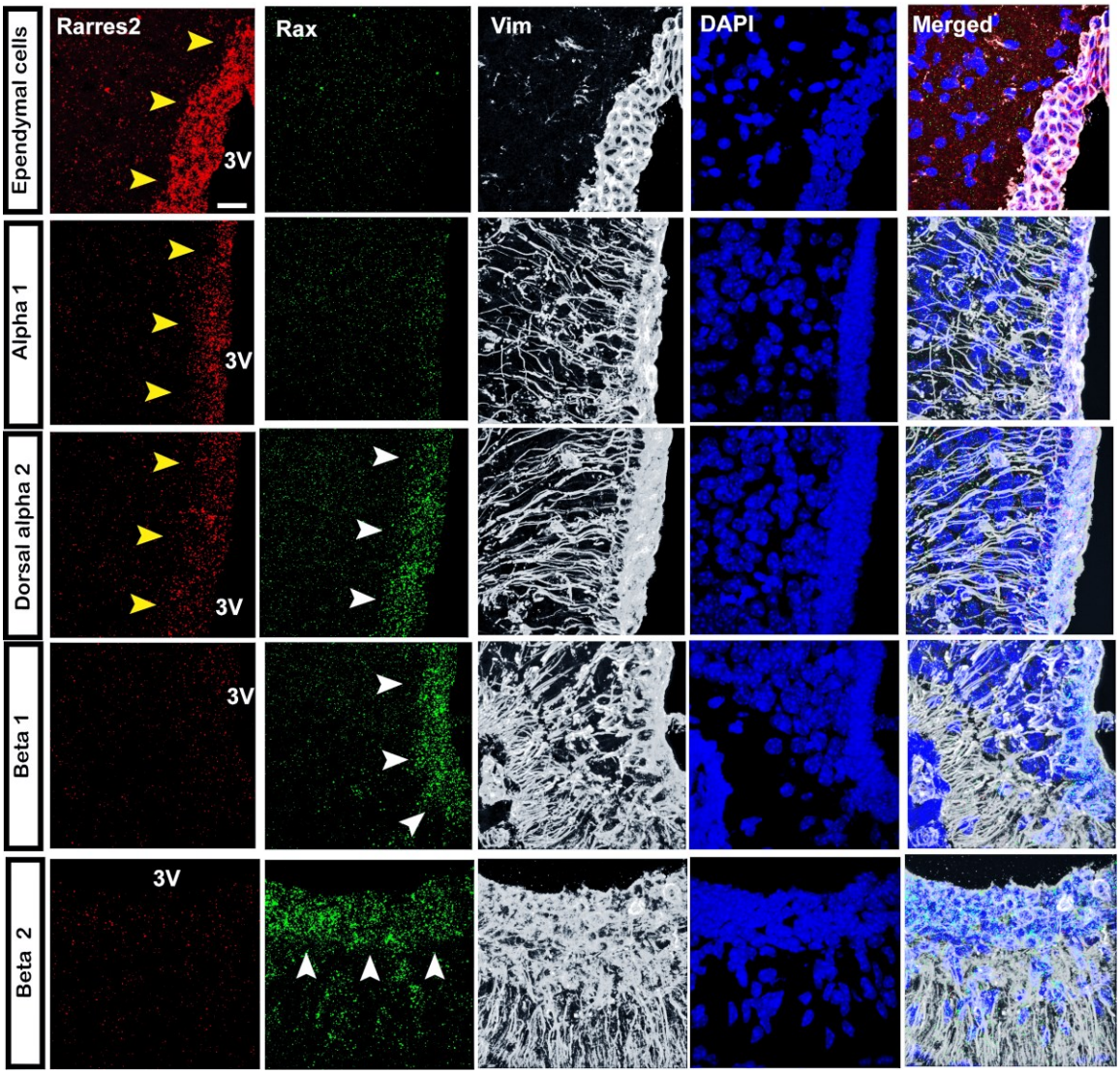

Figure 3.5. Rax and Rarres2 expression along the ventro-dorsal axis of the medial hypothalamus

Confocal z-stack reconstruction of double fISH for Rarres2 (red) and Rax (green) mRNA and immunohistochemistry for Vimentin (VIM) (white). Rarres2 mRNA is expressed predominantly in the most dorsal region of the third ventricular wall where ependymal cells are more abundant (yellow arrow heads). There is some expression of Rarres2 in the dorsal α2 tanycytes were some ependymal cells intercalate with tanycytes. Rax mRNA is only expressed in the ventral region of the third ventricular wall where tanycytes are abundant (α2, β1, β2). 3V: third ventricle. Scale bar: 20μm

Figure 3.6.

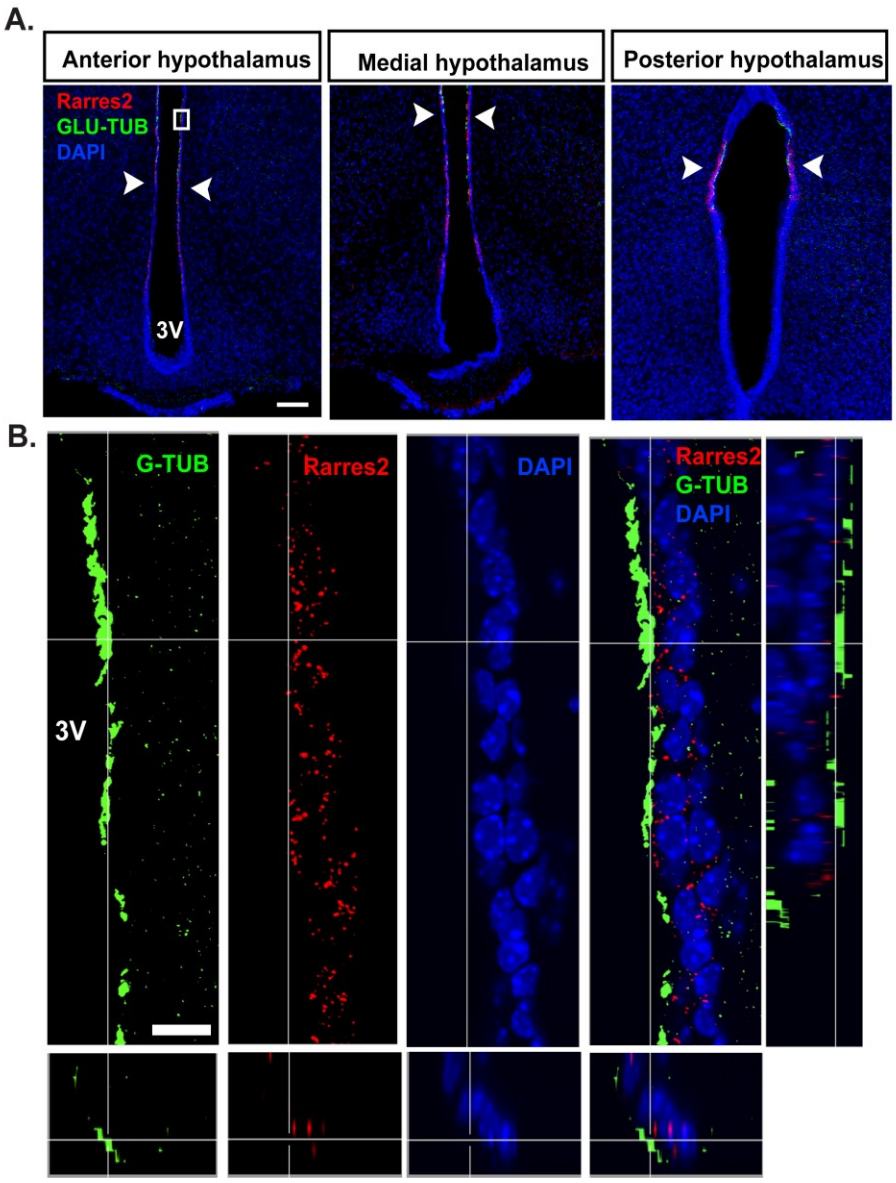

Figure 3.6. Rarres2 is expressed in ependymal cells
A. Confocal *z*-stack reconstruction of Rarres2 fISH (red) and Detyrosinated tubulin (G-TUB) IHC (green). G-TUB is expressed in the dorsal region of the hypothalamic third ventricular wall along the anterior-posterior axis similar to Rarres2 expression (white arrow heads). Scale bar: 100µm. **B**. Orthogonal view of Rarres2 mRNA and G-TUB IHC in ependymal cells identified by the expression of G-TUB in their motile cilia (green). 3V:third ventricle. Scale bar: 20 µm.

Figure 3.7.

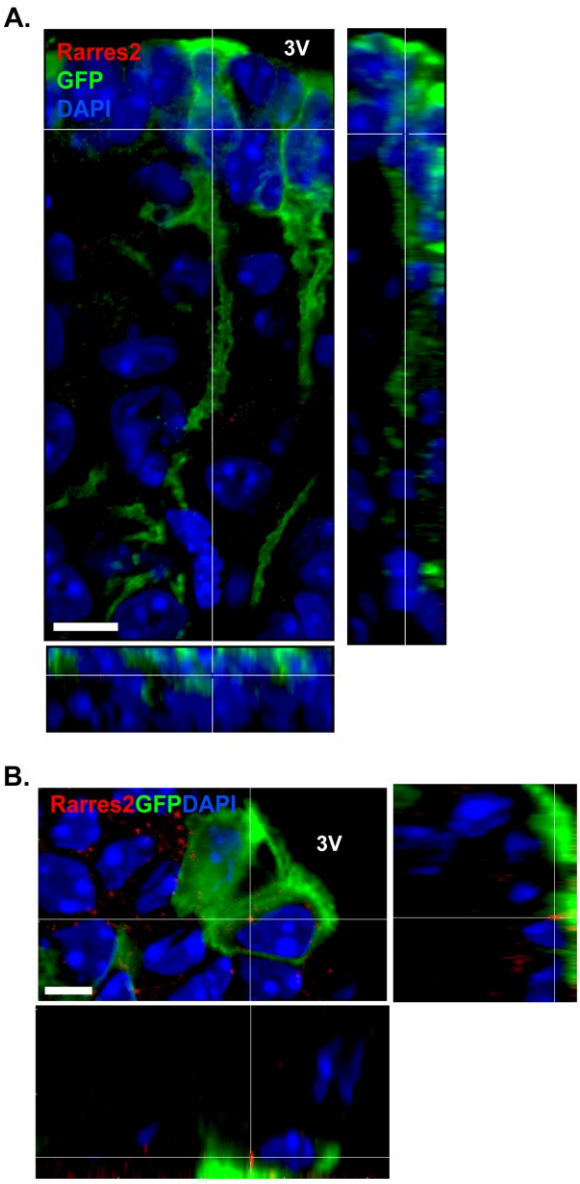

Figure 3.7. Rarres2 is specifically expressed in ependymal cells
A, B. Orthogonal view of confocal image of Rarres2 fISH (red), membrane tagged GFP IHC (green) in adult $Rax^{+/+}$;Nestin:$CreER^{T2/+}$;$TdTomEGFP^{/+}$ mice (P48). Rarres2 mRNA is not expressed in α2 tanycytes **(A)** but it is expressed in ependymal cells **(B)**. Both tanycytes and ependymal cells expressed membrane tagged GFP (green). 3V: third ventricle. Scale bars: 20 μm.

Figure 3.8.

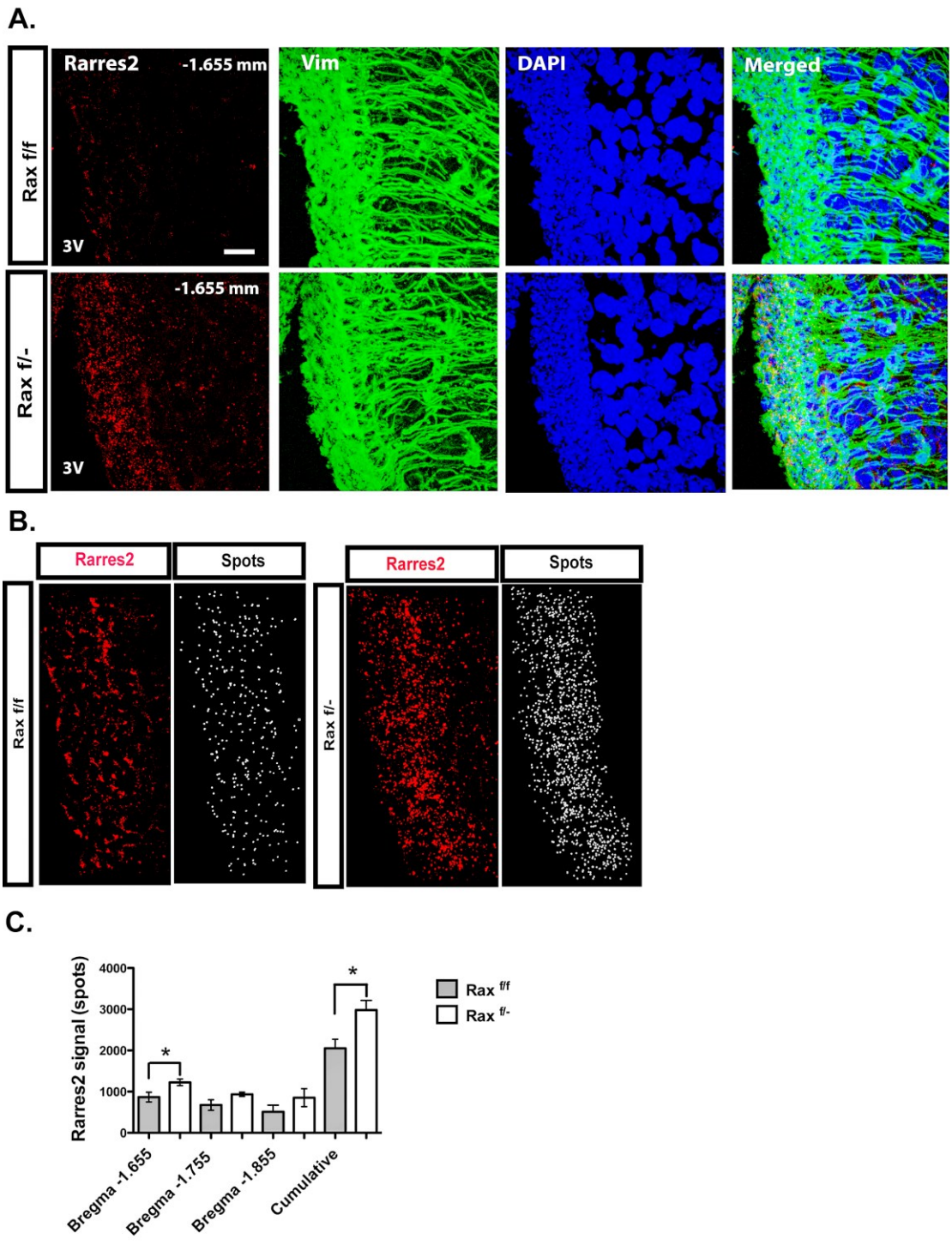
A.
Rax f/f
Rarres2
-1.655 mm
3V
Vim
DAPI
Merged
Rax f/-
-1.655 mm
3V
B.
Rarres2
Spots
Rax f/f
Rarres2
Spots
Rax f/-
C.
Rarres2 signal (spots)
4000
3000
2000
1000
0
*
*
Rax f/f
Rax f/-
Bregma -1.655
Bregma -1.755
Bregma -1.855
Cumulative

Figure 3.8. Ventralization of Rarres2 mRNA in Rax haploinsuficient mice
A. Confocal *z*-stack reconstruction of Rarres2 fISH (red) and vimentin IHC (green). Rarres2 mRNA is more abundant in the α2 zone (immediately ventral to the deflection point, DP) of $Rax^{f/-}$ mice compared to $Rax^{f/f}$ controls. **B.** Three-dimensional reconstruction of Rarres2 mRNA using the spot tool of the Imaris software. **C.** Quantification of Rarres2 mRNA in the α2 zone at three different bregma points. Cumulative indicates the sum of Rarres2 signal along the three different bregma points. Unpaired t-test (n=3), Bregma -1.655 p=0.05, Cumulative p=0.04.

Figure 3.9.

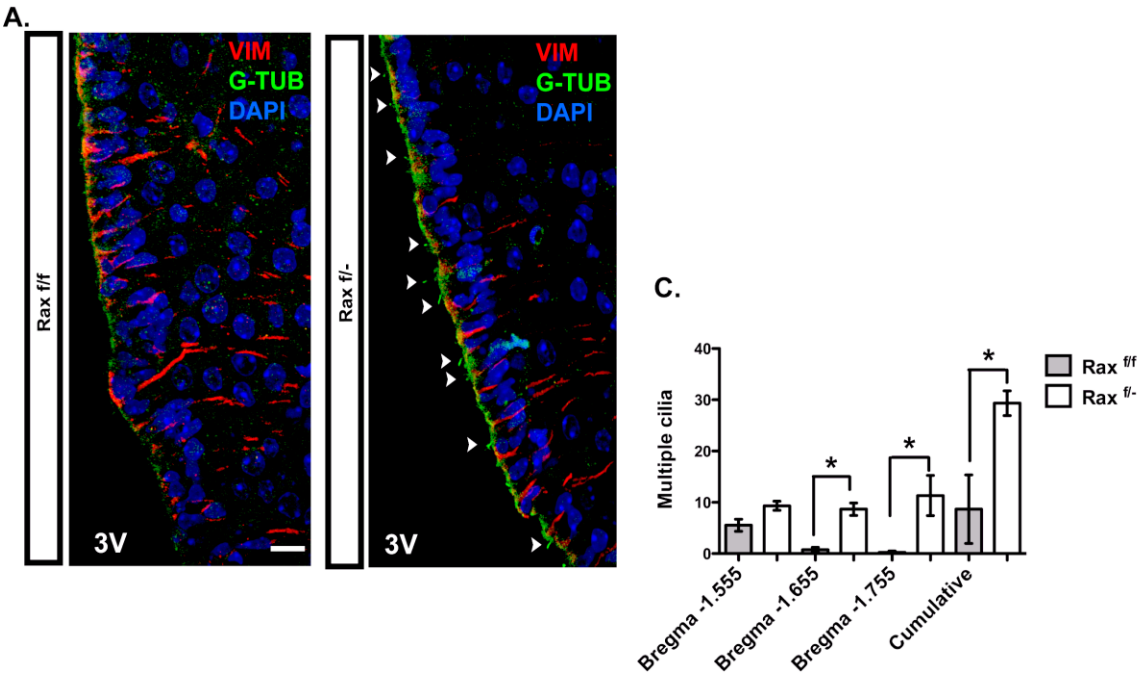

Figure 3.9. Increased multiple cilia in the tanycytic zone of Rax haploinsuficient mice

Immunohistochemistry of vimentin (Vim, red) and detyrosynated tubulin (G-TUB, green). **A.** G-TUB^{+} are more abundant in the tanycytic zone of Rax Rax$^{f/-}$ mice compared to Rax$^{f/f}$ mice (white arrow heads). **B.** Quantification of multiple cilia in each optical slice of *z*-stack confocal pictures at three different bregma points. Cumulative indicates the sum of multiple cilia along the three different bregma points. Unpaired t-test Rax$^{f/f}$ (n=4), Rax$^{f/-}$ (n=3). Bregma -1.655 p= 0.001, bregma -1.755 p=0.02, cumulative p=0.04.

Figure 3.10.

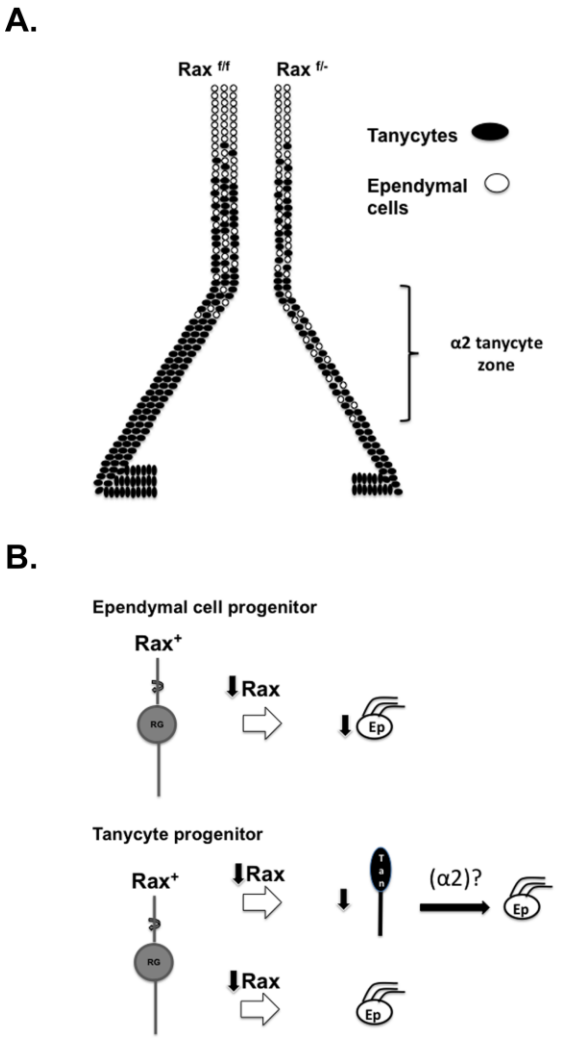

Figure 3.10. Schematic representation of Rax role in tanycyte and ependymal cell development

Rax is required for the proliferation of glia cells located in ventricular wall of the developing hypothalamus. **A.** Reduction of Rax gene dose during the development of $Rax^{f/-}$ mice leads to a thinner ventricular wall and ectopic presence of ependymal cells in the tanycytic zone. **B**. The thinner ventricular wall might be originated because of hypoproliferation of the radial glia resulting in reduction of its progeny, the ependymal cells (Ep) and tanycytes (Tan). The presence of ventral ependymal cells might result from tanycyte progenitor differentiation toward an ependymal cell phenotype due to reduced Rax dose. Alternatively, it might result from transdifferentiation of some α2 tanycytes in ependymal cells induced by reduced Rax signaling. RG: Radial glia, Ep: Ependymal cells, Tan: Tanycytes.

3.4. Materials and methods

Mice

$Rax^{f/f}$ mice were a generous donation of Peter Mathers. These mice were bred to the germline Cre mouse line Ella-Cre to generate $Rax^{+/-}$. Rax heterozygous mice where crossed back to Rax $^{f/f}$ mice generating Rax $^{f/-}$.

P45 $Rax^{+/+}$;Nestin:$CreER^{T2/+}$;$tdTomatoEGFP^{/+}$ where generated and induced as previously described (see **Chapter 2**)

Tamoxifen preparation and administration. P45 $Rax^{+/+}$;Nestin:$CreERT2^{/+}$; $tdTomatoEGFP^{/+}$ mice where induced as previously described (see **Chapter 2**)

Genotyping of Rax, Cre and GFP were performed as previously described **(**see **Chapter 2).**

Brain tissue collection was performed as previously described **(**see **Chapter 2).**

Fluorescent *in situ* hybridization (fISH) and immunohistochemistry (IMH)

Rarres2 probe was made from Rarres2 AW048638 clone. Optimal time for reaction of Rarres2 probe during fISH was 30-1h. Antibody used for G-TUB staining during fISH/IHC was rabbit anti-Detyrosinated tubulin 1:500 dilution.

The procedure was performed as previously described (see **Chapter 2**).

Hypothalamus dissections

$Rax^{f/f}$ (n=6) and $Rax^{f/-}$ (n=6) mice were sacrificed with CO_2 and their hypothalamus was immediately dissected. Brains were placed ventral side up, immobilize with needles and submerged in PBS1X during dissection. An initial incision was made in the midline, followed by two more lateral cuts made ~2mm away from the midline originating two rectangular pieces of tissue. Each of them were placed in its side

to performed two cuts, a rostral cut made just anterior to the occulomotor nerve (nervus occulomotorius) and a caudal cut made posterior to the red nucleus. Hypothalami were placed in eppendorf tubes and store at -20°C until the RNA extraction.

RNA extraction and RT-PCR

mRNA was extracted using RNeasy Mini kits (Qiagen). RNA was quantified using NanoDrop 1000 spectrophotometer (Thermo Scientific), and Superscript II reverse transcriptase (Invitrogen) was used to create cDNA from 1000 ng of RNA. Levels of mRNA for specific genes were quantified with Power SYBR green PCR master mix (Applied Biosystems). The RT-PCR output generated a Ct value which was transformed to ΔCt by normalizing each sample to 18S gene (18S fwd – GCAATTATTCCCCATGAACG and 18S rev- GGCCTCACTAAACCATCCAA). The ΔΔCt value was then calculated relative to the average control ΔCt value.

Primers were obtained from the validated pools of primers in the PrimerBank website (Spandidos, Wang, Wang, & Seed, 2010; Spandidos et al., 2008)(http://pga.mgh.harvard.edu/primerbank/), except for Hes5 primers which were donated by Nicholas Gaiano. Primer sequences used for RT-PCR were:

Rax fwd-TGGGCTTTACCAAGGAAGACG and Rax rev-GGTAGCAGGGCCTAG-TAGCTT, Rarres2 fwd-GCTGATCTCCCTAGCCCTATG Rarres2 rev- CCAATCA-CACCACTAACCACTTC, Gpr50 fwd-AGAGCAACATGGGACCTACAA, Gpr50 rev-GCCAGAATTTCGGAGCTTCTTG, Hes1 fwd-CCAGCCAGTGTCAACACGA and Hes1 rev-AATGCCGGGAGCTATCTTTCT, Foxj1 fwd- GCC TCC CTA CTC GTA TGC CA and Foxj1 rev - GCC GAC AGG GTG ATC TTG G, Vimentin fwd-CGTCCACACGCACCTACAG and Vimentin rev- GGGGGATGAGGAATAGAGG

CT, GFAP fwd-CCCTGGCTCGTGTGGATTT and GFAP rev-GACCGATACCACTCCTCTGTC, Hes5 fwd- 5'-AGA AAA ACC GAC TGC GGA AGC C-3' and Hes5 rev- CGC GGC GAA GGC TTT GCT.

Image acquisition

Low resolution images of chromogenic *in situ* hybridization and DAPI were obtained in an axioskop 2 mot plus from Carl Zeiss equipped with an Axiovision software and using a 10X objective.

z stack images were taken in a Zeiss LSM510 Meta confocal microscope using a 63X or 100X objective and digital zoom 0.7 or 1 and equipped with a Zen 2009 software. To make sure that the *z* stack images to be used for quantification in the two genotype groups ($Rax^{f/f}$ and $Rax^{f/-}$) were taken in identical conditions, we collected them together during the same confocal session and using the same pinhole, gain and contrast.

The landmarks used for the identification of the different tanycytes along the ventro-dorsal axis of the medial hypothalamus were the following (see Figure 1.1): Medial zone of the ME (β2 tanycytes), lateral evagination of the infundibular recess (LEIR) (β1 tanycytes), immediately ventral the deflection point (DFP) (α2 tanycytes), immediately dorsal to the DFP (α1 tanycytes), roof of the third ventricle (ependymal cells).

Identification of bregma points along the anterior-posterior axis was done comparing our images with the Allen Mouse Brain Atlas (Sunkin et al., 2013) and using the shape of the ME, the lateral region of *par tuberalis* and the shape of the different hypothalamic nuclei stained with DAPI as landmarks.

Image analysis

Quantification of *z* stack images was done by one blind evaluator and using the Imaris software version 7.1.1. Rax and Rarres2 fISH signal was quantified using the automatic three- dimensional quantification of spots followed by editing for excess or lack of signal detection. Quantification of DAPI volume was done semi-automatically using the cell tool of the software and manually adjusting the threshold to correspond to the area of interest. Visualization of volume reconstruction was done with the surface tool of Imaris and visualization of the two-dimensional images of the *z* stacks were obtained by grouping the z stack in the ImageJ software.

Cilia quantification was performed in brain sections from $Rax^{f/f}$ and $Rax^{f/-}$ stained with G-TUB which labels cilia, and Vim which labels ependymal cells and tanycytes. Confocal z-stack images of the α2 tanycytic zone were analyzed for the presence of multiple cilia as follows: each digital slide of the confocal z-stack was visualized in the slice gridded viewer of the Imaris software. One blind observer manually counted the number of cilia longer than 2µm present in each square of the grid for each digital slide. Cilia shorter than 2µm were excluded because it most likely corresponded to primary cilia. When a cilium was clearly part of a cilia cluster it was counted only once.

Statistical analysis

All quantifications were analyzed for statistical significance in the GraphPad Prism software using a two tailed unpaired t-test and considering $p<0.05$ as significant.

Chapter 4

Rax haploinsuficient mice display changes in the hypothalamic CSF-brain barrier

4.1. Introduction

The ependymal layer lining the ventricles forms a barrier between the cerebrospinal fluid (CSF) filled ventricle and the adjacent neurons (CSF-brain barrier) that regulates the permeability of water and solutes across the ventricular wall (Del Bigio, 1995; Bruni et al., 1985). This barrier is dynamic and controlled by multiple protein-protein interactions as well as post-translational modifications of the components of the tight junctions. These proteins include claudins, junction-associated MARVEL proteins (e.g. occludins), and junction adhesion molecules (JAMS). Also, adapter molecules such as membrane associated guanylate kinase homologues (MAGUKs), ZO-1, ZO-2 and ZO-3 are important for the binding of occludins and claudins to the cytoskeleton (Tsukita, Furuse, & Itoh, 1999). Ependymal tight junctions not only separate the brain from molecules present in the CSF, but also mediate important signaling pathways that control gene expression, cell proliferation and differentiation (Matter & Balda, 2003; Steed, Balda, & Matter, 2010). Ependymal junctions are particularly common in circumventricular organs (CVOs) in which the blood brain barrier (BBB) is absent. It seems that the presence of tight junctions between ependymal cells in the ventricular wall of the CVOs compensates for the absence of tight junctions in the endothelial cells characteristic of the BBB (Norsted, Gomuc, & Meister, 2008; Rodriguez et al., 2010).

In addition to the barrier properties of ependymal cells, they have an alternate

function as facilitators of communication between the CSF and the brain (Del Bigio, 1995; Bruni et al., 1985). The paracellular permeability of the ependymal layer that allows the communication between CSF and adjacent neurons in brain parenchyma, occurs because of the ability of the ependymal cells to form gap junctions as demonstrated both in culture (Gabrion et al., 1998; Bouille, Mesnil, Barriere, & Gabrion, 1991) and *in vivo* (Jarvis & Andrew, 1988; Brightman, 1965). Gap junctions allow the transfer of water and small molecules from the CSF to the parenchyma and are formed by the coupling of connexin channels from adjacent cells. These cell junctions are essential during development and in the mature brain (Dere & Zlomuzica, 2012).

A recent paper described the distribution of tight junction proteins in the wall of the third ventricle of the mouse medial hypothalamus. The authors reported that tight junction proteins had a differential distribution along the third ventricular wall of the medial hypothalamus. Dorsally, the ventricular wall of the tuberal hypothalamus expressed several tight junction proteins including occludin, ZO-1, claudin1 and claudin5, forming a very organized "honeycomb-like" pattern characteristic of tight junctions. A similar pattern was observed in the ventricular layer of the median eminence (ME) as would be expected in a CVO. Interestingly, they found that in the zone between the most dorsal (ependymal zone) and most ventral (ME) region of the third ventricular wall, the honeycomb-like pattern becomes progressively disorganized ventrally until it was absent in the α2 tanycytic zone at the level of the ArcN. The disorganization of tight junctions between the tanycytes in the ArcN suggested that there was differential CSF-brain permeability at this level. To test that hypothesis they used Evans Blue (EB) dye, which is a low-molecular-mass tracer that has high affinity for

albumin and diffuses across paracellular spaces (Fry, Mahley, Weisgraber, & Oh, 1977). They found that EB easily diffused and distributed in the ArcN leading the authors to conclude that there is open communication between the CSF and the neurons in the ArcN (Mullier et al., 2010).

There are few studies characterizing the permeability of the CSF-brain barrier under abnormal circumstances and the only available studies are performed in mouse models of acute or chronic hydrocephalus. One study, which evaluated the differences between EB diffusion in an acute obstructive hydrocephalus model, found no difference in EB diffusion between hydrocephalic and normal brains (Nyberg-Hansen, Torvik, & Bhatia, 1975). A more recent study used a mouse model of chronic congenital hydrocephaly. The *hyh* mouse (*hy*drocephalus with *h*op gate), features large areas where ependymal cells are lost and replaced by reactive astrocytes, which assume some of the ependymal cell functions. In these mice the tracers HRP and lanthanum nitrate where able to cross the reactive astrocytic regions in the lateral ventricles, which showed similar paracellular permeability when compared to the wild type mice (Roales-Bujan et al., 2012). This study suggested that astrocytes are required for the compensatory mechanisms that ensure a normal communication between the CSF and adjacent neurons despite abnormal circumstances.

To our knowledge there are no studies addressing the paracellular permeability of the third ventricular wall wherein a reduced number of tanycytes and ependymal cells or when an abnormal distribution of ependymal cells is present. For this reason we studied the permeability of the third ventricular wall in the Rax haploinsuficient mice. We have previously found that Rax haploinsuficient mice have a thinner ventricular wall due to a

reduction in tanycytes and ependymal cells. These mice also have ectopic presence of ependymal cells in the ventricular wall adjacent to the ArcN (see **Chapter 3**). We hypothesized that this change in the composition and distribution of the cells in the third ventricular wall will impact the diffusion of EB from the CSF to the hypothalamic parenchyma. To test this hypothesis we injected EB in the lateral ventricle of these mice and quantified the EB in the hypothalamic parenchyma. We found that in Rax haploinsuficient mice there was a reduced distal diffusion of EB.

4.2. Results

4.2.1. Rax haploinsuficient mice display reduced distal diffusion of Evans Blue

One minute after injecting 1µl of 1% EB in the lateral ventricle of $Rax^{f/f}$ and $Rax^{f/-}$ mice we found that there was a reduction of EB distal diffusion in the medial hypothalamus of the Rax haploinsuficient mice. EB distal diffusion was higher in the hypothalamus compared to other brain regions adjacent to the ventricular compartments (Figure 4.1B). Within the hypothalamus, EB diffusion varied along the anterior to posterior axis in both genotypes with no distal diffusion in the anterior hypothalamus, and more distal diffusion in the medial and posterior hypothalamus (Figure 4.1C). Based on these results and owing to the fact that we wished to compare our results with the previous report of EB diffusion by Mullier et al. 2010, we only quantified EB in the medial hypothalamus. To determine the distal diffusion of the EB we quantified the total amount of EB in all the brain sections of the medial hypothalamus as well as the EB in the parenchyma using the pixel quantification method within ImageJ. The distal diffusion was calculated as a ratio between the levels of EB in the parenchyma of each brain section divided by the total amount of EB in the same brain section. In $Rax^{f/-}$ mice

the distal diffusion was significantly lower than the diffusion in the $Rax^{f/f}$ (Figure 4.1D). Furthermore, most diffusion in both genotypes was located ventrally near the ArcN, and dorsally near the DMH where ependymal cells are abundant. When we compared the distribution of EB along the ventricular wall (ventral to dorsal axis) we did not find any statistically significant differences between genotypes (Figure 4.1E).

4.3. Discussion

We have investigated the permeability of the ventricular wall in Rax haploinsuficient mice which have a reduced number of ependymal cells and tanycytes along the hypothalamic third ventricular wall and ectopic presence of ependymal cells at the level of the ArcN. We found that in Rax haploinsuficient mice there was a reduced distal diffusion of EB from the CSF to the parenchyma of the medial hypothalamus.

The cellular composition of the ventricular wall influences the amount EB distal diffusion

First, we observed that there was proximal EB diffusion along the anterior to posterior hypothalamic axis but EB distal diffusion was only present in the medial and posterior hypothalamus. This might be related to the variable composition of the hypothalamic ventricular wall along this axis. The anterior hypothalamus is composed exclusively of ependymal cells while tanycytes are only present in a small area at the floor of the third ventricle. In contrast, the medial and posterior hypothalamus features more tanycytes than ependymal cells (Rodriguez et al., 2005). We also saw some distal diffusion from the lateral ventricles or from the dorsal third ventricle to the adjacent parenchyma where there are scattered tanycytes.

Our observation suggests that distal diffusion of EB is higher in hypothalamic

areas enriched with tanycytes. Both tanycytes and ependymal cells can form gap junctions which explain the proximal diffusion of a tracer, but only tanycytes have long processes that project distally from the ventricle. Tanycytes might facilitate distal diffusion of EB either by endocytosis of the EB followed by transcellular transport or by paracellular transport between tanycytic processes. EB has high affinity for albumin and both paracellular and transcellular transport of albumin has being reported in endothelial cells (Minshall, Tiruppathi, Vogel, & Malik, 2002). Also, other tracers such as wheat germ agglutinin (WGA) and horseradish peroxidase (HRP) have been observed to follow dual trafficking pathways with diffusion between tanycyte cell bodies as well as transcytosis along tanycytic processes occurring (Rodriguez et al., 2005).

The organization of intercellular spaces between the tanycytic processes could facilitate the movement of molecules parallel to tanycytic processes.

Taken together our observations suggest that EB diffusion is higher in brain areas enriched with tanycytes such as the medial and posterior hypothalamus and that tanycytes might facilitate distal EB diffusion through paracellular and/or intracellular transport.

EB diffusion was found in the tuberal hypothalamus not only in the ArcN and ependymal zone but also in the transition zone

We observed that in the $Rax^{f/f}$ mice the distribution of the EB was similar to what was previously reported by Mullier at el. who found diffusion in the ArcN and in the ependymal zone of the medial hypothalamus (Mullier et al., 2010). However, we also found diffusion in the transition zone at the level of VMH and DMH where α1 tanycytes and ependymal cells are present. Even though Mullier et al. did not observe diffusion in the α1 tanycyte zone, it could be expected based on the disorganized honeycomb like

expression pattern of the tight junction molecules at this level, and because of the previously reported expression of gap junction proteins, such as connexin-43, between the α1 tanycytes which may facilitate paracellular diffusion (Rodriguez et al., 2010). It is possible that in addition to the expression of tight junction or gap junction markers, other factors influence the diffusion of molecules from the CSF to the hypothalamus. Furthermore, Mullier et al. reported restricted diffusion of EB in the ArcN at a specific bregma point in the tuberal hypothalamus without describing his findings at other bregma locations. This is an important point because we found that EB diffusion varies along the anterior to posterior axis.

As a consequence it remains unclear if Mullier et al. did observe diffusion of EB at the level of α1 at other bregma points which may not have been reported. Finally, the differences between our study and Mullier's findings may also be the result of differences in experimental conditions. Even thought we tried to replicate experiments exactly, using the same volume and concentration of EB and sacrificing the mice 1 minute after the injection, other variables are very difficult to replicate. For example, the precision and consistency of injection into the lateral ventricle, a key factor determining the amount of EB that reaches the third ventricle and diffuses to the hypothalamic parenchyma, is not easily reproducible especially between experimenters.

Based on previous reports of α1 tanycyte expression of connexin-43 (Rodriguez et al., 2010) and the disorganized honey comb pattern expression of their tight junction molecules (Mullier et al., 2010), the distal diffusion of EB at the level of the α1 tanycytes that we observed was expected despite its discrepancy with previous reports.

In addition, we found reduced distal diffusion of EB in the medial hypothalamus

of Rax haploinsuficeint mice. If distal EB diffusion is facilitated by the presence of tanycytes, the reduction of tanycytes in our Rax haploinsuficient mice would explain a reduction in distal EB diffusion. However the reduction of EB was not only observed in the tanycyte zone (ventral) but also in the ependymal region (dorsal).

This suggests that there might be other factors affecting permeability of the hypothalamic ventricular wall beyond simple reduction in the number of tanycytes. One of these factors could be the distribution of cell-cell junctions in the tanycytic and ependymal zones. There are abundant gap junctions between ependymal cells and tanycytes of the hypothalamic third ventricular wall while there are functional tight junctions only in the floor of the hypothalamic third ventricle which lacks a BBB; here a tight protective layer of ependymal cells is required to prevent direct contact between the CSF and ME axons and neurons (Rodriguez et al., 2005; Peruzzo et al., 2000). Since paracellular permeability depends on the type of intercellular junctions (gap junctions facilitate diffusion while tight junctions restrict diffusion) ,the reduction of distal diffusion of EB in our Rax haploinsuficient mice suggests a compensatory increase of tight junctions resulting from a reduced number of cells along the third ventricular wall. Unfortunately, we could not perform staining with antibodies against tight or gap junction proteins because of the instability and highly hydrophilic nature of EB which impeded combined immunohistochemistry together with EB visualization.

Our data shows that there is a reduced distal diffusion of EB in the Rax haploinsuficient mice, which could be the result of a compensatory increase in tight junctions between those remaining tanycytes available in the ventricular wall and/or because of a reduced availability of tanycyte processes facilitating EB distal diffusion.

Characterization of hypothalamic function will be required to detect phenotypic abnormalities resulting from ventricular permeability in Rax haploinsuficient mice

Finally, we found that reduction of EB diffusion was not associated with any abnormal gross behavioral phenotype. Since EB has a high affinity for albumin, which is present in blood and CSF, changes in EB diffusion would reflect the protein permeability of the vascular endothelium and the ependymal epithelium respectively. EB is broadly used to study the integrity of the blood-brain-barrier (BBB) after stroke or other challenges (Yang et al., 2012; Geng et al., 2012; Zeng et al., 2012) and has been utilized, although less frequently, to assess changes in CSF-brain permeability in normal and hydrocephalic brains.

We used EB to study the CSF-brain barrier assuming that any changes in EB diffusion across the ventricular wall would indicate changes in protein permeability. Protein mediated signaling between the CSF and adjacent neurons is important for normal brain development and function (Dziegielewska, Knott, & Saunders, 2000; Sharma & Johanson, 2007). Signaling may be receptor-mediated or may occur by paracellular transport (Agnati et al., 1995). It has been suggested that based on the expression of cell-cell junctions and the pattern of EB diffusion in the ArcN, there is an open communication between the CSF and this nucleus (Mullier et al., 2010). Several proteins have been proposed to diffuse to the ArcN and participate in function of this nucleus such as T4, prolactin and leptin (Rodriguez et al., 2010).

As a consequence it would be expected that changes in protein permeability will affect hypothalamic function. However, the Rax haploinsuficient mice that were used in this study did not present any gross anatomical or behavioral abnormalities. This could

be explained because the reduced protein diffusion induces subtle changes which will only be detected with more specialized physiological and behavioral studies of hypothalamic functions such as measurements of hormonal levels. Conversely, the reduction in the number of cells in the Rax haploinsuficient mice might activate compensatory mechanisms which protect against the presence of physiological abnormalities.

In summary, our data shows that Rax haploinsuficient mice have a reduced distal diffusion of EB along the entire third ventricular wall of the medial hypothalamus, this functional phenotype was not associated with any gross behavioral phenotype. Reduction of EB diffusion could be the result of a reduced availability of tanycyte processes facilitating EB distal diffusion or because of an increase in tight junctions between the fewer ependymal cells and tanycytes available in the ventricular wall. In order to elucidate the role of intercellular junctions in our Rax haploinsuficient mice, it would be necessary to perform ventricular injections with more stable tracers such as fluorescein (FITC), which are retained after immunohistochemistry and would allow for co-staining with antibodies against tight junction and gap junction molecules. These studies may reveal the correlation between the distribution of this junction molecules and the diffusion of the tracers.

Figure 4.1.

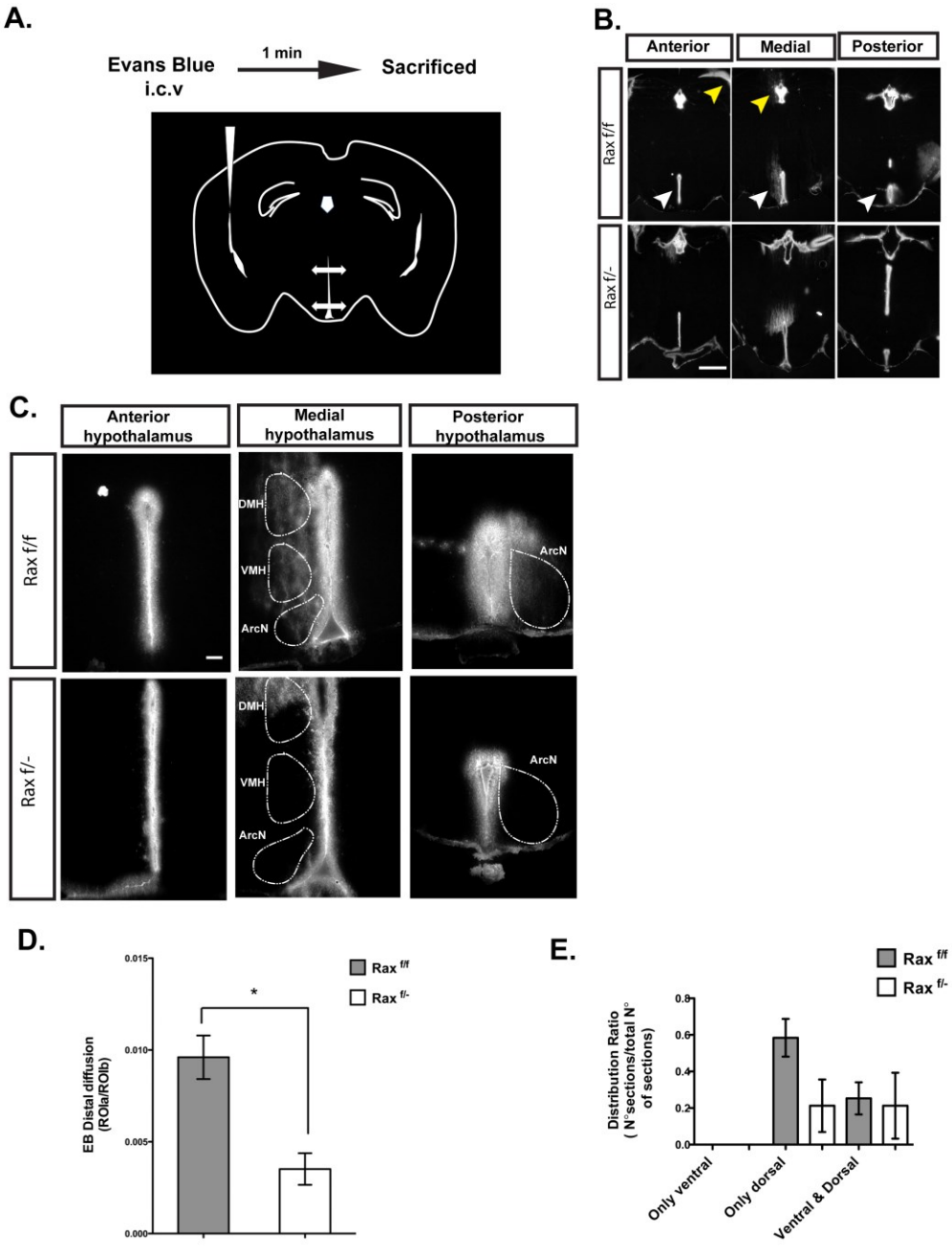
A.
Evans Blue
i.c.v
1 min
Sacrificed
B.
Anterior
Medial
Posterior
Rax f/f
Rax f/-
C.
Anterior hypothalamus
Medial hypothalamus
Posterior hypothalamus
Rax f/f
Rax f/-
DMH
VMH
ArcN
D.
EB Distal diffusion (ROIa/ROIb)
Rax f/f
Rax f/-
*
E.
Distribution Ratio (N°sections/total N° of sections)
Rax f/f
Rax f/-
Only ventral
Only dorsal
Ventral & Dorsal

Figure 4.1. Reduced diffusion of Evans blue in Rax haploinsuficient mice
A. Schema of Evans Blue injection protocol. EB was injected in the lateral ventricle of adult (P45) mice who were sacrificed 1 min after the injection. **B.** EB distribution in the brain. There was more distal diffusion in the hypothalamus (white arrow heads) than in other brain regions. Some distal diffusion is present in the dorsal third ventricle (yellow arrow head, anterior) and the lateral ventricles (yellow arrow head, medial). **C.** Closer view of **B.** Distribution of EB in the hypothalamus. The EB diffusion in the anterior hypothalamus was only proximal. Distal diffusion was observed in the medial and posterior hypothalamus. In the medial hypothalamus distal diffusion was present in the ArcN, VMH and DMH. In the posterior hypothalamus distal diffusion is present in the ArcN. **D.** Quantification of distal diffusion of the EB in the medial hypothalamus. The distal diffusion was calculated as a ratio between the amount of EB (measured as pixels) in the parenchyma of each brain section (ROIa) divided by the total amount of EB (parenchyma and ventricle) in the same brain section (ROIb). In $Rax^{f/-}$ mice the distal diffusion was significantly lower than the diffusion in the $Rax^{f/f}$. **E.** Distribution of EB in the ventro-dorsal axis. There was no exclusive ventral diffusion in any genotype. No significant difference between genotypes was found when the distribution of EB along the ventricular wall was compared (only dorsal Vs ventral & dorsal). Unpaired t-test of distal EB diffusion in the medial hypothalamus $Rax^{f/f}$ (n= 3, 44 sections) Vs $Rax^{f/-}$ n=3, 41 sections) p (ROIa/ROIb)=0.001. Unpaired t-test $Rax^{f/f}$ (n= 3, 44 sections) Vs $Rax^{f/-}$ n=3, 41 sections) p(only dorsal)=0.10, p (ventral & dorsal)=0.85. Scale bars: 500μm (**B**) and 100μm (**C**).

4.3. Materials and methods

Mice

The Rax $^{f/f}$ and Rax $^{f/-}$ mice used for these experiments were generated and maintained as previously described (see **Chapter 3**).

Evans blue preparation

Evans Blue (EB) powder dye content 75% (Sigma) was dissolved in sterile 0.9% saline solution to a 1% concentration. The EB solution was prepared fresh and kept in the darkness at RT until the intracerebroventricular injection (i.c.v).

Canulation and intracerebroventricular injections

Mice were anesthetized with an i.p injection of a Domitor (medetomidine, selective α-2-receptor adrenergic agonist) (1mg/kg) and Ketamine (NMDA antagonist) (80 mg/kg) cocktail in a 5:2 ratio (Dormitor:Ketamine). The scalp incision area of the anesthetized mice was prepared for surgery by shaving off their hair followed by swabbing their skin with a Povidone-Iodine swab stick, an antiseptic germicide, and ethanol 70%. The mice were then placed in a stereotaxic instrument (Kopf) by adjusting the incisor and ear bars an elevating the mice to a skull level position. An incision was made into the skin along the midline of the scalp starting at a point slightly posterior from between the eyes to a point approximately 1 mm caudal to lambda reference point.

Then, a hole was drilled into the skull 0.6 mm caudal to bregma and 1.2 mm lateral to midline. In order to allow for the cannula to adhere into place, the surface of the skull was etched with a sterile scalpel, coated with super-glue and etched again with a scalpel when the glue was dry. An extra-thin walled 24-gauge stainless steel cannula was inserted 2.2 mm below the skull surface, and secured in place using dental cement. A 30-

guage obturator was inserted into the cannula to maintain patency. The wound around the base of the dental cement was closed using Sofsilk sutures. To prevent hypothermia and death, the mice were kept on a heating pad set at 40°C. Finally, mice received an i.c.v injection of 1ul of 1% EB into the lateral ventricle using a disinfected stainless steel injector Hamilton Syringe connected by polyethylene tubing. Administration of EB lasted around 3-4 seconds and the injector was kept inside the cannula for one minute after the EB was administered. Then, the injector was removed and the mice where decapitated with scissors. The brain were collected and immediately embedded and frozen in O.C.T and stored at -80°C.

Tissue collection

Fresh frozen coronal hypothalamic sections were collected by sectioning in a cryostat at 40 μm starting from the middle of the anterior hypothalamus to the end of the posterior hypothalamus. Sections from each brain were immediately mounted in Superfrost Plus slides (Fisher) and allowed to dry at room temperature in the dark for around 20 minutes.

Imaging acquisition

Brain blocks were photographed during sectioning with a regular camera to visualize the gross distribution of EB in the brain ventricles.

Images of the brain sections were obtained with an axioskop 2 mot plus from Carl Zeiss equipped with an Axiovision software and using a 5X and 10X objective. Two sets of pictures were taken in this axioscop, the first set was taken right after the slides were dried and it was used to examine the general distribution of EB in the third ventricle. The second set was taken around four months after the initial set of pictures and it was used to obtain images for pixel quantification. Slides were frozen at -80°C during the period of time between the two set of pictures and defrosted at room temperature in the dark for 15 minutes prior to image acquisition

Image analysis

All 10X images from the entire medial hypothalamus of each mice were used for pixel quantification using the ImageJ software as follow. All images had the same background subtraction and brightness adjustment before converting them in binary images (0 or 255 pixels). The threshold used for all image was the same and was set automatically after choosing the *maxentropy* thresholding method. Then, two different

regions of interest (ROI) were drawn in each image for quantification: ROI(b) was a fixed rectangular box which contained all pixels in the third ventricle and the adjacent hypothalamic parenchyma where EB diffused. ROI(a) was an irregular shaped ROI different for each image and contained only the pixels in the parenchyma. When there were no pixels in the parenchyma we assigned a default number of pixels which was the lowest number of pixels in the entire sample (359) to be able to calculate a ratio. The total amount of pixels for each ROI was the "area measurement" resulting from the *analyze measure* tool of the software. Finally, the distal diffusion of EB was calculated as a ratio of the EB in the parenchyma (ROIa) divided by the total amount of EB in the medial hypothalamus (ROIb), Ratio= (ROIa/ROIb).

Statistical analysis

The ratio for each image (ROIb/ROIa) in the $Rax^{+/+}$ mice (n=3, total images=44) were compared with the ratio for each image in $Rax^{+/-}$ mice (n=3, total images=41) and analyzed for statistically significant difference using an unpaired non parametric two tail Mann-Whitney test using $p< 0.05$ as significant.

This test was implemented in the graph pad Prism software.

Chapter 5

RAX protein is secreted by terminally differentiated tanycytes and is internalized by other hypothalamic cells

5.1. Introduction

Rax gene codes for a transcription factor (TF) of the homeoprotein family (RAX) (Furukawa et al., 1997). Homeoproteins are characterized by a highly conserved homeodomain fold consisting of three α helices connected by short loops. The third C-terminal α helix binds to the major grove of DNA to regulate transcription (Laughon, 1991). Homeoproteins are essential for embryonic development and morphogenesis (Pick & Heffer, 2012). In the nervous system, homeoproteins participate in neurogenesis, neuronal differentiation and axon guidance leading to the compartmentalization of the brain and map formation (Kiecker & Lumsden, 2005; Wigle & Eisenstat, 2008). It has classically been accepted that homeoproteins function in a cell autonomous way by regulating transcription of numerous genes including membrane receptors, cell adhesion molecules and growth factor-like molecules, as well as other transcription factors (Gehring et al., 1994; Choo & Russell, 2011). However, growing evidence indicates that homeoproteins can also function in a paracrine fashion, being secreted and consequently internalized by nearby cells. This novel, non-cell autonomous mechanism of homeoprotein function operates not only during development but also in adulthood (Brunet, Di Nardo, Sonnier, Beurdeley, & Prochiantz, 2007).

The first evidence of paracrine secretion of homeoproteins emerged in 1991 when Joliot et al. found that the *Drosophila* homeoprotein Antennapedia was internalized by neurons, reached the nucleus and induced neuronal differentiation (Joliot, Pernelle, Deagostini-Bazin, & Prochiantz, 1991). The internalization of Antennapedia was enabled by the presence of a 16 amino acid (aa) sequence in the homeodomain region, now called Penetratin (Le Roux, Joliot, Bloch-Gallego, Prochiantz, & Volovitch, 1993; Derossi, Joliot, Chassaing, & Prochiantz, 1994). Penetratin allows the delivery of hydrophilic cargos into cells and it represents one of the first members of an increasing family of natural and synthetic cell penetrating peptides (CPPs) (Dupont, Prochiantz, & Joliot, 2011; Prochiantz, 2011; Jones & Sayers, 2012). The mechanism of homeoprotein cell internalization is not completely understood but available data suggest that it does not require a receptor (Le Roux et al., 1993), occurs mainly by direct translocation and/or endocytosis (Duchardt, Fotin-Mleczek, Schwarz, Fischer, & Brock, 2007; Letoha et al., 2003; Christiaens et al., 2004) and requires specific aa within the internalization sequence, including a tryptohphan in position 48 (48W) (Le Roux et al., 1993).

In addition to Antennapedia, other homeoproteins have being shown to act in a non-cell autonomous way to regulate developmental processes that include: guidance of retinal growth cones and retinotectal patterning (Engrailed1-En1 and Engrailed2-En2, collectively Engrailed) (Brunet et al., 2005; Wizenmann et al., 2009), eye development and migration of oligodedrocyte precursors in the neural tube (Pax6) (Lesaffre, Joliot, Prochiantz, & Volovitch, 2007; Di Lullo et al., 2011), and visual cortical plasticity (Otx2) (Sugiyama et al., 2008). Among these homeoproteins, the sequence and secretion of En2 are the best characterized. In addition to an internalization sequence, En2 contains an 11

aa secretion sequence embedded in a nuclear export sequence (NES), as well as a nuclear localization sequence (NLS) (Joliot et al., 1998; Maizel, Bensaude, Prochiantz, & Joliot, 1999). En2 secretion involves several steps. First, En2 is translated in the ribosome and its possession of an NLS allows it to pass through the nucleus. Second, once in the cytoplasm, En2 associates with membrane fractions of cholesterol and glycosphingolipids forming rafts or caveolae-like vesicles (Joliot et al., 1997). This packing process is regulated by phosphorylation of the En2 N-terminal region by casein kinase II (Maizel et al., 2002). Finally, En2 is secreted into the extracellular space where it is internalized by adjacent cells and induces local protein translation leading to guidance of retinal growth cones and retinotectal patterning (Brunet et al., 2005).

Although they have prominent developmental functions, expression of several homeoproteins persists throughout adulthood, suggesting that they play relevant but poorly understood roles in cellular function throughout life. Growing evidence shows that homeoproteins in adult mice play a key role in neuroprotection and neuronal function (Joshi et al., 2011). It has being shown that En1 haploinsuficient mice display a progressive degeneration of mesecephalic dopaminergic (mDA) neurons, leading to a severe motor and behavioral phenotype similar to human Parkinson's disease (PD) (Sgado et al., 2006). Interestingly, it has being shown that in En1 haploinsuficient mice, infusion of En2 above the substantia nigra stops cell death of mDA neurons (Sonnier et al., 2007). The authors showed that En2 infused into the extracellular space was internalized by En1-deficient mDA neurons and stop their death which demonstrates that En1 and En2 have an equivalent ability to regulate mDA neuron survival (Sonnier et al., 2007).

Recently, it has being shown that exogenous Engrailed-1 and Engrailed-2 protect mDA neurons from 1-methyl-4-phenyl-1,2,3,6-tetrahydropyridine (MPTP), a mitochondrial complex I toxin used to model Parkinson's disease in animals (Alvarez-Fischer et al., 2011). The mechanism of Engrailed-mediated cell protection involves Engrailed phosphorylation of the eukaryotic translation initiation factor 4E (eIF4E) and eIF4E binding protein 2, which regulates translation of two subunits of the mitochondrial complex I, Ndufs1 and Ndufs3 (Topisirovic et al., 2005; Alvarez-Fischer et al., 2011). In addition to the Engrailed role in mDA survival, Engrailed infused into adult mouse brains increases striatal dopamine and induces changes in motor behavior (Alvarez-Fischer et al., 2011). Around 200 homeoproteins share the binding site to eIF4E, suggesting that regulation of protein translation may be a common mechanism of action of these proteins, but it has not being demonstrated yet (Topisirovic & Borden, 2005).

Another homeoprotein transcription factor involved in neuroprotection is Otx2. During development, this homeoprotein is required for photoreceptor cell fate determination (Nishida et al., 2003). Interestingly, Otx2 mRNA is found in photoreceptors and bipolar cells whereas Otx2 protein is found in photoreceptors, bipolar cells and retinal ganglion cells (RGCs) (Koike et al., 2007; Rath, Morin, Shi, Klein, & Moller, 2007). The presence of Otx2 protein in RGCs suggested that Otx2 might be taken up by RGCs from bipolar cells and/or photoreceptors. In fact, it has being shown that Otx2 infused into the eyes can be trans-synaptically transferred to parvalbumin cells in the visual cortex, where Otx2 participates in the opening of the critical period for ocular dominance plasticity (Sugiyama et al., 2008). In addition to Otx2's essential role during retinal development, it has being shown *in vivo* that secretion and internalization

of Otx2 in adult mice is essential for the survival of RGCs in a NMDA-mediated excitotoxic model (Torero Ibad et al., 2011). We have shown that Rax participates in the proliferation of tanycyte progenitors and continues to be expressed in terminally differentiated tanycytes, where its functional role remains unknown. Even though Rax has been widely studied in the retina, evidence of RAX protein secretion, either within the retina or in any other structure in the visual system, has not been found during development or adulthood (Furukawa et al., 1997; Mathers et al., 1997). Moreover, to our knowledge, RAX protein expression in the hypothalamus has never being studied. To begin deciphering the role of Rax in terminally differentiated tanycytes and explore the possibility of RAX secretion in the hypothalamus, we characterized RAX protein expression in the adult murine hypothalamus. Also, we attempted to eliminate Rax in terminally differentiated tanycytes by viral infection of $Rax^{f/f}$ mice and through a genetic approach. We found that RAX protein is present in hypothalamic cells which do not have Rax mRNA expression, including ependymal cells, adjacent parenchymal cells and neurons in the lateral hypothalamic area (LHA). In addition, we found that RAX protein is abundant in the median eminence (ME), especially in the palisade layer, and that RAX is secreted *in vitro*. Finally, significant Rax elimination in the majority of terminally differentiated tanycytes was not possible to achieve with any of the two approaches used.

5.2. Results

5.2.1. RAX protein distribution differs from Rax mRNA distribution in the hypothalamus

To understand the role of Rax in hypothalamic terminally differentiated tanycytes, we examined RAX protein expression in adult mice (P45). At low resolution, RAX

protein was found in the ventral portion of the wall of the third ventricle along the anterior to posterior axis of the hypothalamus and in the ME in a distribution similar to Rax mRNA (Figure 5.1, compare with Figure 2.2 in **Chapter 2**). However, RAX protein signal differed from Rax mRNA in two regions; the more external layer of the median eminence (palisade layer), where RAX protein was abundant and Rax mRNA is low, and in the roof of the third ventricle of the posterior hypothalamus, where there is no Rax mRNA due to the presence of ependymal cells (Figure 5.1, compared with Figure 2.2 in **Chapter 2**). At higher resolution, we also found RAX protein in the roof of the third ventricle of the tuberal hypothalamus (Figure 5.2) and in all the layers of the ME, from the ependymal layer, where β2 tanycyte cell bodies are located (TL), to the more external palisade layer (PL) where β2 and β1 tanycyte processes end (Figure 5.2). Interestingly, within the ME, RAX protein signal was observed in close proximity to the trajectory of tanycyte processes and appeared to accumulate in the PL (Figure 5.2).

Low-resolution imaging also revealed RAX protein signal adjacent to the third ventricle and in lateral hypothalamic cells. In the anterior portion of the tuberal hypothalamus, some of these RAX-positive cells seemed to be located in the DMH and distally in the LHA (Bregma -1.455 and -1.555). In the medial portion of tuberal hypothalamus (Bregma -1.555, -1.655, -1.855), RAX-positive cells aggregated in the LHA and their number decreased posteriorly, where they disappear from the LHA and appear in the PH (Bregma -1.955 and -2.005) (Figure 5.3). These cells were not observed in either the Rax mRNA fISH or in control immunostaining that did not include the anti-Rax primary antibody (Figure 5.4A). Furthermore, in a $Rax^{+/+}$;$NestinCreERT2^{/+}$;$R26RYFP^{/+}$ mouse, induced at P45 with 4-OHT, RAX protein

staining showed that the LHA RAX-positive cells did not express nestin and were instead positive for the neuronal marker Hu (Figure 5.4 B).

Interestingly, RAX protein signal outside tanycyte nuclei, including all layers of the ME, ependymal cells and in the hypothalamic parenchyma, had a granular appearance whereas RAX protein signal inside tanycytes nuclei was smooth, or a combination of smooth and granular (Figure 5.2). The granular signal associated with the smooth signal in tanycyte cell bodies increased dorsally, starting in β tanycytes, became more abundant in the α tanycytes and changed to a exclusively granular pattern in the roof of the third ventricle, where ependymal cells are located (Figure 5.2). Moreover, RAX signal in the hypothalamic parenchyma sometimes formed ring shapes around DAPI stained nuclei, suggestive of cytoplasmic localization of RAX protein in parenchymal cells (Figure 5.2). Finally, abundant, widely dispersed RAX granular signal was observed in the intercellular spaces of ventricle adjacent nuclei (DMH, VMH, ArcN) and was much lower in the LHA (Figure 5.2 and Figure 5.6).

5.2.2. Viral mediated elimination of Rax in terminally differentiated tanycytes

We attempted to eliminate Rax by i.c.v injection of AAV1-GFP-Cre into P45 $Rax^{f/f}$ mice. Four weeks after injection, mice were sacrificed (Figure 5.5 A) and AAV1-infected cells, identified by their expression of GFP, were observed in the ventricular wall and in the hypothalamic parenchyma (Figure 5.5B). Ventricular GFP^{+} cells corresponded to ependymal cells (Figure 5.7) and tanycytes, whose cell bodies and processes were both labeled with GFP (Figure 5.5B). In ventral regions, tanycytes were effectively infected but the efficiency decreased dorsally where ependymal cells are

located (Figure 5.7). In the hypothalamic parenchyma, we observed GFP^+ cells, as well as blood vessels enveloped by GFP^+ tanycyte processes (Figure 5.5B).

To determine whether infection with AAV1-Cre-GFP was sufficient to eliminate RAX in $Rax^{f/f}$ mice, we examined RAX protein signal along the wall of the third ventricle as well as in the LHA in brain sections from $Rax^{f/f}$-AAV1-Cre-GFP and $Rax^{+/+}$-AAV1-Cre-GFP mice. We compared RAX protein signal in these sections to sections from $Rax^{f/f}$-AAV1-Cre-GFP mice in which the primary antibody was omitted during staining. We found that RAX signal in ependymal cells, LHA cells and tanycytes was clearly distinct from signal in the no anti-Rax control, indicating that RAX protein signal profile was specific and did not correspond to background (Figure 5.6 to 5.10). There were no qualitative differences in total RAX protein signal in the ependymal cells, LHA cells and α tanycytes of the $Rax^{f/f}$-AAV1-Cre-GFP mice compared to $Rax^{+/+}$-AAV1-Cre-GFP controls (Figure 5.6 and Figure 5.10), suggesting that infection with AAV1-Cre-GFP did not eliminate RAX protein from these cells. However, in β2 tanycytes we did observed some qualitative differences between brain sections from $Rax^{f/f}$-AAV1-Cre-GFP (n=3) and $Rax^{+/+}$-AAV1-Cre-GFP (n=2) mice. In $Rax^{+/+}$-AAV1-Cre-GFP β2 tanycytes, RAX granules were closely associated with their processes, both proximal and distal to their cell bodies (Figure 5.11A). In contrast, in $Rax^{f/f}$-AAV1-Cre-GFP mice, some infected □2 tanycytes (GFP^+ Rax^- nuclei) did not have RAX associated with their processes, and in some cases, did not seem to have any process (Figure 5.11 B). Furthermore, RAX signal in β2 tanycyte cell bodies of $Rax^{f/f}$-AAV1-Cre-GFP mice looked predominantly granular instead of smooth as is seen in the $Rax^{+/+}$-AAV1-Cre-GFP mice. Finally, overall RAX signal in the ME was reduced in $Rax^{f/f}$-AAV1-Cre-GFP

mice and had a disorganized distribution that did not seem to follow tanycyte processes (Figure 5.11A).

5.2.3. RAX is secreted by tanycytes

We have shown that RAX protein is expressed in brain regions where there is no Rax mRNA (ependymal cells, adjacent hypothalamic parenchymal cells, intercellular spaces LHA neurons and the external layer of the ME). In addition, we found that RAX protein signal has a granular appearance in those regions and that it is closely associated with β tanycyte processes especially in their terminals located in the palisade region of the ME. Finally, we observed that RAX protein is absent from the processes of GFP^{+} Rax^{-} β2 tanycytes in $Rax^{f/f}$-AAV1-Cre-GFP mice. Together, these observations suggest that RAX is secreted by tanycytes. To start exploring this hypothesis, we performed protein alignment of mouse RAX protein with the four murine homeoproteins known to be secreted *in vivo*: Pax6, Engrailed 1 and 2, and Otx2 (Brunet et al., 2005; Lesaffre et al., 2007; Di Lullo et al., 2011; Sugiyama et al., 2008). Spatazza *et al* has suggested a consensus secretion and internalization sequence based on the aligment of ten homeoproteins known to be secreted and internalized *(Spatazza et al., 2013)*. Using Spatazza's consensus sequences as a reference, we found that RAX contains the consensus secretion sequence except for the third position where it has a "V" instead of an "L" or an "I". However, V is an aliphatic amino acid, as are "L" and "I". In addition, RAX contains the entire consensus internalization sequence, including the tryptophan (W), which is essential for translocation into live cells (Le Roux *et al.* 1993) (Figure 5.12 A). Furthermore, we observed that mouse RAX and human RAX protein are identical in the homeodomain region (100% homology) containing the secretion and internalization

sequence (Figure 5.12 B). Based on this *in silico* analysis and RAX protein signal in the hypothalamus, we wanted to test RAX secretion *in vitro*, along with other homeoprotein TFs. When three different cell lines (293T, MDCK and GT1-7) were transfected with human RAX clones, RAX protein secretion was observed in all three cell lines. However, the level of RAX secretion was about half as efficient as that of the positive control En2 (Figure 5.13).

5.2.4. Genetic conditional ablation of Rax in terminally differentiated tanycytes does not result in a significant reduction of Rax mRNA

RAX protein distribution in the hypothalamus, the *in silico* analysis of RAX protein sequence, and the *in vitro* secretion of RAX, strongly suggest that RAX is secreted by hypothalamic tanycytes. If tanycytes are the source of secreted RAX in the hypothalamus, an elimination of Rax mRNA in terminally differentiated tanycytes should lead to a reduction of RAX protein in ependymal cells, LHA and hypothalamic parenchyma and ME. Because viral infection of terminally differentiated tanycytes in $Rax^{f/f}$ mice with AAV1-Cre-GFP only led to a reduction in β2 RAX secretion and did not significantly reduce RAX in the majority of tanycytes, we attempted to eliminate Rax in terminally differentiated tanycytes through a genetic approach. $Rax^{f/f}$ mice were bred to mice expressing inducible Cre recombinase ($CreER^{T2}$) under control of the nestin promoter, which is specific for progenitors throughout the CNS, including tanycytes (Lee D. *et al.* 2012). Double transgenic $Rax^{f/f}$;Nestin:$CreER^{T2}$ and $Rax^{f/-}$;NestinCreERT2 mice were induced with 4-OHT at P45 and sacrificed five days later. Unfortunately, we did not see any significant difference in Rax signal in terminally differentiated tanycytes between the two genotypes when Rax mRNA was quantified using image analysis

(Figure 5.14). As a consequence, we did not quantify RAX protein distribution differences between genotypes.

5.3. Discussion

We have shown that Rax mRNA in the hypothalamus is expressed only in tanycytes and in the ME. Surprisingly we have also found that RAX protein is expressed in hypothalamic areas where there is no Rax mRNA. In the dorsal area of the tuberal hypothalamus, RAX protein is present not only in terminally differentiated tanycytes but also in ependymal cells, neurons of the LHA and other hypothalamic parenchymal cells as well as in the intercellular space. Ventrally, RAX protein is found in the ME along β tanycyte processes and is especially abundant in the palisade layer where tanycyte processes terminate. The mismatch between Rax mRNA and RAX protein signal distribution in the hypothalamus is suggestive of RAX secretion. In fact, *in silico* analysis of RAX protein homeodomain region revealed the presence of homeoprotein secretion and internalization sequences. In addition, *in vitro* secretion analysis of human RAX protein confirmed the ability of RAX to be secreted. Together our data suggest that RAX protein is secreted by tanycytes. α tanycytes secrete RAX directly from their cell bodies to the hypothalamic parenchyma where it is then internalized into ventricle adjacent cells . RAX also reaches dorsal ependymal cells and distal neurons of the LHA and cells of the PH. In the β tanycytes, RAX protein is translated and transported along the tanycyte processes and is secreted in the ME, especially in the more external palisade layer where tanycyte processes terminate. We found that viral-mediated elimination of RAX in terminally differentiated tanycytes leads to a partial reduction of RAX only in the β2 tanycytes, but did not alter RAX in the majority of tanycytes, especially dorsal α

tanycytes. Conditional genetic approaches aimed at ablating Rax were also not effective in blocking RAX production in tanycytes.

RAX is secreted by tanycytes and is internalized by adjacent and distal cells

Rax is a homeoprotein TF. The role of homeoproteins during development has being widely studied and findings indicate that they are essential for transcriptional regulation of genes involved in cell positioning (Pick & Heffer, 2012). In contrast, their function in the adult organism is poorly understood.

Recently, Spatazza et al. suggested a consensus secretion and internalization sequence based on the alignment of ten homeoproteins known to be secreted. Secretion of six of these proteins has only been tested *in vitro* (HoxA5, HoxB4, HoxB8, HoxC8, Pdx1, Emx2) (Spatazza et al., 2013), whereas the other four have been studied *in vivo* (Pax6, En1/2, Otx2) (Lesaffre et al., 2007; Di Lullo et al., 2011; Brunet et al., 2005; Wizenmann et al., 2009; Sugiyama et al., 2008). Interestingly, we found that RAX contains these consensus sequences. The similarity between Rax and other known secreted homeoproteins strongly suggests that RAX could share functional properties with these proteins. It is important to highlight that the secretion and internalization sequences are located in the homeodomain, which is highly conserved within the homeoprotein family and across species (Laughon, 1991). This conservation suggests that most homeoproteins should have the ability to be secreted and internalized. However, secretion and internalization have only been demonstrated for a few members of this large family (Prochiantz & Joliot, 2003; Spatazza et al., 2013).

Since mouse and human RAX have identical homeodomain sequences, we tested RAX secretion *in vitro* using human RAX clones transduced into three different cells

lines and confirmed RAX secretion in all cell lines. However, RAX secretion was not as strong as En2 secretion, which was used as a positive control. This difference in secretion efficiency could be due to variability in the inherent secretion ability of the different homeoproteins and due to the influence of cell culture conditions on individual homeoprotein secretion.

RAX secretion was further suggested by the distribution of its protein signal. We found that in the tuberal hypothalamus RAX protein is present in areas where no Rax mRNA can be detected. It is unlikely that the observed RAX staining found in this study correspond to non specific signal; the antibody was raised against a very specific peptide region of RAX protein (PKAPAGGSESSPPAAPGFVPEYEATRP), followed by affinity purification with the same peptide and specificity was confirmed by western blot (Muranishi et al., 2011). Furthermore, RAX staining with this antibody in the retina showed specific signal in the expected layers (Muranishi et al., 2011) without any evidence of secretion (personal communication). In addition, in our experiments we used control staining from which the primary antibody was omitted, and these lacked the characteristic RAX signal seen in our experimental samples. Taken together, we believe that the RAX signal observed corresponded to real RAX protein distribution in the hypothalamus.

Interestingly, RAX signal presented two different patterns, a smooth signal mostly found in the nuclei and a granular signal found in hypothalamic areas that lack Rax mRNA. Similar granular signals have been observed in secreted En2 stainings (Joliot et al., 1991; Layalle et al., 2011) and FITC-labeled homeodomains (Spatazza et al., 2013), suggesting that RAX granular signal corresponds to RAX secretory granules. Rax

granules are abundant in β tanycyte processes but absent from α tanycyte processes. However, RAX protein is observed in hypothalamic parenchyma adjacent to α tanycytes. Thus, RAX secretion from α tanycytes does not seem to require tanycyte processes. RAX granules can be seen in the ventricular layer, suggesting that in the α tanycytes RAX is translated mainly in their cell bodies, packed and secreted directly from the cell body, not through the processes. Once RAX is secreted from α tanycytes, the internalization sequence will allow RAX internalization by ventricle adjacent cells, which accounts for the presence of RAX in the intercellular space and surrounding parenchymal DAPI stained nuclei. RAX could also reach ependymal cells from α1 tanycytes by secretion followed by lateral translocation along the wall of the third ventricle.

Several rounds of internalization and secretion could move RAX from cell to cell laterally away from the ventricle and dorsally to the ependymal cells. This mechanism of RAX diffusion is similar to the known mechanism of morphogene gradient formation by planar transcytosis (Entchev & Gonzalez-Gaitan, 2002). Interestingly, it has being proposed that homeoproteins, in addition to regulating the expression of morphogenes, can behave as morphogenes themselves (Brunet et al., 2007). Brunet et al. has suggested that the intercellular passage of homeoproteins seems to be a simple mechanism for the transfer of positional information during morphogenesis (Brunet et al., 2007). Indeed, this phenomenon has already been demonstrated for En2 (Wizenmann et al., 2009; Layalle et al., 2011) and Pax6 (Lesaffre et al., 2007; Di Lullo et al., 2011). However, the purpose of gradient formation in mature organisms remains unclear. Also, RAX function in ependymal cells and ventricle adjacent hypothalamic cells is completely unknown.

Intriguingly, we found RAX signal in LHA neurons and in cells of the PH. Even though planar transcytosis can move a molecule further form its source, it will become diluted with distance and, as a consequence, this mechanism would not explain how RAX reaches the LHA and PH. Most likely RAX would reach the LHA neurons by trans-synaptic transport as has being reported for Otx2 in the visual system *(Sugiyama et al., 2008)*. This hypothesis is supported by the presence of abundant projections from the DMH to the LHA, some of which have been implicated in regulating wakefulness (Thompson, Canteras, & Swanson, 1996). Interestingly, Rax expression in mature pineal gland increases during the light period of the day (Rohde, Klein, Moller, & Rath, 2011). Also, it has been reported that tanycytes have transcriptional changes in response to light (Kameda, Arai, & Nishimaki, 2003; Bolborea et al., 2011). These published data, together with our observation of RAX protein in terminally differentiated tanycyte and LHA neurons, raises the possibility that Rax mRNA of terminally differentiated tanycytes could change in response to light and that RAX protein could be trans-synaptically transferred to the LHA to transmit photoperiodic information. Simultaneously, RAX might be contributing to the survival of LHA neurons similar to the role of En2 in mDA neurons (Sonnier et al., 2007).

RAX is translated and transported along β tanycyte processes and secreted in the palisade layer

In Chapter 2, we reported that Rax mRNA was found in all layers of the ME. Also, it is known that tanycytes have ribosomes in their processes and, which could be involved in translating mRNAs (Rodriguez et al., 2005). In this chapter we have described that RAX protein is closely associated with β tanycyte process and it is

abundant in the palisade layer of the ME where β tanycyte processes end and where Rax mRNA is low. Together, the presence of Rax mRNA in the ME in association with Vim^+ processes, the abundance of ribosomes in tanycyte processes and the RAX protein granular signal in the tanycyte terminals suggest that RAX can be translated in tanycyte processes, packed in secretory granules and transported to β tanycyte terminals where it is secreted. It is known that β1 tanycytes have the ability to secrete transforming growth factor α (TGFα) and PGE2 after estrogen stimulation, which in turns regulate release of GnRH *(Prevot et al., 1999; Prevot et al., 2003; de Seranno et al., 2004; de Seranno et al., 2010)*. Also, it has been shown that pyroglutamyl peptidase II mRNA, which encodes a highly specific membrane-bound metallopeptidase that inactivates TRH in the extracellular space (Charli et al., 1998), is present along β2 tanycytes process and it accumulates in the palisade layer of the ME where PPII protein contributes to the regulation of the amount of TRH released into the portal circulation (Sanchez et al., 2009). This is similar to our observations of Rax mRNA and RAX protein signal distribution in β2 tanycytes and ME. Interestingly, the secretory ability of tanycytic process terminals seems to be an exclusive property of β tanycytes, which have a well-developed smooth endoplasmic reticulum, tubular structures and multiple vesicles in their terminals, ultrastructural characteristics not present in the α tanycytes (Rodriguez et al., 2005). Such a divergence in morphological features would explain the absence of RAX granular signal in the α tanycytes processes.

The abundance of RAX in the most external layer of the ME is intriguing, as the palisade layer is almost completely devoid of cell bodies. This layer is primarily composed of cell fibers passing to the infundibulum from various nuclei, which penetrate

the PL and terminate in the capillaries of the primary plexus, where the fibers release neuropeptides into the portal circulation (Ojeda et al., 2008). TGFα, PGE2 and PPII secretion in the palisade layer leads to regulation of GnRH and TRH, respectively, thus, raising the possibility that RAX protein might be regulating neuropeptide release. Another possibility is that RAX secreted in the PL could diffuse to more internal ME layers to promote the survival of median eminence cells, including newborn neurons. In fact, we found RAX protein in all layers of the ME and in deep ME cell nuclei that are unlikely to be tanycytes. Also, it has been reported that homeoproteins promote cell survival through the control of protein translation (Sonnier et al., 2007) and that β2 tanycytes can give rise to neurons in the ME (Lee et al., 2012). Thus, RAX might contribute to the survival of these newborn neurons together with other factors secreted in the ME. Furthermore, RAX could also provide cues for neuronal differentiation of progenitors in the ME similar to the homeoprotein Pax6 in the adult SVZ (Hack et al., 2005; Kohwi, Osumi, Rubenstein, & Alvarez-Buylla, 2005).

Attempt to eliminate Rax using viral and conditional genetic ablation was not effective

RAX viral infection in $Rax^{f/f}$ mice led to an inefficient RAX elimination, leaving a large population of tanycytes as infected, yet RAX^{+} cells (RAX^{+} GFP^{+}). Interestingly, AAV1-Cre-GFP infection in Rax $^{f/f}$ mice induced an increase in RAX granules in the tanycyte layer of the ME and a reduction of RAX in tanycyte processes and in the medial and external layers of the ME. This switch in protein localization might indicate that in non-infected tanycytes, RAX was predominantly translated in the cell bodies, not in the processes of β tanycytes and that it was secreted from the cell body directly to adjacent

infected tanycytes, giving the appearance of inefficient RAX elimination (GFP^+, RAX^+ cells). However, this intriguing observation requires confirmation through a quantitative analysis of mice with a longer AAV1-Cre-GFP infection which will increase the number of infected α and β tanycytes (Passini et al., 2003), and, as a consequence, allow the characterization of the role of RAX not only in tanycytes but also in other hypothalamic cells that internalize RAX.

Genetic conditional ablation of Rax in terminally differentiated tanycytes was expected to occur since we were able to induce a 50% decrease of Rax mRNA in developing tanycytes. However we did not observe any significant change of Rax mRNA levels in terminally differentiated tanycytes. This might be caused by the intrinsic nature of the $NestinCreER^{T2}$ mouse line, which is known to lead to a mosaic elimination of target genes (Balordi & Fishell, 2007), making it difficult to achieve a significant reduction of Rax in tanycytes. As the same cre line was used successfully during development to induce a significant reduction of Rax, the mosaicism associated with the $NestinCreER^{T2}$ line seems to be greater in terminally differentiated tanycytes. Such age dependent variation in the efficiency of cre activation has been described for several inducible Cre lines (Michael, Brennan, & Robertson, 1999; Postic & Magnuson, 2000). A more effective Cre line specific for tanycytes will be necessary to eliminate Rax in tanycytes and to evaluate the consequent phenotype.

In conclusion, our data strongly suggest that RAX protein is secreted by terminally differentiated tanycytes. RAX secretion from β tanycytes occurs through their processes, whereas the α tanycytes secrete RAX directly from their cell bodies. Secreted RAX is internalized by ependymal cells, ventricle adjacent hypothalamic cells and distal

neurons of the LHA (Figure 5.13). Further experiments to determine the *in vivo* distribution of RAX protein by i.c.v injection of biotinylated RAX or FITC-labeled RAX will confirm RAX ability to translocate cells. Also, *in vitro* testing of RAX secretion in cultured tanycytes together with a broad elimination of Rax in tanycytes through a long AAV1-Cre-GFP infection of $RAX^{f/f}$ mice or through a genetic conditional ablation of Rax using a more effective tanycyte specific cre line will confirm that tanycytes are the source of secreted RAX in the hypothalamus. Finally, immunohistochemical characterization of RAX^{+} hypothalamic parenchymal cells and specific blocking of RAX in the extracellular space will facilitate the understanding of the functional role that RAX secretion plays in adult hypothalamic cells.

Figure 5.1.

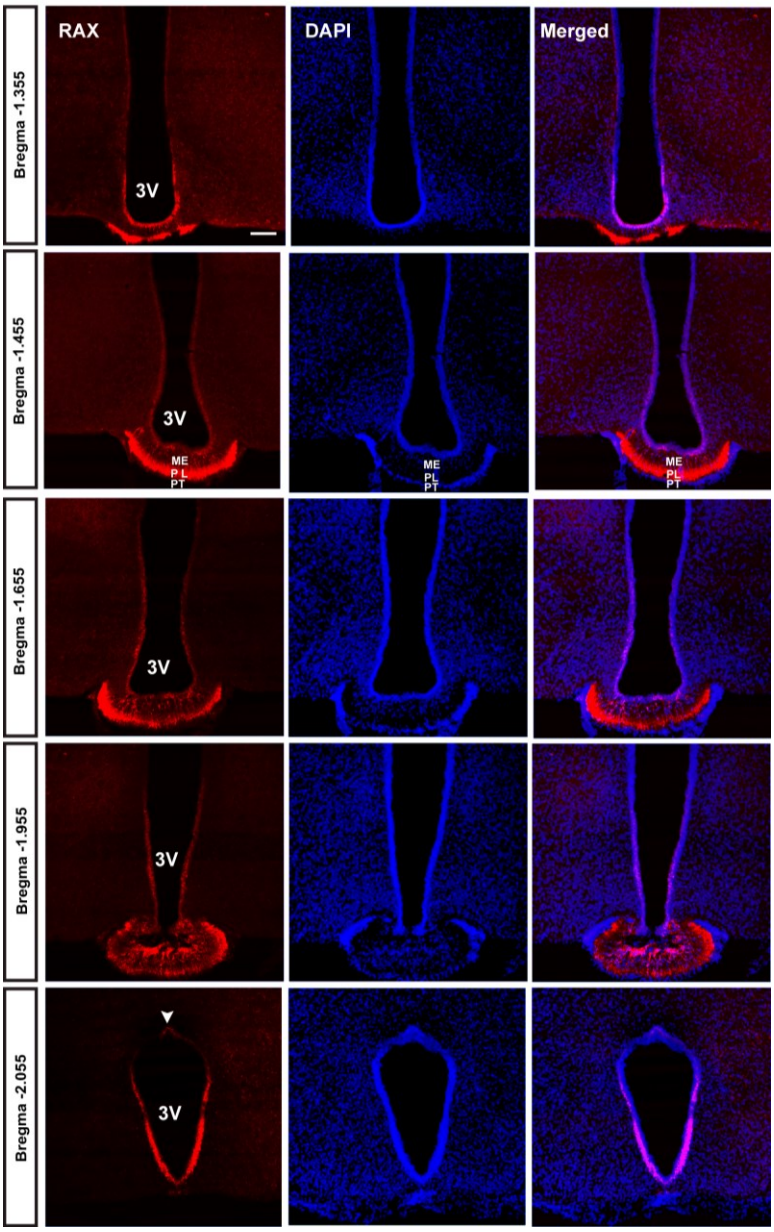

Figure 5.1. RAX protein expression in the ventricular wall of the tuberal hypothalamus

RAX IHC (red) in the tuberal hypothalamus of adult (P45) C57BL/6 wild type mouse. RAX is present in the wall of the third ventricle along the anterior to posterior axis of the tuberal hypothalamus. RAX is particularly abundant in the most external layer of the ME (palisade layer, PL). RAX signal is seen in the roof of the third ventricle of the most posterior portion of the tuberal hypothalamus where ependymal cells are located (white arrow head). Weaker RAX signal is present throughout the hypothalamic parenchyma. 3V: third ventricle, ME: median eminence, PL: Palisade layer, PT: pars tuberalis, Scale bar: 20μm.

Figure 5.2.

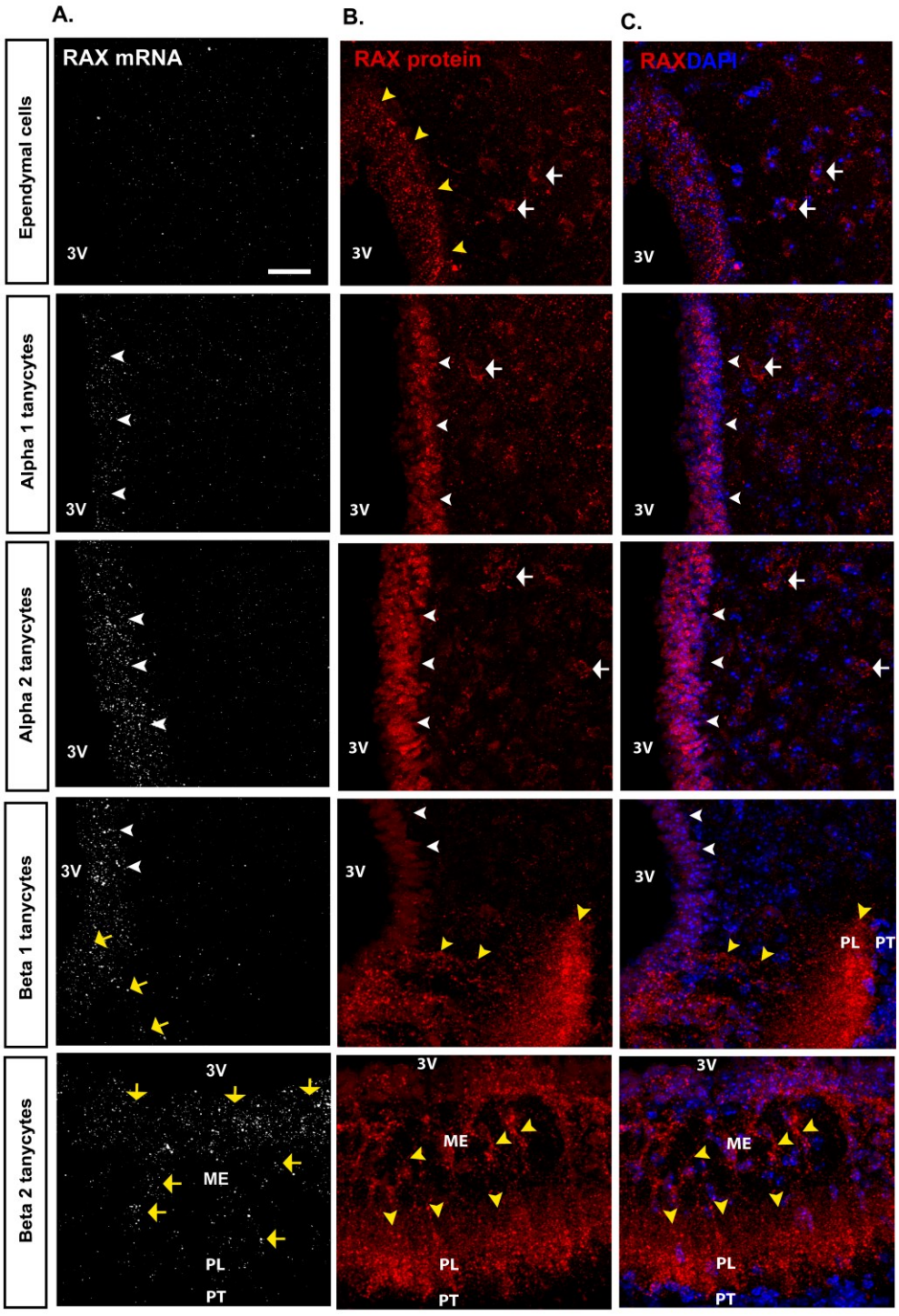
A.
B.
C.
RAX mRNA
RAX protein
RAXDAPI
Ependymal cells
Alpha 1 tanycytes
Alpha 2 tanycytes
Beta 1 tanycytes
Beta 2 tanycytes
3V
ME
PL
PT

Figure 5.2. RAX protein distribution in the wall of the third ventricle differs from Rax mRNA expression

Rax fISH (white), RAX IHC (red), and DAPI (blue) in adult (P45) C57BL/6 wild type mice. **A.** Rax mRNA is expressed the in cell bodies of terminally differentiated α tanycytes located in the wall of the ventral third ventricle (white arrow heads) and in the cell bodies and processes of β1 and β2 tanycytes in the median eminence (ME) (yellow arrows). **B and C**. RAX protein is not only found in terminally differentiated α and β tanycytes (white arrow heads), but also in ependymal cells and adjacent hypothalamic parenchyma. In addition, RAX is particularly abundant in the most external palisade layer (PL) of the ME (yellow arrow heads). Protein expression in terminally differentiated tanycytes is seen either as a smooth signal in tanycyte nuclei (white arrow heads in β1 tanycytes) or as a combination of smooth and granular signal (α tanycytes). The combined signal increases progressively along the dorsal axis until it becomes completely granular in the ependymal cells (yellow arrow heads). RAX granules are also found in the intercellular space of adjacent hypothalamic nuclei and also form ring shapes suggestive of a cytoplasmic localization of RAX protein in parenchymal cells (white arrows) 3V: Third ventricle. PL: Palisade layer, PT: pars tuberalis, ME: Median eminence. Scale bar: 20μm

Figure 5.3.

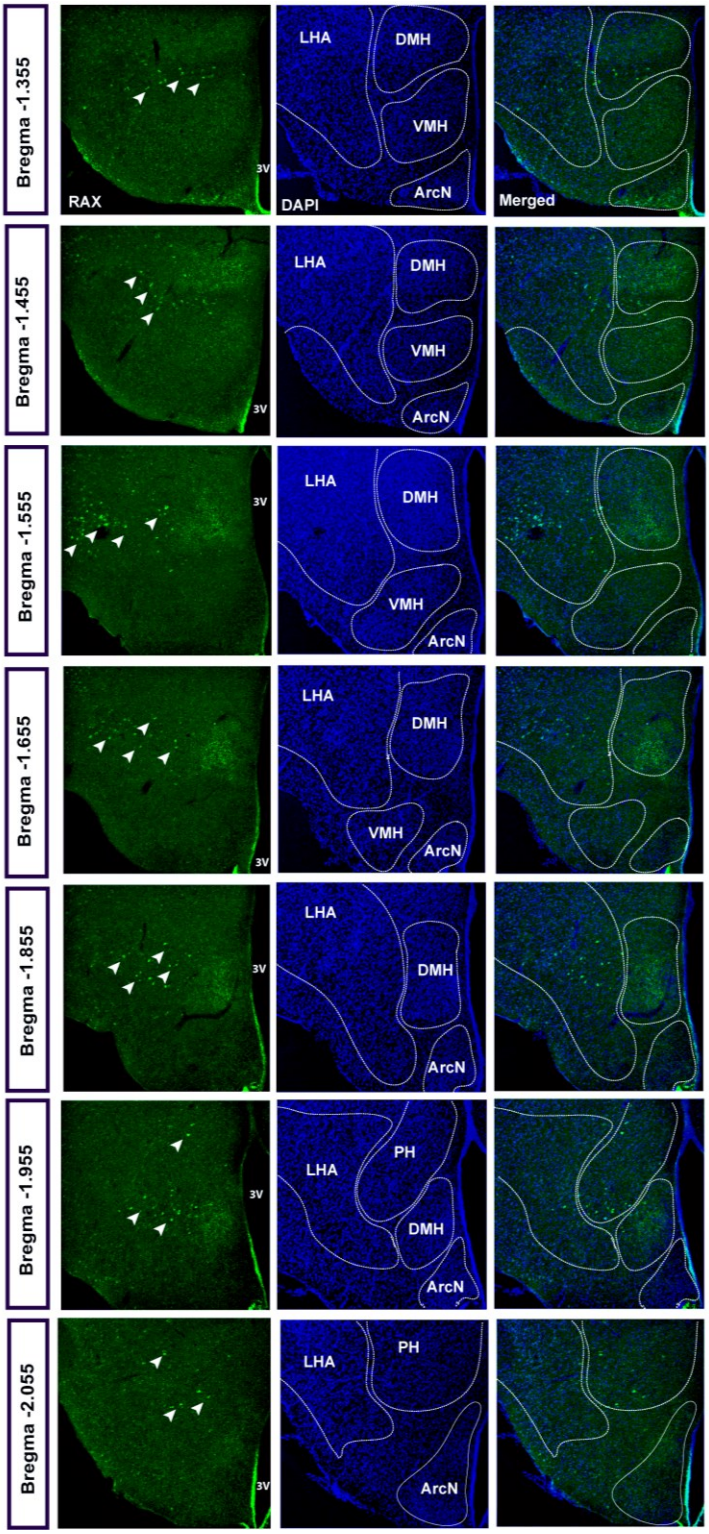
Bregma -1.355
RAX
3V
LHA
DMH
VMH
ArcN
DAPI
Merged
Bregma -1.455
Bregma -1.555
Bregma -1.655
Bregma -1.855
Bregma -1.955
PH
Bregma -2.055

Figure 5.3. RAX is present in the lateral hypothalamic area and in the posterior hypothalamic area

RAX IHC (green) across the anterior to posterior axis of the tuberal hypothalamus of adult (P45) C57BL/6 wild type mice. In the anterior portion of the tuberal hypothalamus (Bregma -1.355), RAX^+ cells (white arrow heads) are located close to the ventricle, primarily in the ventral portion of the DMH. In the medial portion of the tuberal hypothalamus (Bregma -1.555 to -1855), RAX^+ cells are located distal to the ventricle within the LHA. In the more posterior portion of the tuberal hypothalamus (Bregma -1.955 and -2.055), RAX^+ cells are mainly located in the PH. RAX protein is also present in the wall of the third ventricle at all bregma points of the tuberal hypothalamus. DMH: Dorsomedial hypothalamus, VMH: ventromedial hypothalamus, ArcN: Arcuate nucleus, LHA: Lateral hypothalamic area, PH: Posterior hypothalamic area, 3V: third ventricle.

Figure 5.4.

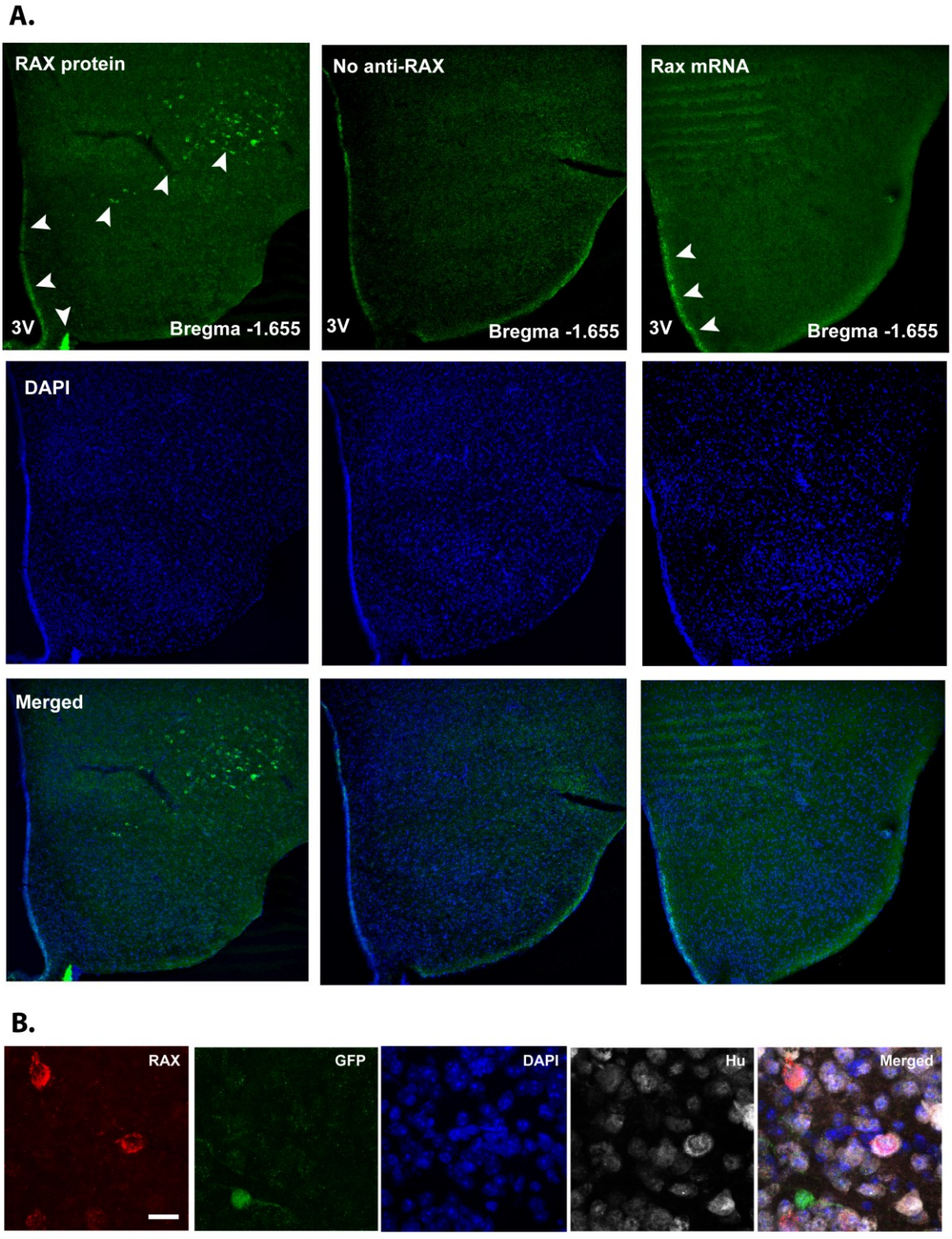
A.
RAX protein
No anti-RAX
Rax mRNA
3V
Bregma -1.655
3V
Bregma -1.655
3V
Bregma -1.655
DAPI
Merged
B.
RAX
GFP
DAPI
Hu
Merged

Figure 5.4. RAX protein in the lateral hypothalamic area is localized in neurons
A. RAX IHC with and without primary antibody and RAX fISH in the lateral region of the tuberal hypothalamus of adult (P45) C57BL/6 wild type mice. RAX protein (left panel) is present in lateral hypothalamic cells (distal white arrow heads) as well as in the wall of the third ventricle and the lateral palisade layer of the ME (white arrow heads adjacent to the ventricle). Rax mRNA (right panel) is present in the ventral portion of the ventricular wall. RAX^{+} cells in the LHA are neither observed in the control IHC with no primary antibody (middle panel) nor in the Rax fISH (right panel).. 3V: third ventricle. **B.** Immunohistochemistry for RAX (red), GFP (green), and Hu (white) in the LHA of tamoxifen-induced $Rax^{+/+}$; Nestin:$CreERT2^{R26RYFP}$ adult (P45) mouse. RAX is found in Hu^{+} cells of the LHA and is not found in $Nestin^{+}$ cells. In LHA neurons, RAX protein adopts a ring shape suggestive of cytoplasmic localization. Scale bar: 20μm.

Figure 5.5.

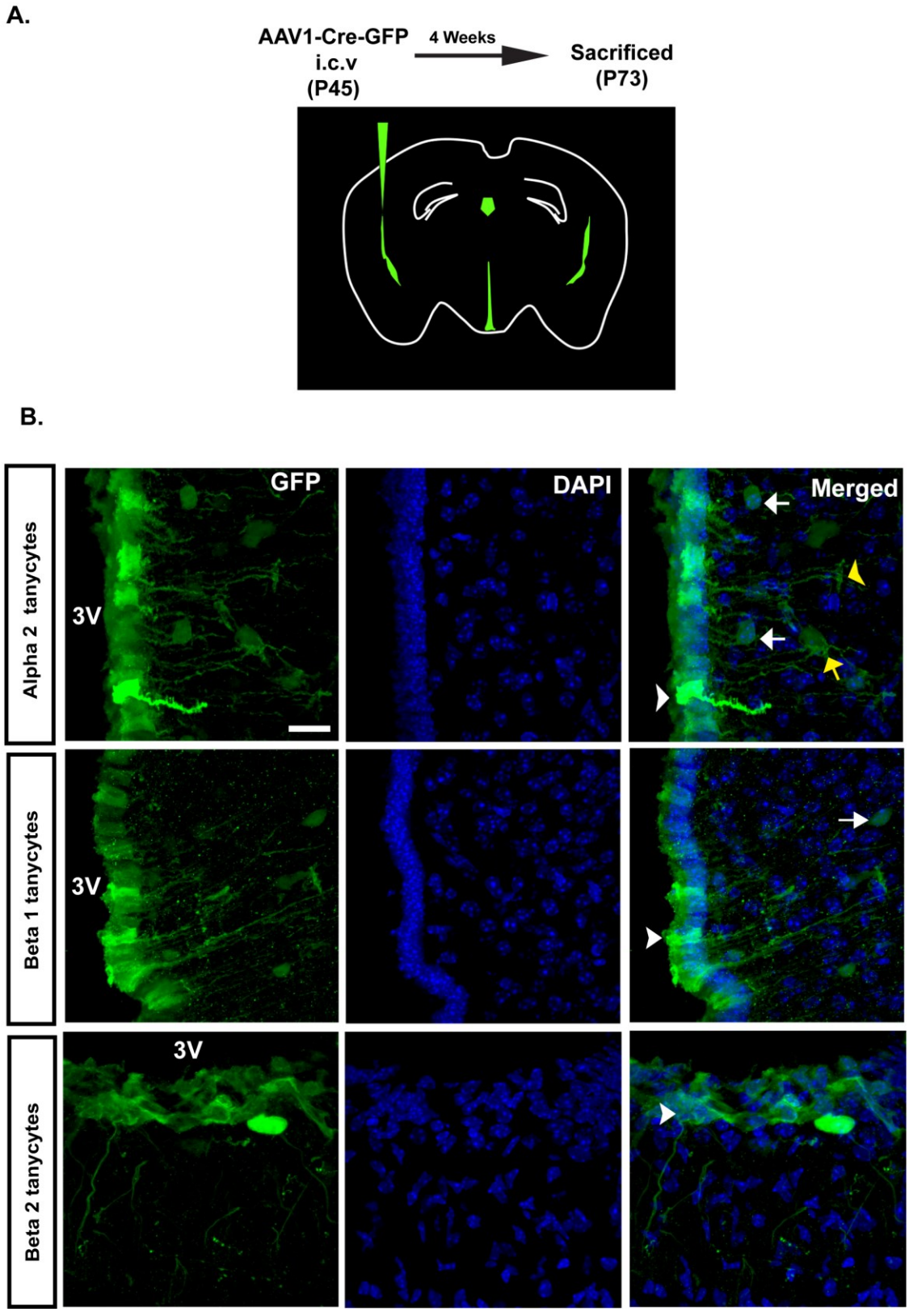
A.
AAV1-Cre-GFP
i.c.v
(P45)
4 Weeks
Sacrificed
(P73)
B.
Alpha 2 tanycytes
Beta 1 tanycytes
Beta 2 tanycytes
GFP
DAPI
Merged
3V
3V
3V

Figure 5.5. AAV1 viral infection of tanycytes and hypothalamic parenchymal cells

A. Cartoon illustrating the AAV1-Cre-GFP injection site and experimental timecourse. 1ul of AAV1-Cre-GFP was administered i.c.v in adult (P45) C57BL/6 wild type mice; mice were then sacrificed 4 weeks later (P73). **B.** GFP is found in tanycyte cell bodies and processes (white arrow heads) as well as in some cells in the hypothalamic parenchyma (white arrows). Some GFP^+ cells in the parenchyma are associated with tanycyte processes (yellow arrow). GFP labeled processes are also associated with blood vessels (yellow arrow head). 3V: third ventricle. Scale bar: 20μm

Figure 5.6.

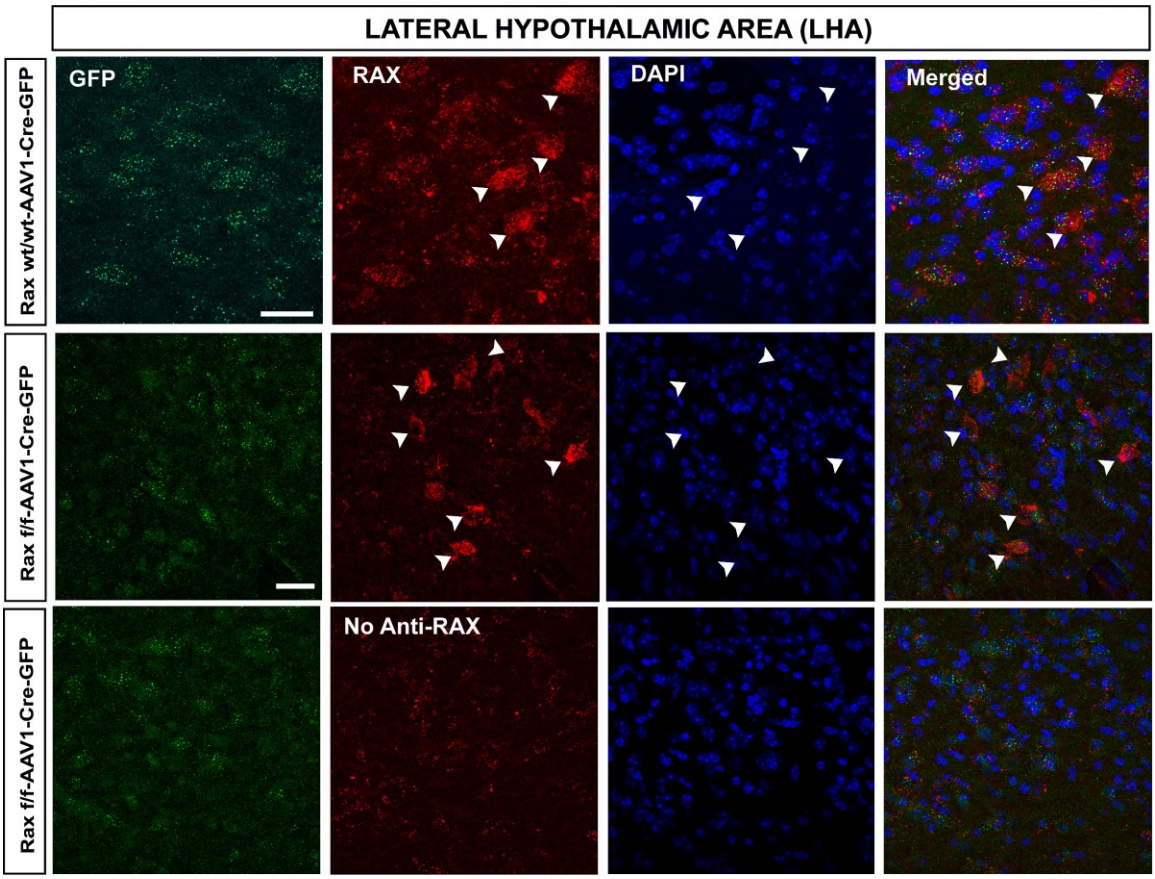

Figure 5.6. RAX protein in lateral hypothalamic cells
RAX protein (red) and GFP expression (green) in $Rax^{f/f}$ and $Rax^{wt/wt}$ mice four weeks after i.c.v injection of AAV1-Cre-GFP virus; images are maximum intensity projections of confocal z-stacks. RAX protein is found in lateral hypothalamic cells (white arrow heads). RAX protein is still present in LHA cells of $Rax^{f/f}$-AAV1-Cre-GFP. Negative control with no primary antibody (No anti-Rax) does not have specific granules and signal corresponds to background. 3V: Third ventricle. Scale bar: 20µm

Figure 5.7.

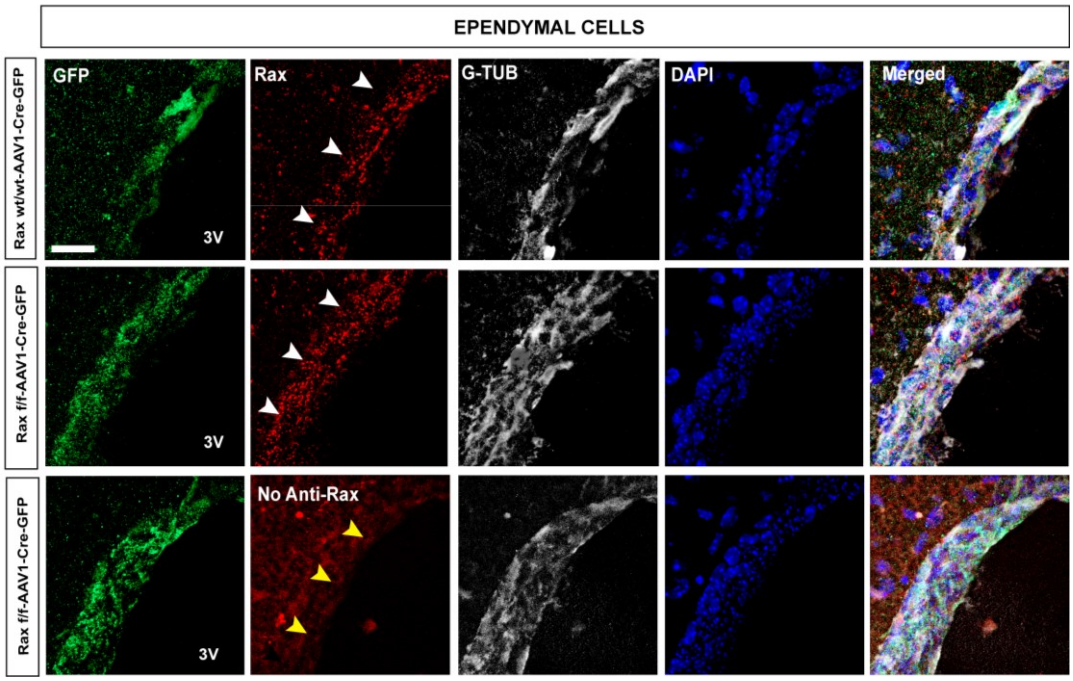

Figure 5.7. RAX protein in the third ventricle ependymal cells infected with AAV1-Cre-GFP

RAX protein (red), GFP expression (green), and G-TUB (white) in $Rax^{f/f}$ and $Rax^{wt/wt}$ mice four weeks after i.c.v injection of AAV1-Cre-GFP virus; images are maximum intensity projections of confocal z-stacks. RAX protein is found in ependymal cells ($G\text{-}TUB^{+}$) in a granular pattern (white arrow heads). Negative control with no primary antibody (No anti-Rax) does not have RAX^{+} granules and signal corresponds to background (yellow arrow heads). RAX protein is still present in ependymal cells of $Rax^{f/f}$-AAV1-Cre-GFP mice compared to $Rax^{wt/wt}$-AAV1-Cre-GFP control mice. 3V: third ventricle. Scale bar: 20µm

Figure 5.8.

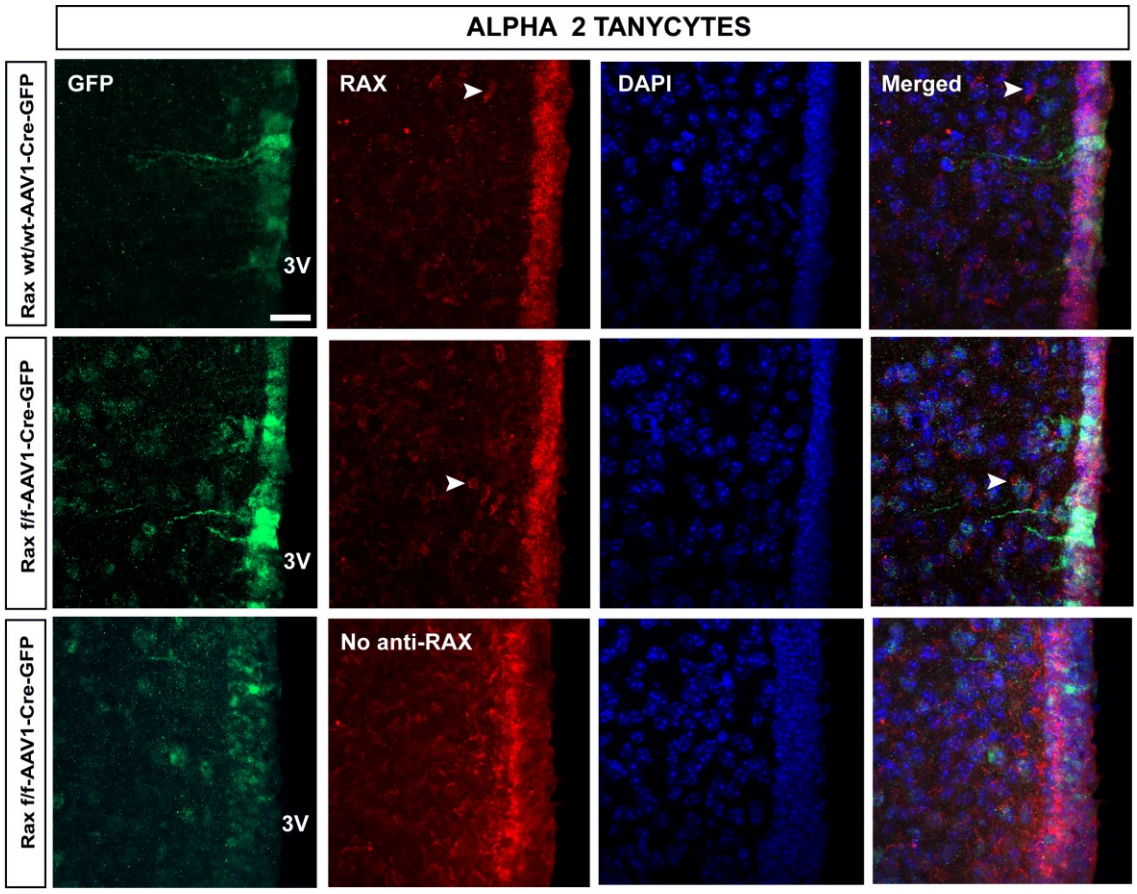

Figure 5.8. RAX protein in α2 tanycytes infected with AAV1-Cre-GFP virus
RAX protein (red) and GFP expression (green) in the α2 tanycytes of Rax $^{f/f}$ and Rax$^{wt/wt}$ mice four weeks after i.c.v injection of AAV1-Cre-GFP virus; images are maximum intensity projections of confocal z-stacks. RAX is found in the ventricular wall where tanycyte cell bodies are located. RAX signal persists in Rax$^{f/f}$-AVV1-Cre-GFP mice, indicating that RAX protein is apparently not reduced in α2 tanycytes of Rax $^{f/f}$-AAV1-Cre-GFP mice compared to Rax$^{wt/wt}$-AAV1-Cre-GFP control mice. Granular RAX signal is found in tanycytes and in the hypothalamic parenchyma, where RAX surrounds DAPI^{+} nuclei in a manner suggestive of cytoplasmic location (white arrow heads). RAX signal in both genotypes is distinct from the signal in the no anti-RAX control IHC. 3V: third ventricle. Scale bar: 20 μm.

Figure 5.9.

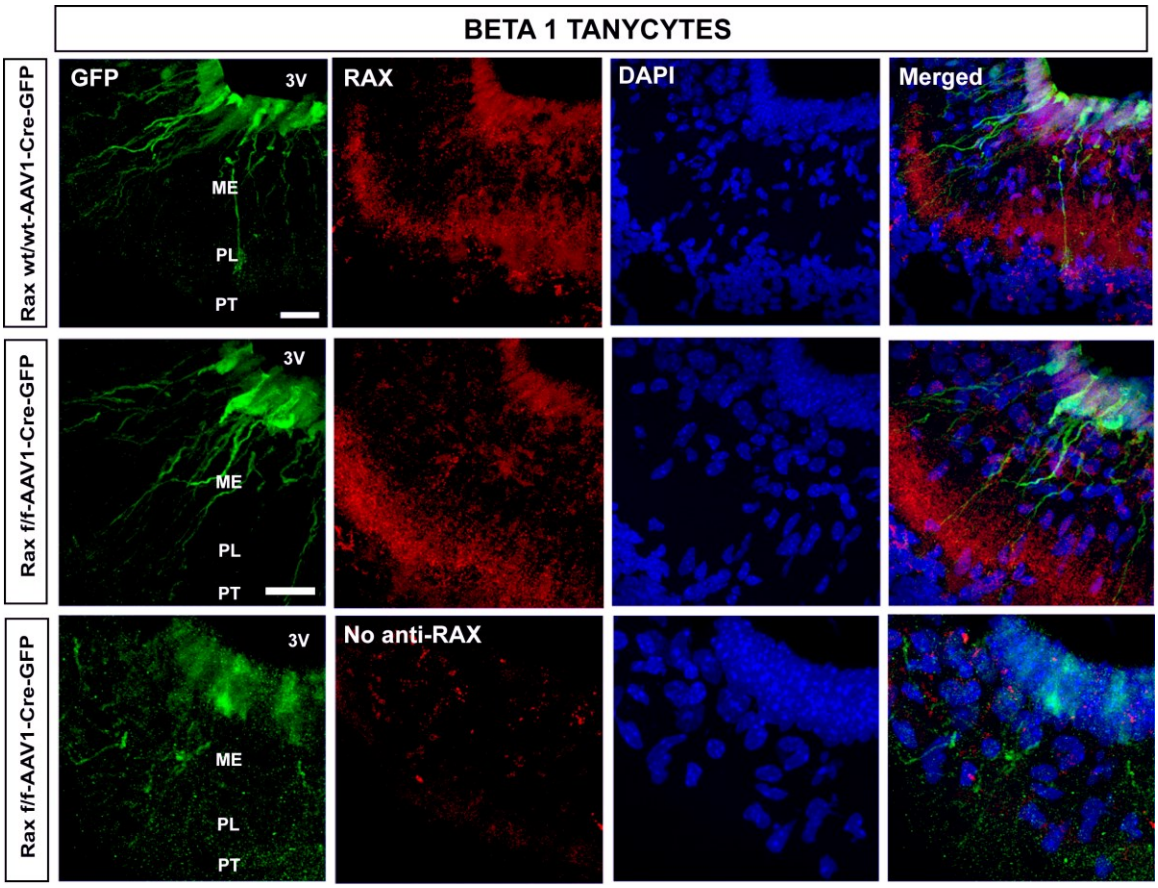

Figure 5.9. RAX protein in β1 tanycytes infected with AAV1-Cre-GFP
RAX protein (red) and GFP expression (green) in the β1 tanycytes of $Rax^{f/f}$ and $Rax^{wt/wt}$ mice four weeks after i.c.v injection of AAV1-Cre-GFP virus; images are maximum intensity projections of confocal z-stacks. RAX protein is found in β1 tanycyte cell bodies and in the medial and lateral ME, especially in the PL. RAX signal in both genotypes is distinct from the signal in the No anti-RAX control. RAX signal is apparently not reduced in the $Rax^{f/f}$-AAV1-Cre-GFP mice compared to $Rax^{wt/wt}$-AAV1-Cre-GFP control mice. PL: Palisade layer, PT: Pars tuberalis, ME: median eminence. 3V: third ventricle. Scale bars: 20 μm.

Figure 5.10.

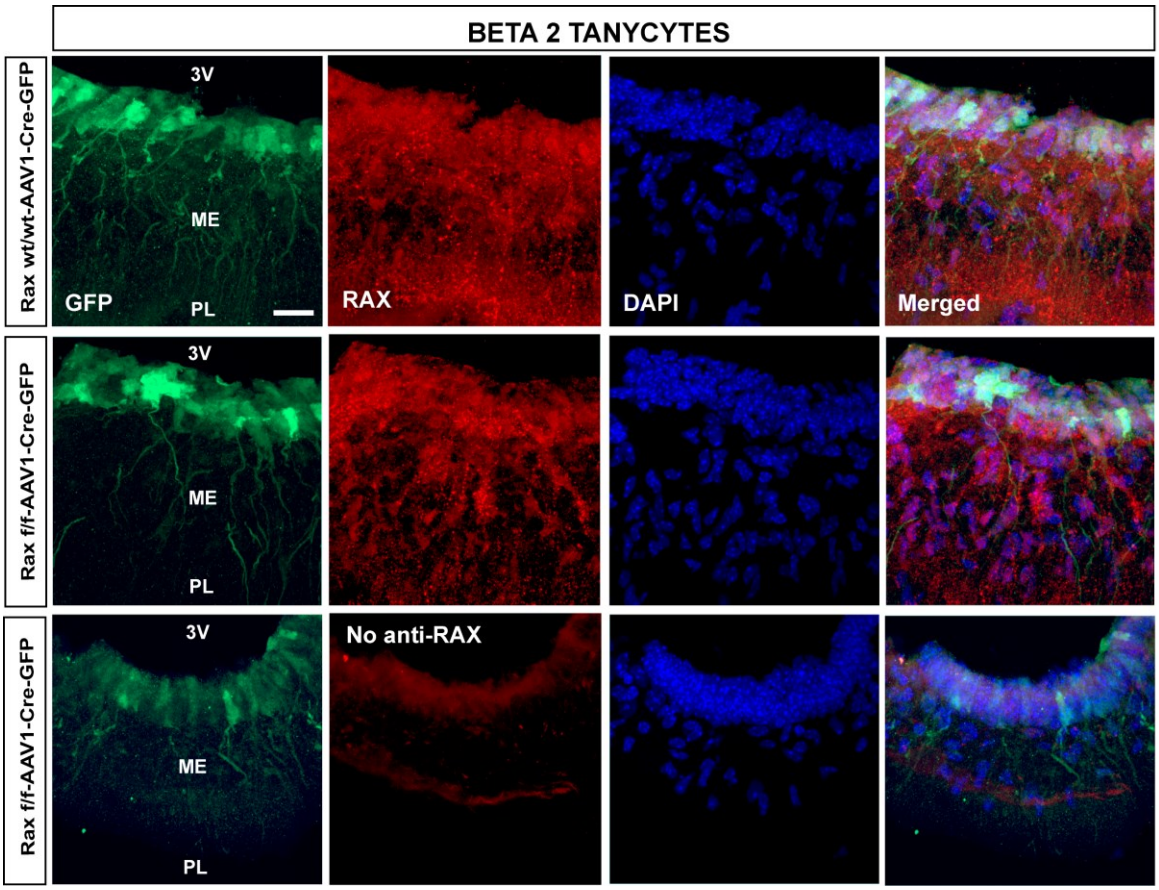

Figure 5.10. RAX protein in β2 tanycytes of AAV1-Cre-GFP infected mice
RAX protein (red) and GFP expression (green) in the β2 tanycytes of $Rax^{f/f}$ and $Rax^{wt/wt}$ mice four weeks after i.c.v injection of AAV1-Cre-GFP virus; images are maximum intensity projections of confocal z-stacks. RAX is found in β2 tanycyte cell bodies, ME and PL. RAX protein in the ME seems to follow the trajectory of tanycyte processes. RAX signal is partially reduced in the ME and PL of $Rax^{f/f}$-AAV1-Cre-GFP mice compared to $Rax^{wt/wt}$-AAV1-Cre-GFP control mice. RAX signal in both genotypes is distinct from the signal in the No anti-RAX control. PL: palisade layer, ME: median eminence. 3V: third ventricle. Scale bar: 20 μm.

Figure 5.11.

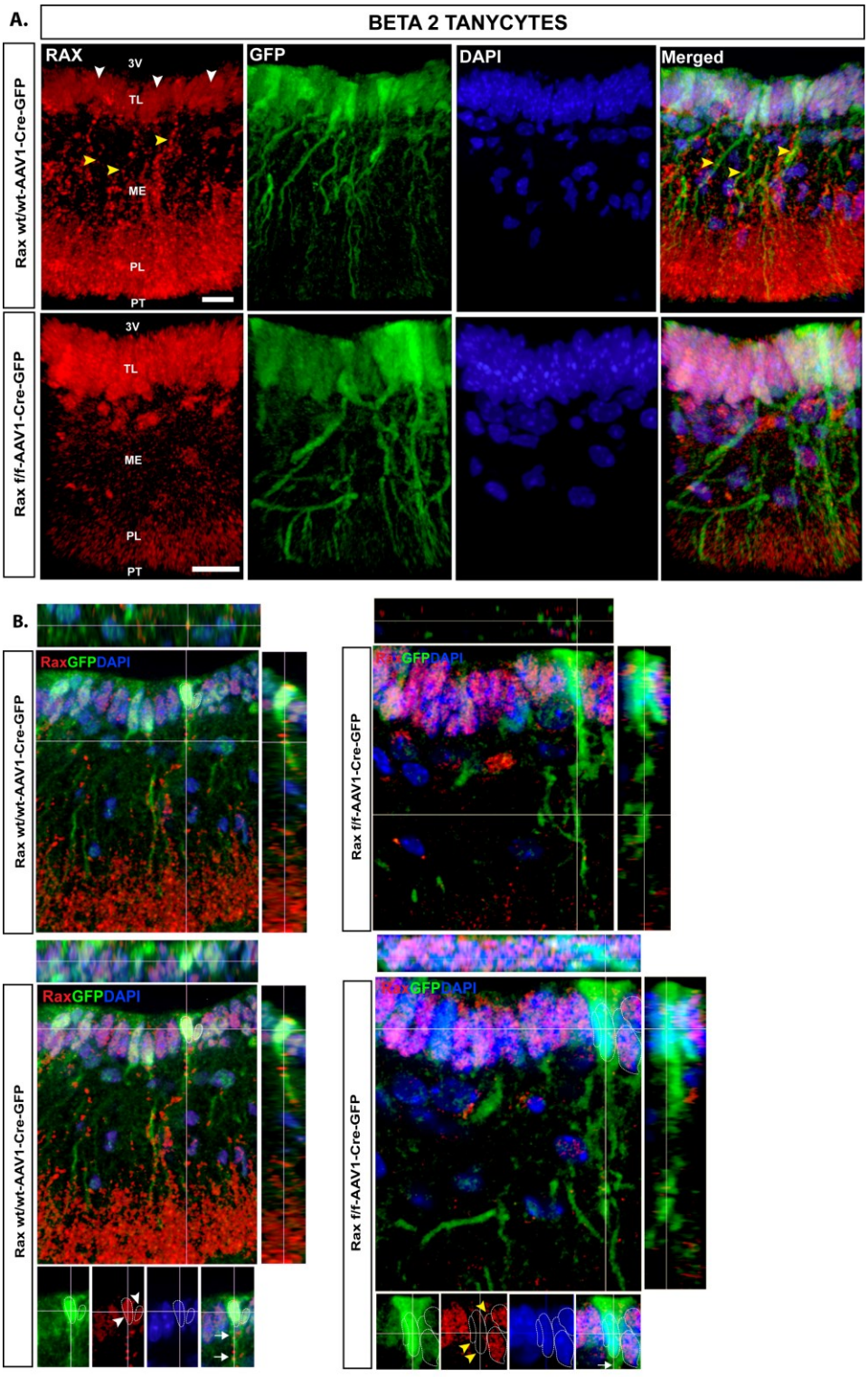
A.
BETA 2 TANYCYTES
RAX
GFP
DAPI
Merged
3V
TL
ME
PL
PT
Rax wt/wt-AAV1-Cre-GFP
Rax f/f-AAV1-Cre-GFP
B.
RaxGFPDAPI
GFPDAPI

Figure 5.11. RAX protein in the median eminence of AAV1-Cre-GFP infected mice
A. RAX protein (red) and GFP expression (green) in the median eminence in β2 tanycytes of $Rax^{f/f}$ and $Rax^{wt/wt}$ mice four weeks after i.c.v injection of AAV1-Cre-GFP virus. β2 tanycytes of both genotypes are infected with the virus (GFP^+ cells in the TL of the ME). RAX signal in the cell bodies of $Rax^{wt/wt}$ -AVV1-Cre-GFP β2 tanycytes is predominantly smooth (white arrow heads), whereas RAX signal in the tanycyte processes is granular (yellow arrow heads). RAX signal in the β2 cell bodies is increased in $Rax^{f/f}$-AAV1-Cre-GFP mice and appears more granular compared to $Rax^{wt/wt}$,AVV1-Cre-GFP mice. In contrast, RAX protein is reduced in the ME and PL of $Rax^{f/f}$-AAV1-Cre-GFP mice compared to $Rax^{wt/wt}$ AVV1-Cre-GFP mice. **B.** Orthogonal views of the images in *A* at the level of the tanycyte processes (top) and tanycyte cell bodies (bottom). RAX signal in the ME is closely associated with tanycyte processes (**B** top left). RAX^+ cell bodies (white arrow heads) have RAX in their cell processes (white arrows, B bottom left), RAX^- cell bodies (yellow arrow heads) do not have RAX in their processes (**B** top right and **B** bottom right). TL: β2 tanycyte layer, ME: median eminence, PL: Palisade layer, PT: Pars tuberalis. 3V: third ventricle. Scale bars: 15μm.

Figure 5.12.

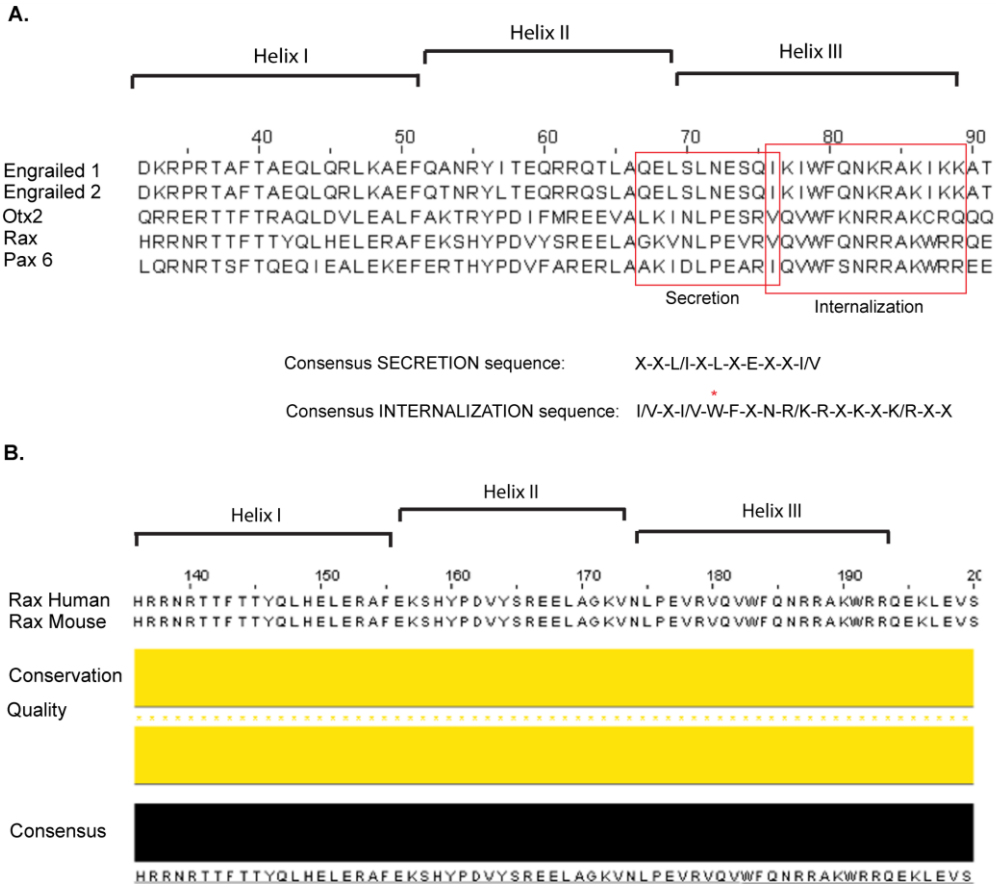

Figure 5.12. Rax contains the consensus homeoprotein secretion and internalization sequences.

A. Homeodomain aligment of Rax and other homeoproteins known to be secreted and internalized *in vivo.* Boxed areas correspond to the secretion and internalization sequences. RAX contains the consensus secretion sequence except for the third position where it does not have an "L" or "I" but instead has a "V". However, V is an aliphatic aa as L and I are. RAX does contain the entire consensus internalization sequence including the tryptophan (W), which is essential for translocation into live cells (red asterisk). Consensus secretion and internalization sequences obtained and modified from Spatazza J. et al. 2013. **B.** Protein alignment of human and mouse RAX homeodomain region. Human and mouse RAX have identical homeodomain sequences.

Figure 5.13.

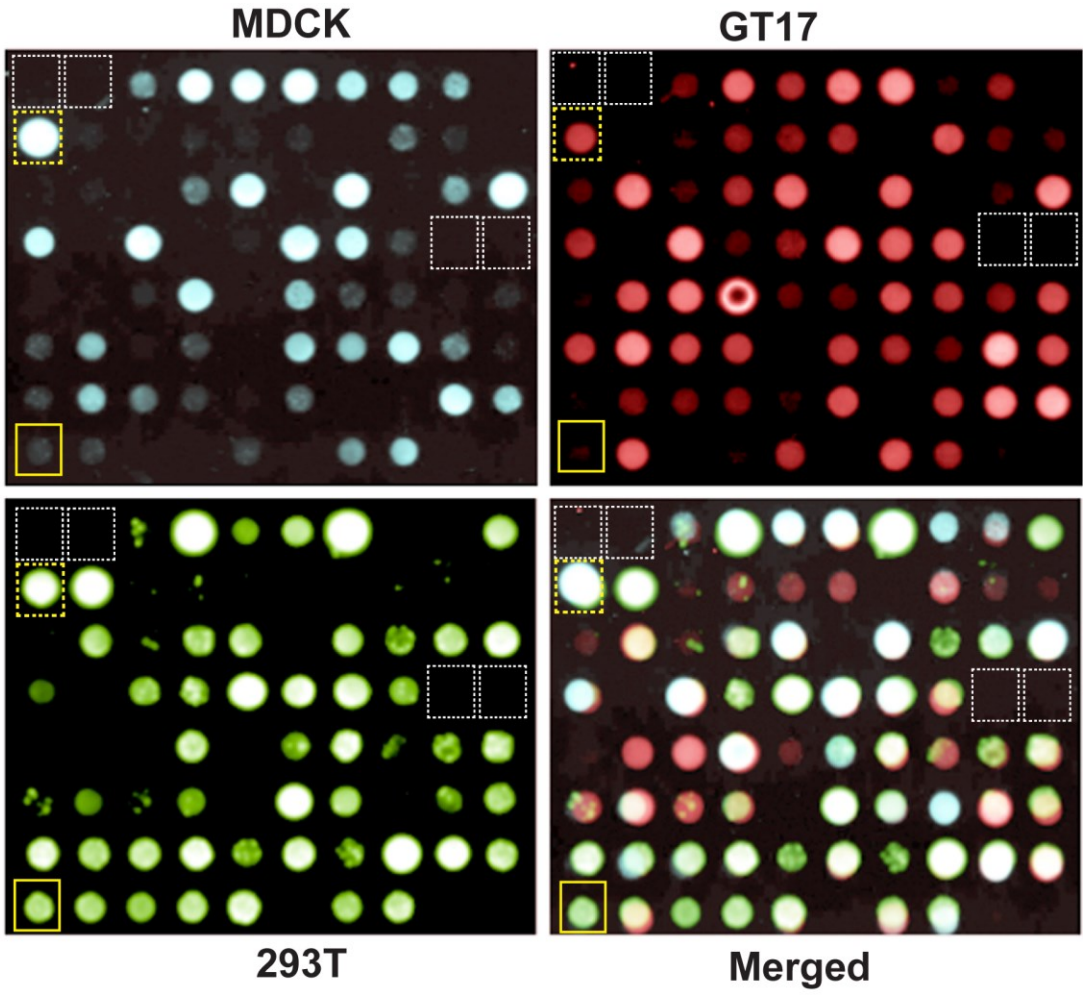

Figure 5.13. Human RAX is secreted *in vitro*
In vitro testing of RAX protein secretion using dot blot. RAX protein is secreted from the three cell lines tested (MDCK, GT17, and 293T; yellow square) but at lower levels than the known secreted homeoprotein En2 (positive control, yellow dashed square). No secretion is seen in the negative control homeoproteins MEIS1 and MEIS 2 as well as Luc^{+} and Luc^{-} (white dashed squares). Remaining wells contain additional homeoproteins tested for secretion.

Figure 5.14.

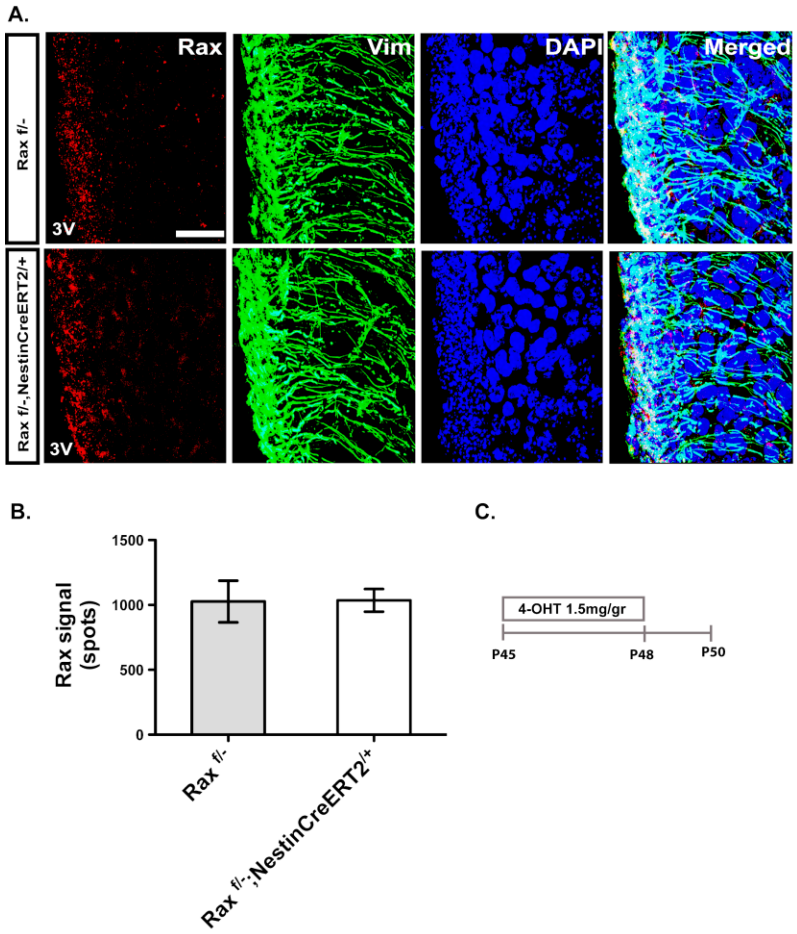

Figure 5.14. No reduction of Rax mRNA in terminally differentiated tanycytes using a Rax conditional allele ablation.
A. Confocal *z*-stack reconstruction of Rax fISH (red) and Vimentin IHC (green) in the α2 tanycyte zone of $Rax^{f/-}$ and $Rax^{f/-}$;$NestinCreER^{T2/+}$ adult mice (P45). **B.** Quantification of Rax mRNA signal using the spot tool of Imaris. There is no reduction of Rax mRNA in 4-OHT induced $Rax^{f/-}$;$Nestin:CreER^{T2/+}$ mice compared to $Rax^{f/-}$ mice. Unpaired t-test (n=3), p= 0.92. **C.** Diagram of the 4-OHT induction protocol. Mice received 1.5mg/gr of 4-OHT i.p. once a day for three days and were sacrificed 1 day after the last dose. 3V: Third ventricle. Scale bar: 20μm.

Figure 5.15.

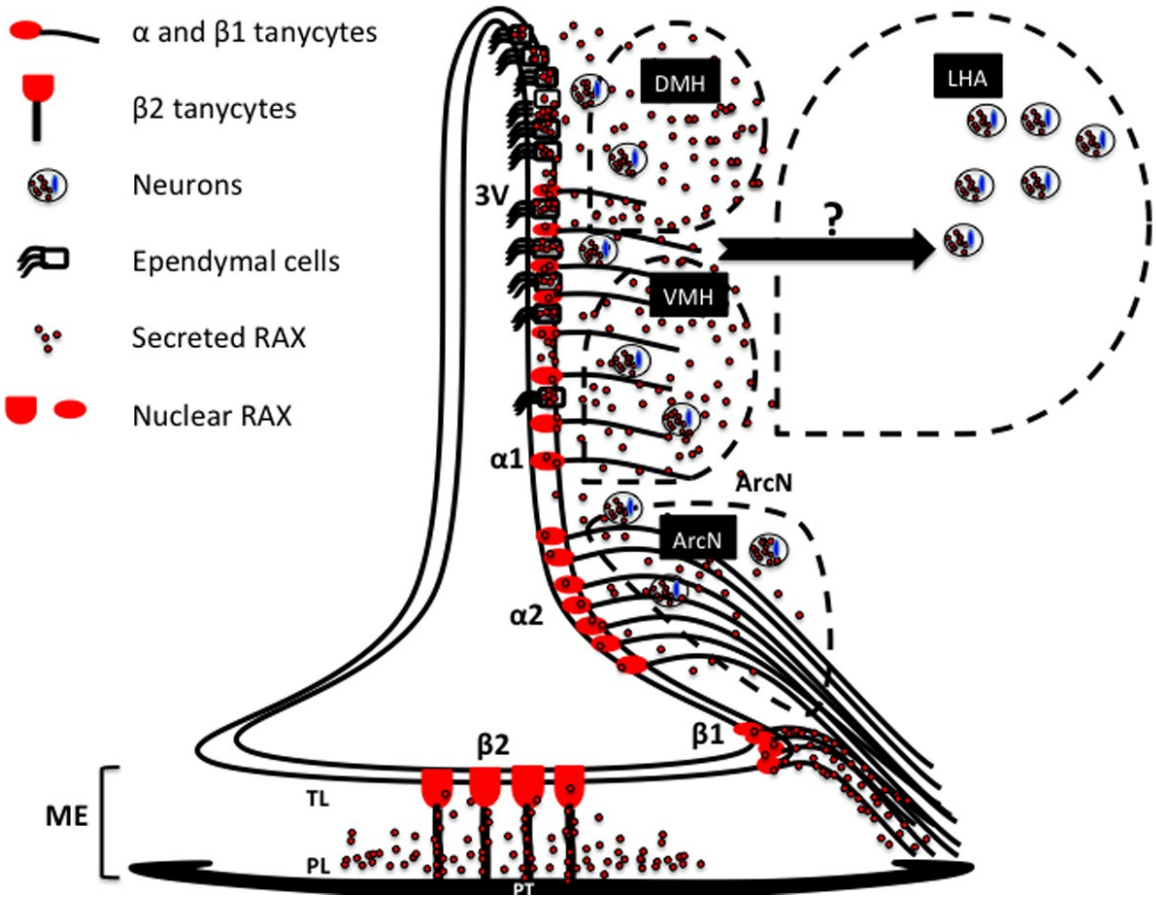

Figure 5.15. Schematic representation of RAX protein secretion in the hypothalamus

RAX protein is synthetized and secreted from α and β tanycytes. α tanycytes secrete RAX directly to the intercellular space of the hypothalamic parenchyma from where it translocates to adjacent hypothalamic cells. RAX also translocates to ependymal cells, likely from the closest α1 tanycytes. RAX secretion from α tanycytes does not involve tanycyte processes. In contrast, β tanycytes translate Rax mRNA in their cell bodies and processes, transport RAX protein along the process and secrete it through their process terminals in the most external palisade layer (PL) from were it seems to diffuse to more internal ME layers. RAX protein reaches specific neurons in the lateral hypothalamic area (LHA) through an unknown mechanism which probably involves transynaptic transport of RAX through projections from the DMH to the LHA. Alpha and β tanycytes secrete RAX to adjacent and distal cells possibly to regulate transcription and/or translation to promote their survival. 3V: third ventricle, PL: Palisade layer, PT: Pars tuberalis, ME: Median eminence, DMH: Dorsomedial Hypothalmic nucleus, VMH: Ventromedial Hypothalamic nucleus, ArcN: Arcuate Nucleus.

5.4. Materials and methods

Mice

$Rax^{f/-}$;Nestin:$CreER^{T2/+}$

$Rax^{f/-}$;Nestin:$CreER^{T2/+}$ were generated as follow; first, $Rax^{f/f}$ and $Rax^{f/-}$ mice were bred to Nestin:$CreERT2^{/+}$ mice generating $Rax^{f/+}$;Nestin:$CreERT2^{/+}$.. and $Rax^{+/-}$;Nestin:$CreERT2^{/+}$. Second, $Rax^{f/+}$;Nestin:$CreER^{T2/+}$. were crossed to mice with the same genotype generating $Rax^{f/f}$;Nestin:$CreERT2^{/+}$. Third, these mice were then crossed to $Rax^{+/-}$;Nestin:$CreERT2^{/+}$ to generate $Rax^{f/-}$;Nestin:$CreER^{T2/+}$.

$Rax^{f/f}$ in a C57BL/6 background

$Rax^{f/f}$ mice donated by Dr. Peter Mathers had a mixed background, and as a consequence they were backcrossed for five generations with C57BL/6 wild type mice to generated $Rax^{f/+}$ mice in a C57BL/6 background. After the last backcross, $Rax^{f/+}$ mice were bred to each other to generate $Rax^{f/f}$ offspring. C57BL/6 wild type mice were purchased from Charles Rivers.

$Rax^{+/+}$;Nestin:$CreERT2^{R26RstopYFP}$

$Rax^{+/+}$; Nestin:$CreERT2^{R26RstopYFP}$ were donated by Daniel Lee. Cre activity was induced by injecting mice with 0.15mg/gr of 4-OHT at P45 and mice were sacrificed three days later (P48) to perform GFP and RAX protein staining followed by image analysis in the LHA.

Tamoxifen preparation and administration, brain tissue collection, genotyping and Rax mRNA fluorescent *in situ* hybridization (fISH) combined with Vimentin immunohistochemistry were performed as previously described **(**see **Chapter 2).**

Brain tissue sectioning and immunohistochemistry (IHC)

Coronal hypothalamic free floating sections were collected by sectioning brains with a cryostat at 40 μm starting from the middle of the anterior hypothalamus to the end of the posterior hypothalamus. Serial sections were collected in PB 0.5X in individual wells of 48 well plates (Falcon). Right after cutting, brain sections where examined under the light microscope to choose sections containing only the tuberal hypothalamus and the anterior region of the posterior hypothalamus for a total of ten to twelve sections per brain. Sections were stored at -20°C in anti-freezing solution (30% glycerol, 30% ethylene glycol, 10% PBS 2X and 30% DI water) until IHC was performed. Immunohistochemistry of RAX and GFP was performed on free-floating sections as follows: Permeabilization/blocking were performed using PBS plus solution (0.3% Triton 100X and 5% normal horse serum in 0.1M PBS 1X) for 15 minutes followed by blocking in Superblock (ScyTek) for 5 minutes. For Hu staining, sections where submerged in TE 1X pH 8 and heated at 80°C in a water bath for 20 minutes before blocking with Superblock. Sections were then incubated O/N at 4°C with primary antibodies prepared in permeabilizing/blocking solution. On the following day, brain sections were incubated with Alexa secondary antibodies in PBS plus for 2 hrs at RT at 1:500 dilution. Primary antibodies used were: chicken anti-GFP (1:1000, Aves Lab), guinea pig anti-RAX (1:1000, donated by Dr. Furukawa from Osaka Bioscience Institute, Japan) and mouse anti-Hu 1:100 (Invitrogen). DAPI staining was performed by submerging the sections in a DAPI solution 1:5000 in PBS 1X for 10 minutes. When the staining was finished, sections were mounted on Superfrost Plus slides (Fisher), dried for around 5 min at RT in the darkness and covered with 100 μl of Vectashield hard-set Mounting Medium with DAPI (Vector laboratories). Vectashield covered slides were allowed to dry in the dark

for 1 hour and stored at 4°C until image acquisition. The no anti-RAX control staining was performed simultaneously with the anti-Rax staining in identical conditions except that they received 1 µl of PBS plus solution instead of Rax primary antibody.

Canulation and intracerebroventricular injections of AVV1-Cre-GFP viruses

AAV1-Cre-GFP viruses were purchased from Vector Biolabs as premade viruses suspended in PBS with 5% glycerol at a concentration of 1 X 10^{13} GC/ml. Adult Rax $^{f/f}$ and Rax $^{+/+}$ mice (P45) were canulated as previously described (see **Chapter 4**) except that these mice received 1ul of AAV1-Cre-GFP virus into the lateral ventricle using a disinfected stainless steel injector Hamilton Syringe connected by polyethylene tubing after canulation. This was followed by 3 boluses 5-10 min apart of Antisedan, an α2 antagonist, at a total dose of 2 mg/kg to promote awakening from anesthesia. To facilitate recovery and prevent hypothermia, the mouse was kept on a heating pad set at 40°C and received an i.p injection of Banamine analgesic (2.5 mg/kg) upon renewing ambulation. Injected mice were kept alive for 4 weeks, during which they were monitored weekly for any gross changes in behavior or body weight. Typically, one week post-surgery mice returned to pre-surgical behavior and recovered their body weight. At P73 (4 weeks later) mice were sacrificed and their brains were collected as previously described (see **Chapter 3**).

Image acquisition was performed as previously described (see **Chapters 2 and 3).**

Image analysis

The landmarks used for the identification of tanycytes along the ventro-dorsal axis of the medial hypothalamus were described previously (see **Chapter 3**). The identification of Bregma points along the anterior-posterior axis and the identification of hypothalamic

nuclei were accomplished as previously described (see **Chapter 3**).

RAX protein signal from Rax $^{f/f}$; AVV1-Cre-GFP and Rax $^{+/+}$; AVV1-Cre-GFP mice was assessed qualitatively in snapshot images obtained in the Imaris software; no quantitative analysis of RAX signal was performed. Orthogonal views of β tanycyte confocal *z* stack images in Rax$^{f/f}$;AVV1-Cre-GFP and Rax$^{+/+}$;AVV1-Cre-GFP mice were also obtained in the Imaris software.

***In silico* protein homeodomain sequence analysis**

Rax, Otx2, Engrailed (En1/ En2) and Pax6 mouse protein sequences were obtained from the NCBI protein database. All available mouse sequences of different lengths for each protein were selected and aligned to each other with the online CrustalW2 software (available at http://www.ebi.ac.uk/Tools/msa/clustalw2/) to verify that they corresponded to the same protein. Then, the homeodomain sequence of the longest protein version was used for the multiple sequence alignment with the same software. The secretion and internalization sequences were identified in the analyzed proteins by comparing the second and third helix sequences of Pax6, Otx2 and Rax with the published En1/2 internalization sequences (Brunet et al., 2007; Spatazza et al., 2013). Rax protein human sequence was also obtain from NCBI protein and its homeodomain was aligned with the Rax mouse sequence using the CrustalW2. NCBI accession numbers of protein sequences used are: En1 mouse (EDL39793), En2 mouse (EDL37227), Pax6 mouse (AAL38015), Otx2 mouse (CAA48755), Rax mouse (NP_038861.2), Rax human (NP_038463.2).

Rax protein secretion

Rax protein secretion testing was performed in the lab of Dr. Jin Woo Kim at the

Korea Advanced Institute of Science and Technology (KAIST) through a collaboration with our laboratory and as part of his human secretome project. Human cDNA clones were donated by our laboratory and were obtained from Invitrogen. These clones were introduced into pCAGIG-V5-GW and/or pLumio-V5 vectors and were transfected into Human Embryonic Kidney 293 cells (293T), Madin-Darby Canine Kidney Epithelial Cells (MDCK Line) and the neuronal hypothalamic cell line GT1-7 which is an immortalized cell line derived from mature GnRH neurons. Protein detection was performed using dot blot. Protein secretion was classified as positive or negative after comparing the intensities of positive (En2) and negative (vector only or c-Myc) controls in the same dot-blot membrane with protein expression levels examined by Western blot and viability of transfected cells. The control values of protein levels where then compared overall with the experimental samples. Each experiment was done in all cell lines in triplicate. More details of the secretion test cannot be disclosed due to Dr. Jin Woo Kim´s ongoing patenting process.

Chapter 6

Generation of two Rax knock-in mouse lines to study tanycytes development and function

6.1. Introduction

Rax is expressed in retinal progenitors and ventral forebrain progenitors which give rise to the hypothalamus and posterior pituitary (Furukawa et al., 1997; Mathers et al., 1997). Although Rax has being widely characterized in the developing and postnatal retina (Muranishi, Terada, & Furukawa, 2012). Rax expression and its function in ventral forebrain progenitors are poorly understood. We have previously shown that Rax is specifically expressed in tanycyte progenitors and in progenitors that might give rise to ventral hypothalamic nuclei (see **Chapter 2,** Figure 2.1B). Also, we have shown that Rax haploinsuficiency leads to reduction of tanycytes and ependymal cells and an ectopic presence of ependymal cells in the α2 tanycytic zone. Even though both events seem to be associated with changes in the CSF-brain barrier permeability in the hypothalamus, it does not affect the gross phenotype of these mice (see **Chapters 3 and 4**). The reduction of tanycytes and ependymal cells seems to be originated by a reduction of proliferation and/or a reduced survival of progenitors (see **Chapter 3**). This demonstrates that Rax plays an important role in the development of ependymal cells and hypothalamic tanycytes. Interestingly, it has being recently shown that embryonic disruption of Rax expression in parenchymal ventral hypothalamic progenitors leads to a defect in the specification of VMH and ArcN neurons (Lu et al., 2013). Together, this data shows that Rax is essential for the proper development and function of hypothalamic neurons,

ependymal cells and tanycytes and it also raises the question of the potential connection between both progenitor pools (ventricular and parenchymal) and the specific cell populations originated from them.

Based on the chronological expression of Rax in the hypothalamic primordium in which Rax appears first in the ventricular lumen (E11.5) and later in the developing nuclei (E12.5) it is possible to speculate that some Rax^{+} ventricular progenitors migrate to the parenchyma to give rise to neurons while other stay in the ventricle to give rise to tanycytes and ependymal cells. Conversely, they might correspond to two different pools of progenitors, one parenchymal pool which originates VMH and ArcN neurons earlier (E10 to E16) and a ventricular pool which gives rise to tanycytes and ependymal cells later (E16 to E19). Interestingly, Rax transcript disappears from ventral hypothalamic nuclei but remains through adulthood in terminally differentiated tanycytes (see **Chapter 2**, Figure 2.2). Since Rax is expressed in retinal and hypothalamic progenitors, it is possible to speculate that terminally differentiated tanycytes retain Rax expression because they retain progenitor characteristics in adult mice. In fact, we have shown that β2 postnatal tanycytes can give rise to neurons in the ME (Lee et al., 2012), but it is unknown if other tanycytes such as α tanycytes could give rise to neurons in other hypothalamic areas during development or adulthood.

Prospective inducible genetic fate mapping (PIGFM) of Rax progenitors is necessary to determine the identity of cells derived from Rax^{+} progenitors and to determine if terminally differentiated tanycytes could give rise to neurons either in basal conditions of after challenges such as hypothalamic injury. In order to perform a PIGFM is necessary to develop an inducible Cre line which could be activated at specific

developmental points and it the cells under study (spatiotemporal specificity) (Joyner & Zervas, 2006). In addition, a conditional tanycytic and hypothalamic Rax:Cre line will allow the conditional ablation of genes expressed in ventricular and parenchymal Rax^{+} progenitors to understand the transcriptional control of tanycytes and ventral hypothalamic nuclei development. Recently, it was reported the generation of a conditional Rx-tTA: TetOp-Cre knock-in mouse which after being crossed with Z/EG reporter mice showed Cre activity in the retina, pituitary and peripheral tissues (Plageman, Jr. & Lang, 2012). However, Rx-tTA:TetOp-Cre activity in the adult hypothalamus was not characterized in these mice (Plageman, Jr. & Lang, 2012) leaving as an open question if this Cre line will be useful for studying tanycyte development and function.

Furthermore, in order to understand the role of tanycytes in adult hypothalamic function is necessary to generate mouse models in which tanycytes could be selectively eliminated. Several attempts have being done to achieve selective elimination of terminally differentiated tanycytes which contributed to the understanding of tanycytes role in the regulation of the GnRH axis. In 1985, Rodríguez et al. filled the third ventricle with an epoxy resin leading to a massive tanycyte elimination known as experimental tanycytectomy (Rodriguez et al., 2005). This epoxy resin induced several timed changes in the third ventricle starting with obliteration of the 3V, followed by degeneration of tanycytes processes and ending with the reorganization of the infundibular recess (IR) and a re-establishment of CSF circulation but in complete absence of α and β tanycytes which were replaced by cells that seem to correspond to astrocytes (Rodriguez et al., 2005). Also, the GnRH fibers ending in the ME showed

major modifications; even though these fibers were still present they were randomly distributed in the lateral regions of the ME and there was no tanycytic cuff separating the GnRH axonal terminals from the portal circulation. This suggested that GnRH endings where still able to release GnRH into the portal circulation and indeed, when they measured LH and FSH there was no difference compared to control rats (Rodriguez, Peña, Aguado, & Schoebitz, 1985). Nevertheless, the authors found that the epoxy resin-injected rats were not able to produce the peak of LH that is expected during the afternoon of the proestrous necessary for ovulation (Rodriguez et al., 1985).

These observations suggested that tanycytes were necessary for the pulse of GnRH release into the portal circulation required for ovulation but not for its tonic release. It has being shown by electron microscopy, that β1 tanycyte processes surround GnRH axonal terminals in the ME during proestrous avoiding their direct contact with the portal circulation. However, during the estrous surge, tanycytes appeared retracted and GnRH axons are in direct contact with blood vessels (Prevot et al., 1999). Although these observations provided some insight in the importance of an intact ventral hypothalamus in the regulation of GnRH release in the ME, the dramatic changes achieved with experimental tanycytectomy in all the cellular components of the ventricular and subventricular layers as well as in adjacent neurons and axons makes difficult to assigned a specific role of tanycytes in the regulation of the neuroendocrine systems and in other hypothalamic functions.

Another attempt to eliminate tanycytes consisted in the electrocoagulation of tanycytes. In contrast to the findings described above, tanycytes injured with electrocoagulation did not induce any changes in LH and FSH or in reproductive

competence (Nozaki, Uemura, & Kobayashi, 1980). This disagreement is likely to be originated by the difference in the tanycytectomy methods utilized in these experiments and the possibility that in the electrocoagulation experiments some intact tanycytes that were not injured, regenerated and repaired the damaged regions as has being shown to happen when tanycytes are injured with alloxan (Sanders et al., 2004). Independent of these contrasting findings, it is evident that these studies used strategies that are not tanycyte specific and have little reproducibility.

A more selective strategy to conditionally ablate tanycytes would include the crossing of an inducible Cre line specific for tanycytes (inducible Rax:Cre) with a mouse line that after Cre activation would induce cell death such as the ROSA26:lox-EGFP-stop-lox-DTa. These mice express EGFP broadly and can only express DTa (diphtheria toxin fragment a) after Cre-mediated recombination of a stop signal (Ivanova et al., 2005). As a consequence, breeding of this line to a Rax:Cre inducible line will lead to a specific ablation of Rax-expressing cells due to DTa toxicity. Alternatively, a tanycyte specific DTa line crossed to an inducible Cre line expressed in tanycytes or a tanycyte specific DTa line infected with Cre virus delivered by intracerebroventricular injections will also allow the elimination of tanycytes in a specific and time controlled manner. However, neither an inducible Cre line specific for tanycytes or a tanycyte specific DTa line have yet been generated.

Since Rax is specifically expressed in hypothalamic ventricular progenitors and in terminally differentiated tanycytes, we designed the targeting vectors for two knock-in mice under the control of Rax promoter, Rax:lox-EGFP-stop-lox-DTa mice and Rax:CreER^{T2} to allow both Cre-dependent regulation of gene function in tanycytes and

selective ablation of tanycytes. The Rax:CreER^{T2} will express a CreER^{T2} fusion protein consisting of a Cre recombinase (Cre) and a triple mutant form of the human Estrogen receptor ligand binding domain (ER^{T2}) which does not bind its natural ligand (17β estradiol) but has high affinity for its synthetic estrogen antagonist 4-hydroxytamoxifen (4-OHT) and ICI 182,780 (Feil, Wagner, Metzger, & Chambon, 1997). CreER^{T2} is restricted to the cytoplasm by a heat shock protein 90 (Hsp90) however when CreER^{T2} binds its ligand it translocates to the nucleus to induce recombination of DNA regions containing lox sites in Rax expressing cells (reporters and/or conditional alleles). The Rax:lox-EGFP-stop-lox-DTa carrying mice will express EGFP in the Rax expressing cells which after Cre mediated recombination of the stop signal will express DTa leading to cell death (Ivanova et al., 2005).

We have successfully generated Rax:CreER^{T2} mice which have being crossed with the reporter line Ai9tdTomato (Ai9). Characterization of Rax:CreER$^{T2/+}$;Ai9tdTomato$^{/+}$ mice demonstrated strong and specific Cre activity in postnatal tanycytes, cells in the median eminence and in Müller glia in the retina. In contrast, the Rax:lox-EGFP-stop-lox-DTa mice have not yet been generated. We expect that these mouse lines will allow us to advance our understanding of hypothalamic tanycyte development and function.

6.2. Results

6.2.1. Generation of RaxCreER^{T2} knock-in mice

We generated two vectors; the Rax:CreER^{T2} targeting vector and a control vector using a combination of regular cloning and recombineering (Figure 6.1A). The control vector was created in order to generate a PCR protocol to test correct 3' insertion into the

Rax locus. Both vectors were submitted to the Johns Hopkins transgenic core facility to perform electroporation into embryonic stem cells (ES cells) from sv129 mice. After the third electroporation attempt, ES cell colonies with correct 3' insertion (tested by PCR) and 5' insertion (tested by southern blot) were submitted to the transgenic core facility for karyotyping and injection into pronuclei of fertilized eggs obtained from sv129 female mice (Figure 6.1B and C). As a result we obtained several male and female chimeras which were breed to C57BL/6 mice to test germ line transmission of the targeted locus. Agouti mice resulting from these breeding were expected to carry the Rax:CreER^{T2-}neo targeted locus and were genotyped for Cre and the neomycin cassette. Finally, mice carrying the Rax:CreER^{T2-}neo targeted locus were breed to FLpeR mice to remove the neo cassette. The resulting Rax:CreER$^{T2/+}$ knock-in mice were fertile and viable and do not have any gross phenotype resulting from the Rax haploinsuficiency.

6.2.2. Rax:CreER^{T2} activity in the postnatal hypothalamus is specific to tanycytes and some cells in the median eminence.

To characterize Rax:CreER^{T2} spatiotemporal expression, we bred Rax:CreER$^{T2/+}$ to the reporter line Ai9tdTomato generating Rax:CreER$^{T2/+}$;Ai9tdTomato$^{/+}$ mice. The Ai9tdTomato mouse reporter line has a lox-flanked stop cassette which prevents transcription of the downstream red fluorescent protein variant (tdTomato) (Madisen et al., 2010). When bred to any Cre mice it is expected that the resulting offspring will have the stop cassette deleted in the Cre-expressing cells resulting in expression of tdTomato (Madisen et al., 2010). Because this reporter construct is driven by a CAG promoter inserted into the Gt(ROSA)26Sor locus, tdTomato expression is determined by which cells express Cre recombinase which in the hypothalamus are the tanycytes and cells in

the median eminence (see **Chapter 2**). We characterized Rax:CreER^{T2} activity in postnatal Rax:CreER$^{T2/+}$;Ai9TdTomato$^{/+}$ mice induced at early (P5) and later postnatal ages (P18). At early postnatal ages mice received 0.3mg of 4-OHT or corn oil by gavage once a day at P5, P7 and P11 and they were sacrificed at P15 (Figure 6.2). At later postnatal ages mice received 0.3mg of 4-OHT at P18, P19 and 1mg of 4-OHT at P21 and P22 by gavage and were sacrificed at P23 (Figure 6.3).

In 4-OHT induced mice we observed tdTomato signal in the cell bodies and processes of hypothalamic α and β tanycytes but not in the ependymal cells (Figure 6.2B). The presence of tdTomato signal in tanycytes was confirmed by co-labeling with vimentin in tanycyte cell bodies and processes (Figure 6.2D and Figure 6.3C). Furthermore, there was abundant tdTomato signal in the ME corresponding to tanycyte processes and disperse cells located in the medial and external layers (Figure 6.2B and 6.3). Interestingly, some of the ME cells expressing tdTomato were co-labeled with Sox2, a neuronal progenitor marker (Graham, Khudyakov, Ellis, & Pevny, 2003). Futhermore, we observed tdTomato signal in the hypothalamic parenchyma of Rax:CreER$^{T2/+}$; Ai9tdTomato$^{/+}$ mice. To rule out the possibility that some of the parenchymal tdTomato signal was originated by leakiness of the reporter line, we examined oil treated mice. We rarely saw any tdTomato signal in these mice brain (data not shown) and it was almost completely absent in the hypothalamus (Figure 6.2B).

TdTomato signal in the ME and hypothalamic parenchyma is currently being carefully examined using IHC and confocal imaging at higher resolution. Also, a whole brain search of tdTomato signal is in process to support the specificity of Rax:CreER$^{T2/+}$, so far neither a specific nor a significant signal has being observed in other brain regions

outside the hypothalamus except for a transient early postnatal expression in a cerebellar lobe.

6.2.3. Transient expression of Rax in a subregion of the cerebellum

When mice are induced at P5, tdTomato signal was observed bilaterally in granular cells of the flocculus lod of the postnatal cerebellum but it was completely absent when mice were induced at P18 (Figure 6.4). The singal in Rax:CreER$^{T2/+}$;Ai9tdTomato$^{/+}$ mice is in agreement with the Rax mRNA expression (from E13.5 to P14) that has being reported in the Allen Mouse Brain Atlas in the same area where we observed tdTomato signal.

6.2.4. Rax:CreER^{T2} activity in the postnatal retina is specific to Müller glia

Rax expression in the retina has being widely characterized. It is known that in postnatal mice, Rax expression becomes restricted to MG and progressively declines until it becomes undetectable by P13.5 (Furukawa et al., 1997; Mathers et al., 1997). We analyzed the retinas of Rax:CreER$^{T2/+}$;Ai9tdTomato$^{/+}$ mice induced at P5, P7 and P11, when Rax is still expressed in MG. We found that tdTomato co-labels with the MG marker p27 demonstrating that Rax:CreER$^{T2/+}$ activity is specific to Rax expressing cells in the retina (Figure 6.5).

6.2.5. Attempt to generate Rax:lox-EGFP-stop-lox-DTa mice

We generated the Rax:lox-EGFP-stop-lox-DTa targeting vector and a control vector using a combination of classical cloning and recombineering (Figure 6.6). We have submitted the targeting vector to the Johns Hopkins Transgenic Core five times and we had finally obtained two clearly positive clones by PCR but have not obtained any positive results by southern blot yet apparently due to a sensitivity problem in the

southern blot protocol. We are currently in the process of southern blot verification.

6.3. Discussion

Taking advantage of the specific expression of Rax in hypothalamic tancytes, we generated an inducible Cre mouse line driven by the Rax promoter, the Rax:CreER$^{T2/+}$ mouse line. For an initial spatiotemporal characterization of our mouse line we generated Rax:CreER$^{T2/+}$;Ai9tdTomato$^{/+}$ and induced them at postnatal ages. In these double transgenic mice we showed that Cre activity within the brain is specific of hypothalamic tanycytes and cells located in the medial and external layers of the median eminence. Outside the hypothalamus, transient early postnatal Cre activity is observed in the flocculus lobe of the cerebellum where Rax mRNA is transiently expressed. Also, as expected, we found specific postnatal Rax:CreER^{T2} activity in the retinal MG. Thus, the overall distribution of tdTomato signal coincides with the Rax expressing areas demonstrating that there is little to none ectopic Cre activity of our Rax:CreER^{T2} mouse line. We expect that this mouse lines will contribute to the understanding of tanycyte development and function as well as to the study of other Rax expressing cells outside the brain such as MG in the retina.

Rax:CreER^{T2} mice are viable, fertile and efficiently recombine the Ai9tdTomato reporter

We have shown that Rax haploinsuficient mice have a reduction in the number of tanycytes and ependymal cells, an ectopic presence ependymal cells in the α2 tanycytic zone and a reduction of the Evans Blue tracer distal diffusion (see **Chapters 3 and 4**). However, these mice are viable and fertile and they do not manifest any change in their gross phenotype. Similarly, Rax:CreER$^{T2/+}$ mice are haploinsuficient for the Rax allele

and are normal and fertile. Our previous characterization of Rax haploinsuficiency provides a baseline for interpreting any phenotype arising from elimination of any conditional allele in hypothalamic tanycytes.

Rax:CreER^{T2} activity in the postnatal hypothalamus is specific to tanycytes and cells in the median eminence

We induced Rax:CreER$^{T2/+}$;Ai9tdTomato$^{/+}$ at P5, P7 and P11 when tanycytes differentiation and maturation is in progress (Altman & Bayer, 1978; Rutzel & Schiebler, 1980). Also we induced them at later postnatal ages (P18, P19, P21 and P22) when tanycyte maturation has not finished. In both cases we were able to visualize tanycyte cell bodies and processes. In addition, some parenchymal signal was observed which might correspond to blood vessels, ectopic Cre expression or leakiness of the reporter. We have previously shown that blood vessels surrounded by tanycytes processes are visible when their processes are labeled (see **Chapter 1**, Figure 1.1 and see **Chapter 6** Figure 5.5B). Another explanation for the parenchymal signal is the presence of ectopic Cre activity due to a transient ectopic hypothalamic Cre expression during development as has being reported in other Cre lines (Smith, 2011). Finally, to rule out the possibility of leakiness of the reporter we used oil treated controls. Leakiness of the reporter would be originated by a weak stop signal that allows tdTomato expression without previous Cre mediated excision of the lox surrounding the stop signal. We did not observed any significant tdTomato signal in the oil controls demonstrating that these reporter is reliably reflecting the spatiotemporal activity of Rax:CreER$^{T2/+}$.

Interestingly, we observed tdTomato signal in the ME not only in tanycytes cell bodies and processes but also in disperse cells located in the medial and external layers of

the ME. We have previously shown that there is Rax mRNA in some ME cells and that some of those cells also express Gpr50, a gene known to be expressed in tanycytes (see **Chapter 2,** Figure 2.4). Besides, we have shown that some ME cells expressed RAX protein (See **Chapter 5,** Figure 2.6). Based on our previous characterization of Rax expression, the tdTomato signal in the ME of Rax:CreER$^{T2/+}$;Ai9tdTomato$^{/+}$ mice is expected but the identity of these cells is still unknown. Interestingly, we have found that Rax^{-}expressing cells in the ME also expressed the neuronal progenitor Sox2. Since β2 tanycytes also express Sox2 and some ME cells expressed the tanycyte marker Gpr50 and Rax, it is possible that ME cells expressing tdTomato correspond to displaced β2 tanycytes cell bodies as was described earlier by Rodríguez (Rodriguez et al., 1979). However, ME cells expressing tdTomato are in the medial and the external layers of the median eminence making unlikely that they correspond to terminally differentiated β2 tanycytes. As a consequence, Rax^{+}, Sox2^{+} cells might correspond to an intermediate progenitor arising from β2 tanycytes or immature newly generated β2 tanycytes. This is supported by published data showing that tanycytes can proliferate and differentiate into neurons under basal conditions (Cifuentes et al., 2011; Lee et al., 2012) as well as in response to growth factors (Perez-Martin et al., 2010) and high fat diet (Lee et al., 2012).

Finally, ME cells expressing tdTomato might correspond to a tanycyte-independent population of Rax+ progenitors or they might even correspond to neurons, astrocytes or microglia. As a consequence their definitive identification needs a through immunohistochemical characterization.

Rax:CreER^{T2} activity outside the hypothalamus is specific to Rax expressing cells

We have shown that in the adult mouse brain Rax expression is present in the

hypothalamic tanycytes and within the ME (see **Chapter 2**), also it has being published that Rax is also expressed in the pineal gland and posterior pituitary of adult mice (Rohde et al., 2011). Furthermore, at later postnatal ages MG are the only retinal cells expressing Rax but this signal disappears after P13.5 (Furukawa et al., 1997; Mathers et al., 1997). We have found that Rax:CreER$^{T2/+}$;Ai9tdTomato$^{/+}$ mice reliably replicate the expected expression within the hypothalamus and in the retina. We are in the process of verifying expression in the other Rax expressing brain areas including the pineal gland and posterior pituitary. Interestingly, we also found transient postnatal Rax:CreER^{T2} activity in the cerebellum which agrees with the reported embryonic and early postnatal Rax expression in this brain region in the Allen Mouse Brain Atlas (Sunkin et al., 2013). Transient expression in cells different from hypothalamic tanycytes need to be taken into account when exploring the resulting phenotype of eliminating conditional alleles in Rax expressing cells or when attempting to selectively eliminate them.

Although crossing a Cre line to a reporter is routinely done to characterize spatiotemporal expression, in some cases it might not be replicated when the same Cre line is crossed to other reporters, or when trying to delete conditional alleles due to the variability of Cre activity in different genetic backgrounds (Smith, 2011) and the variable accessibility of the Cre to different lox containing loci. Thus, our characterization of Rax:CreER^{T2}; Ai9tdTomato$^{/+}$ suggest that Rax:CreER^{T2} is a reliable and efficient tool to study tanycytes development and function but its efficiency might vary depending on the target loci. Also, it is necessary to characterize Rax:CreER^{T2} activity in older mice due to possibility of variable Cre activity at different ages as has being reported for other inducible Cre lines (Michael et al., 1999; Postic & Magnuson, 2000).

In summary, we have generated a viable and fertile tanycyte-specific Cre mouse line, the Rax:CreER$^{T2/+}$, which within the hypothalamus is specifically expressed in tanycytes and some cells the ME which might correspond to newborn tanycytes. As a consequence Rax:CreER$^{T2/+}$ can have a variety of uses including elimination of conditional alleles in tanycytes, selective elimination of tanycytes after crossing to a DTa expressing mouse line and prospective genetic labeling of tanycytes. Also, this line can be use to study other Rax expressing populations such as retinal progenitors and MG in the retina. Its utility in the pineal gland and posterior pituitary needs to be further addressed when the characterization of Rax:CreER^{T2} activity is completed.

Figure 6.1.

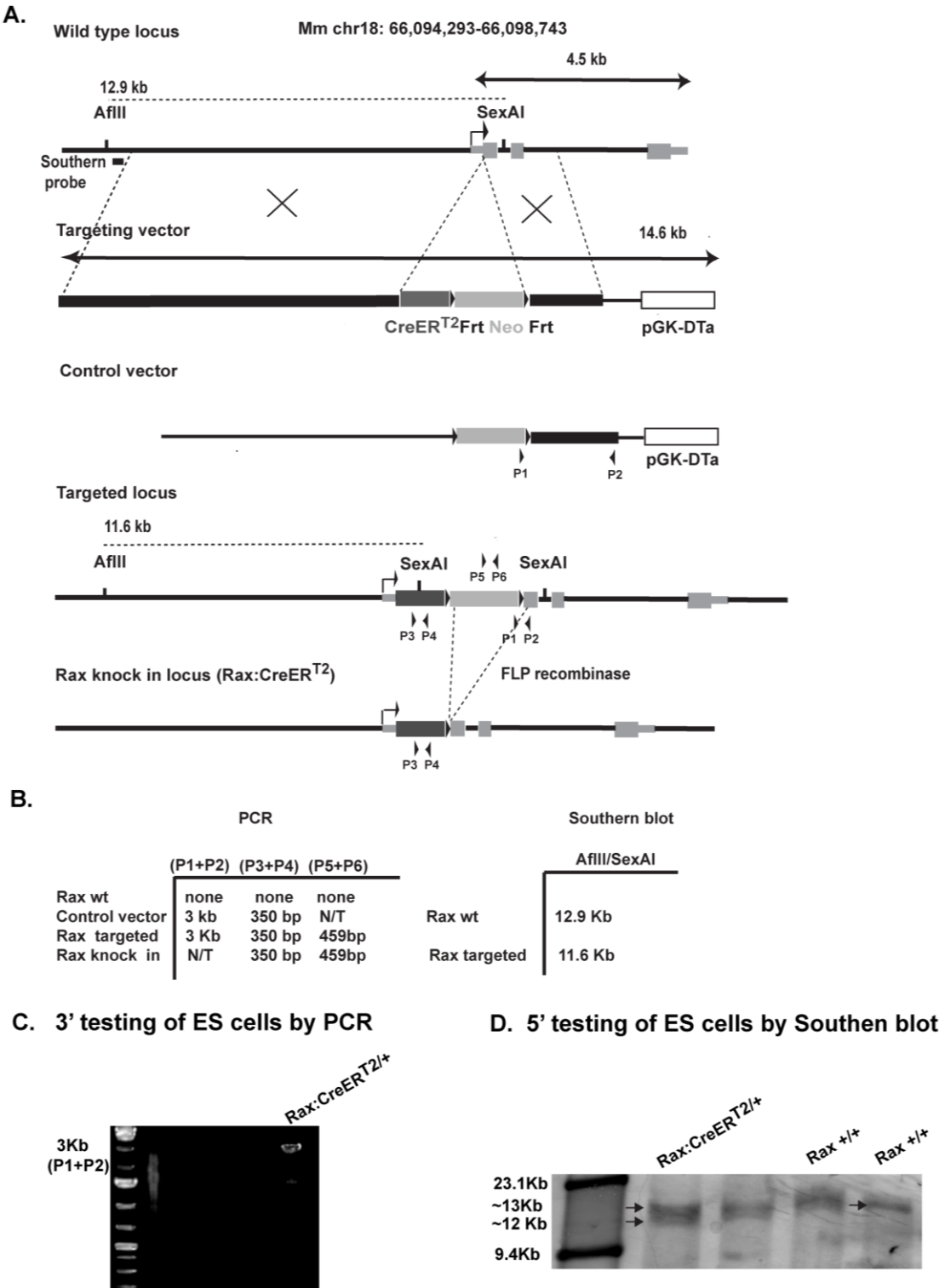
A.
Wild type locus
Mm chr18: 66,094,293-66,098,743
4.5 kb
12.9 kb
AflII
SexAI
Southern probe
Targeting vector
14.6 kb
CreER^{T2}Frt Neo Frt
pGK-DTa
Control vector
P1
P2
pGK-DTa
Targeted locus
11.6 kb
AflII
SexAI
P5 P6
SexAI
P3 P4
P1 P2
Rax knock in locus (Rax:CreER^{T2})
FLP recombinase
P3 P4
B.
PCR
Southern blot
(P1+P2) (P3+P4) (P5+P6)
AflII/SexAI
Rax wt none none none
Control vector 3 kb 350 bp N/T
Rax targeted 3 Kb 350 bp 459bp
Rax knock in N/T 350 bp 459bp
Rax wt 12.9 Kb
Rax targeted 11.6 Kb
C. 3' testing of ES cells by PCR
Rax:CreER$^{T2/+}$
3Kb (P1+P2)
D. 5' testing of ES cells by Southen blot
Rax:CreER$^{T2/+}$
Rax +/+
Rax +/+
23.1Kb
~13Kb
~12 Kb
9.4Kb

Figure 6.1. Generation of Rax:CreER^{T2} knock-in mice

A. Schematic representation of the generation of Rax:CreER$^{T2/+}$ knock-in mice. Rax:CreER^{T2} targeting vector and a control vector were generated using a combination of regular cloning and recombineering. The control vector was created in order to generate a PCR protocol to test correct 3' insertion in the Rax locus (primers P1 and P2). Embryonic stem cells (ES cells) from 129/sv mice were electroporated with either the targeting vector or the control vector. Following electroporation, the targeting vector was inserted by homologous recombination into the Rax locus in frame and six nucleotides downstream from the first ATG. In order to generate chimeras, ES cells with correct 3' insertion (tested by PCR) and 5' insertion (tested by southern blot) were injected in the pronuclei of fertilized eggs obtained from 129/sv female mice. The neo cassette was removed from Rax:CreER^{T2} –neo mice carrying the targeted locus by breeding them to FLPe mice. Rax:CreER^{T2}; FLPe$^{/+}$ mice were tested by PCR for the absence of the neo cassette (primers P5 and P6) and the presence of Cre recombinase (primers P3 and P4). **B.** Expected band sizes of the PCR and southern blot testing protocols. **C.** PCR and Southern blot in DNA from ES cell clones tested for correct insertion of the targeting vector into the Rax locus. The 3' testing was done by PCR using a forward primer located inside the second intron of Rax gene and a reverse primer located in the neomycin cassette generating a 3Kb fragment (see also **A.)**. The 5' testing was performed by Southern blot using DNA double digested with AfIIl and SexAI followed by hybridization with a probe located 11.2 kb upstream of the first Rax ATG. The targeting vector locus introduced an additional SexAI site closer to the AfIII site which generated a DNA fragment (11.6 Kb) shorter than the wild type DNA fragment (12.9Kb).

Figure 6.2.

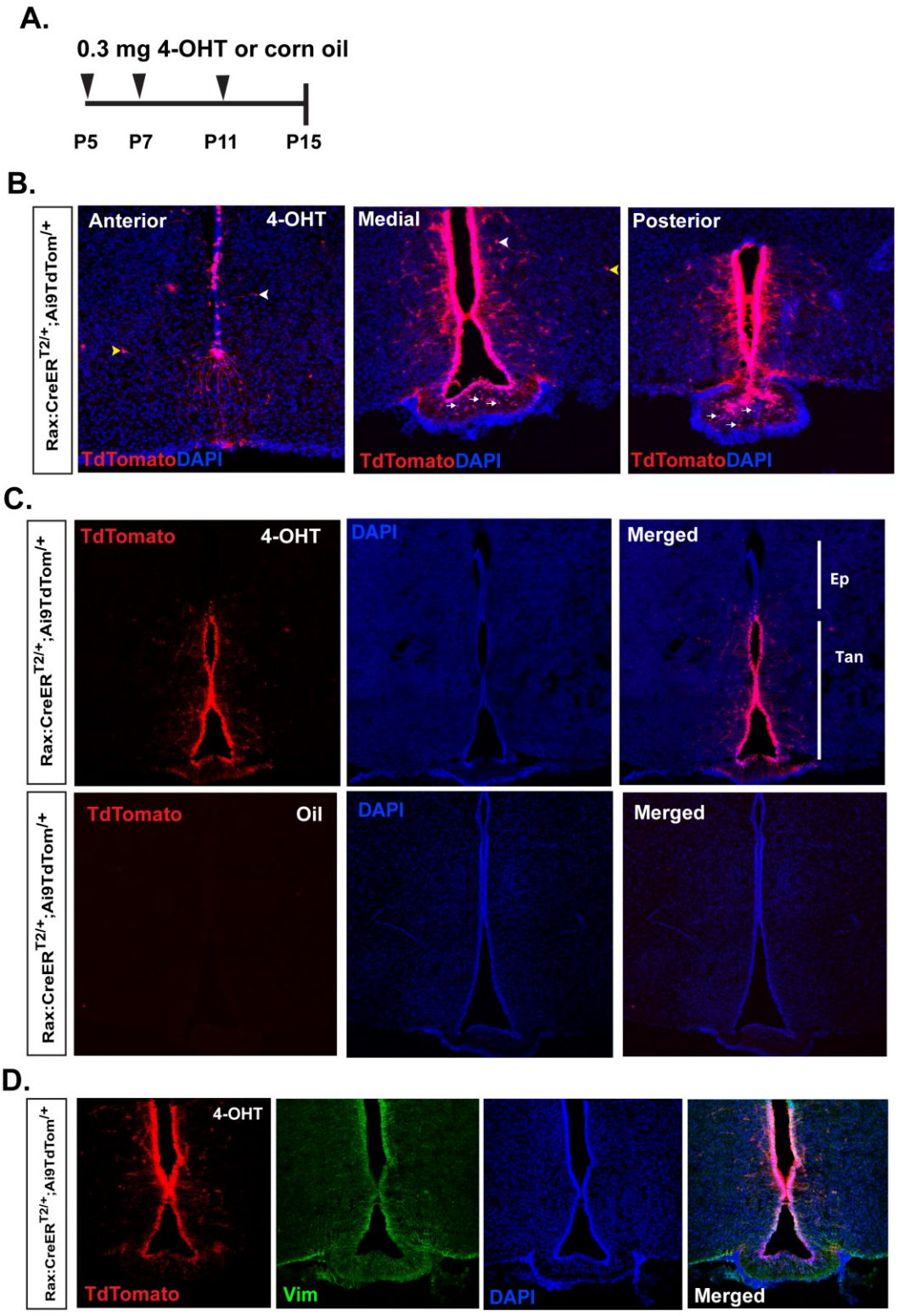
A.
0.3 mg 4-OHT or corn oil
P5
P7
P11
P15
B.
Rax:CreER$^{T2/+}$;Ai9TdTom$^{/+}$
Anterior
4-OHT
TdTomatoDAPI
Medial
TdTomatoDAPI
Posterior
TdTomatoDAPI
C.
Rax:CreER$^{T2/+}$;Ai9TdTom$^{/+}$
TdTomato
4-OHT
DAPI
Merged
Ep
Tan
Rax:CreER$^{T2/+}$;Ai9TdTom$^{/+}$
TdTomato
Oil
DAPI
Merged
D.
Rax:CreER$^{T2/+}$;Ai9TdTom$^{/+}$
4-OHT
TdTomato
Vim
DAPI
Merged

Figure 6.2. Rax:CreER^{T2} activity in the postnatal hypothalamus is specific of tanycytes and some cells in the median eminence

Confocal images of Rax:CreER$^{T2/+;}$Ai9tdTomato$^{/+}$ mice. **A.** Diagram of 4-Hydroxytamoxifen (4-OHT) administration. Mice received 0.3mg of 4-OHT orally by gavage once a day at P5, P7 and P11 and were sacrificed at P15. **B.** Cre recombinase activity along the anterior to posterior axis of the hypothalamus (20X). There is specific cre activity in tanycytes of the anterior, medial and posterior hypothalamus. Tanycyte cell bodies and processes can be visualized directly without staining due to the presence of Ai9tdtomato expression after 4-OHT induction of Rax:CreER^{T2} . Some tdTomato signal is observed in the hypothalamic parenchyma proximal (white arrow heads) and distal to the ventricle (yellow arrow heads). Proximal signal might correspond to cells or blood vessels surrounded by tanycytic processes as is seen in the anterior section (white arrow head). Distal signal seems to correspond to either ectopic cre activity or leakiness in the reporter. Signal in the median eminence corresponds to β tanycyte processes and Rax^{+} cells of unknown identity (white arrows). **C.** Tile confocal images of Rax:CreER$^{T2/+;}$Ai9tdTomato$^{/+}$ mice injected with 4-OHT or oil (20X). Tdtomato signal is present in tanycytes (Tan) but it is not observed in the ependymal cells (Ep). Ai9tdTomato reporter is not leaky in the hypothalamus as is seen in the oil control. **D.** Tdtomato signal in the tanycyte cell bodies and processes co-labels with vimentin (green) (20X).

Figure 6.3.

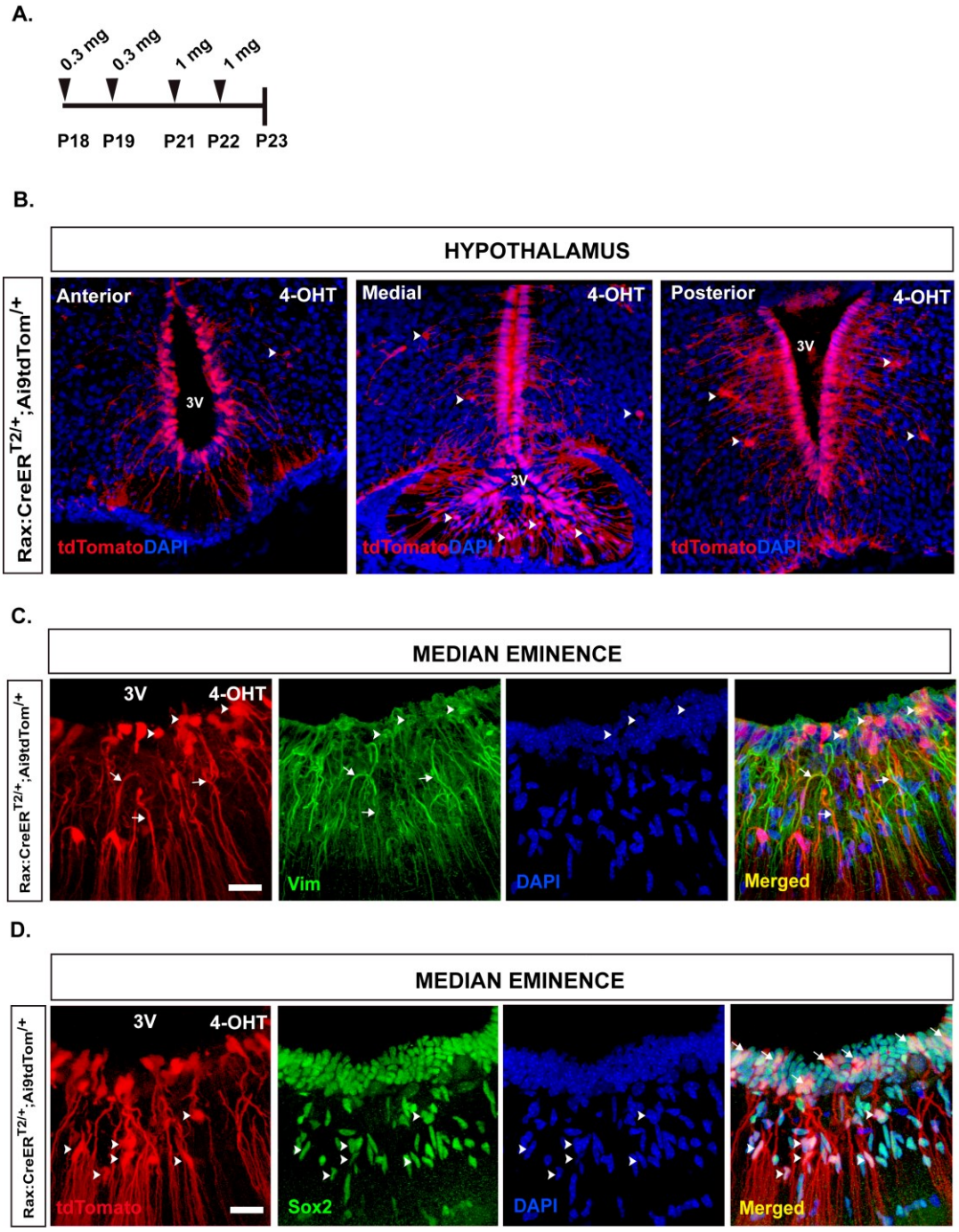
A.
0.3 mg
0.3 mg
1 mg
1 mg
P18 P19 P21 P22 P23
B.
HYPOTHALAMUS
Rax:CreER^T2/+;Ai9tdTom/+
Anterior
4-OHT
3V
tdTomatoDAPI
Medial
4-OHT
3V
tdTomatoDAPI
Posterior
4-OHT
3V
tdTomatoDAPI
C.
MEDIAN EMINENCE
Rax:CreER^T2/+;Ai9tdTom/+
3V
4-OHT
Vim
DAPI
Merged
D.
MEDIAN EMINENCE
Rax:CreER^T2/+;Ai9tdTom/+
3V
4-OHT
tdTomato
Sox2
DAPI
Merged

Figure 6.3. Rax:CreER^{T2} activity at later postnatal ages persists in hypothalamic tanycytes and median eminence cells

Confocal images of Rax:CreER$^{T2/+;}$Ai9tdTomato$^{/+}$ mice. **A.** Diagram of 4-Hydroxytamoxifen (4-OHT) administration. Mice received 0.3mg of 4-OHT orally by gavage once a day at P18, P19 and 1mg at P21, P22 and were sacrificed at P23. **B.** At later postnatal ages (P18 to P22) Rax:CreER^{T2} activity is similar to P5 activity; tdTomato signal is present in tanycytes of the anterior, medial and posterior hypothalamus, as well as in cells in medial and external layers of median eminence. Also, there is some tdTomato signal in hypothalamic parenchyma frequently associated with tanycytes processes (white arrow heads). **C.** Confocal *z*-stack reconstruction of the median eminence of the tuberal hypothalamus stained with vimentin (green). Tanycytes cells bodies (white arrow heads) and tanycyte processes (white arrows) are co-labeled with vimentin and Ai9tdTomato. Scale bar: 20μm. 3V: third ventricle **D.** Confocal *z*-stack reconstruction of the median eminence of the tuberal hypothalamus stained with Sox2 (green). Beta tanycytes are co-labeled with Sox2 and Ai9Tdtomato (white arrow heads). Furthermore, cells in the medial layer of the median eminence are co-labeled with Sox2 (white arrow heads). Scale bar: 20μm. 3V: third ventricle.

Figure 6.4.

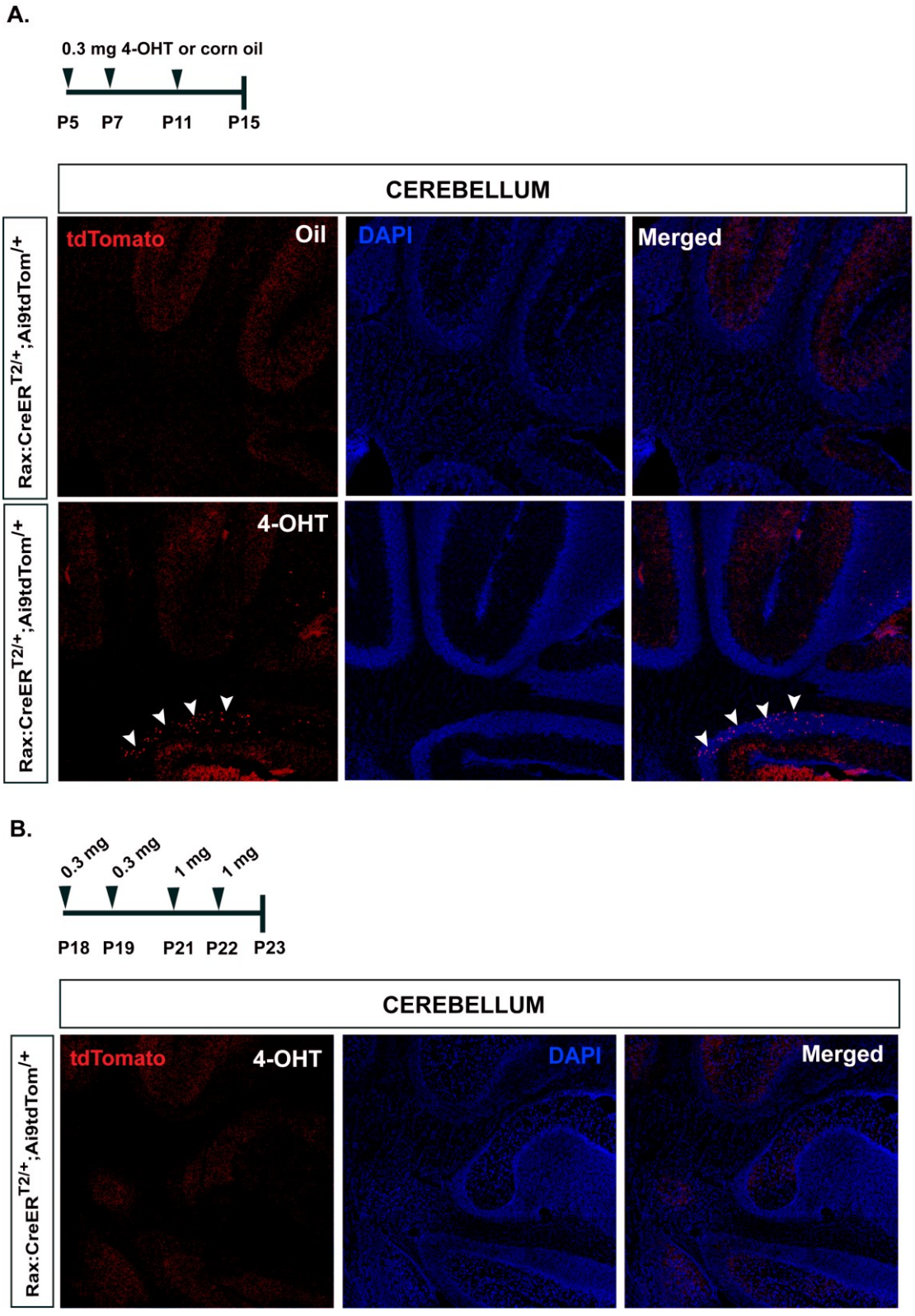
A.
0.3 mg 4-OHT or corn oil
P5
P7
P11
P15
CEREBELLUM
tdTomato
Oil
DAPI
Merged
Rax:CreER$^{T2/+}$;Ai9tdTom$^{/+}$
4-OHT
Rax:CreER$^{T2/+}$;Ai9tdTom$^{/+}$
B.
0.3 mg
0.3 mg
1 mg
1 mg
P18
P19
P21
P22
P23
CEREBELLUM
tdTomato
4-OHT
DAPI
Merged
Rax:CreER$^{T2/+}$;Ai9tdTom$^{/+}$

Figure 6.4. Transient early postnatal Rax:CreER^{T2} activity in the cerebellum
A. Confocal images of the cerebellum of Rax:CreER$^{T2/+}$;Ai9tdTomato$^{/+}$ mice induced at early postnatal ages (P5). Mice received corn oil or 0.3mg of 4-OHT at P5, P7, P11 by gavage and were sacrificed at P15. There is tdTomato signal in cells of a ventral cerebellar lobe. **B.** Confocal images of the cerebellum of Rax:CreER^{T2};Ai9tdTomato$^{/+}$ mice induced at later postnatal ages (P19). Mice received 0.3mg of 4-OHT at P18, P19 and 1mg of 4-OHT at P21 and P22 by gavage and were sacrificed at P23. TdTomato signal in the ventral cerebellar lobe is not observed indicating that Rax cerebellar expression in this areas is transient.

Figure 6.5.

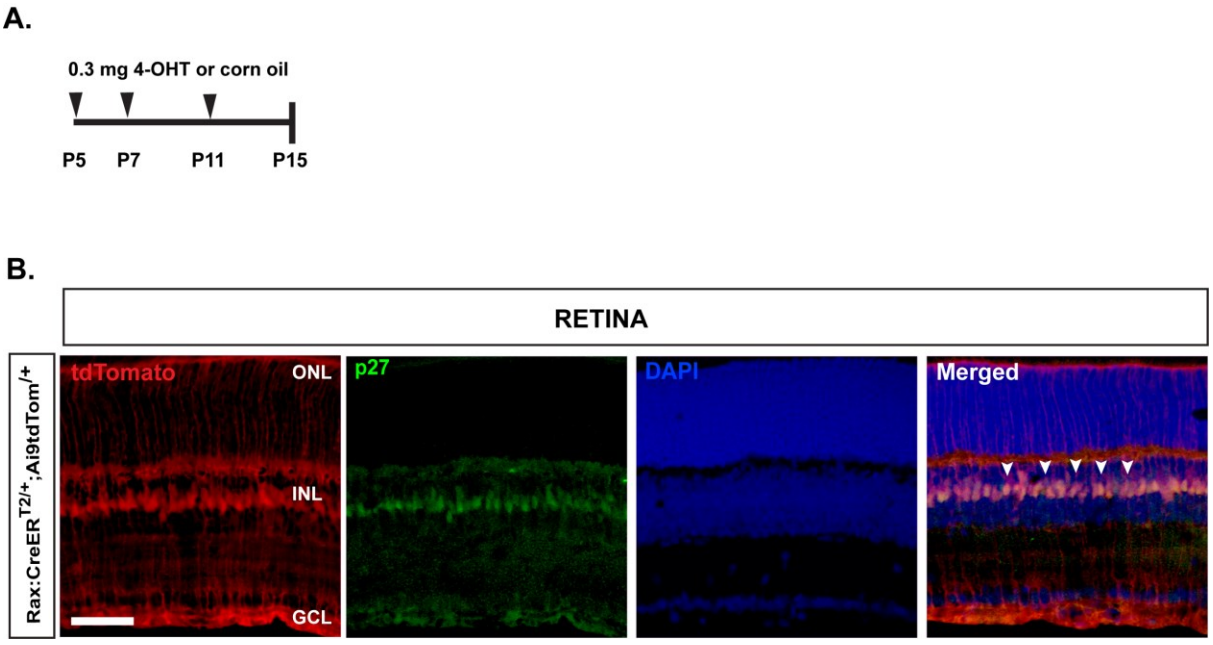

Figure 6.5. Postnatal Rax:CreER^{T2} activity in the retina is specific of Muller glia
Confocal *z*-stack reconstruction of retinas from Rax:CreER$^{T2/+}$;Ai9tdTomato$^{/+}$ mice induced with 4-OHT. **A.** Mice received 4-OHT or corn oil by gavage at P5, P7, P11 and they were sacrificed at P15. **B.** Tdtomato labels the entire Müller glia (MG) cell bodies. MG end feet extend across the entire retina from the ONL to the INL. MG end feet form the inner limiting membrane (area by the GCL) and the outer limiting membrane (area between the ONL and the photoreceptor outer segments). Also, MG end feet envelop the synaptic plexa of the inner and outer plexiform layers (areas between the ONL and INL and the area between the INL and GCL). The nuclear MG marker p27 co-labels with tdTomato. Scale bar: 40um**.**

Figure 6.6.

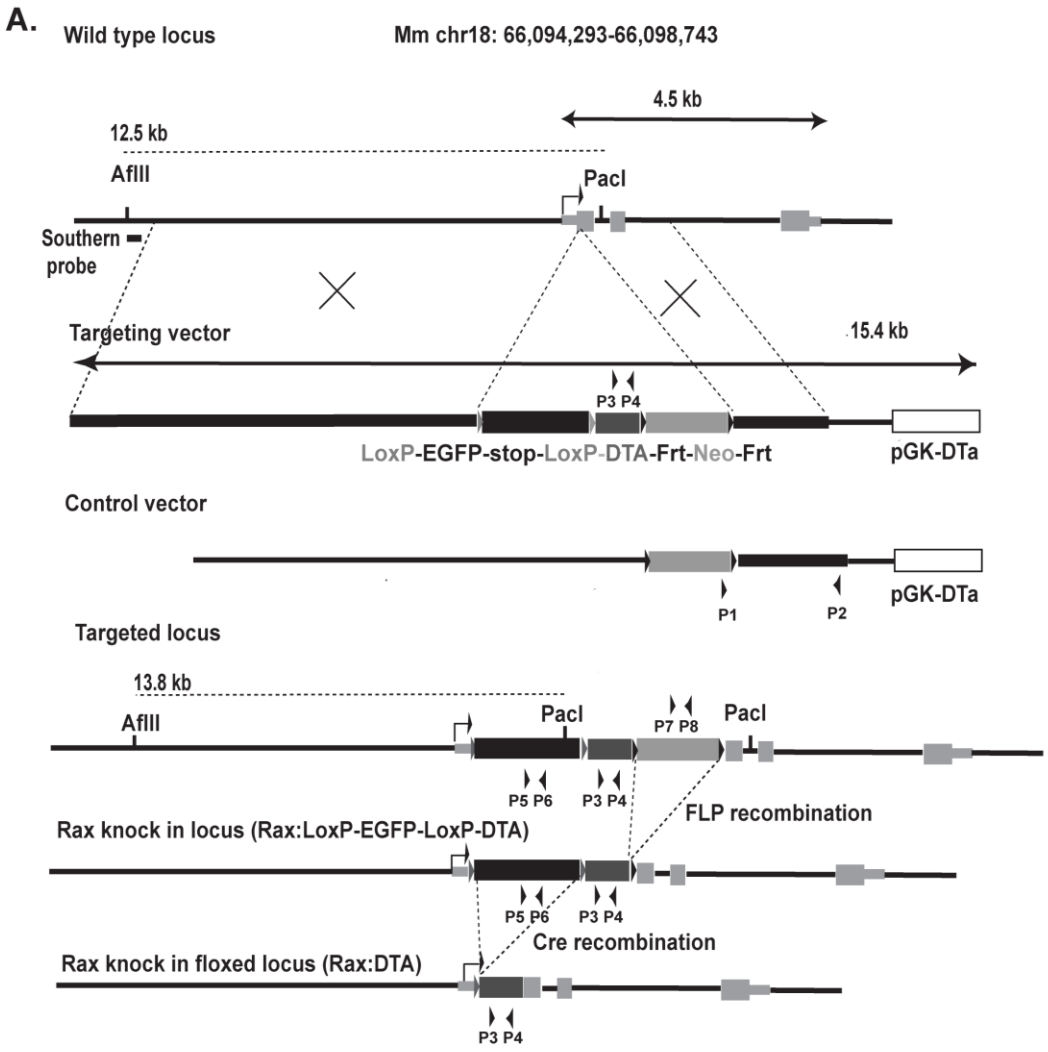

B.

	PCR				Southern blot	
	(P1+P2)	(P3+P4)	(P5+P6)	(P7+P8)		AflII/PacI
Rax wt	none	none	none	none		
Control vector	3 kb	550bp	500bp	N/T	Rax wt	12.5 Kb
Rax targeted	3 Kb	550bp	500bp	459bp		
Rax knock in	N/T	550bp	500bp	459bp	Rax targeted	13.8 Kb

Figure 6.6. Generation of Rax: lox-EGFP-stop-lox-DTa knock-in targeted locus
A. Schematic representation of the generation of Rax:lox-EGFP-stop-lox-DTA knock-in construct. Rax:lox-EGFP-stop-lox-DTA targeting vector and a control vector were generated using a combination of regular cloning and recombineering. The control vector was created in order to generate a PCR protocol to test correct 3' insertion in the Rax locus (primers P1 and P2). Embryonic stem cells (ES cells) from 129/sv mice were electroporated with either the targeting vector or the control vector. Following electroporation, the targeting vector was inserted by homologous recombination into the Rax locus in frame and six nucleotides downstream from the first ATG. In order to generate chimeras, ES cells with correct 3' insertion (tested by PCR) and 5' insertion (tested by southern blot) were injected in the pronuclei of fertilized eggs obtained from 129/sv female mice. However, none ES cells with the correct targeted locus have not being obtained yet. If positive ES cells are obtained, the neo cassette is going to be removed, from mice carrying the targeted locus, by crossing them with flp mice. Rax: lox-EGFP-stop-loxP-DTa knock in mice will be tested for the absence of a the neo cassette (primers P7 and P8) and presence of EGFP (primers P3 and P4) and DTA (primers P3 and P4). **B.** Expected band sizes of the PCR and southern blot protocol

6.4. Materials and methods

Mice

C57BL/6J wild type

C57BL/6J wild type mice were purchased from Charles Rivers and were bred to chimeric mice to determine germline transmission of the Rax:CreER^{T2} targeted locus.

FLPeR mice

The neomycin cassette was removed using FLpeR mice donated by Dr. Jeremy Nathans from Johns Hopkins. These mice correspond to the Jackson's repository 129S4/SvJaeSor-Gt(ROSA)26Sortm1(FLP1)Dym/J stock number 003946. FLPeR mice have a widespread expression of the FLPe variant of the Saccharomyces cerevisiae FLP1 recombinase gene driven by the Gt(ROSA)26Sor promoter. FLP-mediated recombination in Rax:CreER^{T2}-neo;ROSA26FLpeR mice containing a neomycin cassette flanked by FRT sites, resulted in the elimination of the neomycin cassette and generation of Rax:CreER^{T2} knock-in mouse. The FLPeR was bred out of the mouse line after the neomycin cassette elimination.

Ai9tdTomato reporter mice

Ai9tdTomato mice were a generous donation from Dr. Xinzhong Dong at Johns Hopkins. These mice correspond to the Jackson's repository B6;129S6-Gt(ROSA)26Sortm9(CAG-tdTomato)Hze/J mouse line Stock No. 007905. The Ai9tdTomato reporter mouse line has a lox-flanked stop cassette which prevents transcription of the downstream red fluorescent protein variant (tdTomato). When bred to any Cre mice it is expected that the resulting offspring will have the stop cassette deleted in the Cre-expressing cells resulting in expression of tdTomato. Because this

reporter construct is driven by a CAG promoter inserted into the Gt(ROSA)26Sor locus, tdTomato expression is determined by which cells express Cre recombinase.

Genotyping

Tail DNA was extracted as previously described (see **Chapter 3**).

Cre genotyping was done as previously described (see **Chapter 3**).

DTa genotyping

DTa genotyping was performed using the following primers fwd 5'-TCGTACCACGGGACTAAACC-3' and rev 5'-GTTAATTAATTAGAGCTTTAAATCTCT-3' originating a 550 PCR product. The PCR protocol used was: 94°C for 5', 94°C for 30 sec, 55°C for 30 sec, 68°C for 45 min, repeat steps 2-4 30 times, 72° C for 5, 4°C hold.

Neomycin cassette genotyping

Neomycin cassette genotyping of the RaxCreERT2; ROSA26FLpeR mice was done with the following primers: fwd 5'-GGCGCGAGCCCTGATGCTC-3' and rev 5'-TTGGGTGGAGAGGCTATTCGGCTATGAC-3' originating a 459bp PCR product. The PCR protocol used was: 94°C for 5', 94°C for 30 sec, 63°C for 30 sec, 68°C for 45 min, repeat steps 2-4 30 times, 72° C for 5, 4°C hold.

Ai9tdTomato genotyping

Ai9tdTomato genotyping was done using the fwd primer 5'-CTGTTCCTG TACGGCATGG-3' and the rev primer 5'-GGCATTAAAGCAGCGTATCC-3' which originated a 296bp PCR product. The PCR protocol was: 94°C 5 min, 94°C 30 sec, 55°C 45 sec, 72°C 45 sec repeat steps 2-4 35 times, 72°C 7 min and 4°C hold.

Generation of the pBSA vector

We designed a multicloning site to clone the different cassettes for our targeting and control vector. The multicloning site was generated as follows: first, we identified the restriction enzyme sites (RE) needed for cloning the cassettes into the vector and designed a 102bp single strand DNA sense and antisense sequence using vector NTI. This ssDNA consisted of eigth unique RE sites (SacII, NsiI, PacI, MluI, NotI, BsiWI, ApaI, AtaII) separated from each other by three adenines (AAA). Both ssDNA were added in an equimolar concentration (100uM) in miliQ water, the solution was heated at 94°C in a water bath and allowed to slowly cool down at RT to allow formation of a double stranded DNA (dsDNA). The resulting dsDNA was sequenced in both directions and was later cloned into a pBluscript SK(-) which has had its multicloning site previously removed (pBSA).

Generation of Rax:lox-EGFP-stop-lox-DTa and Rax:CreER^{T2} targeting and control vectors

We used recombineering to retrieve a 14kb fragment from a C57black/6 background Bacterial Artificial Chromosome (BAC) containing the Rax locus as well as a long and short arm. Briefly, we electroporated the entire BAC into SW106 cells and grow them O/N at 30°C. Colonies were tested for the presence of the BAC by PCR amplification of random fragments inside the BAC. Then, SW106 cells containing the BAC were electroporated with a pGK-DTa vector containing two previously cloned 500 bp retrieving arms (a 3' arm and a 5' arm) homologous to the ends of the chosen 14kb BAC region. For the control vector, the 500 bp 3' arm was homologous to the BAC region 500kb downstream from the 3' arm used for the targeting vector with the intention

to generate a longer short arm in the control vector to design a PCR ES cells screening protocol.

Finally, we activated the recombineering machinery of the SW106 cells (containing the BAC and the pGK-DTa vector) by shaking and heating at 42°C which induced the retrieval of the 14Kb BAC region by homologous recombination between the BAC and the 3' and 5' 500 bp arms of the pGK-DTa vector. The resulting vector (pGK-DTa-LA-Rax-SA) consisting of the Rax locus (4.5 Kb), an upstream 7.5Kb long arm (LA), a short 2Kb arm (SA) and the negative selection cassette pGK-DTa, was used for a second round of recombineering with the vectors containing either the lox-EGFP-stop-lox-DTa-neo or the CreER^{T2}-neo targeting constructs.

The Rax:lox-EGFP-stop-lox-DTa-neo and Rax:CreER^{T2}-neo constructs were generated simultaneously using traditional cloning as follows: first, we cloned two 500 pb arms homologous to the Rax sequence upstream (5' arm) and downstream (3' arm) from the eighth nucleotide downstream the adenine of the Rax first translation start site (USCS genome browser July 2007 (NCBI37/mm9) Assembly) into the pBSA vector that we generated previously. Second, we introduced a neomycin cassette in between the two short Rax homologous arms. Then, we cloned the lox-EGFP-stop-lox-DTa cassette obtained from Dwight Bergels laboratory (Kang et al., 2010) or the CreER^{T2} obtain from Addgene (pCAG-CreERT2, Plasmid 14797) upstream the neomycin cassette generating the lox-EGFP-stop-lox-DTa-neo and the CreER^{T2}-neo constructs. The resulting lox-EGFP-stop-lox-DTa-neo cassette or CreER^{T2}-neo cassettes were inserted into the Rax locus by recombineering between the 500 bp arms of the lox-EGFP-stop-lox-DTa-neo or the CreER^{T2}-neo constructs and the pGK-DTa-LA-Rax-SA vector. As a consequence, we

generated the targeting vectors Rax:CreER^{T2}-neo and Rax:lox-EGFP-stop-lox-DTa-neo which were sequenced and submitted to the Johns Hopkins transgenic core for electroporation into sv129 ES cells.

The control construct was generated in the same way than the targeting vectors except that the control construct contained only the neomycin cassette and its short arm was 1Kb longer. A longer short arm allowed the standardization of a PCR protocol to test correct 3' insertion into the Rax locus. In this PCR protocol the forward primer aligned to the second intron of Rax and the reverse primer aligned to the neomycin cassette originating a 3Kb fragment only when the constructs where inserted in the correct location.

Sequencing of the targeting and control vectors

Rax:CreER^{T2}-neo and Rax:lox-EGFP-stop-lox-DTa-neo targeting vectors and control vector DNA were submitted to the sequencing core at Johns Hopkins for sequencing using forward primers expanding the entire construct including the long and short arms. We verified the sequences of the long and short arms using the BLAT tool from the University of California Santa Cruz genome browser (UCSC genome browser July 2007 (NCBI37/mm9) Assembly). The Rax:CreER^{T2}-neo, Rax:lox-EGFP-stop-lox-DTa-neo and control vector sequences were verified by comparing the resulting sequence with the expected sequence built in vector NTI. Primers used for sequencing were designed using the automatic sequencing primers designer in Vector NTI.

Digestion and DNA purification of targeting and control vectors

Rax:CreER^{T2} and Rax:lox-EGFP-stop-lox-DTa targeting and control vectors were linearized using the fast digest AscI restriction enzyme from ThermoScientific (FD1894).

The digesting cocktail was prepared as suggested by the manufacturer. The incubation time was 1 hour at 37°C. Digested fragments were run in an agarose gel using the uncut plasmid as a control.

The DNA of the digested targeting and control vectors were purified by mixing 1:1 volume of phenol:chloroform:isoamyl alcohol (25:24:1) and the digested reaction containing around 50ug of total vector DNA. This mixture was vortexed for 15 minutes at RT. The supernatant was transferred to a new tube containing a precipitation cocktail consisting of 20µl of 3M Sodium acetate and 1000 µl of 100% EtOH. The precipitation was promoted by incubating the mixture at -80°C overnight. Next day, the precipitation reaction was centrifuged at 4°C for 15 minutes and the supernatant was centrifuged for 15 minutes at 4°C in 1500µl of 70% EtOH. This centrifugation process was repeated twice when a DNA pellet was observed. The DNA pellet was dried at RT for around 15 minutes and the DNA was re-suspended in PBS 1X.

The targeting and control vector DNA were submitted to the Johns Hopkins transgenic core for electroporation into sv129 ES cells following protocols available at their web site: http://www.hopkinsmedicine.org/core/Transgenic_Core/protocols.html

DNA extraction from sv129 ES cell electroporated clones

The Johns Hopkins transgenic core performed the DNA extraction from the ES cells electroporated with the targeting or control constructs following protocols available at their web site: http://www.hopkinsmedicine.org/core/Transgenic_Core/protocols.html.

ES cell colonies screening by PCR

Embryonic stem cell colonies electroporated with either the targeting construct (Rax:CreER^{T2} and Rax:lox-EGFP-stop-lox-DTa) or the control construct were screened

for correct locus insertion by PCR amplification of a 3kb DNA fragment using a forward primer located in chromosome 18 within the second intron of the Rax gene fwd 5'-TTTGTCATTTCCCCTCGTAG-3' and a reverse primer located in the neomycin cassette 5'-CTTCTATCGCCTTCTTGACG-3'. This genotyping was performed using the following PCR touchdown protocol: 95°C 5 min, 94°C 30min, 70°C 1min; minus 1°C each cycle (15 times), 72°C 3min, 94°C 30sec, 55°C 30sec 30X, 72°C 3min, 72°C 7min, 4°C hold.

Southern blot

ES cell colonies that tested positive by PCR for correct 3' insertion into the Rax locus and the ES cell colonies electroporated with the control vector were grown further and their DNA was extracted using the Blood & Cell Culture DNA Mini Kit from Qiagen (Cat. 13323) following the manufacturer's protocol.

Purified DNA was digested with AfIII and SexAI (Rax:CreER^{T2}-neo construct) or with Aflll and PacI (Rax:lox-EGFP-stop-lox-DTa-neo construct) and used for Southern blot. We designed a 511bp probe amplified by PCR from a wild type C57BL/6J DNA using the following primers: forward 5'-ATGCATTTAGATGCCTGATTGCCAAT-3' and reverse 5'-ACGCGTCAAAACCACAGTAAACCAAG-3'. This probe hybridized upstream the long arm of each targeted locus. The probe labeling and Southern blot were performed using the DIG-High Prime DNA Labeling and Detection Starter Kit I from Roche (Cat. 11745832910) following the manufacturer's protocol.

Karyotyping and ES cells pronuclear injection was performed at the Johns Hopkins transgenic core following their protocols.

Tamoxifen preparation and administration

4-hydroxytamoxifen powder (4-OHT) (Sigma) was dissolved in 100% EtOH to a concentration of 0.05mg/µl. The 4-OHT dissolved in EtOH was aliquoted (100/µl) and each aliquot was mixed with corn oil (Sigma) in a ratio of 1:5 (4-OHT:oil). The EtOH was evaporated from the mixture and the 4-OHT was dissolved in the oil by vacuum centrifugation and heat for 7.5 minutes. Then, the 4-OHT:oil solution was administered to the Rax:CreER$^{T2/+}$;Ai9tdTomato$^{/+}$ mice by gavage. Mice induced at P5, P7 and P11 and sacrificed at P15 received 0.3mg of 4-OHT daily. Mice induced at later postnatal ages received 0.3mg at P18 and P19 and 1mg at days P21 and P22. Rax:CreERT2$^{/+}$;Ai9TdTomato$^{/+}$ oil treated mice received corn oil by gavage.

Brain tissue collection

Mice brain were collected as previously described (see **Chapter 2**). Coronal hypothalamic free floating sections were obtained by sectioning in a cryostat at 40 µm starting from the middle of the anterior hypothalamus to the end of the posterior hypothalamus. Sections were floated in PB 0.5X and serially distributed in individual wells of an RNAse free 48 well plate (Falcon). Sections were stored at -20°C in anti-freezing solution until they were used for the experiments.

Eye tissue collection and staining

We dissected the eyes from RaxCreER^{T2};Ai9tdTomato mice treated with 4-OHT. These eyes where cryopreserved, sectioned and stained using previously described protocols (de Melo, Peng, Chen, & Blackshaw, 2011). The antibody used for MG labeling was mouse anti-P27 antibody at 1:200 dilution from BD Transduction Labs Cat# 610241 (Clone57/Kip1/p27).

Immunohistochemistry of brain sections

Vimentin IHC was performed in floating sections as follows. Slides were washed with PBS 1X for 15 minutes followed by blocking in Superblock (ScyTek) for 5 minutes. Then, Sections were permeabilized/blocked in PBS plus solution (0.3% Triton 100X and 5% normal horse serum in 0.1M PBS 1X) and incubated O/N at 4°C with goat anti-vimentin (1:500) from Aves Lab or rabbit anti-Sox2 (1:500) prepared in PBS plus solution. Next day, slides were washed/permeabilized using PBST (PBS 1X plus Triton 0.1%) for 30 minutes and incubated with Alexa secondary antibodies in PBS plus for 2 hrs at RT at 1:500 dilution. DAPI staining was performed by submerging the slides in a DAPI solution 1:5000 in PBS1X. Tdtomato was detected directly from the tissue without IHC staining.

Image acquisition

Single plane and *z*-stack confocal images were obtained in a Zeiss LSM510 Meta confocal microscope equipped with a Zen 2009 software and using a 10X, 20X or 63X objective and digital zoom 1. Tile pictures were obtained in a 3X3 or 3X2 frame. Confocal images for the two groups ($RaxCreER^{T2}$;$Ai9tdTomato^{/+}$ treated with 4-OHT and $RaxCreER^{T2}$;$Ai9tdTomato^{/+}$ treated with corn oil) were taken in identical conditions, using the same pinhole, gain and contrast.

Images for the different treatments were analyzed qualitatively for the presence or absence of signal and the co-labeling with cell specific markers.

Chapter 7.

Conclusions

- Rax is required for the proliferation and/or survival of progenitors that give rise to hypothalamic tanycytes and ependymal cells of the third ventricle.
- Rax haploinsuficiency leads to the ectopic presence of ependymal cells in the α2 tanycytic zone.
- Hypocellularity of the third ventricle in Rax haploinsuficient mice originates changes in CSF-brain permeability but it does not lead to changes in the gross phenotype of these mice.
- Rax protein is secreted from tanycytes and internalized by adjacent and distal hypothalamic cells.
- Rax:CreER^{T2} mice are a reliable tool to study hypothalamic tanycyte development and function.

This study represents the first throughout characterization of a transcription factor involved in tanycyte development which lead to the generation of the Rax:CreER^{T2} mouse line that can be used to study tanycyte development and function. Also, we have reported for the first time that Rax transcription factor protein is secreted by tanycytes in the adult murine hypothalamus which will open a new field of research on the function of tanycyte-secreted homeoproteins.

Bibliography

Agnati, L. F., Zoli, M., Stromberg, I., & Fuxe, K. (1995). Intercellular communication in the brain: wiring versus volume transmission. Neuroscience, 69, 711-726.

Altman, J. & Bayer, S. A. (1978). Development of the diencephalon in the rat. III. Ontogeny of the specialized ventricular linings of the hypothalamic third ventricle. J.Comp Neurol., 182, 995-1015.

Alvarez-Bolado, G., Paul, F. A., & Blaess, S. (2012). Sonic hedgehog lineage in the mouse hypothalamus: from progenitor domains to hypothalamic regions. Neural development, 7, 4-7.

Alvarez-Fischer, D., Fuchs, J., Castagner, F., Stettler, O., Massiani-Beaudoin, O., Moya, K. L. et al. (2011). Engrailed protects mouse midbrain dopaminergic neurons against mitochondrial complex I insults. Nature neuroscience, 14, 1260-1266.

Andreazzoli, M., Gestri, G., Cremisi, F., Casarosa, S., Dawid, I. B., & Barsacchi, G. (2003). Xrx1 controls proliferation and neurogenesis in Xenopus anterior neural plate. Development (Cambridge, England), 130, 5143-5154.

Asbreuk, C. H., van Schaick, H. S., Cox, J. J., Smidt, M. P., & Burbach, J. P. (2002). Survey for paired-like homeodomain gene expression in the hypothalamus: restricted expression patterns of Rx, Alx4 and goosecoid. Neuroscience, 114, 883-889.

Balordi, F. & Fishell, G. (2007). Mosaic removal of hedgehog signaling in the adult SVZ reveals that the residual wild-type stem cells have a limited capacity for self-

renewal. The Journal of neuroscience : the official journal of the Society for Neuroscience, 27, 14248-14259.

Batailler, M., Mullier, A., Sidibe, A., Delagrange, P., Prevot, V., Jockers, R. et al. (2012). Neuroanatomical distribution of the orphan GPR50 receptor in adult sheep and rodent brains. Journal of neuroendocrinology, 24, 798-808.

Blackshaw, S., Scholpp, S., Placzek, M., Ingraham, H., Simerly, R., & Shimogori, T. (2010). Molecular pathways controlling development of thalamus and hypothalamus: from neural specification to circuit formation. The Journal of neuroscience : the official journal of the Society for Neuroscience, 30, 14925-14930.

Bleier, R. (1971). The relations of ependyma to neurons and capillaries in the hypothalamus: a Golgi-Cox study. The Journal of comparative neurology, 142, 439-463.

Bolborea, M., Laran-Chich, M. P., Rasri, K., Hildebrandt, H., Govitrapong, P., Simonneaux, V. et al. (2011). Melatonin controls photoperiodic changes in tanycyte vimentin and neural cell adhesion molecule expression in the Djungarian hamster (Phodopus sungorus). Endocrinology, 152, 3871-3883.

Bouille, C., Mesnil, M., Barriere, H., & Gabrion, J. (1991). Gap junctional intercellular communication between cultured ependymal cells, revealed by lucifer yellow CH transfer and freeze-fracture. Glia, 4, 25-36.

Brightman, M. W. (1965). The distribution within the brain of ferritin injected into cerebrospinal fluid compartments. II. Parenchymal distribution. The American Journal of Anatomy, 117, 193-219.

Bringmann, A., Iandiev, I., Pannicke, T., Wurm, A., Hollborn, M., Wiedemann, P. et al. (2009). Cellular signaling and factors involved in Muller cell gliosis: neuroprotective and detrimental effects. Progress in retinal and eye research, 28, 423-451.

Bringmann, A. & Wiedemann, P. (2012). Muller glial cells in retinal disease. Ophthalmologica.Journal international d'ophtalmologie.International journal of ophthalmology.Zeitschrift fur Augenheilkunde, 227, 1-19.

Brunet, I., Di Nardo, A. A., Sonnier, L., Beurdeley, M., & Prochiantz, A. (2007). The topological role of homeoproteins in the developing central nervous system. Trends in neurosciences, 30, 260-267.

Brunet, I., Weinl, C., Piper, M., Trembleau, A., Volovitch, M., Harris, W. et al. (2005). The transcription factor Engrailed-2 guides retinal axons. Nature, 438, 94-98.

Brunetti, L., Di, N. C., Recinella, L., Chiavaroli, A., Leone, S., Ferrante, C. et al. (2011). Effects of vaspin, chemerin and omentin-1 on feeding behavior and hypothalamic peptide gene expression in the rat. Peptides, 32, 1866-1871.

Bruni, J. E. (1998). Ependymal development, proliferation, and functions: a review. Microscopy research and technique, 41, 2-13.

Bruni, J. E., Del Bigio, M. R., & Clattenburg, R. E. (1985). Ependyma: normal and pathological. A review of the literature. Brain research, 356, 1-19.

Byerly, M. S. & Blackshaw, S. (2009). Vertebrate retina and hypothalamus development. Wiley interdisciplinary reviews.Systems biology and medicine, 1, 380-389.

Cardona-Gomez, G. P., Chowen, J. A., & Garcia-Segura, L. M. (2000). Estradiol and progesterone regulate the expression of insulin-like growth factor-I receptor and insulin-like growth factor binding protein-2 in the hypothalamus of adult female rats. Journal of neurobiology, 43, 269-281.

Casarosa, S., Amato, M. A., Andreazzoli, M., Gestri, G., Barsacchi, G., & Cremisi, F. (2003). Xrx1 controls proliferation and multipotency of retinal progenitors. Molecular and cellular neurosciences, 22, 25-36.

Charli, J. L., Vargas, M. A., Cisneros, M., de, G. P., Baeza, M. A., Jasso, P. et al. (1998). TRH inactivation in the extracellular compartment: role of pyroglutamyl peptidase II. Neurobiology (Bp), 6, 45-57.

Charlton, H. (2008). Hypothalamic control of anterior pituitary function: a history. Journal of neuroendocrinology, 20, 641-646.

Chauvet, N., Parmentier, M. L., & Alonso, G. (1995). Transected axons of adult hypothalamo-neurohypophysial neurons regenerate along tanycytic processes. J.Neurosci.Res., 41, 129-144.

Chauvet, N., Prieto, M., & Alonso, G. (1998). Tanycytes present in the adult rat mediobasal hypothalamus support the regeneration of monoaminergic axons. Exp.Neurol., 151, 1-13.

Chauvet, N., Privat, A., & Alonso, G. (1996). Aged median eminence glial cell cultures promote survival and neurite outgrowth of cocultured neurons. Glia, 18, 211-223.

Choo, S. W. & Russell, S. (2011). Genomic approaches to understanding Hox gene function. Advances in Genetics, 76, 55-91.

Christiaens, B., Grooten, J., Reusens, M., Joliot, A., Goethals, M., Vandekerckhove, J. et al. (2004). Membrane interaction and cellular internalization of penetratin peptides. European journal of biochemistry / FEBS, 271, 1187-1197.

Cifuentes, M., Perez-Martin, M., Grondona, J. M., Lopez-Avalos, M. D., Inagaki, N., Granados-Duran, P. et al. (2011). A comparative analysis of intraperitoneal versus intracerebroventricular administration of bromodeoxyuridine for the study of cell proliferation in the adult rat brain. J.Neurosci.Methods, 201, 307-314.

Coppola, A., Meli, R., & Diano, S. (2005). Inverse shift in circulating corticosterone and leptin levels elevates hypothalamic deiodinase type 2 in fasted rats. Endocrinology, 146, 2827-2833.

Cortes-Campos, C., Elizondo, R., Carril, C., Martinez, F., Boric, K., Nualart, F. et al. (2013). MCT2 expression and lactate influx in anorexigenic and orexigenic neurons of the arcuate nucleus. PLoS One, 8, e62532.

Cortes-Campos, C., Elizondo, R., Llanos, P., Uranga, R. M., Nualart, F., & Garcia, M. A. (2011). MCT expression and lactate influx/efflux in tanycytes involved in glia-neuron metabolic interaction. PloS one, 6, e16411.

Croteau, W., Davey, J. C., Galton, V. A., & St Germain, D. L. (1996). Cloning of the mammalian type II iodothyronine deiodinase. A selenoprotein differentially expressed

and regulated in human and rat brain and other tissues. The Journal of clinical investigation, 98, 405-417.

De Groot, L. J. (1999). Dangerous dogmas in medicine: the nonthyroidal illness syndrome. The Journal of clinical endocrinology and metabolism, 84, 151-164.

de Melo, J., Peng, G. H., Chen, S., & Blackshaw, S. (2011). The Spalt family transcription factor Sall3 regulates the development of cone photoreceptors and retinal horizontal interneurons. Development (Cambridge, England), 138, 2325-2336.

de Seranno, S., d'Anglemont de Tassigny, X., Estrella, C., Loyens, A., Kasparov, S., Leroy, D. et al. (2010). Role of estradiol in the dynamic control of tanycyte plasticity mediated by vascular endothelial cells in the median eminence. Endocrinology, 151, 1760-1772.

de Seranno, S., Estrella, C., Loyens, A., Cornea, A., Ojeda, S. R., Beauvillain, J. C. et al. (2004). Vascular endothelial cells promote acute plasticity in ependymoglial cells of the neuroendocrine brain. The Journal of neuroscience : the official journal of the Society for Neuroscience, 24, 10353-10363.

de, V. F., Picart, R., Jacque, C., & Tixier-Vidal, A. (1981). Glial fibrillary acidic protein. A cellular marker of tanycytes in the mouse hypothalamus. Dev.Neurosci., 4, 457-460.

Del Bigio, M. R. (1995). The ependyma: a protective barrier between brain and cerebrospinal fluid. Glia, 14, 1-13.

Dellmann, H. D., Lue, L. F., & Bellin, S. I. (1987). Neurosecretory axon regeneration into intrahypothalamic neural lobe allografts: neurophysin immunohistochemistry and fine structure. Experimental brain research.Experimentelle Hirnforschung.Experimentation cerebrale, 67, 543-555.

Dere, E. & Zlomuzica, A. (2012). The role of gap junctions in the brain in health and disease. Neuroscience and biobehavioral reviews, 36, 206-217.

Derossi, D., Joliot, A. H., Chassaing, G., & Prochiantz, A. (1994). The third helix of the Antennapedia homeodomain translocates through biological membranes. The Journal of biological chemistry, 269, 10444-10450.

Di Lullo, E., Haton, C., Le Poupon, C., Volovitch, M., Joliot, A., Thomas, J. L. et al. (2011). Paracrine Pax6 activity regulates oligodendrocyte precursor cell migration in the chick embryonic neural tube. Development (Cambridge, England), 138, 4991-5001.

Diano, S., Naftolin, F., Goglia, F., & Horvath, T. L. (1998). Fasting-induced increase in type II iodothyronine deiodinase activity and messenger ribonucleic acid levels is not reversed by thyroxine in the rat hypothalamus. Endocrinology, 139, 2879-2884.

Didier, M., Harandi, M., Aguera, M., Bancel, B., Tardy, M., Fages, C. et al. (1986). Differential immunocytochemical staining for glial fibrillary acidic (GFA) protein, S-100 protein and glutamine synthetase in the rat subcommissural organ, nonspecialized ventricular ependyma and adjacent neuropil. Cell and tissue research, 245, 343-351.

Doetsch, F., Garcia-Verdugo, J. M., & Alvarez-Buylla, A. (1997). Cellular composition and three-dimensional organization of the subventricular germinal zone in the adult mammalian brain. The Journal of neuroscience : the official journal of the Society for Neuroscience, 17, 5046-5061.

Duchardt, F., Fotin-Mleczek, M., Schwarz, H., Fischer, R., & Brock, R. (2007). A comprehensive model for the cellular uptake of cationic cell-penetrating peptides. Traffic (Copenhagen, Denmark), 8, 848-866.

Duenas, M., Luquin, S., Chowen, J. A., Torres-Aleman, I., Naftolin, F., & Garcia-Segura, L. M. (1994). Gonadal hormone regulation of insulin-like growth factor-I-like immunoreactivity in hypothalamic astroglia of developing and adult rats. Neuroendocrinology, 59, 528-538.

Dupont, E., Prochiantz, A., & Joliot, A. (2011). Penetratin story: an overview. Methods in molecular biology (Clifton, N.J.), 683, 21-29.

Dziegielewska, K. M., Knott, G. W., & Saunders, N. R. (2000). The nature and composition of the internal environment of the developing brain. Cellular and molecular neurobiology, 20, 41-56.

Edlund, T. & Jessell, T. M. (1999). Progression from extrinsic to intrinsic signaling in cell fate specification: a view from the nervous system. Cell, 96, 211-224.

Eiraku, M., Takata, N., Ishibashi, H., Kawada, M., Sakakura, E., Okuda, S. et al. (2011). Self-organizing optic-cup morphogenesis in three-dimensional culture. Nature, 472, 51-56.

Entchev, E. V. & Gonzalez-Gaitan, M. A. (2002). Morphogen gradient formation and vesicular trafficking. Traffic (Copenhagen, Denmark), 3, 98-109.

Ernst, M. C. & Sinal, C. J. (2010). Chemerin: at the crossroads of inflammation and obesity. Trends in endocrinology and metabolism: TEM, 21, 660-667.

Fehm, H. L., Kern, W., & Peters, A. (2006). The selfish brain: competition for energy resources. Progress in brain research, 153, 129-140.

Feil, R., Wagner, J., Metzger, D., & Chambon, P. (1997). Regulation of Cre recombinase activity by mutated estrogen receptor ligand-binding domains. Biochemical and biophysical research communications, 237, 752-757.

Fekete, C., Gereben, B., Doleschall, M., Harney, J. W., Dora, J. M., Bianco, A. C. et al. (2004). Lipopolysaccharide induces type 2 iodothyronine deiodinase in the mediobasal hypothalamus: implications for the nonthyroidal illness syndrome. Endocrinology, 145, 1649-1655.

Fernandez-Galaz, M. C., Morschl, E., Chowen, J. A., Torres-Aleman, I., Naftolin, F., & Garcia-Segura, L. M. (1997). Role of astroglia and insulin-like growth factor-I in gonadal hormone-dependent synaptic plasticity. Brain research bulletin, 44, 525-531.

Fernandez-Galaz, M. C., Torres-Aleman, I., & Garcia-Segura, L. M. (1996). Endocrine-dependent accumulation of IGF-I by hypothalamic glia. Neuroreport, 8, 373-377.

Fliegauf, M., Benzing, T., & Omran, H. (2007). When cilia go bad: cilia defects and ciliopathies. Nature reviews.Molecular cell biology, 8, 880-893.

Fliers, E., Unmehopa, U. A., & Alkemade, A. (2006). Functional neuroanatomy of thyroid hormone feedback in the human hypothalamus and pituitary gland. Mol Cell Endocrinol., 251, 1-8.

Fry, D. L., Mahley, R. W., Weisgraber, K. H., & Oh, S. Y. (1977). Simultaneous accumulation of Evans blue dye and albumin in the canine aortic wall. The American Journal of Physiology, 233, H66-H79.

Furukawa, T., Kozak, C. A., & Cepko, C. L. (1997). Rax, a Novel Paired-Type Homeobox Gene, shows Expression in the Anterior Neural Fold and Developing Retina. Proceedings of the National Academy of Sciences of the United States of America, 94, 3088-3093.

Furukawa, T., Mukherjee, S., Bao, Z. Z., Morrow, E. M., & Cepko, C. L. (2000). rax, Hes1, and notch1 promote the formation of Muller glia by postnatal retinal progenitor cells. Neuron, 26, 383-394.

Gabrion, J. B., Herbute, S., Bouille, C., Maurel, D., Kuchler-Bopp, S., Laabich, A. et al. (1998). Ependymal and choroidal cells in culture: characterization and functional differentiation. Microscopy research and technique, 41, 124-157.

Garcia, M., Millan, C., Balmaceda-Aguilera, C., Castro, T., Pastor, P., Montecinos, H. et al. (2003). Hypothalamic ependymal-glial cells express the glucose

transporter GLUT2, a protein involved in glucose sensing. Journal of neurochemistry, 86, 709-724.

Garcia, M. & Vecino, E. (2003). Role of Muller glia in neuroprotection and regeneration in the retina. Histology and histopathology, 18, 1205-1218.

Garcia-Segura, L. M. (2009). Hormones and brain Plasticity. New York: Oxford.

Garcia-Segura, L. M., Lorenz, B., & DonCarlos, L. L. (2008). The role of glia in the hypothalamus: implications for gonadal steroid feedback and reproductive neuroendocrine output. Reproduction (Cambridge, England), 135, 419-429.

Garcia-Segura, L. M., Rodriguez, J. R., & Torres-Aleman, I. (1997). Localization of the insulin-like growth factor I receptor in the cerebellum and hypothalamus of adult rats: an electron microscopic study. Journal of neurocytology, 26, 479-490.

Gehring, W. J., Qian, Y. Q., Billeter, M., Furukubo-Tokunaga, K., Schier, A. F., Resendez-Perez, D. et al. (1994). Homeodomain-DNA recognition. Cell, 78, 211-223.

Geng, X., Ren, C., Wang, T., Fu, P., Luo, Y., Liu, X. et al. (2012). Effect of remote ischemic postconditioning on an intracerebral hemorrhage stroke model in rats. Neurological research, 34, 143-148.

Geng, Y., Yu, Q., Sicinska, E., Das, M., Bronson, R. T., & Sicinski, P. (2001). Deletion of the p27Kip1 gene restores normal development in cyclin D1-deficient mice. Proceedings of the National Academy of Sciences of the United States of America, 98, 194-199.

Gharib, S. D., Wierman, M. E., Shupnik, M. A., & Chin, W. W. (1990). Molecular biology of the pituitary gonadotropins. Endocrine reviews, 11, 177-199.

Givalois, L., Arancibia, S., Alonso, G., & Tapia-Arancibia, L. (2004). Expression of brain-derived neurotrophic factor and its receptors in the median eminence cells with sensitivity to stress. Endocrinology, 145, 4737-4747.

Gould, S. J., Howard, S., & Papadaki, L. (1990). The development of ependyma in the human fetal brain: an immunohistological and electron microscopic study. Brain research.Developmental brain research, 55, 255-267.

Graham, V., Khudyakov, J., Ellis, P., & Pevny, L. (2003). SOX2 functions to maintain neural progenitor identity. Neuron, 39, 749-765.

Guadano-Ferraz, A., Obregon, M. J., St Germain, D. L., & Bernal, J. (1997). The type 2 iodothyronine deiodinase is expressed primarily in glial cells in the neonatal rat brain. Proceedings of the National Academy of Sciences of the United States of America, 94, 10391-10396.

Hack, M. A., Saghatelyan, A., de, C. A., Pfeifer, A., Ashery-Padan, R., Lledo, P. M. et al. (2005). Neuronal fate determinants of adult olfactory bulb neurogenesis. Nature neuroscience, 8, 865-872.

Hajos, F. & Basco, E. (1984). The surface-contact glia. Adv.Anat.Embryol.Cell Biol., 84, 1-79.

Harik, S. I., Hall, A. K., Richey, P., Andersson, L., Lundahl, P., & Perry, G. (1993). Ontogeny of the erythroid/HepG2-type glucose transporter (GLUT-1) in the rat nervous system. Brain research.Developmental brain research, 72, 41-49.

Herwig, A., Ross, A. W., Nilaweera, K. N., Morgan, P. J., & Barrett, P. (2008). Hypothalamic thyroid hormone in energy balance regulation. Obes.Facts., 1, 71-79.

Hiney, J. K., Srivastava, V., Nyberg, C. L., Ojeda, S. R., & Dees, W. L. (1996). Insulin-like growth factor I of peripheral origin acts centrally to accelerate the initiation of female puberty. Endocrinology, 137, 3717-3728.

Ivanova, A., Signore, M., Caro, N., Greene, N. D., Copp, A. J., & Martinez-Barbera, J. P. (2005). In vivo genetic ablation by Cre-mediated expression of diphtheria toxin fragment A. Genesis (New York, N.Y.: 2000), 43, 129-135.

Jain, R., Pan, J., Driscoll J.A., Wisner, J. W., Huang, T., Gunsten, S. P. et al. (2010). Temporal relationship between primary ad motile ciliogenesis in airway epithelial cells. Am J Respir Cell Mol Biol., 43, 731-739.

Jarvis, C. R. & Andrew, R. D. (1988). Correlated electrophysiology and morphology of the ependyma in rat hypothalamus. The Journal of neuroscience : the official journal of the Society for Neuroscience, 8, 3691-3702.

Joliot, A., Maizel, A., Rosenberg, D., Trembleau, A., Dupas, S., Volovitch, M. et al. (1998). Identification of a signal sequence necessary for the unconventional secretion of Engrailed homeoprotein. Current biology : CB, 8, 856-863.

Joliot, A., Pernelle, C., Deagostini-Bazin, H., & Prochiantz, A. (1991). Antennapedia homeobox peptide regulates neural morphogenesis. Proceedings of the National Academy of Sciences of the United States of America, 88, 1864-1868.

Joliot, A., Trembleau, A., Raposo, G., Calvet, S., Volovitch, M., & Prochiantz, A. (1997). Association of Engrailed homeoproteins with vesicles presenting caveolae-like properties. Development (Cambridge, England), 124, 1865-1875.

Jones, A. T. & Sayers, E. J. (2012). Cell entry of cell penetrating peptides: tales of tails wagging dogs. Journal of controlled release : official journal of the Controlled Release Society, 161, 582-591.

Joshi, R. L., Torero Ibad, R., Rheey, J., Castagner, F., Prochiantz, A., & Moya, K. L. (2011). Cell non-autonomous functions of homeoproteins in neuroprotection in the brain. FEBS letters, 585, 1573-1578.

Joyner, A. L. & Zervas, M. (2006). Genetic inducible fate mapping in mouse: establishing genetic lineages and defining genetic neuroanatomy in the nervous system. Developmental dynamics : an official publication of the American Association of Anatomists, 235, 2376-2385.

Kameda, Y., Arai, Y., & Nishimaki, T. (2003). Ultrastructural localization of vimentin immunoreactivity and gene expression in tanycytes and their alterations in hamsters kept under different photoperiods. Cell and tissue research, 314, 251-262.

Kang, S. H., Srivastava, I., Fukaya, M., De Biase, L., Takebayashi, H., & Bergles, D. E. (2010). Inducible ablation of NG2+ glial cells in the adult brain. Society for Neuroscience .

Ref Type: Abstract

Kapsimali, M., Caneparo, L., Houart, C., & Wilson, S. W. (2004). Inhibition of Wnt/Axin/beta-catenin pathway activity promotes ventral CNS midline tissue to adopt hypothalamic rather than floorplate identity. Development (Cambridge, England), 131, 5923-5933.

Kiecker, C. & Lumsden, A. (2005). Compartments and their boundaries in vertebrate brain development. Nature reviews.Neuroscience, 6, 553-564.

King, J. C. & Rubin, B. S. (1994). Dynamic changes in LHRH neurovascular terminals with various endocrine conditions in adults. Hormones and behavior, 28, 349-356.

Kohwi, M., Osumi, N., Rubenstein, J. L., & Alvarez-Buylla, A. (2005). Pax6 is required for making specific subpopulations of granule and periglomerular neurons in the olfactory bulb. J.Neurosci., 25, 6997-7003.

Koike, C., Nishida, A., Ueno, S., Saito, H., Sanuki, R., Sato, S. et al. (2007). Functional roles of Otx2 transcription factor in postnatal mouse retinal development. Molecular and cellular biology, 27, 8318-8329.

Kokoeva, M. V., Yin, H., & Flier, J. S. (2005). Neurogenesis in the hypothalamus of adult mice: potential role in energy balance. Science (New York, N.Y.), 310, 679-683.

Kozlowski, G. P. & Coates, P. W. (1985). Ependymoneuronal specializations between LHRH fibers and cells of the cerebroventricular system. Cell and tissue research, 242, 301-311.

Krisch, B. & Leonhardt, H. (1978). The functional and structural border of the neurohemal region of the median eminence. Cell and tissue research, 192, 327-339.

Laemle, L. K. & Rusa, R. (1992). VIP-like immunoreactivity in the suprachiasmatic nuclei of a mutant anophthalmic mouse. Brain research, 589, 124-128.

Larsen, P. R., Kronenberg, H. M., Melmed, S., & Polonsky, S. (2002). Williams Texbook of Endocrinology. (10 ed.) Philadelphia: Saunders.

Laughon, A. (1991). DNA binding specificity of homeodomains. Biochemistry, 30, 11357-11367.

Lavado, A. & Oliver, G. (2011). Six3 is required for ependymal cell maturation. Development (Cambridge, England), 138, 5291-5300.

Layalle, S., Volovitch, M., Mugat, B., Bonneaud, N., Parmentier, M. L., Prochiantz, A. et al. (2011). Engrailed homeoprotein acts as a signaling molecule in the developing fly. Development (Cambridge, England), 138, 2315-2323.

Le Roux, I., Joliot, A. H., Bloch-Gallego, E., Prochiantz, A., & Volovitch, M. (1993). Neurotrophic activity of the Antennapedia homeodomain depends on its specific DNA-binding properties. Proceedings of the National Academy of Sciences of the United States of America, 90, 9120-9124.

Lechan, R. M. & Fekete, C. (2004). Feedback regulation of thyrotropin-releasing hormone (TRH): mechanisms for the non-thyroidal illness syndrome. J Endocrinol.Invest, 27, 105-119.

Lee, D. A., Bedont, J. L., Pak, T., Wang, H., Song, J., Miranda-Angulo, A. et al. (2012). Tanycytes of the hypothalamic median eminence form a diet-responsive neurogenic niche. Nature neuroscience, 15, 700-702.

Lesaffre, B., Joliot, A., Prochiantz, A., & Volovitch, M. (2007). Direct non-cell autonomous Pax6 activity regulates eye development in the zebrafish. Neural development, 2, 2.

Letoha, T., Gaal, S., Somlai, C., Czajlik, A., Perczel, A., & Penke, B. (2003). Membrane translocation of penetratin and its derivatives in different cell lines. Journal of Molecular Recognition : JMR, 16, 272-279.

Liu, Y. & Rao, M. S. (2004). Glial progenitors in the CNS and possible lineage relationships among them. Biology of the cell / under the auspices of the European Cell Biology Organization, 96, 279-290.

Lu, F., Kar, D., Gruenig, N., Zhang, Z. W., Cousins, N., Rodgers, H. M. et al. (2013). Rax is a selector gene for mediobasal hypothalamic cell types. J Neurosci., 33, 259-272.

Ma, C., Papermaster, D., & Cepko, C. L. (1998). A unique pattern of photoreceptor degeneration in cyclin D1 mutant mice. Proceedings of the National Academy of Sciences of the United States of America, 95, 9938-9943.

Ma, Y. J., Berg-von der Emde, K., Moholt-Siebert, M., Hill, D. F., & Ojeda, S. R. (1994). Region-specific regulation of transforming growth factor alpha (TGF alpha) gene expression in astrocytes of the neuroendocrine brain. The Journal of neuroscience : the official journal of the Society for Neuroscience, 14, 5644-5651.

Madisen, L., Zwingman, T. A., Sunkin, S. M., Oh, S. W., Zariwala, H. A., Gu, H. et al. (2010). A robust and high-throughput Cre reporting and characterization system for the whole mouse brain. Nature neuroscience, 13, 133-140.

Maizel, A., Bensaude, O., Prochiantz, A., & Joliot, A. (1999). A short region of its homeodomain is necessary for engrailed nuclear export and secretion. Development (Cambridge, England), 126, 3183-3190.

Maizel, A., Tassetto, M., Filhol, O., Cochet, C., Prochiantz, A., & Joliot, A. (2002). Engrailed homeoprotein secretion is a regulated process. Development (Cambridge, England), 129, 3545-3553.

Marcet, B., Chevalier, B., Luxardi, G., Coraux, C., Zaragosi, L. E., Cibois, M. et al. (2011). Control of vertebrate multiciliogenesis by miR-449 through direct repression of the Delta/Notch pathway. Nature cell biology, 13, 693-699.

Markakis, E. A. (2002). Development of the neuroendocrine hypothalamus. Front Neuroendocrinol., 23, 257-291.

Marsili, A., Sanchez, E., Singru, P., Harney, J. W., Zavacki, A. M., Lechan, R. M. et al. (2011). Thyroxine-induced expression of pyroglutamyl peptidase II and inhibition

of TSH release precedes suppression of TRH mRNA and requires type 2 deiodinase. J.Endocrinol., 211, 73-78.

Mathers, P. H., Grinberg, A., Mahon, K. A., & Jamrich, M. (1997). The Rx homeobox gene is essential for vertebrate eye development. Nature, 387, 603-607.

Mathew, T. C. (2008). Regional analysis of the ependyma of the third ventricle of rat by light and electron microscopy. Anatomia, Histologia, Embryologia, 37, 9-18.

Matter, K. & Balda, M. S. (2003). Signalling to and from tight junctions. Nature reviews.Molecular cell biology, 4, 225-236.

Medina-Martinez, O., Amaya-Manzanares, F., Liu, C., Mendoza, M., Shah, R., Zhang, L. et al. (2009). Cell-autonomous requirement for rx function in the mammalian retina and posterior pituitary. PloS one, 4, e4513.

Michael, S. K., Brennan, J., & Robertson, E. J. (1999). Efficient gene-specific expression of cre recombinase in the mouse embryo by targeted insertion of a novel IRES-Cre cassette into endogenous loci. Mech.Dev., 85, 35-47.

Millan, C., Martinez, F., Cortes-Campos, C., Lizama, I., Yanez, M. J., Llanos, P. et al. (2010). Glial glucokinase expression in adult and post-natal development of the hypothalamic region. ASN neuro, 2, e00035.

Millhouse, O. E. (1971). A Golgi study of third ventricle tanycytes in the adult rodent brain. Zeitschrift fur Zellforschung und mikroskopische Anatomie (Vienna, Austria : 1948), 121, 1-13.

Minshall, R. D., Tiruppathi, C., Vogel, S. M., & Malik, A. B. (2002). Vesicle formation and trafficking in endothelial cells and regulation of endothelial barrier function. Histochemistry and cell biology, 117, 105-112.

Mohacsik, P., Zeold, A., Bianco, A. C., & Gereben, B. (2011). Thyroid hormone and the neuroglia: both source and target. Journal of thyroid research, 2011, 215718.

Monroe, B. G. & Paull, W. K. (1974). Ultrastructural changes in the hypothalamus during development and hypothalamic activity: the median eminence. Progress in brain research, 41, 185-208.

Mullier, A., Bouret, S. G., Prevot, V., & Dehouck, B. (2010). Differential distribution of tight junction proteins suggests a role for tanycytes in blood-hypothalamus barrier regulation in the adult mouse brain. The Journal of comparative neurology, 518, 943-962.

Muranishi, Y., Terada, K., & Furukawa, T. (2012). An essential role for Rax in retina and neuroendocrine system development. Development, growth & differentiation, 54, 341-348.

Muranishi, Y., Terada, K., Inoue, T., Katoh, K., Tsujii, T., Sanuki, R. et al. (2011). An essential role for RAX homeoprotein and NOTCH-HES signaling in Otx2 expression in embryonic retinal photoreceptor cell fate determination. The Journal of neuroscience : the official journal of the Society for Neuroscience, 31, 16792-16807.

Muzumdar, M. D., Tasic, B., Miyamichi, K., Li, L., & Luo, L. (2007). A global double-fluorescent Cre reporter mouse. Genesis (New York, N.Y.: 2000), 45, 593-605.

Nakao, N., Ono, H., Yamamura, T., Anraku, T., Takagi, T., Higashi, K. et al. (2008). Thyrotrophin in the pars tuberalis triggers photoperiodic response. Nature, 452, 317-322.

Nishida, A., Furukawa, A., Koike, C., Tano, Y., Aizawa, S., Matsuo, I. et al. (2003). Otx2 homeobox gene controls retinal photoreceptor cell fate and pineal gland development. Nature neuroscience, 6, 1255-1263.

Norsted, E., Gomuc, B., & Meister, B. (2008). Protein components of the blood-brain barrier (BBB) in the mediobasal hypothalamus. Journal of chemical neuroanatomy, 36, 107-121.

Nozaki, M., Uemura, H., & Kobayashi, H. (1980). Hypothalamo-hypophysial function following the lesion of tanycytes in the median eminence of the rat. Cell and tissue research, 209, 225-238.

Nyberg-Hansen, R., Torvik, A., & Bhatia, R. (1975). On the pathology of experimental hydrocephalus. Brain research, 95, 343-350.

O'Callaghan, C., Sikand, K., & Rutman, A. (1999). Respiratory and brain ependymal ciliary function. Pediatr.Res., 46, 704-707.

Ohyama, K., Das, R., & Placzek, M. (2008). Temporal progression of hypothalamic patterning by a dual action of BMP. Development (Cambridge, England), 135, 3325-3331.

Ojeda, S. R., Lomniczi, A., & Sandau, U. S. (2008). Glial-gonadotrophin hormone (GnRH) neurone interactions in the median eminence and the control of GnRH secretion. Journal of neuroendocrinology, 20, 732-742.

Olney, J. W. (1971). Glutamate-induced neuronal necrosis in the infant mouse hypothalamus. An electron microscopic study. Journal of neuropathology and experimental neurology, 30, 75-90.

Orellana, J. A., Saez, P. J., Cortes-Campos, C., Elizondo, R. J., Shoji, K. F., Contreras-Duarte, S. et al. (2012). Glucose increases intracellular free Ca(2+) in tanycytes via ATP released through connexin 43 hemichannels. Glia, 60, 53-68.

Osakada, F., Ikeda, H., Mandai, M., Wataya, T., Watanabe, K., Yoshimura, N. et al. (2008). Toward the generation of rod and cone photoreceptors from mouse, monkey and human embryonic stem cells. Nature biotechnology, 26, 215-224.

Passini, M. A., Watson, D. J., Vite, C. H., Landsburg, D. J., Feigenbaum, A. L., & Wolfe, J. H. (2003). Intraventricular brain injection of adeno-associated virus type 1 (AAV1) in neonatal mice results in complementary patterns of neuronal transduction to AAV2 and total long-term correction of storage lesions in the brains of beta-glucuronidase-deficient mice. Journal of virology, 77, 7034-7040.

Paxinos, L. (1994). The rat nervous system . (2 ed.) California: Academic Press.

Pencea, V., Bingaman, K. D., Wiegand, S. J., & Luskin, M. B. (2001). Infusion of brain-derived neurotrophic factor into the lateral ventricle of the adult rat leads to new neurons in the parenchyma of the striatum, septum, thalamus, and hypothalamus. The

Journal of neuroscience : the official journal of the Society for Neuroscience, 21, 6706-6717.

Perez-Martin, M., Cifuentes, M., Grondona, J. M., Lopez-Avalos, M. D., Gomez-Pinedo, U., Garcia-Verdugo, J. M. et al. (2010). IGF-I stimulates neurogenesis in the hypothalamus of adult rats. The European journal of neuroscience, 31, 1533-1548.

Peruzzo, B., Pastor, F. E., Blazquez, J. L., Schobitz, K., Pelaez, B., Amat, P. et al. (2000). A second look at the barriers of the medial basal hypothalamus. Experimental brain research.Experimentelle Hirnforschung.Experimentation cerebrale, 132, 10-26.

Pick, L. & Heffer, A. (2012). Hox gene evolution: multiple mechanisms contributing to evolutionary novelties. Annals of the New York Academy of Sciences, 1256, 15-32.

Plageman, T. F., Jr. & Lang, R. A. (2012). Generation of an Rx-tTA: TetOp-Cre knock-in mouse line for doxycycline regulated Cre activity in the Rx expression domain. PloS one, 7, e50426.

Postic, C. & Magnuson, M. A. (2000). DNA excision in liver by an albumin-Cre transgene occurs progressively with age. Genesis (New York, N.Y.: 2000), 26, 149-150.

Prevot, V., Cornea, A., Mungenast, A., Smiley, G., & Ojeda, S. R. (2003). Activation of erbB-1 signaling in tanycytes of the median eminence stimulates transforming growth factor beta1 release via prostaglandin E2 production and induces cell plasticity. The Journal of neuroscience : the official journal of the Society for Neuroscience, 23, 10622-10632.

Prevot, V., Croix, D., Bouret, S., Dutoit, S., Tramu, G., Stefano, G. B. et al. (1999). Definitive evidence for the existence of morphological plasticity in the external zone of the median eminence during the rat estrous cycle: implication of neuro-glio-endothelial interactions in gonadotropin-releasing hormone release. Neuroscience, 94, 809-819.

Prieto, M., Chauvet, N., & Alonso, G. (2000). Tanycytes transplanted into the adult rat spinal cord support the regeneration of lesioned axons. Exp.Neurol., 161, 27-37.

Prochiantz, A. (2011). Homeoprotein intercellular transfer, the hidden face of cell-penetrating peptides. Methods in molecular biology (Clifton, N.J.), 683, 249-257.

Prochiantz, A. & Joliot, A. (2003). Can transcription factors function as cell-cell signalling molecules? Nature reviews.Molecular cell biology, 4, 814-819.

Rath, M. F., Morin, F., Shi, Q., Klein, D. C., & Moller, M. (2007). Ontogenetic expression of the Otx2 and Crx homeobox genes in the retina of the rat. Experimental eye research, 85, 65-73.

Reichenbach, A., Stolzenburg, J. U., Eberhardt, W., Chao, T. I., Dettmer, D., & Hertz, L. (1993). What do retinal muller (glial) cells do for their neuronal 'small siblings'? Journal of chemical neuroanatomy, 6, 201-213.

Roales-Bujan, R., Paez, P., Guerra, M., Rodriguez, S., Vio, K., Ho-Plagaro, A. et al. (2012). Astrocytes acquire morphological and functional characteristics of ependymal cells following disruption of ependyma in hydrocephalus. Acta Neuropathologica, 124, 531-546.

Rodriguez, E. M., Peña, P., Aguado, L. I., & Schoebitz, K. (1985). Current trends in comparative endocrinology. Hong Kong: Hong Kong University Press.

Rodriguez, E. M., Blazquez, J. L., & Guerra, M. (2010). The design of barriers in the hypothalamus allows the median eminence and the arcuate nucleus to enjoy private milieus: the former opens to the portal blood and the latter to the cerebrospinal fluid. Peptides, 31, 757-776.

Rodriguez, E. M., Blazquez, J. L., Pastor, F. E., Pelaez, B., Pena, P., Peruzzo, B. et al. (2005). Hypothalamic tanycytes: a key component of brain-endocrine interaction. Int.Rev.Cytol., 247, 89-164.

Rodriguez, E. M., Gonzalez, C. B., & Delannoy, L. (1979). Cellular organization of the lateral and postinfundibular regions of the median eminence in the rat. Cell and tissue research, 201, 377-408.

Rohde, K., Klein, D. C., Moller, M., & Rath, M. F. (2011). Rax : developmental and daily expression patterns in the rat pineal gland and retina. Journal of neurochemistry, 118, 999-1007.

Rutzel, H. & Schiebler, T. H. (1980). Prenatal and early postnatal development of the glial cells in the median eminence of the rat. Cell and tissue research, 211, 117-137.

Sainsbury, A. & Zhang, L. (2010). Role of the arcuate nucleus of the hypothalamus in regulation of body weight during energy deficit. Mol.Cell Endocrinol., 316, 109-119.

Sanchez, E., Vargas, M. A., Singru, P. S., Pascual, I., Romero, F., Fekete, C. et al. (2009). Tanycyte pyroglutamyl peptidase II contributes to regulation of the hypothalamic-pituitary-thyroid axis through glial-axonal associations in the median eminence. Endocrinology, 150, 2283-2291.

Sanders, N. M., Dunn-Meynell, A. A., & Levin, B. E. (2004). Third ventricular alloxan reversibly impairs glucose counterregulatory responses. Diabetes, 53, 1230-1236.

Satir, P. & Christensen, S. T. (2007). Overview of structure and function of mammalian cilia. Annual Review of Physiology, 69, 377-400.

Segerson, T. P., Kauer, J., Wolfe, H. C., Mobtaker, H., Wu, P., Jackson, I. M. et al. (1987). Thyroid hormone regulates TRH biosynthesis in the paraventricular nucleus of the rat hypothalamus. Science (New York, N.Y.), 238, 78-80.

Selzer, M. E. (2003). Promotion of axonal regeneration in the injured CNS. Lancet Neurol., 2, 157-166.

Seress, L. (1980). Development and structure of the radial glia in the postnatal rat brain. Anat.Embryol.(Berl), 160, 213-226.

Sgado, P., Alberi, L., Gherbassi, D., Galasso, S. L., Ramakers, G. M., Alavian, K. N. et al. (2006). Slow progressive degeneration of nigral dopaminergic neurons in postnatal Engrailed mutant mice. Proceedings of the National Academy of Sciences of the United States of America, 103, 15242-15247.

Sharma, H. S. & Johanson, C. E. (2007). Blood-cerebrospinal fluid barrier in hyperthermia. Progress in brain research, 162, 459-478.

Shimogori, T., Lee, D. A., Miranda-Angulo, A., Yang, Y., Wang, H., Jiang, L. et al. (2010). A genomic atlas of mouse hypothalamic development. Nature neuroscience, 13, 767-775.

Sicinski, P., Donaher, J. L., Parker, S. B., Li, T., Fazeli, A., Gardner, H. et al. (1995). Cyclin D1 provides a link between development and oncogenesis in the retina and breast. Cell, 82, 621-630.

Silver, J. (1977). Abnormal development of the suprachiasmatic nuclei of the hypothalamus in a strain of genetically anophthalmic mice. The Journal of comparative neurology, 176, 589-606.

Siso, S., Jeffrey, M., & Gonzalez, L. (2010). Sensory circumventricular organs in health and disease. Acta Neuropathologica, 120, 689-705.

Smith, L. (2011). Good planning and serendipity: exploiting the Cre/Lox system in the testis. Reproduction (Cambridge, England), 141, 151-161.

Song, Z. & Routh, V. H. (2005). Differential effects of glucose and lactate on glucosensing neurons in the ventromedial hypothalamic nucleus. Diabetes, 54, 15-22.

Sonnier, L., Le Pen, G., Hartmann, A., Bizot, J. C., Trovero, F., Krebs, M. O. et al. (2007). Progressive loss of dopaminergic neurons in the ventral midbrain of adult

mice heterozygote for Engrailed1. The Journal of neuroscience : the official journal of the Society for Neuroscience, 27, 1063-1071.

Spandidos, A., Wang, X., Wang, H., Dragnev, S., Thurber, T., & Seed, B. (2008). A comprehensive collection of experimentally validated primers for Polymerase Chain Reaction quantitation of murine transcript abundance. BMC.Genomics, 9, 633.

Spandidos, A., Wang, X., Wang, H., & Seed, B. (2010). PrimerBank: a resource of human and mouse PCR primer pairs for gene expression detection and quantification. Nucleic Acids Res., 38, D792-D799.

Spatazza, J., Di Lullo, E., Joliot, A., Dupont, E., Moya, K. L., & Prochiantz, A. (2013). Homeoprotein signaling in development, health, and disease: a shaking of dogmas offers challenges and promises from bench to bed. Pharmacological reviews, 65, 90-104.

Steed, E., Balda, M. S., & Matter, K. (2010). Dynamics and functions of tight junctions. Trends in cell biology, 20, 142-149.

Stubbs, J. L., Vladar, E. K., Axelrod, J. D., & Kintner, C. (2012). Multicilin promotes centriole assembly and ciliogenesis during multiciliate cell differentiation. Nature cell biology, 14, 140-147.

Suga, H., Kadoshima, T., Minaguchi, M., Ohgushi, M., Soen, M., Nakano, T. et al. (2011). Self-formation of functional adenohypophysis in three-dimensional culture. Nature, 480, 57-62.

Sugiyama, S., Di Nardo, A. A., Aizawa, S., Matsuo, I., Volovitch, M., Prochiantz, A. et al. (2008). Experience-dependent transfer of Otx2 homeoprotein into the visual cortex activates postnatal plasticity. Cell, 134, 508-520.

Sunkin, S. M., Ng, L., Lau, C., Dolbeare, T., Gilbert, T. L., Thompson, C. L. et al. (2013). Allen Brain Atlas: an integrated spatio-temporal portal for exploring the central nervous system. Nucleic Acids Res., 41, D996-D1008.

Swaab, D. F. (1999). Hypothalamic Peptides in Human Brain Diseases. Trends in endocrinology and metabolism: TEM, 10, 236-244.

Terada, K. & Furukawa, T. (2010). Sumoylation controls retinal progenitor proliferation by repressing cell cycle exit in Xenopus laevis. Developmental biology, 347, 180-194.

Thompson, R. H., Canteras, N. S., & Swanson, L. W. (1996). Organization of projections from the dorsomedial nucleus of the hypothalamus: a PHA-L study in the rat. J.Comp Neurol., 376, 143-173.

Thomzig, A., Wenzel, M., Karschin, C., Eaton, M. J., Skatchkov, S. N., Karschin, A. et al. (2001). Kir6.1 is the principal pore-forming subunit of astrocyte but not neuronal plasma membrane K-ATP channels. Molecular and cellular neurosciences, 18, 671-690.

Topisirovic, I. & Borden, K. L. (2005). Homeodomain proteins and eukaryotic translation initiation factor 4E (eIF4E): an unexpected relationship. Histology and histopathology, 20, 1275-1284.

Topisirovic, I., Kentsis, A., Perez, J. M., Guzman, M. L., Jordan, C. T., & Borden, K. L. (2005). Eukaryotic translation initiation factor 4E activity is modulated by HOXA9 at multiple levels. Molecular and cellular biology, 25, 1100-1112.

Torero Ibad, R., Rheey, J., Mrejen, S., Forster, V., Picaud, S., Prochiantz, A. et al. (2011). Otx2 promotes the survival of damaged adult retinal ganglion cells and protects against excitotoxic loss of visual acuity in vivo. The Journal of neuroscience : the official journal of the Society for Neuroscience, 31, 5495-5503.

Tsukita, S., Furuse, M., & Itoh, M. (1999). Structural and signalling molecules come together at tight junctions. Current opinion in cell biology, 11, 628-633.

Tu, H. M., Kim, S. W., Salvatore, D., Bartha, T., Legradi, G., Larsen, P. R. et al. (1997). Regional distribution of type 2 thyroxine deiodinase messenger ribonucleic acid in rat hypothalamus and pituitary and its regulation by thyroid hormone. Endocrinology, 138, 3359-3368.

Tucker, P., Laemle, L., Munson, A., Kanekar, S., Oliver, E. R., Brown, N. et al. (2001). The eyeless mouse mutation (ey1) removes an alternative start codon from the Rx/rax homeobox gene. Genesis (New York, N.Y.: 2000), 31, 43-53.

VanDunk, C., Hunter, L. A., & Gray, P. A. (2011). Development, maturation, and necessity of transcription factors in the mouse suprachiasmatic nucleus. The Journal of neuroscience : the official journal of the Society for Neuroscience, 31, 6457-6467.

Verma, A. S. & Fitzpatrick, D. R. (2007). Anophthalmia and microphthalmia. Orphanet journal of rare diseases, 2, 47.

Villar, M. J., Ceccatelli, S., Bedecs, K., Bartfai, T., Bredt, D., Synder, S. H. et al. (1994). Upregulation of nitric oxide synthase and galanin message-associated peptide in hypothalamic magnocellular neurons after hypophysectomy. Immunohistochemical and in situ hybridization studies. Brain research, 650, 219-228.

Voigt, P., Ma, Y. J., Gonzalez, D., Fahrenbach, W. H., Wetsel, W. C., Berg-von der Emde, K. et al. (1996). Neural and glial-mediated effects of growth factors acting via tyrosine kinase receptors on luteinizing hormone-releasing hormone neurons. Endocrinology, 137, 2593-2605.

Voronina, V. A., Kozlov, S., Mathers, P. H., & Lewandoski, M. (2005). Conditional alleles for activation and inactivation of the mouse Rx homeobox gene. Genesis (New York, N.Y.: 2000), 41, 160-164.

Walsh, R. J., Brawer, J. R., & Lin, P. L. (1978). Early postnatal development of ependyma in the third ventricle of male and female rats. The American Journal of Anatomy, 151, 377-407.

Wataya, T., Ando, S., Muguruma, K., Ikeda, H., Watanabe, K., Eiraku, M. et al. (2008). Minimization of exogenous signals in ES cell culture induces rostral hypothalamic differentiation. Proceedings of the National Academy of Sciences of the United States of America, 105, 11796-11801.

Wei, L. C., Shi, M., Chen, L. W., Cao, R., Zhang, P., & Chan, Y. S. (2002). Nestin-containing cells express glial fibrillary acidic protein in the proliferative regions

of central nervous system of postnatal developing and adult mice. Brain research.Developmental brain research, 139, 9-17.

Wigle, J. T. & Eisenstat, D. D. (2008). Homeobox genes in vertebrate forebrain development and disease. Clinical genetics, 73, 212-226.

Wizenmann, A., Brunet, I., Lam, J. S., Sonnier, L., Beurdeley, M., Zarbalis, K. et al. (2009). Extracellular Engrailed participates in the topographic guidance of retinal axons in vivo. Neuron, 64, 355-366.

Xu, Y., Tamamaki, N., Noda, T., Kimura, K., Itokazu, Y., Matsumoto, N. et al. (2005). Neurogenesis in the ependymal layer of the adult rat 3rd ventricle. Exp.Neurol., 192, 251-264.

Yamamura, T., Hirunagi, K., Ebihara, S., & Yoshimura, T. (2004). Seasonal morphological changes in the neuro-glial interaction between gonadotropin-releasing hormone nerve terminals and glial endfeet in Japanese quail. Endocrinology, 145, 4264-4267.

Yang, D., Li, S. Y., Yeung, C. M., Chang, R. C., So, K. F., Wong, D. et al. (2012). Lycium barbarum extracts protect the brain from blood-brain barrier disruption and cerebral edema in experimental stroke. PloS one, 7, e33596.

Young, R. W. (1985). Cell differentiation in the retina of the mouse. Anat.Rec., 212, 199-205.

Yu, X., Ng, C. P., Habacher, H., & Roy, S. (2008). Foxj1 transcription factors are master regulators of the motile ciliogenic program. Nature genetics, 40, 1445-1453.

Zeng, X., Asmaro, K., Ren, C., Gao, M., Peng, C., Ding, J. Y. et al. (2012). Acute ethanol treatment reduces blood-brain barrier dysfunction following ischemia/reperfusion injury. Brain research, 1437, 127-133.

Curriculum Vitae

Name	Ana Lucia Miranda-Angulo
Place of Birth	Medellín, Colombia-South America
Date of Birth	October 5, 1975
E-mail	mirandaana012@gmail.com

EDUCATION

Ph.D. Candidate	*2005-curr*	Program in Neuroscience Mentor: Seth Blackshaw **Johns Hopkins, School of Medicine**
M.S.	*2001-2004*	Biomedical Sciences, Genetics **Universidad de Antioquia, School of Medicine,** Colombia
M.D.	*1992-1999*	Medicine **Universidad de Antioquia, School of Medicine,** Colombia
Specialty course	*Sept. 1-* *Dec. 17, 2004*	**National Institutes of Health** Introduction to Medical Genetics
Specialty course	*Sept. 15, 2003-* *Jan. 16, 2004*	National Institutes of Health Neurobiology of Mental Illness
Specialty course	*Dec. 8-* *12, 2003*	**Rockefeller University** Advanced Gene Mapping/Linkage Course

Specialty course	*Nov. 17-21, 2003*	**National Institutes of Health** DNA-Binding Proteins, Transcriptional Regulators and Homeoboxes: Principles and Practice

RESEARCH EXPERIENCE

Doctorate thesis research	*2006-2012*	Laboratory of Seth Blackshaw Ph.D Johns Hopkins, School of Medicine
Laboratory rotations	*2005-2006*	Laboratory of Akira Sawa, Ph.D Laboratory of Nicholas Gaiano Ph.D Johns Hopkins, School of Medicine
Postdoctoral fellowship	*2003-2005*	National Institutes of Mental Health and Pan American Health Organization,USA Mentors: Daniel Weinberger MD., Richard Straub Ph.D., Cynthia Shannon Weickert Ph.D. Project: Genetic association analysis between several candidate genes and schizophrenia.
Master thesis research	*2001-2003*	Research Group in Psychiatry (GIPSI), Universidad de Antioquia, Colombia Mentors: Gabriel Bedoya M.S., Jorge Ospina-Duque M.D. Thesis: Qualitative and quantitative family association analysis in schizophrenic families from Antioquia-Colombia using

		microsatellites near neurodevelopmental genes.
Research Internship	*1999-2001*	Research Group in Psychiatry (GIPSI), Universidad de Antioquia, Colombia Mentors: Gabriel Bedoya M.S., Jorge Ospina-Duque M.D. Project: Linkage analysis of Bipolar I in families from Antioquia-Colombia
Young investigator	*1997-1998*	Molecular Genetics Laboratory, Universidad de Antioquia, Colombia Mentors: Andres Ruiz-Linares Ph.D., Gabriel Bedoya M.S. Project: Linkage analysis of Bipolar I in families from Antioquia

AWARDS AND HONORS

2005	Best article published, Revista Colombiana de Psiquiatría, Colombia.
2004	Poster award, Collegium Internationale Neuro-psychopharmacologicum, Paris.
2004	Graduated with honors, M.S., Biomedical sciences, Universidad de Antioquia, School of Medicine, Colombia.
2003	Postdoctoral fellowship, Pan American Health organization and National Institutes of Health, USA.

PUBLICATIONS

Miranda-Angulo Ana, Byerly, Mardi; Mesa, Janny; Wang, Hong; Blackshaw, Seth. Rax regulates hypothalamic tanycyte differentiation and barrier function in mice. J Comp. Neurol., 2013 Aug 12. Epub ahead of print.

Lee, D. A., Bedont, J. L., Pak, T., Wang, H., Song, J., **Miranda-Angulo, A**., Takiar V.,Charubhumi V., Balordi F., Takebayashi H., Aja S., Fishell G., Blackshaw S. Tanycytes of the hypothalamic median eminence form a diet-responsive neurogenic niche. Nat. Neurosci., 15, 700-702 (Article).

Shimogori T, Lee DA, **Miranda-Angulo A**, Yang Y, Wang H, Jiang L, Yoshida AC, Kataoka A,Mashiko H, Avetisyan M, Qi L, Qian J, Blackshaw S. A genomic atlas of mouse hypothalamic development. Nat Neurosci. 2010 Jun;13(6):767-75. Epub 2010 May 2 (Article).

Barbara Kremeyer, Jenny García, Hanna Kymäläinen, Naomi Wratten, Gabriel Restrepo, Carlos Palacio, **Ana Lucía Miranda**, Carlos López, Margarita Restrepo, Gabriel Bedoya, Linda M. Brzustowicz, Jorge Ospina-Duque, María Patricia Arbeláez, Andrés Ruiz-Linares Evidence for a Role of the NOS1AP (CAPON) Gene in Schizophrenia and Its Clinical Dimensions: An Association Study in a South American Population Isolate. Hum. Hered. 2009; 67:163-173 (Article).

Ana Miranda-Angulo, Cynthia Shannon Weickert, Jenny Wong, William R. Perlman,Sarah E. Ward, Vakkalanka Radhakrishna, Richard E. Straub, Daniel R. Weinberger and Joel E. Kleinman. Variants in the estrogen receptor alpha gene and its mRNA contribute to risk for schizophrenia. Hum. Mol. Gen. 2008; Vol 17, No15, 2293-2309 (Article).

Ana Miranda-Angulo, Lee D., Jian L., QI L., Avetisyan M., Blackshaw S., Genomic analysis of the mouse hypothalamic development. San Diego, California. Society for Neuroscience 2007;776.23/B17 (Poster).

Ana Miranda-Angulo, Cynthia Shannon Weickert, William, R. Perlman, Sarah E. Ward, Joel E. Kleinman, Vakkalanca Radhakrishna , Richard E. Straub, and Daniel R. Weinberger, Variants in the Estrogen Receptor Alpha Gene and its mRNA Isoforms Contribute to Risk for Schizophrenia. XIV World Congress on Psychiatric Genetics, Cagliari, Italy, 2006; October 25-November 3 (Poster).

Miranda A, Garcia J, Lopez C, Gordon D, Palacio C, Restrepo G, Ortiz J, Montoya G, Cardeno C,Calle J, Lopez M, Campo O, Bedoya G, Ruiz-Linares A, Ospina-Duque J. Putative association of the carboxy-terminal PDZ ligand of neuronal nitric oxide synthase gene (CAPON) with schizophrenia in a Colombian population. Schizophr Res. 2006; Feb 28;82(2-3):283-5 (Article).

Ana Miranda, Gabriel Bedoya , Jenny García, Carlos Lopez, Jorge Opina, Jorge Calle, Maria Lopez, Andrés Ruiz, Jorge Ospina. Análisis de ligamiento de esquizofrenia con genes del neurodesarrollo mediante cinco marcadores microsatélites. Revista de Neuro Psiquiatría, 2005;68 (1): 34-46 (Article).

García-Valencia, Jenny; **Miranda, Ana**; Palacio, Carlos; Lopez, Carlos; Ospina, Jorge; Gomez, Juliana. Esquizofrenia y neurodesarrollo. Revista Colombiana de Psiquiatría, 2005; 34(1):63-76 (Review).

Carlos López, **Ana Miranda**, Jenny García, Gabriel Montoya, Carlos Palacio, Gabriel Restrepo, Jorge Calle, Maria López, Natalia González, Alejandro González, Omer Campo, Gabriel Bedoya, Andrés Ruiz, Jorge Ospina. Qualitative and quantitative family based association analysis in schizophrenic families from Antioquia-Colombia using microsatellites near neurodevelopmental genes. Neuropschopharmacology, 2004; vol 7 supplement 1: S261 (Poster).

Ana Miranda, Carlos Lopez, Jenny García, Jorge Ospina. El uso de endofenotipos en el studio del componente genético de la esquizofrenia. Rev. Col. Psiquiatría, 2003; 32

(3):237-59 (Review).

Jorge Ospina-Duque , Mauricio Cuartas-Arias, Luis Carvajal-Carmona, **Ana Miranda**, Ivan Soto, Nicolas Pineda, Jorge Calle , Carlos Lopez, Jenny Garcia , Maria Lopez , Aurora Gallo, Patricia Montoya , Carlos Palacio, Gabriel Bedoya, Andrés Ruiz-Linares. Linkage to bipolar mood disorder in families from Colombia. International Journal of Neuropsychopharmacology, 2002; Vol 5, supplement 1:S114 (Abstract).

Andrés Ruiz, Jorge Ospina, Iván Soto, Gabriel Bedoya, Carlos Palacio, Jorge Calle, Carlos López, Luis Ochoa, Luis Carvajal, Mauricio Cuartas, Daniel Ortiz, Nicolás Pineda, Angela Agudelo, MariaLozano, Aurora gallo**, Ana Miranda**, Lina Serna, Patricia Montoya, Constanza Duque. La población colombiana: encuentro genético de dos mundos. Rev. Colomb. Psiquiatr. 2001;30(3):283-284 (Abstract).

Ospina-Duque, Jorge; Ochoa, Luis; García-Valencia, Jenny; López, Carlos; Calle, Jorge; Carvajal, Luis; Soto, Iván; Pineda, Nicolás; Duque, Constanza; **Miranda, Ana**; Cuartas, Mauricio; Gómez, Juliana; Agudelo, Angela; Montoya, Gabriel; López, María; Gallo, María; Montoya, Claudia; Palacio, Carlos; Bedoya, Gabriel; Mccarthy, Marck; Reus, Víctor; Freimer, Nelson; Ruiz-Linares, Andrés. Loci genéticos asociados al trastorno bipolar: estudios en población colombiana. Rev. Colomb. Psiquiatr. 2001; 30(3):239-47 (Article).

Jorge Ospina, Constanza Duque, Luis Carvajal, Iván Soto, Nicolás Pineda, Daniel Ortiz, Iván Soto, Nicolás Pineda, Mauricio Cuartas, Jorge Calle, Carlos López, Luis Ochoa, Jenny García, Juliana Gómez, Angela Agudelo, Maria Lozano, Aurora Gallo, **Ana Miranda**, Lina Serna, Carlos Palacio Patricia Montoya Gabriel Bedoya, Carlos Palacio, Gabriel Montoya, Maria López, Gabriel Bedoya, Marck McCarthy, Victor Reus, Nelson Freimer, Andrés Ruiz. An association study of bipolar disorder (type 1) with the 5-HTTLPR serotonin transporter polymorphism in a human population isolated from Colombia. Neuroscience letters, 2000; 292:199-202 (Article).

Andrés Ruiz, Gabriel Bedoya, Carlos Palacio, Jorge Calle, Carlos López, Luis Ochoa, Yeny García, Luis Carvajal, Mauricio Cuartas, Daniel Ortiz, Nicolas Pineda, Juliana Gómez, Angela Agudelo, Maria Lozano, Gabriel Montoya, Angelica Ospina, Maria lópez, Aurora Gallo, **Ana Miranda**, Lina Serna, Patricia Montoya, Jorge Ospina. A search for genetic loci involved in predisposition to bipolar mood disorder in the population of Antioquia Colombia. International Journal of Neuropsychopharmacology, 2000; Vol 3 supplement 1:S345 (Abstract).

TEACHING EXPERIENCE

May 2003- curr	Professor in a study commission. Universidad de Antioquia, School of Medicine, Colombia.
Aug. 2011-2012	Tutoring, student research rotation, Undergraduate Neuroscience Program, Johns Hopkins University, USA
Aug. 2009- Dec.2009	Teaching assistant, Introduction to Neuroscience course, Undergraduate Neuroscience Program, Johns Hopkins University, USA.
2001-2002	Adjunct Professor, Human Genetics, Universidad San Martín, School of Medicine, Colombia.